ERDC/CHL TR-11-1

US Army Corps of Engineers®
Engineer Research and Development Center

ERDC
INNOVATIVE SOLUTIONS for a safer, better world

FEMA Region III Storm Surge Study

Coastal Storm Surge Analysis: Storm Forcing

Report 3: Intermediate Submission No. 1.3

Peter Vickery, Dhiraj Wadhera, Andrew Cox, Vince Cardone, Jeffrey Hanson, and Brian Blanton

July 2013

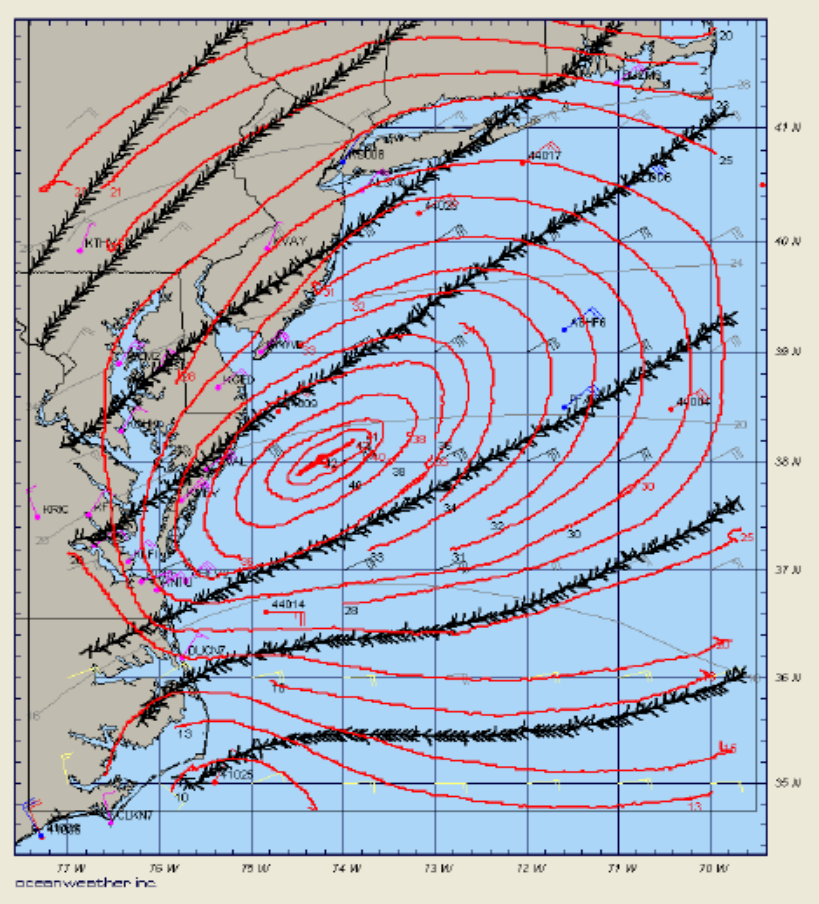

Coastal and Hydraulics Laboratory

The US Army Engineer Research and Development Center (ERDC) solves the nation's toughest engineering and environmental challenges. ERDC develops innovative solutions in civil and military engineering, geospatial sciences, water resources, and environmental sciences for the Army, the Department of Defense, civilian agencies, and our nation's public good. Find out more at www.erdc.usace.army.mil.

To search for other technical reports published by ERDC, visit the ERDC online library at http://acwc.sdp.sirsi.net/client/default.

Coastal Storm Surge Analysis System: Storm Forcing

Report 3: Intermediate Submission No. 1.3

Peter Vickery and Dhiraj Wadhera

Applied Research Associates
8537 Six Forks Road, Suite 600
Raleigh, NC 27615

Andrew Cox and Vince Cardone

Oceanweather, Inc
5 River Road, Suite 1
Cos Cob, CT 06807

Jeffrey L. Hanson

Field Research Facility
US Army Engineer Research and Development Center
1261 Duck Road
Kitty Hawk, NC 27949

Brian Blanton

Renaissance Computing Institute
100 Europa Drive, Suite 540
Chapel Hill, NC 27517

Report 3 of a series; Intermediate Submission 1.3

Prepared for Federal Emergency Management Agency
615 Chestnut Street
One Independence Mall, Sixth Floor
Philadelphia, PA 19106-4404

Under US Army Corps of Engineers Work Unit J64C87

Abstract

The Federal Emergency Management Agency (FEMA), Region III office, has initiated a study to update the coastal storm surge elevations within the states of Virginia, Maryland, and Delaware, and the District of Columbia. The area includes the Atlantic Ocean, the Chesapeake Bay, including its tributaries, and the Delaware Bay. This effort is one of the most extensive coastal storm surge analyses to date, encompassing coastal floodplains in three states and including the largest estuary in the world. The study will replace outdated coastal storm surge stillwater elevations for all Flood Insurance Studies in the study area, and serve as the basis for new coastal hazard analysis and — ultimately — updated Flood Insurance Rate Maps (FIRMs). Study efforts were initiated in August of 2008, and are expected to conclude in 2012.

The storm surge study considers both tropical storms and extratropical cyclones for determination of return period storm surge elevations. The historical record of events in the region has been used to reconstruct wind and pressure fields for significant extratropical cyclone events and to develop a synthetic suite of tropical storm tracks and associated parameters to drive the models. This will support the statistical analysis of storm surge return period elevations. This report, the third of three reports comprising the required Submittal 1 documentation, describes development of the wind and pressure fields required for FEMA Region III storm surge modeling.

Contents

Figures and Tables

Figures

Tables

Preface

This study was conducted for the Federal Emergency Management Agency (FEMA) under Project HSFE03-06-X-0023, "NFIP Coastal Storm Surge Model for Region III" and Project HSFE03-09-X-1108, "Phase II Coastal Storm Surge Model for FEMA Region III." The FEMA technical monitor was Robin Danforth.

The work was performed by the Coastal Processes Branch (HF-C) of the Flood and Storm Protection Division (HF), US Army Engineer Research and Development Center – Coastal and Hydraulics Laboratory (ERDC-CHL). At the time of publication, Mark Gravens was Chief, Coastal Processes Branch; Dr. Ty Wamsley was Chief, Flood and Storm Protection Division; Dr. Jeffrey L. Hanson was the Project Manager; William R. Curtis was Technical Director for Flood and Coastal Storm Research and Development. The Acting Director of CHL was Jose E. Sanchez.

COL Kevin J. Wilson was the Commander of ERDC, and Dr. Jeffery P. Holland was the Director.

Unit Conversion Factors

Multiply	By	To Obtain
degrees (angle)	0.01745329	radians
fathoms	1.8288	meters
feet	0.3048	meters
inches	0.0254	meters
knots	0.5144444	meters per second
miles (nautical)	1,852	meters
miles (US statute)	1,609.347	meters
square miles	2.589998 E+06	square meters
square yards	0.8361274	square meters
yards	0.9144	meters

1 Overview

The Federal Emergency Management Agency (FEMA) is responsible for preparing Federal Insurance Rate Maps (FIRMs) that delineate flood hazard zones in coastal areas of the United States. Under Task Orders HSFE03-06-X-0023 and HSFE03-09-X-1108, the US Army Corps of Engineers (USACE) and project partners are assisting FEMA in the development and application of a state-of-the-art storm surge risk assessment capability for the FEMA Region III domain, which includes the Delaware Bay, Chesapeake Bay, District of Columbia, Delaware-Maryland-Virginia Eastern Shore, Virginia Beach, and all tidal tributaries and waterways connected to these systems. The goal is to develop and apply a complete end-to-end modeling system, with all required forcing inputs, for updating the floodplain levels for coastal and inland watershed communities. Key components of this work include:

1. developing a high-resolution Digital Elevation Map (DEM) for Region III, and converting this to an unstructured modeling grid, with up to 50 m horizontal resolution, for use with the production system;
2. defining the Region III storm hazard in terms of historical extratropical cyclones and synthetic hurricane parameters;
3. preparing an end-to-end modeling system for assessment of Region III coastal storm surge hazards;
4. verifying model accuracy on a variety of reconstructed tropical and extratropical cyclone events;
5. applying the modeling system to compute the 10-, 50-, 100-, and 500- year floodplain levels; and
6. developing a database with GIS tools to facilitate archiving, distribution, and analysis of the various storm surge data products.

Under the direction of FEMA Region III Program Manager, Robin Danforth, USACE assembled a multi-organization partnership to meet the Region III objectives. Work on this project has made extensive use of the capabilities and technology developed for the North Carolina Floodplain Mapping Program (NCFMP). The availability of the NCFMP storm surge modeling system (Blanton et al. 2008) has resulted in a significant cost savings for FEMA Region III. Experts in the fields of coastal storm-surge, wind-driven waves, Geospatial Information Systems (GIS), and high-performance computational systems have worked together in this effort. The project partners and their primary roles are listed in Table 1-1.

Table 1-1. Study team.

Organization	Contacts	Primary Role(s)
US Army Corps of Engineers Field Research Facility (USACE-FRF)	Jeff Hanson Mike Forte Heidi Wadman	Project Manager DEM Construction Model Validations
Applied Research Associates/IntraRisk (ARA)	Peter Vickery Dhiraj Wadhera	Simulated Hurricanes Simulated Hurricanes
ARCADIS	Hugh Roberts John Atkinson Shan Zou	Modeling Mesh Modeling Mesh Modeling Mesh
Elizabeth City State University	Jinchun Yuan	Web/GIS
Oceanweather	Vince Cardone Andrew Cox	Wind Field Reconstructions
Renaissance Computing Institute (RENCI)	Brian Blanton Lisa Stillwell Kevin Gamiel	Modeling System DEM Construction Database/Web/GIS
University of North Carolina- Chapel Hill (UNC-CH)	Rick Luettich	Science Consultant
US Army Corps of Engineers District Offices (NAP, NAO, NAB)	Jason Miller Paul Moye Jared Scott	Bathy/Topo Data Inventory

In addition to the study team, a Technical Oversight Group provided guidance and input to all project phases. This group included members from the following organizations:

1. Chesapeake Bay Research Consortium
2. Delaware Flood Mitigation Program
3. Federal Emergency Management Agency (FEMA)
4. Dewberry, Inc.
5. North Carolina Floodplain Mapping Program
6. USACE Engineer Research and Development Center.

Two prior Submission 1 stand-alone reports (Submission 1.1 by Forte et al. 2011 and Submission 1.2 by Blanton et al. 2011) provided details on the construction of the bathymetric/topographic digital elevation model and preparation of the modeling system including development of the Advanced CIRCulation (ADCIRC) mesh. This report (Submission 1.3) provides the final set of documentation required for Report No. 1 – Scoping and Data Review. The contents of each Submission are listed in Table 1-2. Guidelines for study conduct and documentation appear in FEMA (2007).

Table 1-2. Contents of the Submission 1 report.

Submission	Title	Contents
1.1	FEMA Region III Coastal Storm Surge Analysis: Study Area and Digital Elevation Model (DEM)	Project Overview Study Area DEM Development
1.2	FEMA Region III Coastal Storm Surge Analysis: Computational System	Modeling System Mesh Development
1.3	FEMA Region III Coastal Storm Surge Analysis: Storm Forcing	Hurricane Parameters Extratropical Cyclones

The following chapters describe the development of a synthetic suite of tropical storm tracks, their associated parameters, and the reconstruction of wind and pressure fields for significant extratropical cyclone events in the FEMA Region III coastal domain.

2 Hurricane Parameters

The Joint Probability Method (JPM) for simulating hurricane risk has been used in one form or another since the late 1960s. The original JPM application, while not called JPM, was developed by Russell (1968) for predicting wave loads on offshore structures in the Gulf of Mexico. The approach used by Russell was a full Monte Carlo simulation where hurricanes were modeled using straight-line segments with wind and wave fields computed using hurricane wind and wave models. This methodology was first introduced because the number of historical events (hurricanes) at any one location is insufficient to enable standard statistical techniques (such as extreme value analyses) to estimate flood risk, wave height risk, wind speed risk, etc. For coastal risk assessment, the introduction of long duration synthetic tracks that mimic the behavior of hurricanes while they are offshore (and generating a wave field) was introduced by Resio et al. (2007). Modeling the full storm track of a hurricane for the purpose of developing a wind hazard curve was first introduced by Vickery et al. (2000). These simulation methodologies both model the correlations between storm intensity (central pressure) and radius to maximum winds (*RMW*). Vickery et al. (2009a) modeled a relationship between *RMW* and the Holland *B* (Holland 1980) parameter, whereas Resio et al. (2007) treated the Holland *B* parameter as being deterministic.

The JPM approach is a simulation methodology that relies on the development of statistical distributions of key hurricane input variables (central pressure, radius of maximum winds, translation speed, and heading) and a sampling from these distributions to develop model hurricanes. Heading is the direction of motion of the storm defined as clockwise from north. A storm with a heading of 90 deg is headed east, and one with a heading of -90 deg is heading west. Heading is defined from -180 deg to +180 deg, such that storms with a positive heading have an eastward component and storms with a negative heading have a westward component. The simulation results in a family of modeled storms that preserve the relationships between the various input model components, but provides a means to model the effects and probabilities of storms that have not yet occurred. For this study, a method known as Optimum Sampling (JPM-OS) will be used, which seeks to reduce the number of required simulated storms.

Figures 2-1 through 2-3 show the tracks of historic hurricanes affecting the study region. Of the few hurricanes affecting the study region, none were intense hurricanes. In the absence of sufficient historical data, the approach taken here is to use the synthetic hurricane model described in Vickery et al. (2009a) as a surrogate to develop distributions of central pressure difference, translation speed, and storm heading for storms affecting the study area. Thus, a hybrid approach was used that synthesizes the efficiencies of the JPM with a database of storm statistics generated for a 100,000-year timeframe. The storm statistics were obtained using the synthetic storm modeling approach described in Vickery et al. (2009b).

2.1 Overview of storm sampling and statistical analysis approach

The occurrence of hurricanes in the FEMA Region III domain is rare — on average, once every seven years — and the occurrence of landfalling hurricanes — which, in general, have potential to produce the greatest storm surges — is rarer still. Those hurricanes that have impacted the region during the past 100 years or so, for which data are available, represent a very small subset of the hurricanes that are possible. Vickery et al. (2000, 2009b) present a method for defining what the possibilities of other hurricanes are in terms of tracks, intensity, size, translation speed, and radial changes in the wind field, based on the historical data record for the larger Atlantic coast region. This method involved stochastic simulation of 100,000 hypothetical hurricanes using a Monte Carlo technique; it replicated the statistics of Atlantic coast hurricanes that have influenced the region in terms of tracks and other hurricane parameters.

The approach that is being adopted in this study for characterizing storm water levels and waves utilizes very high resolution computer modeling to maximize accuracy and spatial granularity of model output. Simulation of 100,000 storms using high resolution modeling is not computationally feasible and would require several years to complete, so the number of storms had to be reduced. The JPM was adopted to reduce the number of storms. The JPM is a simulation methodology that relies on the development of statistical distributions of key hurricane input parameters (including central pressure, radius of maximum winds, translation speed and headings or paths); the definition of discrete values for these parameters to adequately represent their statistical distributions; and the definition of a set of storms that have a unique set of parameter values and that are specified to travel along a discrete idealized path. A reduction in the number of storms must be carefully calculated to preserve the inherent

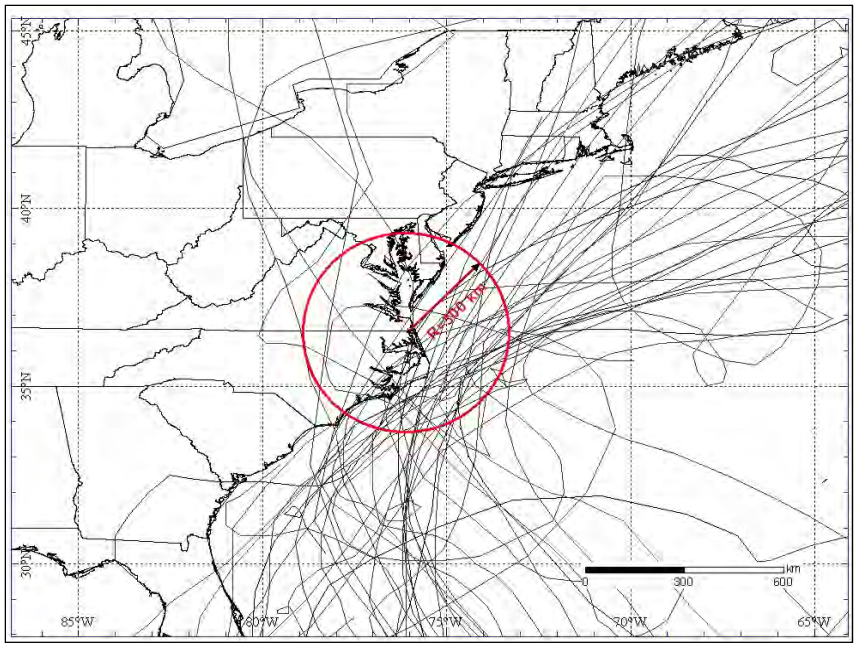

Figure 2-1. Tracks of all hurricanes affecting FEMA Region III for the 1940-2007 period.

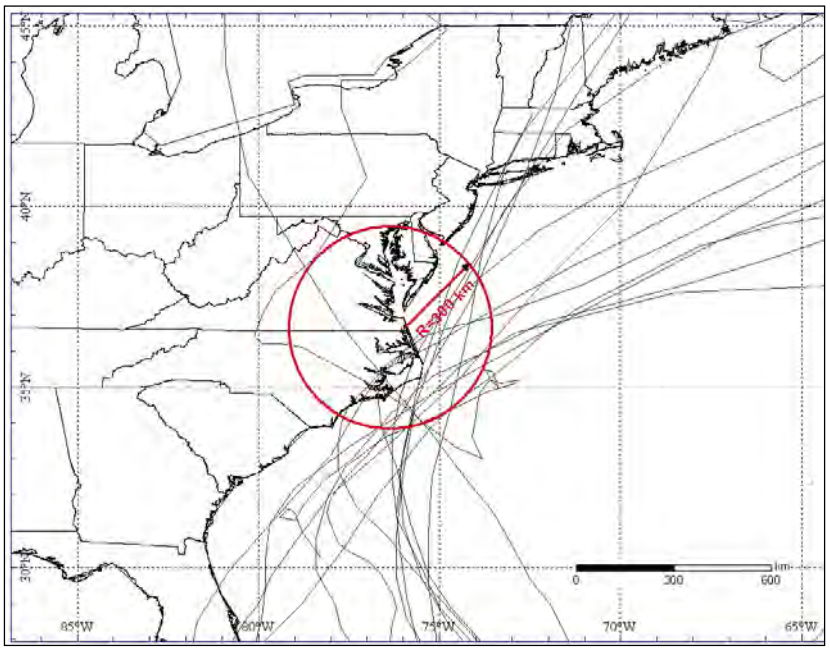

Figure 2-2. Tracks of Category 2 hurricanes affecting FEMA Region III for the 1940-2007 period.

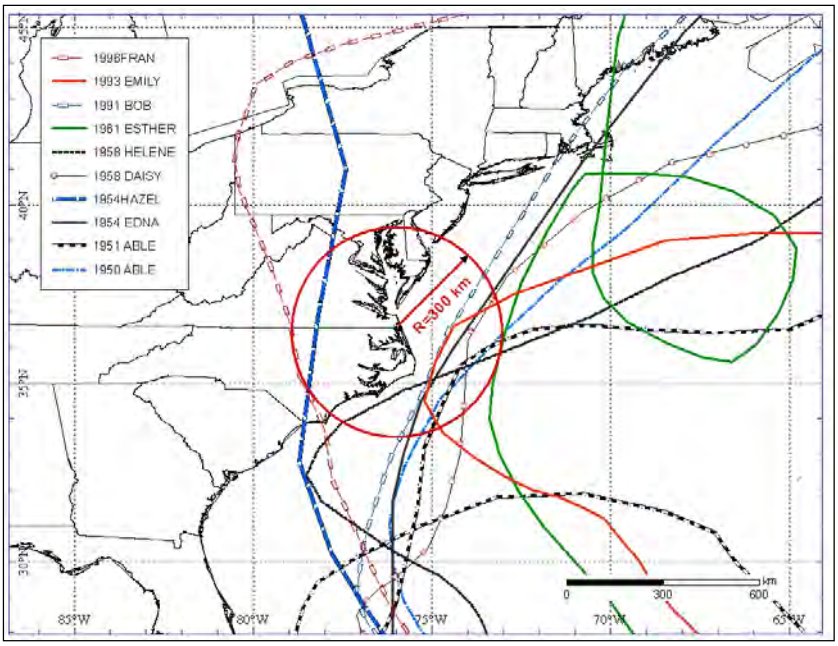

Figure 2-3. Tracks of Category 3 and higher hurricanes affecting FEMA Region III for the 1940-2007 period.

probabilities of hurricane characteristics. The statistics for hurricane parameters and tracks were computed using the method of Vickery et al. (2009b). These statistics were used as the preservation target in the storm reduction process. Another method used to help guide the number reduction process was a coarse grid storm surge model; this model simulated 50,000 of the 100,000 storms. Those results were then used to estimate exceedance probabilities for storm surges throughout the Region III domain. The team eventually reduced the JPM set to 156 storms to preserve the statistics of both the hurricane parameters and their paths, and the storm surge. This storm set reduction process is called an optimal sampling (OS) approach, or JPM-OS.

Through an iterative process, the 50,000 storms were reduced to 17,644; that number was further reduced to a JPM-OS set of 468 storms — each storm with a unique pathway and set of hurricane input parameters. The 468 storms consisted of three classes of storms: one class that made landfall in North Carolina; one class that made landfall along the Virginia/Maryland/Delaware coast; and a third class — bypassing hurricanes — that passed just offshore and near the coast but did not make landfall. The 468-storm set included storms that made landfall either at evenly spaced intervals along the two coastline segments, or — in the case of bypassing hurricanes—at equally spaced points along a shore-perpendicular transect.

An additional reduction in the number of storms (to 156) was made by eliminating variability in the hurricane parameter (the Holland *B* parameter) that controls radial wind speed changes. Eliminating this variability had little effect on storm surge probabilities. This reduction left the storms at unevenly spaced intervals for both landfalling and bypassing hurricanes. Analysis was done to examine the effect of using unevenly spaced storms, compared to evenly spaced storms, and the differences in terms of storm surge probabilities were found to be negligible. The final JPM-OS storm set consisted of 156 unequally spaced storms. The decision to adopt unevenly spaced storms was also done to avoid rerunning storms through the high resolution storm surge and wave models.

The details of the progression to the final JPM-OS set of 156 storms — including the results of analyses performed to inform the storm reduction process — are described in more detail in the following sections.

2.2 Stochastic tracks

The approach for conducting the hurricane simulations for storms affecting the Chesapeake Bay area and coastal Virginia and Delaware makes use of the simulated set of hurricane tracks as given in Vickery et al. (2009b). The simulation methodology is outlined in Figure 2-4. Using this methodology, storms are initiated in the Atlantic Basin at the locations and times observed in the historical record. The storms are moved across the ocean using a Markov-type model, where the position, speed, and heading of each storm at the next time step is determined by sampling from distributions of changes in speed and heading that are primarily functions of the speed and heading of each storm at its respective, current location. Different distributions of changes in storm speed and heading are used in different five degree squares encompassing the Atlantic Basin. The storm intensity, as defined using central pressure, is limited by potential intensity theory (Emanuel 1988).

A simple ocean mixing model (Emanuel et al. 2004) is used to mix cooler waters from beneath the surface of the ocean to limit intensity changes.

Along the coastline of the United States, the model was validated through comparisons of statistical distributions of storm heading, translation speed, distance parameters, central pressure, and frequency. These validations were performed using both landfalling hurricane data as well as the storm data computed at the time a storm is closest to the center of a circle having

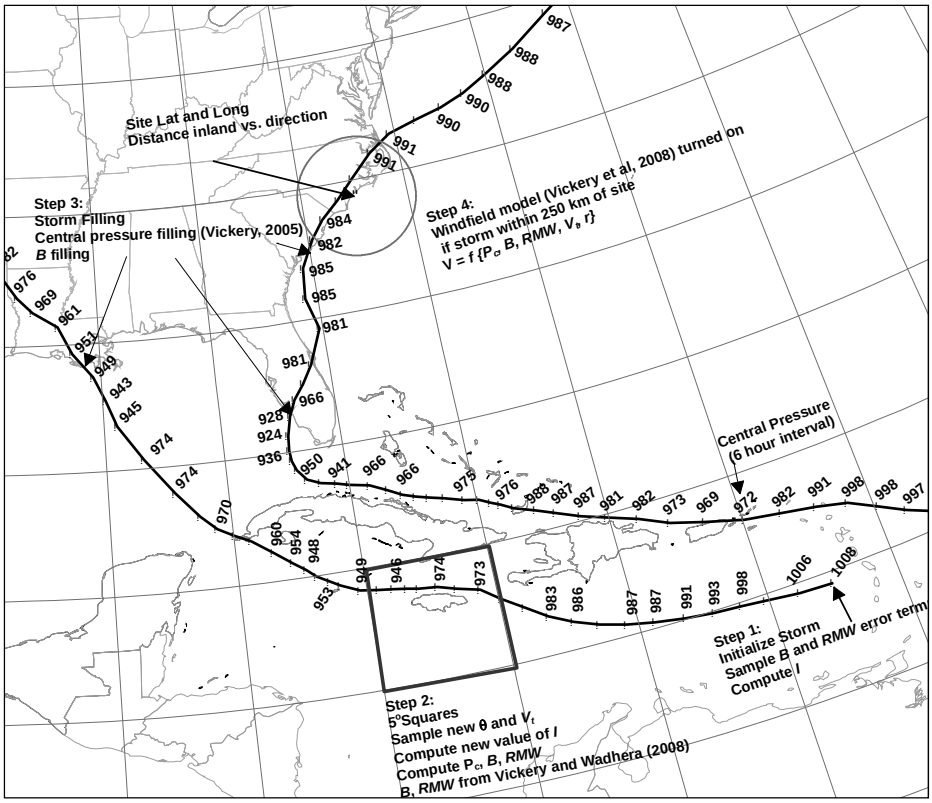

Figure 2-4. Overview of synthetic storm simulation methodology described in Vickery et al. (2009b). In this figure, *I* represents relative intensity as defined in Emanuel (1988), *RMW* is the radius to maximum winds, P_c is the central pressure, *B* is the Holland (1980) pressure profile parameter, Θ is the storm heading, and V_t is the translation speed of the storm.

a radius of 250 km. These sample circles were located at approximately 50 nautical mile increments along the entire coastline of the United States. This synthetic storm model was shown to reproduce the statistics of hurricanes affecting the U.S. coastline from 1900 through 2008, and is capable of simulating hundreds of thousands of years of storms whose statistical characteristics match those of the historic record.

These simulated hurricanes, whose statistical properties are consistent with those affecting the region, were used instead of the extremely limited data associated with historical hurricanes affecting the study area. Figure 2-5 shows milepost locations (MP 150 to MP 3100) and 26 sections of the U.S. coastline. This study was influenced by the statistics of hurricanes affecting MPs 2100 through 2400 and coastline segments 21, 22, 23, and 24. Figure 2-6 shows the areas covered by the 250 km radius circles centered on the mileposts in the region.

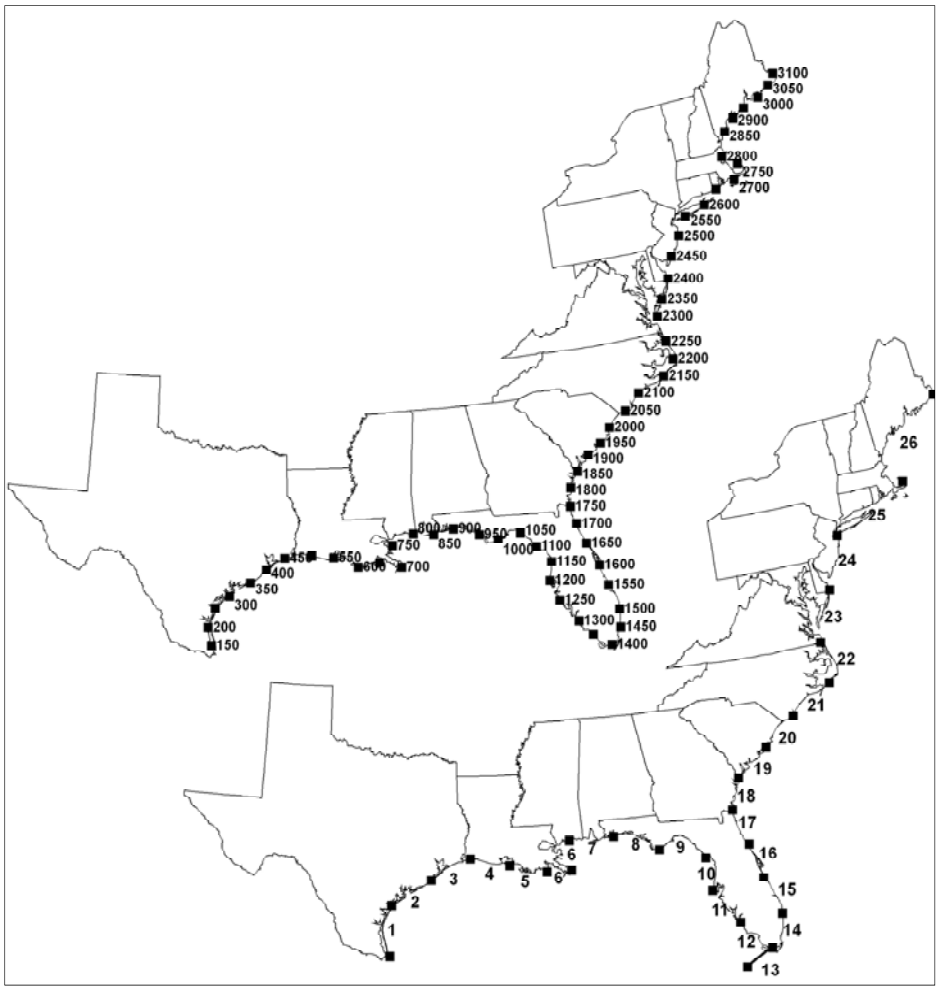

Figure 2-5. Milepost and coastal segments. Each coastal segment (lower map) is about 200 km in length and contains between one and two milepost markers, depending on the exact location of the segment.

Figure 2-7 presents a comparison of modeled (Vickery et al. 2009b) and observed central pressures from hurricanes making landfall along each of the 26 coastal segments shown in Figure 2-5.

As indicated in Figure 2-7, only four hurricanes (with central pressures less than 990 mbar) have made landfall along coastline Segment 22, and no hurricanes made landfall along coastline Segment 23. The hurricane simulation model, which has been run for a period of 100,000 years, generates synthetic hurricanes that make landfall along these coastal segments. The relatively large number of simulated years (100,000) was originally required to enable estimates of long return period (~2000 years or longer) wind speeds.

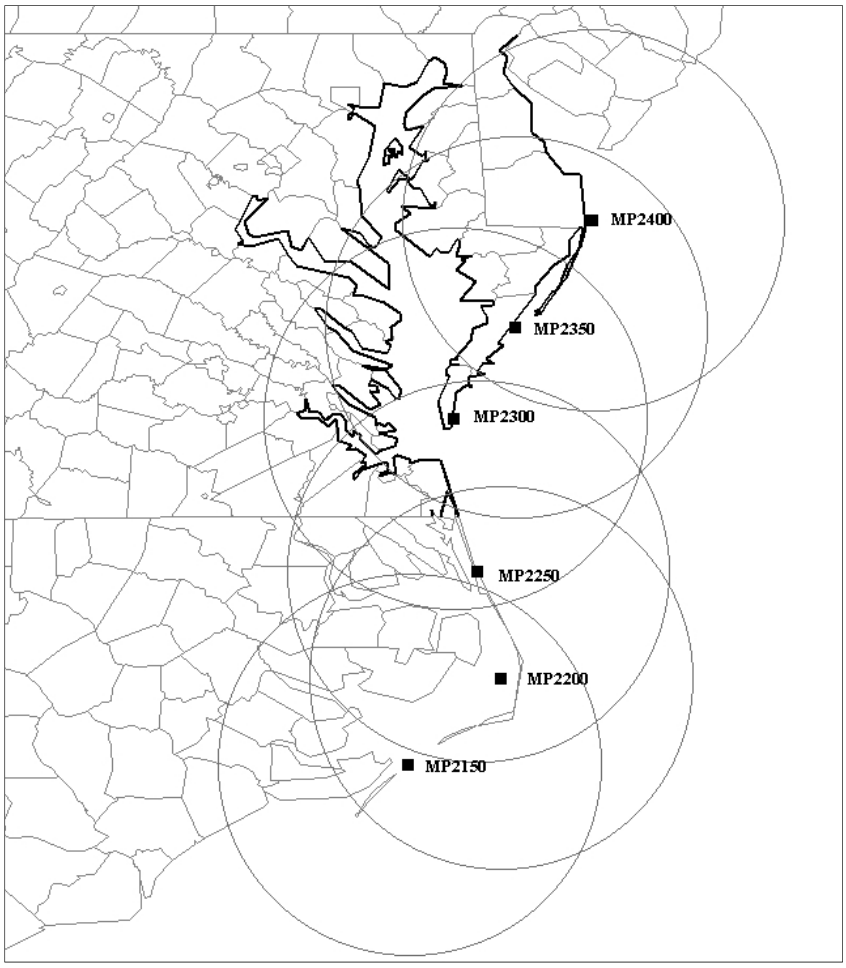

Figure 2-6. Close-up of areas encompassed by the 250 km radius sub-regions used to characterize storms affecting the study region. Darker coastline defines the FEMA Region III coastline.

Figure 2-8 presents a comparison of modeled and observed pressures at the time the storms are closest to the indicated milepost. The comparisons also show good agreement between the modeled and historical central pressure differences. Unlike the comparisons shown in Figure 2-7, which include landfalling hurricanes only, the model and historical data shown in Figure 2-8 includes all tropical cyclones. Hence, the model provides a much larger data set of historic storms to use for comparisons of modeled and historical pressure data. Tests for equivalence of means and variance of the synthetic and historical pressures shown in Figure 2-8 indicate that there is no statistically significant difference (evaluated at the 95th percent confidence interval) between the two data sets. The two distributions at all mileposts pass the Kolmogorov-Smirnov test for equivalence at the 95th percent confidence level.

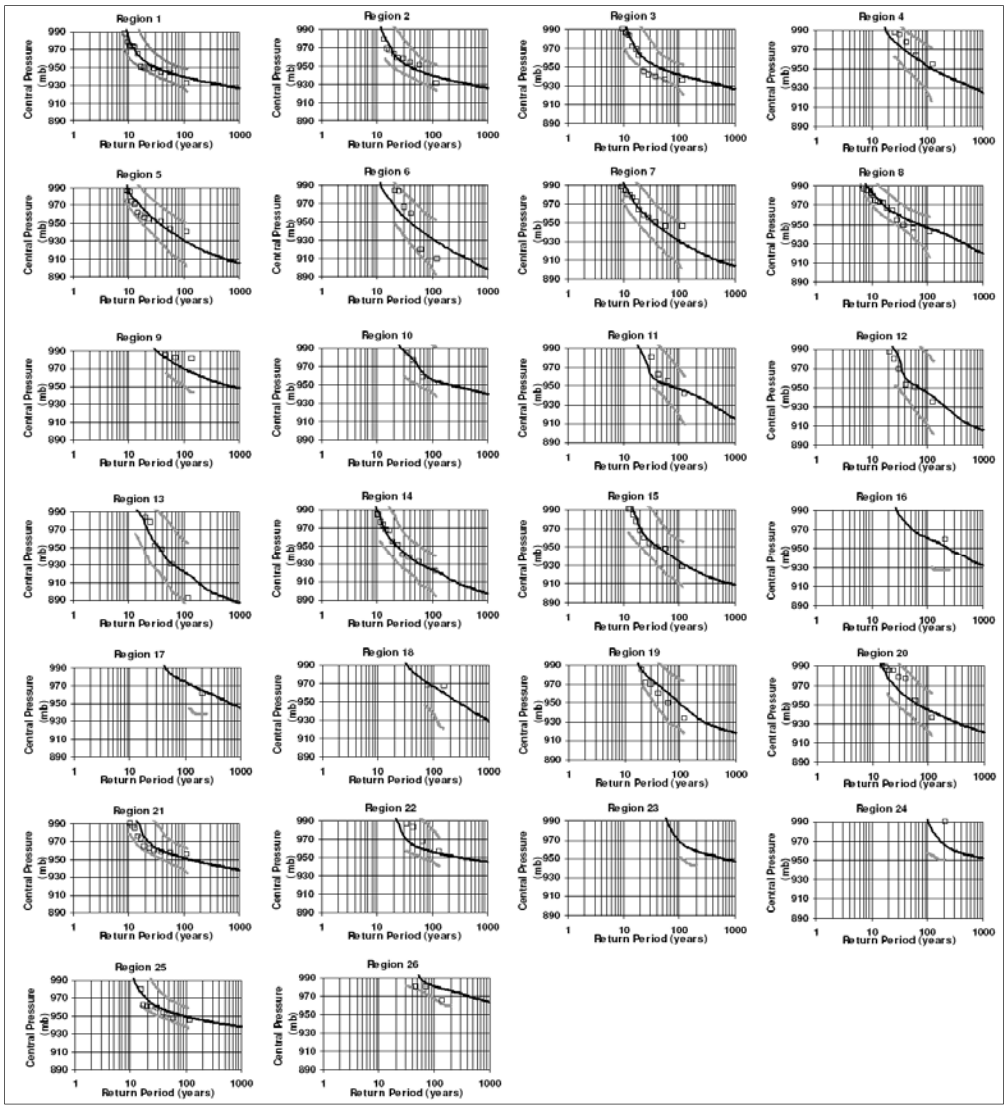

Figure 2-7. Comparison of modeled and observed (1900-2006) central pressures at landfall vs. return period along ~200km coastal segments. Gray lines show 90 % confidence range derived from the modeled empirical distribution. If the upper gray line is not shown, the five percent (lower bound) simulated pressures are less than 990 hPa.

Figures 2-9 and 2-10 present comparisons of the statistics (translation speed and heading) of all simulated and observed tropical cyclones passing within 250 km of Mileposts 2250 and 2300 near the North Carolina and Virginia border. As indicated in Figures 2-7 through 2-9, the statistical distributions of the key tropical cyclone parameters derived from the 100,000 year simulation are seen to be statistically equivalent to those of the short 106 year historical record, but because the synthetic storm set was developed using a 100,000 year simulation, there is a relatively large number of landfalling and close by-passing hurricanes that can be used to define the statistical distributions of the key hurricane parameters for use in the JPM models.

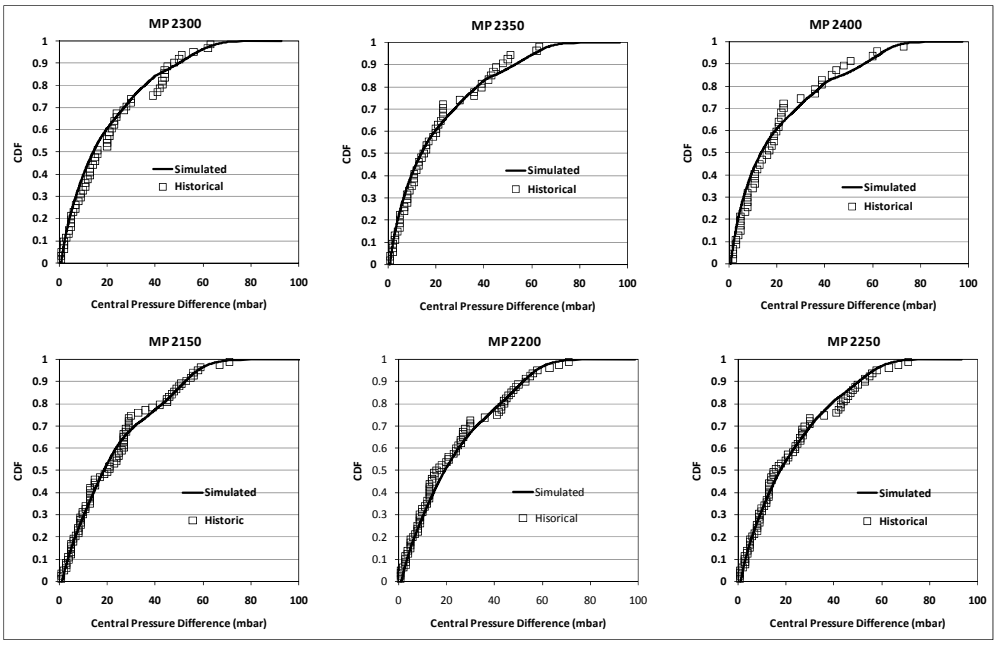

Figure 2-8. Cumulative distributions of central pressures from simulated and historical tropical cyclones passing within 250 km of the indicated milepost. Central pressure represents the value at the time a storm is closest to the indicated milepost.

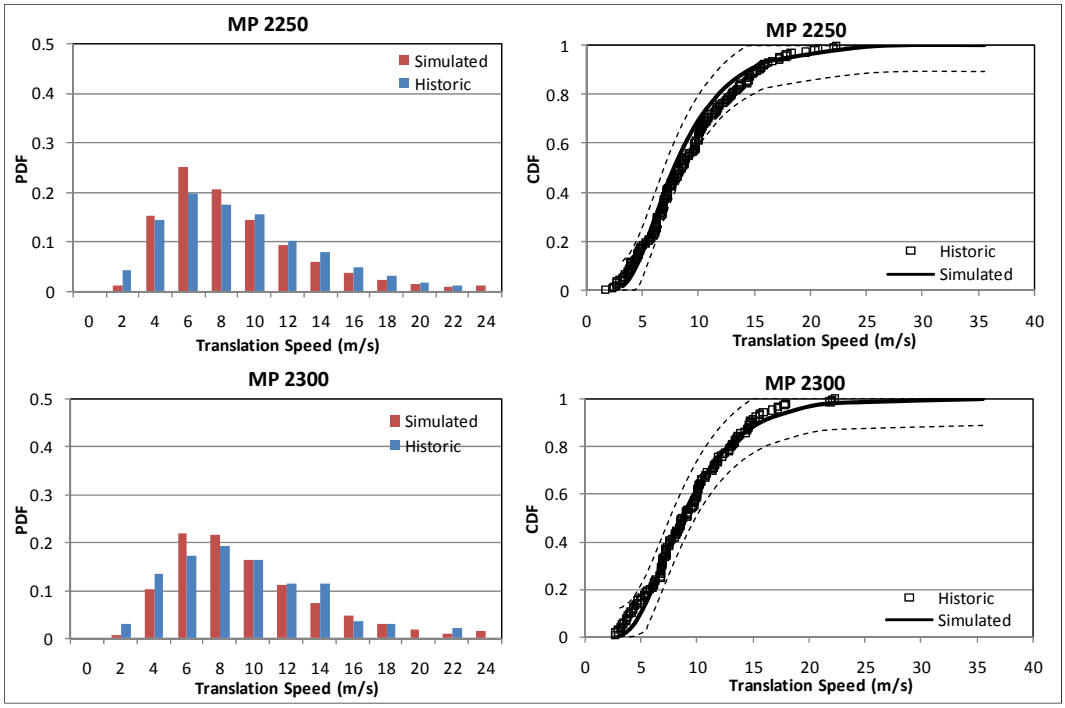

Figure 2-9. Comparisons of translation speeds from simulated and historical tropical cyclones passing within 250 km of the indicated milepost. Dashed lines show the bounds associated with the Kolmogorov-Smirnov test.

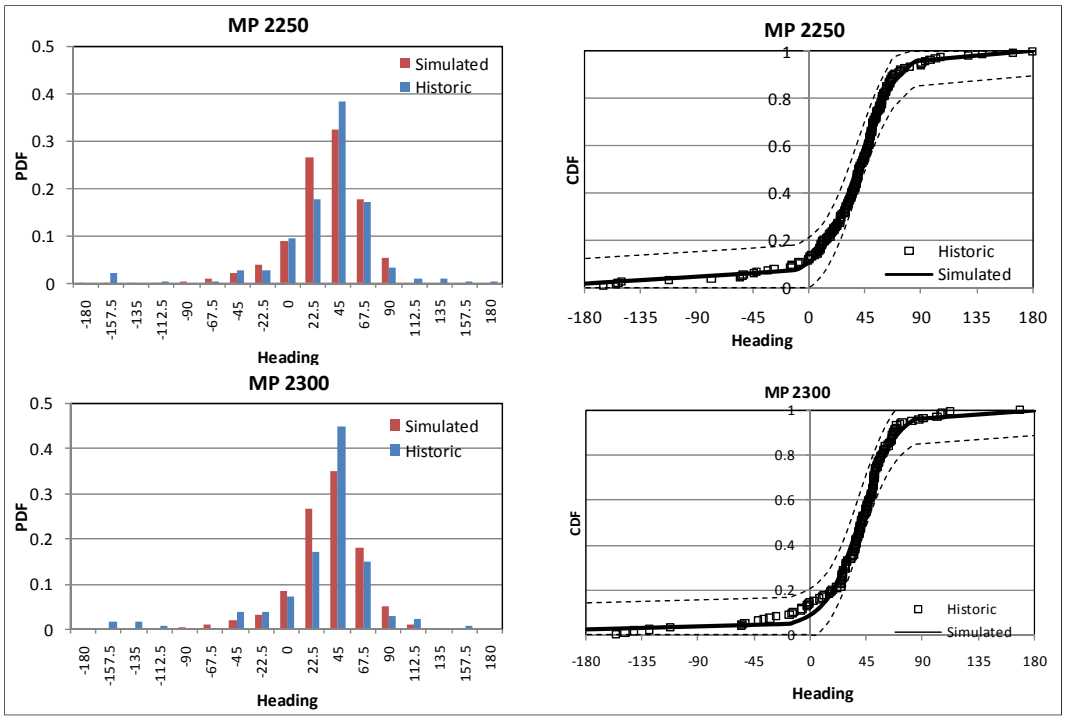

Figure 2-10. Comparisons of storm heading from simulated and historical tropical cyclones passing within 250 km of the indicated milepost. Dashed lines show the bounds associated with the Kolmogorov-Smirnov test. Heading is defined as the direction of storm motion measured clockwise from North. Storms with a positive heading have an eastward component.

In this study, the simulated storms are used to define the statistical distributions and frequencies of hurricanes affecting the Chesapeake Bay and coastal Virginia and Delaware regions. Using the synthetic storm model, 100,000 years of storm tracks were generated and provided to the Renaissance Computing Institute (RENCI) to be used in conjunction with a coarse grid in the Advanced CIRCulation storm surge model (ADCIRC). The storm track data was also used in a simple Holland (1980) windfield model to generate hurricane-induced water elevations in the study region.

2.3 Coarse grid results

A coarse ADCIRC grid was used to provide a baseline from which to compare JPM subset simulations. The coarse grid was derived from the standard ADCIRC east coast 2001 grid by extracting the nodes and elements in the Region III and adjacent areas. There are 8178 nodes and 15450 elements, with a minimum depth of 0.5 m. The grid extends northward to the Delaware/New Jersey coast, southward to Cape Hatteras, and offshore past the continental shelf break, and includes only open water.

The original storm set provided to RENCI for use with the coarse ADCIRC grid contained over 57,000 storms; 17,644 produced a storm surge of at least one meter somewhere in the region "P" shown in Figure 2-11. Figure 2-12 presents the storm surge elevation as a function of the return period at each of the five points shown in Figure 2-11, as well as the maximum storm surge within the region "P," computed from the full storm set (~57,000 storms) in the upper plot and the reduced storm set (17,644 storms) in the lower plot. The full storm set includes all simulated tropical cyclones that pass within 250 km of any of the mileposts shown in Figure 2-6. A comparison of the storm surge hazard curves resulting from the full and reduced storm sets indicates that the elimination of nearly 40,000 weaker or distant storms has virtually no effect on the storm surge elevations for return periods of 10 years and longer.

The storms affecting the region were divided into three classes: namely, storms making landfall along the North Carolina coast, storms making landfall along the Virginia/Delaware coast, and by-passing storms. The line segments associated with these three classes of storms are shown in Figure 2-13.

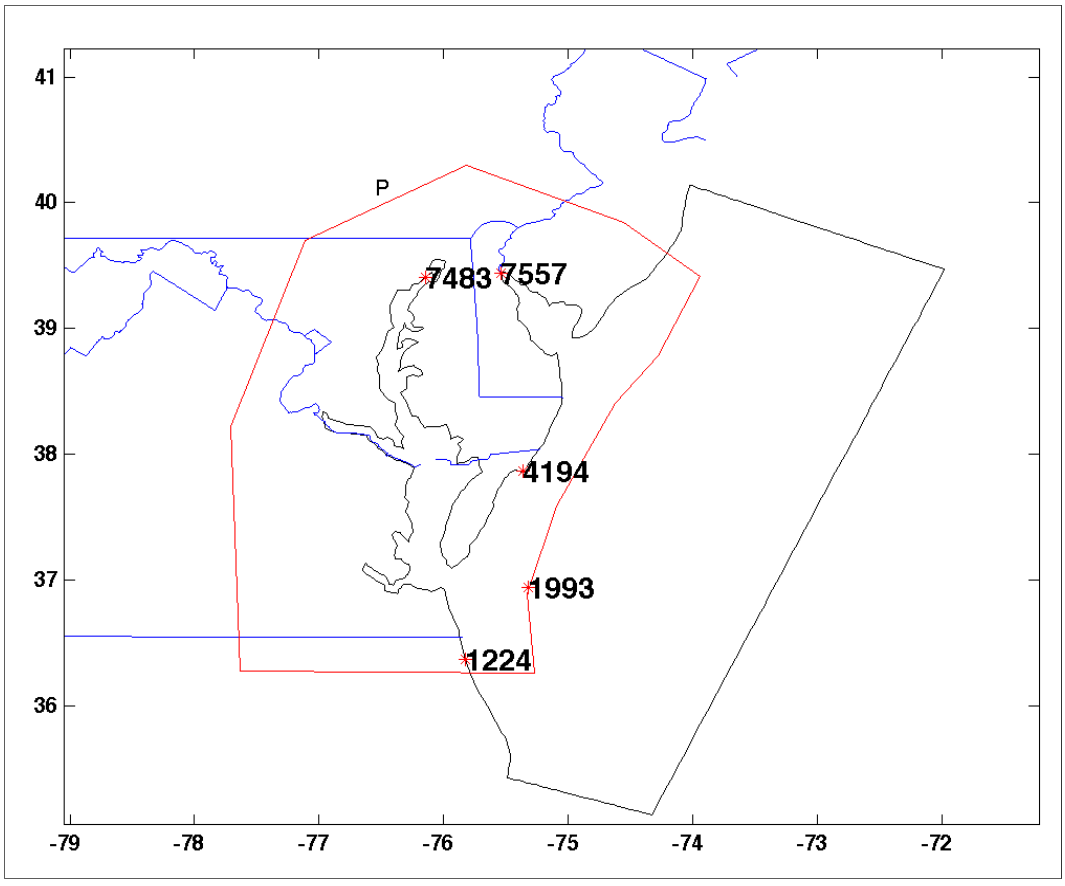

Figure 2-11. Region used for the coarse grid ADCIRC run.

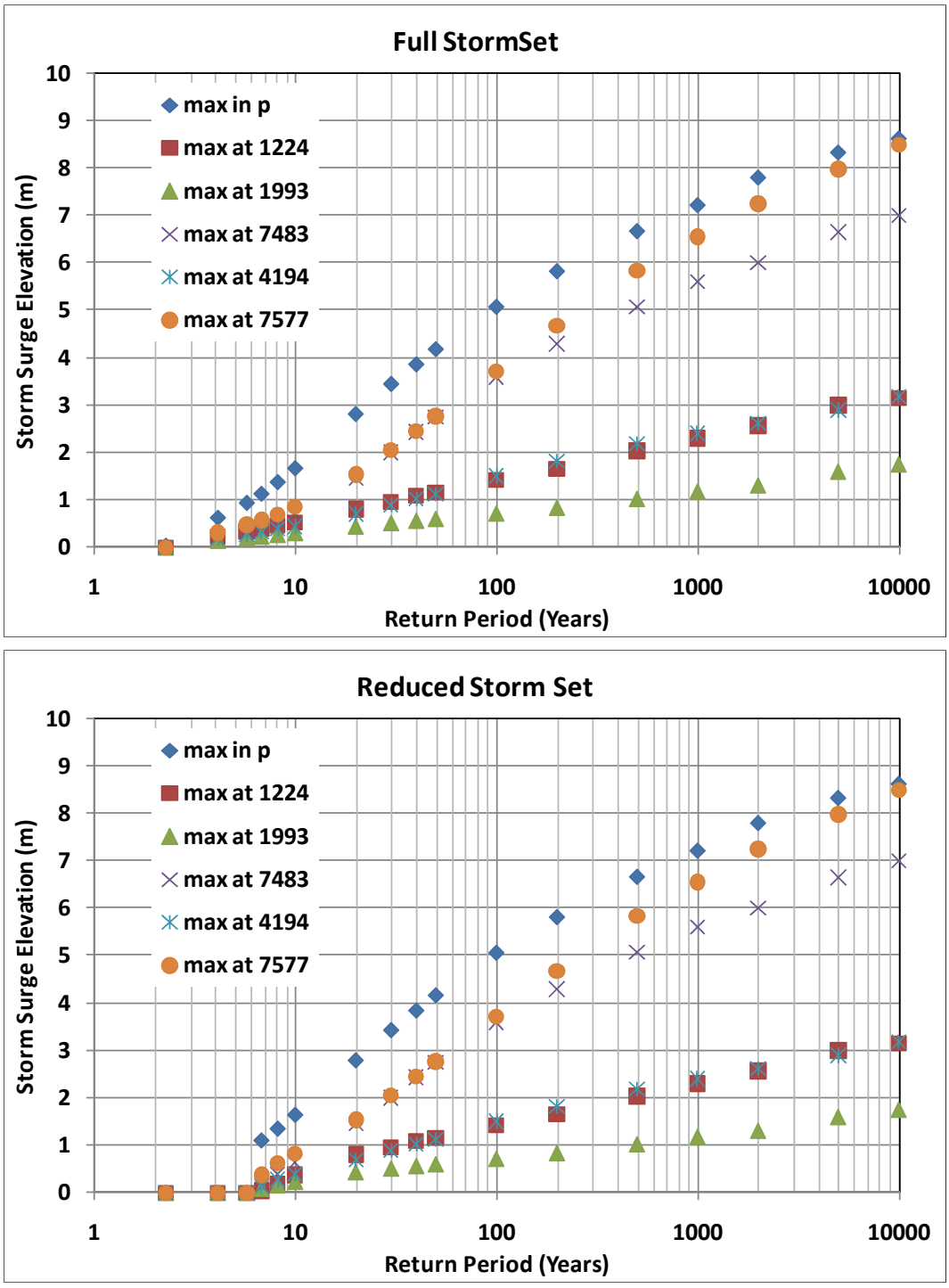

Figure 2-12. Storm surge elevation vs. return period from the coarse grid ADCIRC run.

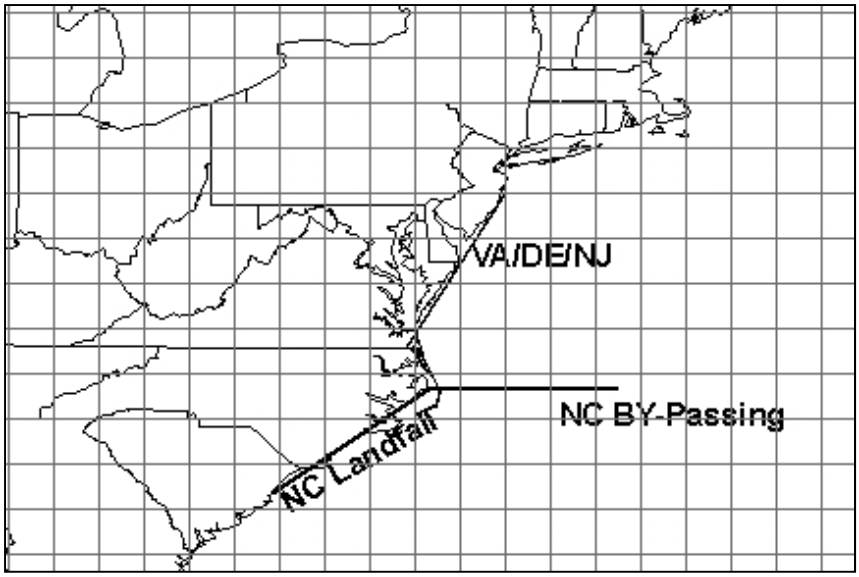

Figure 2-13. Coastal segments used to define hurricane tracks for the Region III Flood Study.

2.4 JPM track selection

Hurricane track parameters (central pressure, translation speed, and heading) and their weights were developed for the three line segments used to define the hurricane risk for the study. Along each of the two coastal segments, the statistical distributions of heading and central pressure are approximated using three discrete values. The distribution for translation speed is characterized using two discrete values. In the first sets of simulations performed during the 2010 timeframe, the distributions of the radius to maximum winds and the Holland *B* parameter were defined using the mean value and the mean $\pm 1.22\sigma_B$, where σ_B is the error term from the regression equations relating *B* to *RMW* and latitude is as described in Vickery and Wadhera (2008). Using the mean $\pm 1.22\sigma_B$ yields a set of *B* values that matches the mean and the variance of the error term from the regression model.

The Holland *B* parameter is modeled using Equation 24 in Vickery and Wadhera (2008) and the radius to maximum winds is modeled using Equation 11 in Vickery and Wadhera (2008). Figure 2-14 presents the mean and $\pm 1.22\sigma$ bounds for the Holland *B* model plotted vs. storm radius to maximum winds. Also provided in Figure 2-14 are the historical values of *B* obtained from hurricane model hindcasts, as described in Vickery and Wadhera (2008).

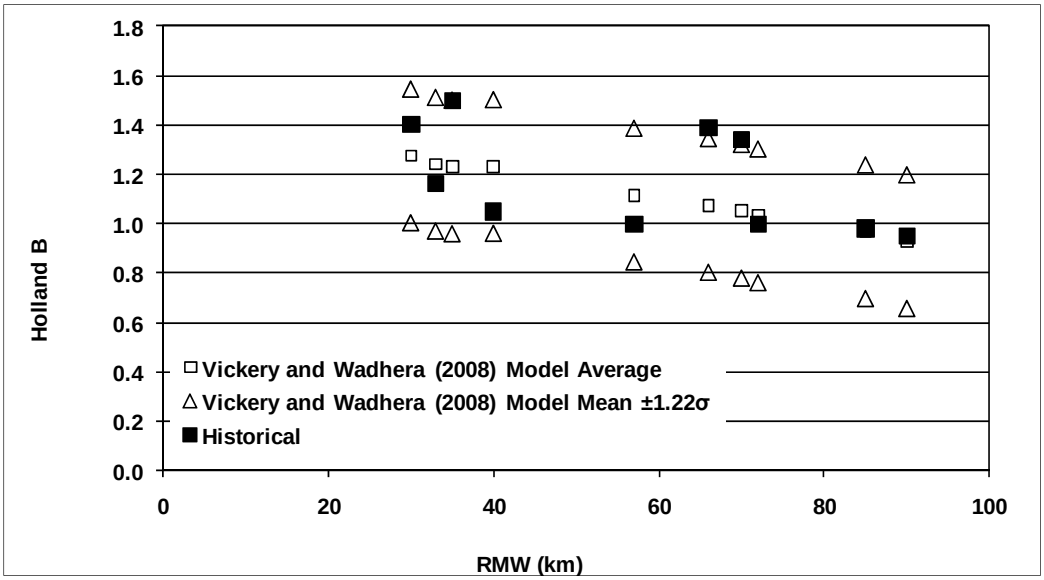

Figure 2-14. Modeled and observed values of the Holland *B* parameter plotted vs. radius to maximum winds. Historical data from recent Atlantic coast landfalling and by-passing hurricanes (excludes Florida).

These *B* values were used in the hurricane wind field model described in Vickery et al. (2009a), which is the same model used in the FEMA Region III production runs, as indicated in the FEMA Region III report entitled *Coastal Storm Surge Analysis: Computational System, Report 2: Intermediate Submission 1.2*, February 2011. As indicated in Figure 2-14, both the model and the data indicate that *B* decreases with increasing radius. It is also noteworthy that the limits defined by $\pm 1.22\sigma_B$ match the limits of the limited historical data.

Figure 2-15 presents the mean and ±1.22σ bounds for the *RMW* model plotted vs. central pressure. Also provided in Figure 2-15 are the historical values of *RMW* obtained from hurricane model hindcasts, as described in Vickery and Wadhera (2008). Both the model and the data indicate that *RMW* decreases with decreasing central pressure. *RMW* also increases with increasing latitude. As in the case of *B*, it was noted that the limits defined by $\pm 1.22\sigma$ match the limits of the limited historical data.

This combination of storm parameters (three radii and three *B* models) results in a total of nine simulated hurricanes for each pressure-heading-translation speed combination. In all cases, the weights were first chosen so that the means and standard deviations of the weighted discrete distributions matched those of the full continuous distributions derived from the stochastic simulation model. An acceptable set of 468 synthetic storms was developed using this approach.

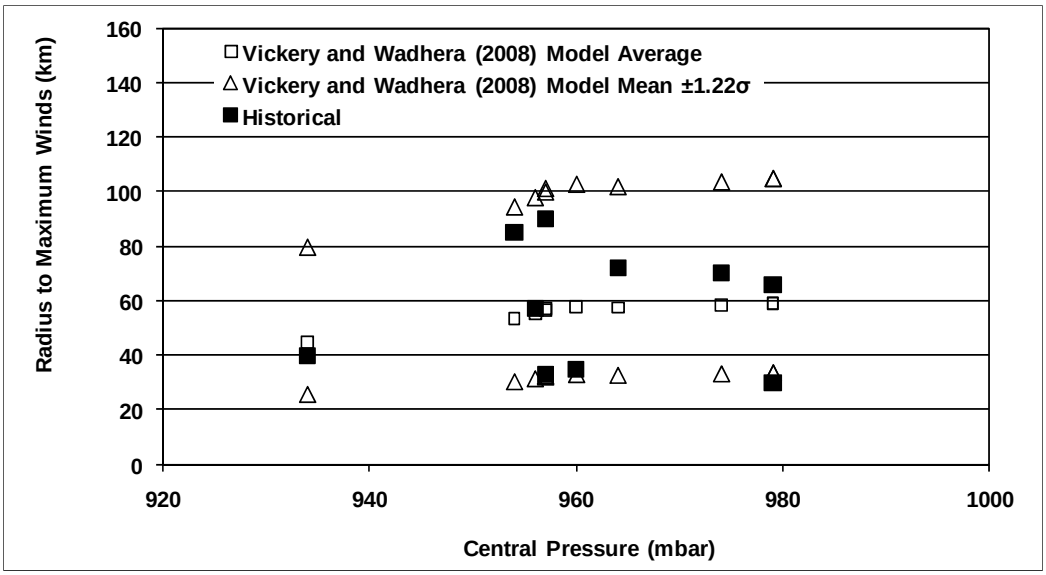

Figure 2-15. Modeled and observed values of radius to maximum plotted vs. central pressures. Historical data from recent Atlantic coast landfalling and by-passing hurricanes (excludes Florida).

Near the end of the track development stage, a sensitivity study was performed where 2/3 of tracks were eliminated (those corresponding to $\pm 1.22\sigma_B$) — leaving only the mean regression model for B — relating B to RMW and latitude. The resulting storm surge estimates associated with a return period of 100 years differed little from those developed using the full set, and a decision was made to proceed with this reduced set of synthetic hurricane tracks. This reduced set of 156 storms contains 1/3 the number of the full 468 storm JPM set.

As will be discussed in Section 2.5, the storm surge estimates resulting from the reduced storm set used in the JPM modeling (156 individual hurricanes) are verified through comparisons to storm surge results derived from 17,644 simulated storms (this number was a subset of the full Monte Carlo simulation storm set).

Figures 2-16 and 2-17 present plots of the maximum storm surges produced using the coarse ADCIRC model runs plotted as a function of each of the three primary variables (heading, translation speed, and central pressure difference), for each of the two coastal landfalling segments. Also shown in Figures 2-16 and 2-17 are the discrete and cumulative distribution functions describing storm heading, central pressure difference, and translation speed. The JPM representation of the Virginia/Delaware/New Jersey

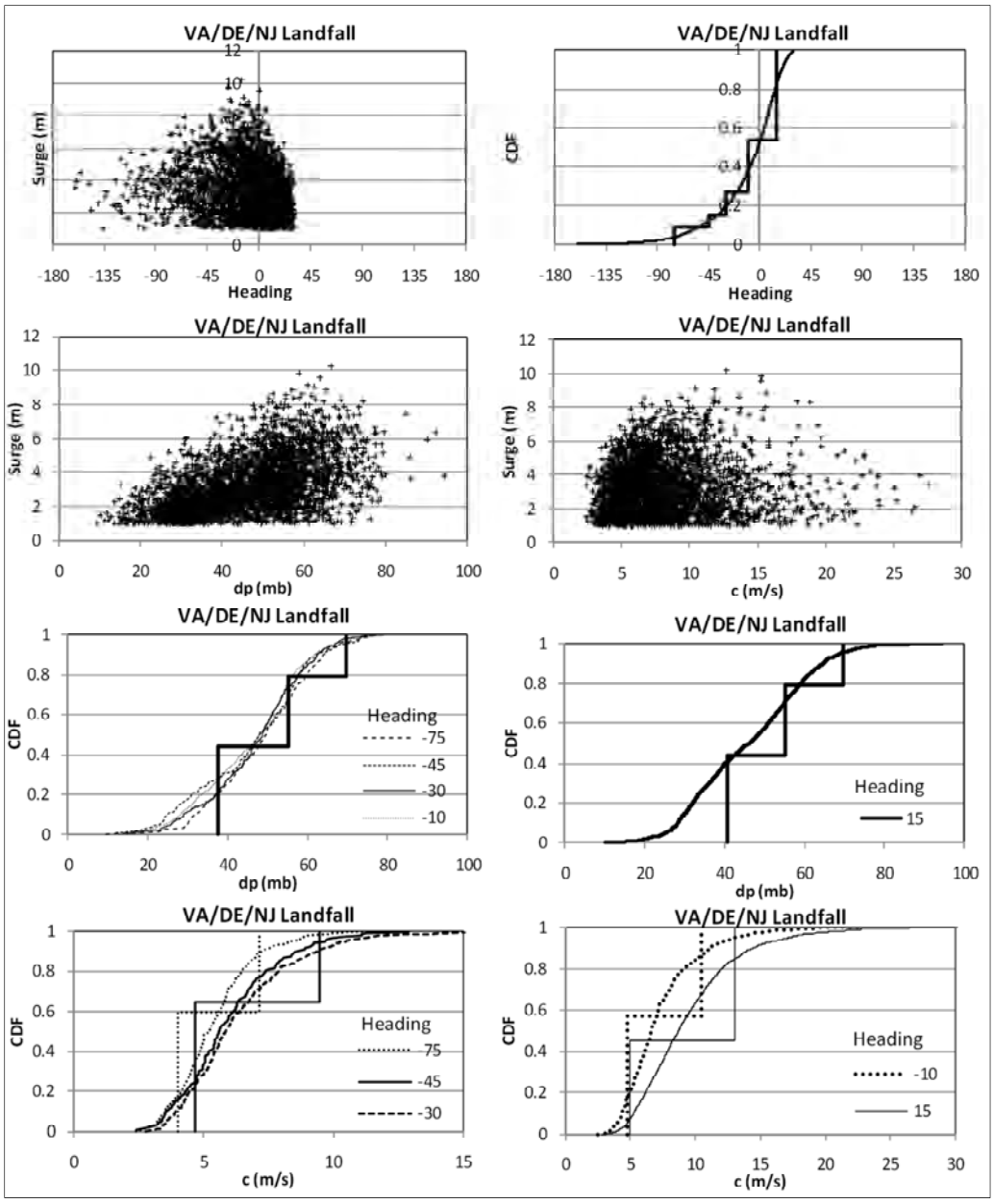

Figure 2-16. Plots of storm surge vs. hurricane parameters and comparisons of continuous and discrete distributions of storm heading, central pressure difference (*dP*), and translation speed (*c*) for Virginia, Delaware and New Jersey landfalling hurricanes. Heading is defined as the direction of motion of the storm measured clockwise from North. Storms with a positive heading have an eastward component. A total of four JPM representations of the translation speed are used to model the translation speed for the five different headings. The same translation speed distribution is used for headings -45 and -30 deg.

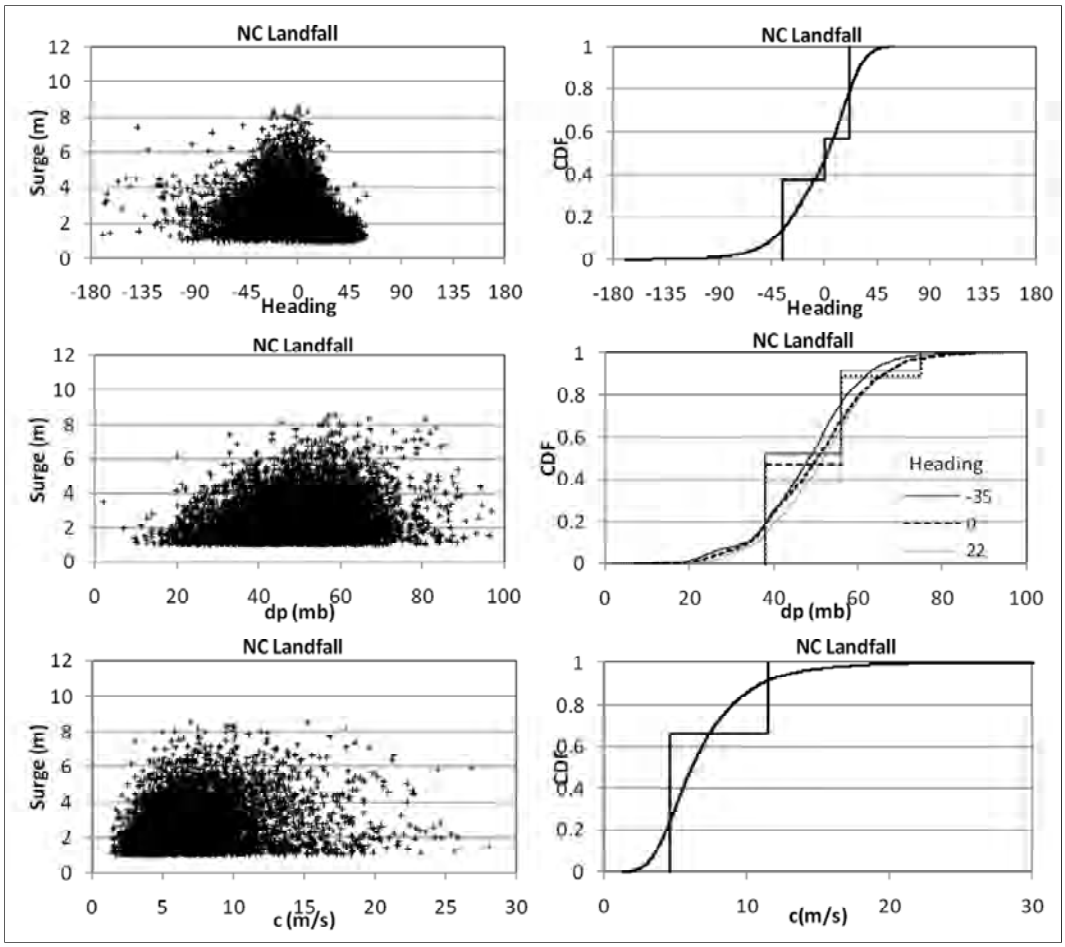

Figure 2-17. Plots of storm surge vs. hurricane parameters and comparisons of continuous and discrete distributions of storm heading, central pressure difference and translation speed for North Carolina landfalling hurricanes. Heading is defined as the direction of motion of the storm measured clockwise from North. Storms with a positive heading have an eastward component. A total of three JPM representations of the translation speed are used to model the translation speed for the three different headings.

landfalling storms is seen to have a distinct bias towards more intense (greater central pressure differences or lower central pressures) landfalling storms than the results of the stochastic set. This distinct bias is intentional and was required to correct for a negative bias in the resulting JPM storm surge estimates (based on the full storm set runs described in Chapter 2.2). In the North Carolina case, no central pressure adjustment was required. Figure 2-17 shows that the JPM tracks reproduce a weak correlation between heading and central pressure that was not evident along other coastal segments. Heading is defined as the direction of storm motion measured clockwise from North, and storms with an eastward component in their motion have positive heading values.

Figure 2-16 (the Virginia/Delaware/New Jersey landfalling storms) demonstrates that there is a different translation speed probability distribution used for each heading (the translation speed distributions for headings -30 and -45 deg are the same), resulting in a set of tracks that maintains the heading-translation speed correlation evident in the stochastic modeling and in the historical record. The r^2 associated with a linear model describing the relationship between heading and translation speed is 0.16; consequently, the team decided that this correlation should be retained in the JPM representation of the hurricanes. In the case of the North Carolina landfalling hurricanes, the corresponding r^2 is only 0.06, and any relationship between heading and translation speed was ignored.

To reproduce both the mean and the variance of the translation speed for the Virginia/Delaware/New Jersey storms using only two discrete values, the separation between the lowest and highest translation speed was found to be relatively large for the eastward heading storms. This large separation is required, as both the mean and the variance of the translation speeds for these eastward heading (re-curving) storms are higher than those for storms having a more westward heading.

In the case of bypassing hurricanes, the distributions of the hurricane's parameters are characterized using only one heading, two values of central pressure, and one translation speed.

Figure 2-18 presents plots of the maximum storm surges produced using the simple ADCIRC model runs performed earlier plotted as a function of each of the three primary variables (heading, translation speed, and central pressure), for the by-passing segment. This figure also shows the discrete and continuous cumulative distribution functions describing storm heading, central pressure difference, and translation speed.

Figure 2-19 shows the cumulative distribution functions (CDFs) of the landfall location (or coast crossing position) of the hurricane tracks along each of the three coastal segments. Three different storm position models are used to describe the track landfall location along the North Carolina and Virginia coastal segments, but only one model is used to define the positioning of the bypassing hurricanes. The track spacing in all cases is obtained using equally spaced positions along the ordinate in Figure 2-19, which yields non-equally spaced positions along the coastal line segment. If the underlying distributions of the track coast crossings were uniform, this equal spacing along the ordinate approach would lead to uniform spacing along the length of the coastal segments.

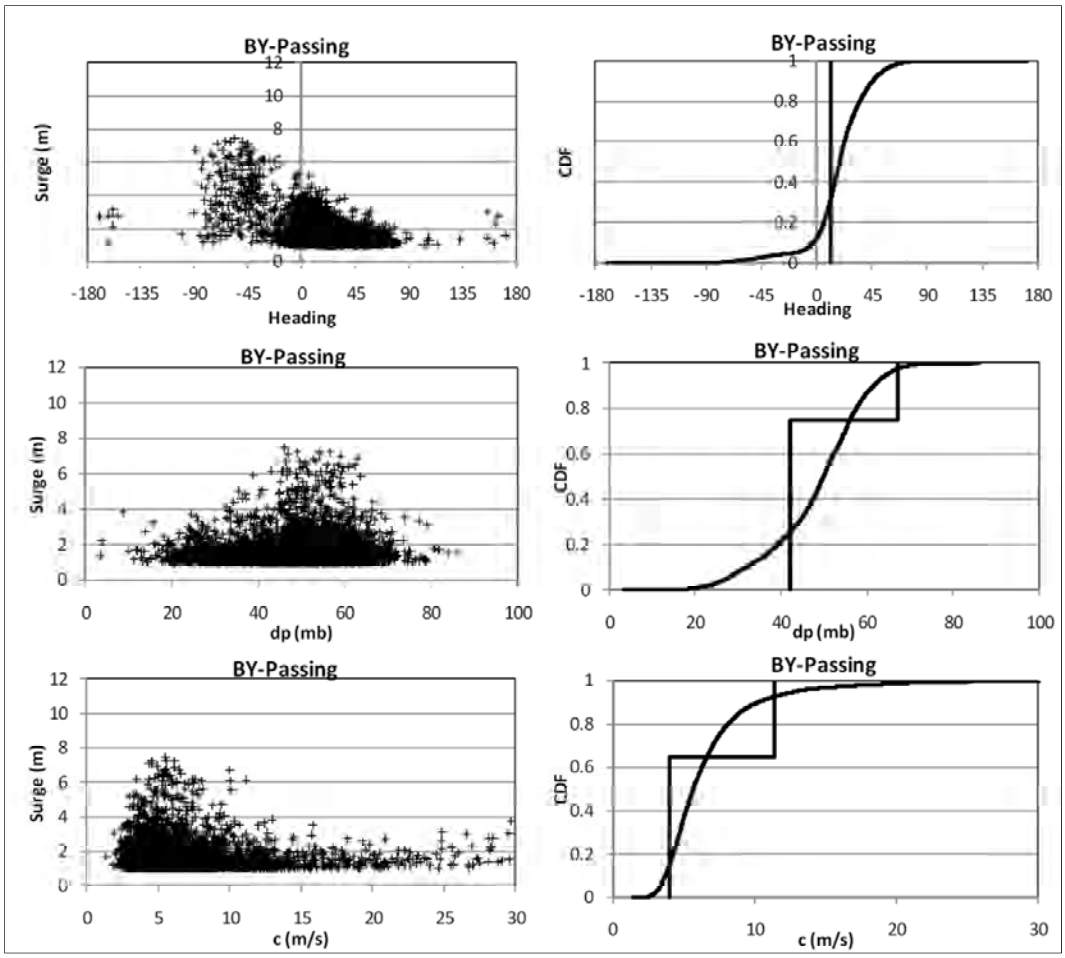

Figure 2-18. Plots of storm surge vs. hurricane parameters and comparisons of continuous and discrete distributions of storm heading, central pressure difference and translation speed for by-passing hurricanes. Heading is defined as the direction of motion of the storm measured clockwise from North. Storms with a positive heading have an eastward component.

The numeric values of the modeled storm parameters and their statistical weights are given in Tables 2-1 and 2-2 for the landfalling coastal segments. The parameter values and weights for the by-passing hurricanes are given in Table 2-3.

The along track variation of central pressure in the JPM hurricanes was treated using the pre-landfall central pressure difference variation model developed during the North Carolina flood study. Once a hurricane makes landfall, the central pressure difference decreases as the hurricane moves inland. The post-landfall filling (increase in central pressure and RMW and a decrease in B) was modeled with the filling models given in Vickery (2005). In the implementation of the filling model for this study, the random error term in the Vickery (2005) model was included rather than simply using the mean filling rate model.

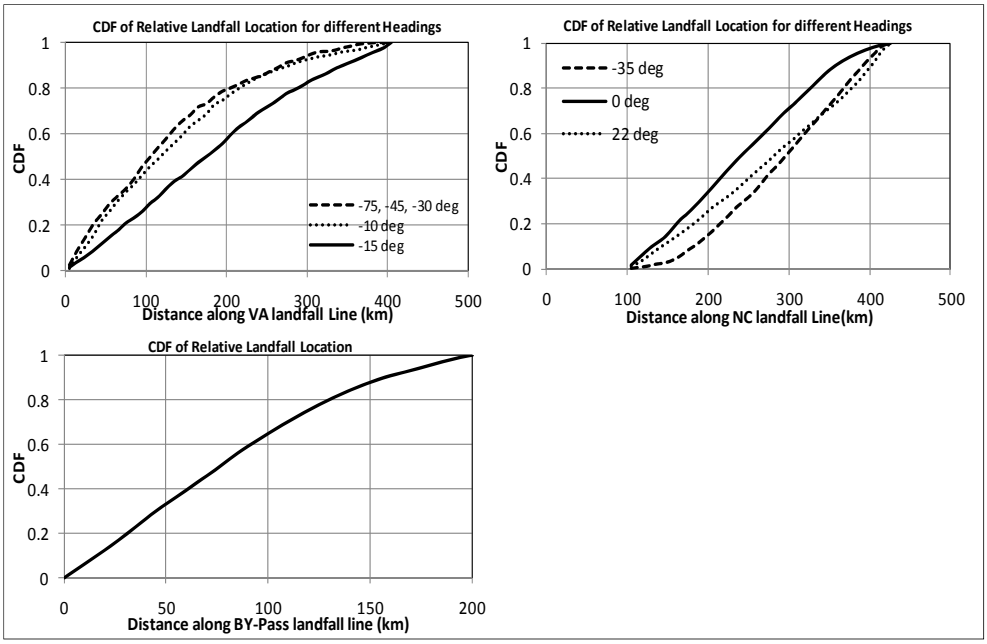

Figure 2-19. Cumulative distribution functions of tracks landfalling along the three coastal segments. The zero position is the leftmost portion of each line segment shown in Figure 2-13.

Table 2-1. Hurricane parameter values and weights for Virginia, Delaware, and New Jersey landfalling hurricanes.

Heading Degrees CW from North	Weight	Central Pressure Difference (mbar)	Weight	Trans Speed (m/sec)	Weight
-75	0.09	34, 51, 65	0.44, 0.35, 0.21	4.0, 7.2	0.60, 0.40
-45	0.06	34, 51, 65	0.44, 0.35, 0.21	4.7, 9.5	0.65, 0.35
-30	0.12	34, 51, 65	0.44, 0.35, 0.21	4.7, 9.5	0.65, 0.35
-10	0.27	34, 51, 65	0.44, 0.35, 0.21	4.8, 10.5	0.57, 0.43
-15	0.47	34, 51, 65	0.44, 0.35, 0.21	5.0, 13.0	0.45, 0.55

Table 2-2. Hurricane parameter values and weights for North Carolina landfalling hurricanes.

Heading Degrees CW from North	Weight	Central Pressure Difference (mbar)	Weight	Trans Speed (m/sec)	Weight
-35	0.37	38, 56, 75	0.52, 0.40, 0.08	4.6, 11.5	0.66, 0.34
0	0.20	38, 56, 75	0.47, 0.42, 0.11	4.6, 11.5	0.66, 0.34
22	0.43	38, 56, 75	0.38, 0.50, 0.12	4.6, 11.5	0.66, 0.34

Table 2-3. Hurricane parameter values and weights for by-passing hurricanes.

Heading Degrees CW from North	Weight	Central Pressure Difference (mbar)	Weight	Trans Speed (m/sec)	Weight
12	1	42,67	0.75,0.25	4.0,11.4	0.65,0.35

Figures 2-20 and 2-21 present comparisons of probability distributions of heading, central pressure, etc., at the time of landfall along the North Carolina and Virginia/Delaware/New Jersey coastal segments. This information is the result of both the stochastic and the JPM models. The comparisons show that the limited numbers of JPM storms combined with the weights reproduce the CDFs from the stochastic simulation reasonably well, with the exception that the full variance of *B* is not reproduced, since *B* is modeled using the mean regression model only. Comparisons resulting from the 468 storm set are provided in Appendix C, where the full distribution of *B* is well reproduced, with the addition of the other 316 storms required when modeling the mean $\pm 1.22\sigma_B$.

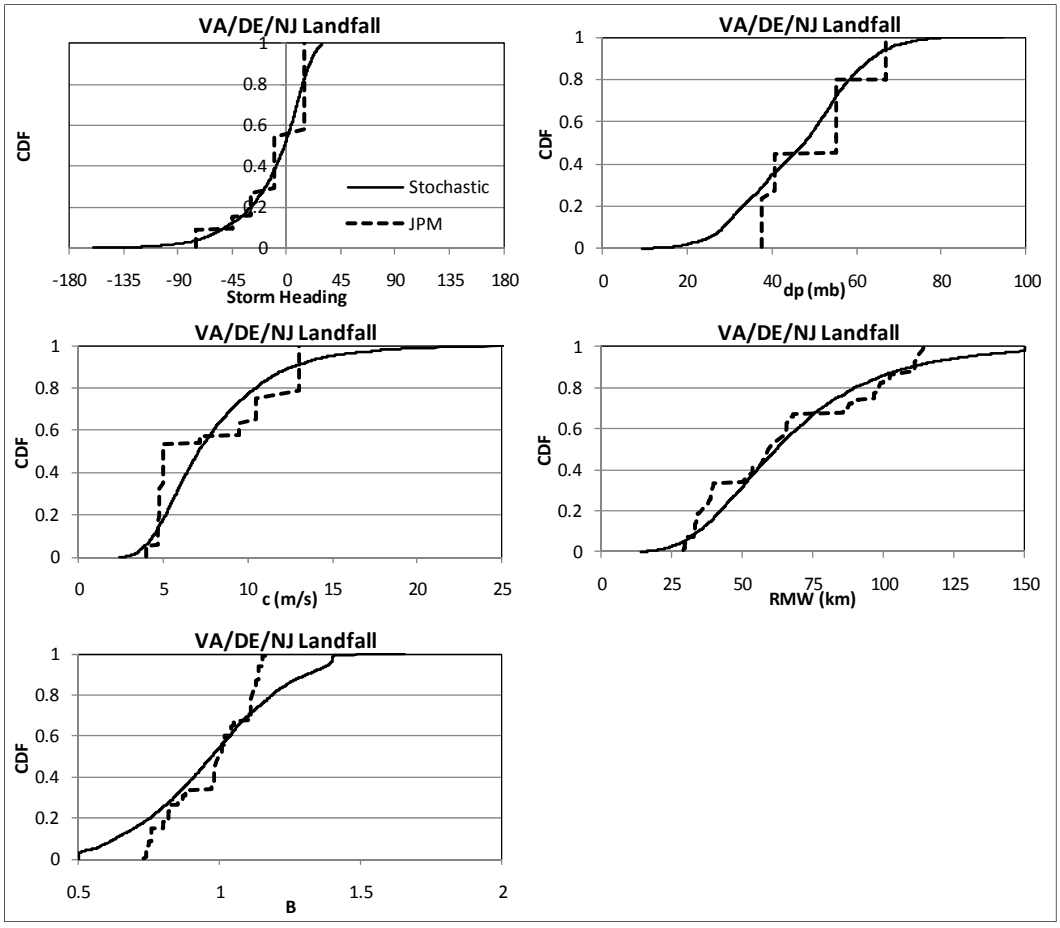

Figure 2-20. Comparison of JPM and stochastic representations of key hurricane parameters at landfall along the VA/DE/NJ coastal segment. Note that although only the mean representation of the Holland *B* parameter was modeled in the JPM set, some variation in *B* is observed due to the correlation of *B* with *RMW* and latitude. Heading is defined as the direction of storm motion measured clockwise from North. Storms with a positive heading have an eastward component. The translation speed is denoted *c*, the central pressure difference is denoted *dP*, and RMW is the radius to maximum winds.

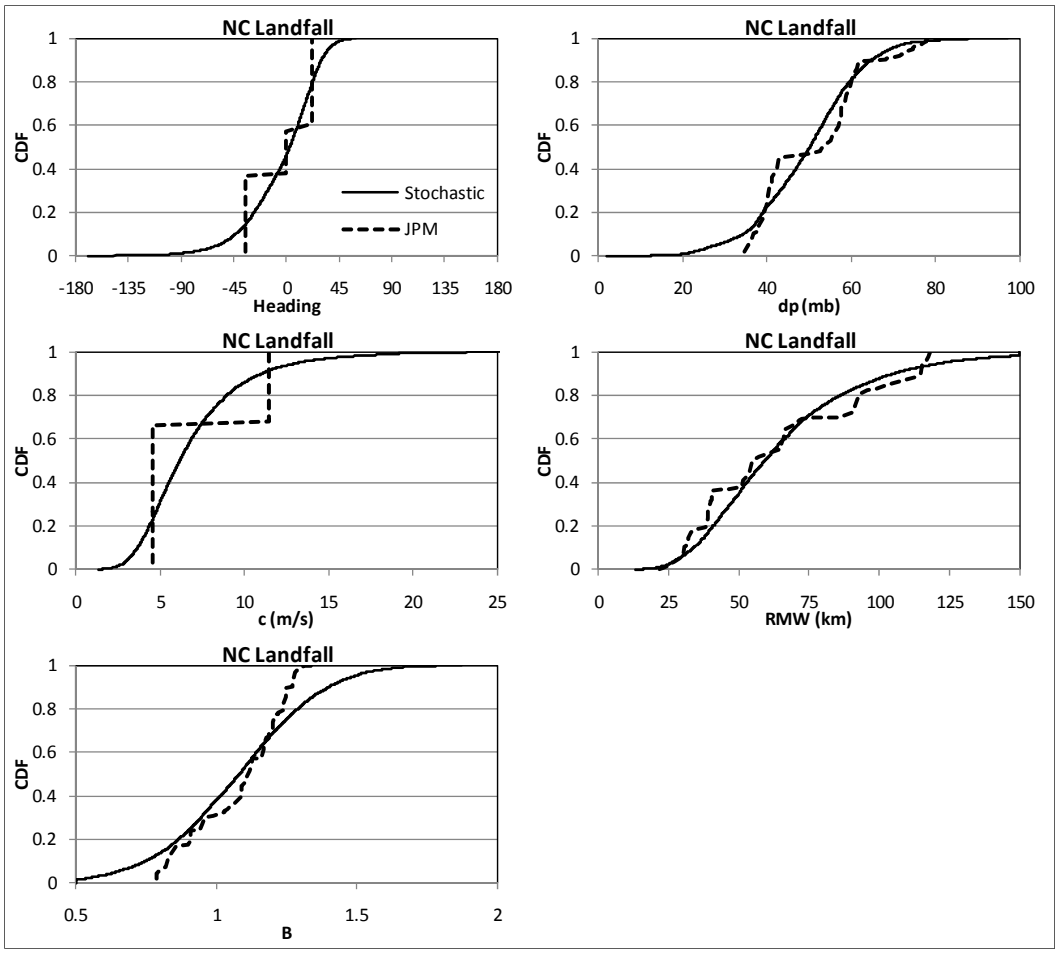

Figure 2-21. Comparison of JPM and stochastic representations of hurricane parameters at landfall along the NC coastal segment. Note that although only the mean representation of the Holland *B* parameter was modeled in the JPM set, some variation in *B* is observed due to the correlation of *B* with *RMW* and latitude. Heading is defined as the direction of storm motion measured clockwise from North. Storms with a positive heading have an eastward component. The translation speed is denoted *c*, the central pressure difference is denoted *dP*, and RMW is the radius to maximum winds.

Recall that the JPM central pressures shown in Figure 2-20 are shifted toward being more intense than the stochastic central pressures, which were found through a trial and error process to be necessary to correct a negative bias in the 100-year return period results.

2.5 Comparison of storm surge hazard curves derived using the JPM approach to those derived from a full stochastic storm set

Results presented in this section are for a set of 156 storm tracks, which were originally a subset of the base (or full JPM) storm set containing 468 simulated tracks. In the full JPM storm set, the variation of the Holland *B* parameters was represented by modeling the mean value and the mean

±1.22 standard deviations but — here in this reduced set — only the mean representation of the Holland *B* parameter is maintained. In the selection of the 156 storms, the tracks associated with the upper and lower bound representations of *B* were removed.

Figure 2-22 presents the nine sets of tracks used in this 156 storm set. To verify that the weighted simulation methodology yields reasonable results, and to determine the return period range over which the results can be considered valid, the team compared the estimates of the predicted hurricane-induced storm surge (derived using the JPM model hurricanes) to those predicted using the 100,000-year simulation of hurricanes. To explore this comparison, the team used a coarse ADCIRC grid and a simple representation of the hurricane wind field. The JPM tracks shown in Figure 2-22 are equally spaced, but this was not the case with the first set of 156 hurricanes (presented in Appendix D). Those original tracks were obtained by removing 312 tracks from the equally spaced set of 468 hurricanes. This first set of 156 storms was produced during a project review meeting where 2/3 of the simulated storms were removed (those corresponding to the upper and lower bound *B* values), with very encouraging results (i.e., small changes in 100-year return period surge elevations). The removal of 2/3 of the storms results in unequally spaced storm tracks, and these were later replaced by nominally equally spaced tracks, the results of which are presented in this section of the report. The results of the unequally spaced results are given in Appendix D, and a summary of the effect of storm spacing is presented at the conclusion of this section.

Figure 2-23 shows the locations of selected sites used to develop plots of still water level vs. return period. These plots are used to compare the full surge hazard curves arising from both the stochastic and JPM simulations. To develop the flood hazard curves associated with the JPM hurricanes, water elevations were computed using the coarse ADCIRC grid for each of the 156 JPM simulated storms. Each JPM hurricane has a probability of occurrence (conditional on a hurricane affecting the study region) equal to the product of the individual parameter weights given in Tables 2-1 through 2-3. The sum of the weights over all three storm types (North Carolina landfalling, Virginia/Delaware/New Jersey landfalling, and by-passing) is equal to unity. The weights in Tables 2-1 through 2-3 have to be multiplied by 0.202, 0.460 and 0.337, respectively, to take into account the relative coastal/by-passing segment crossing rates. The weights are further multiplied by 1/3 to take into account that three values of *RMW* are used for each

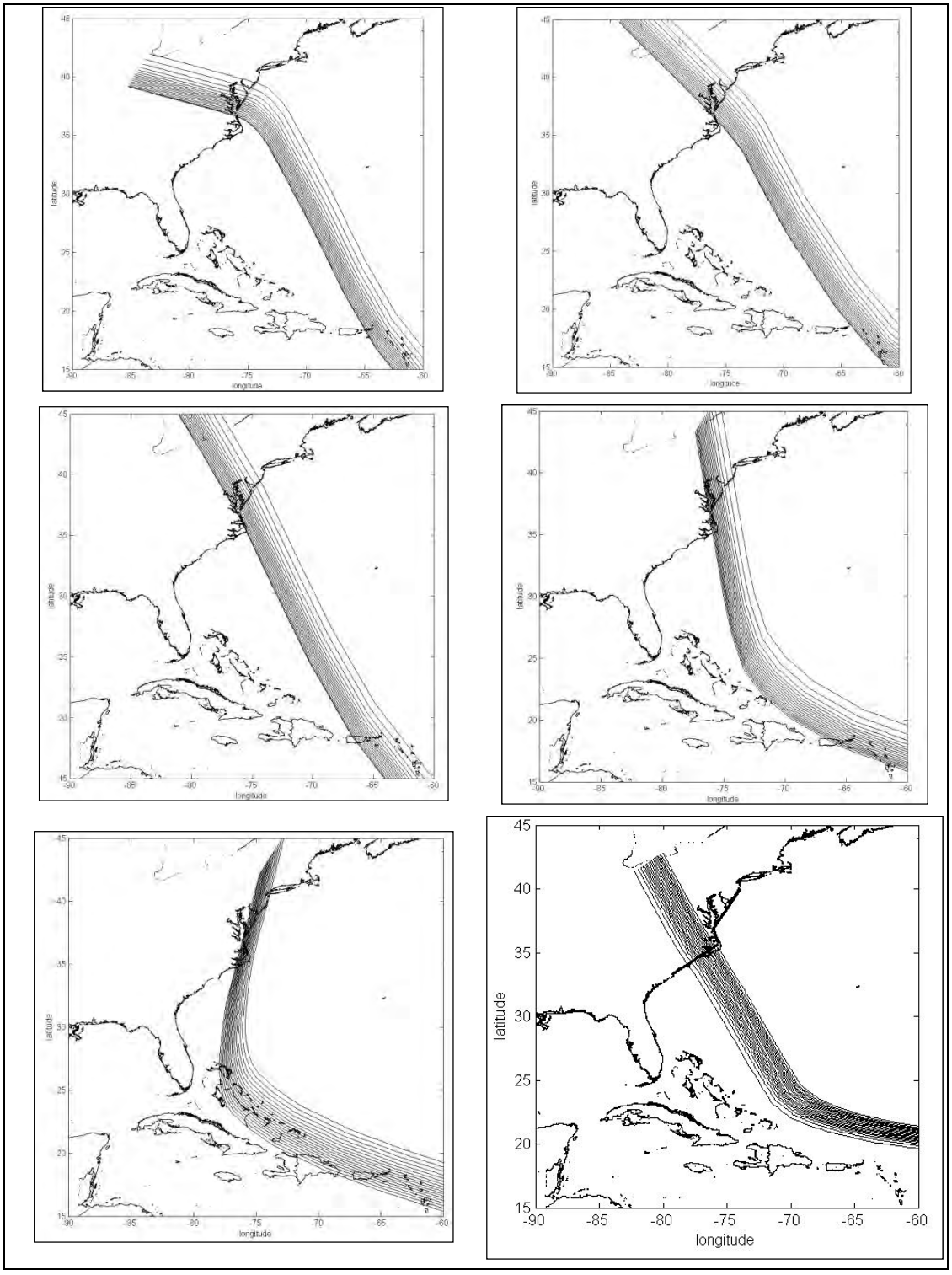

Figure 2-22. Tracks used to define the reduced (JPM) storm set. (continued)

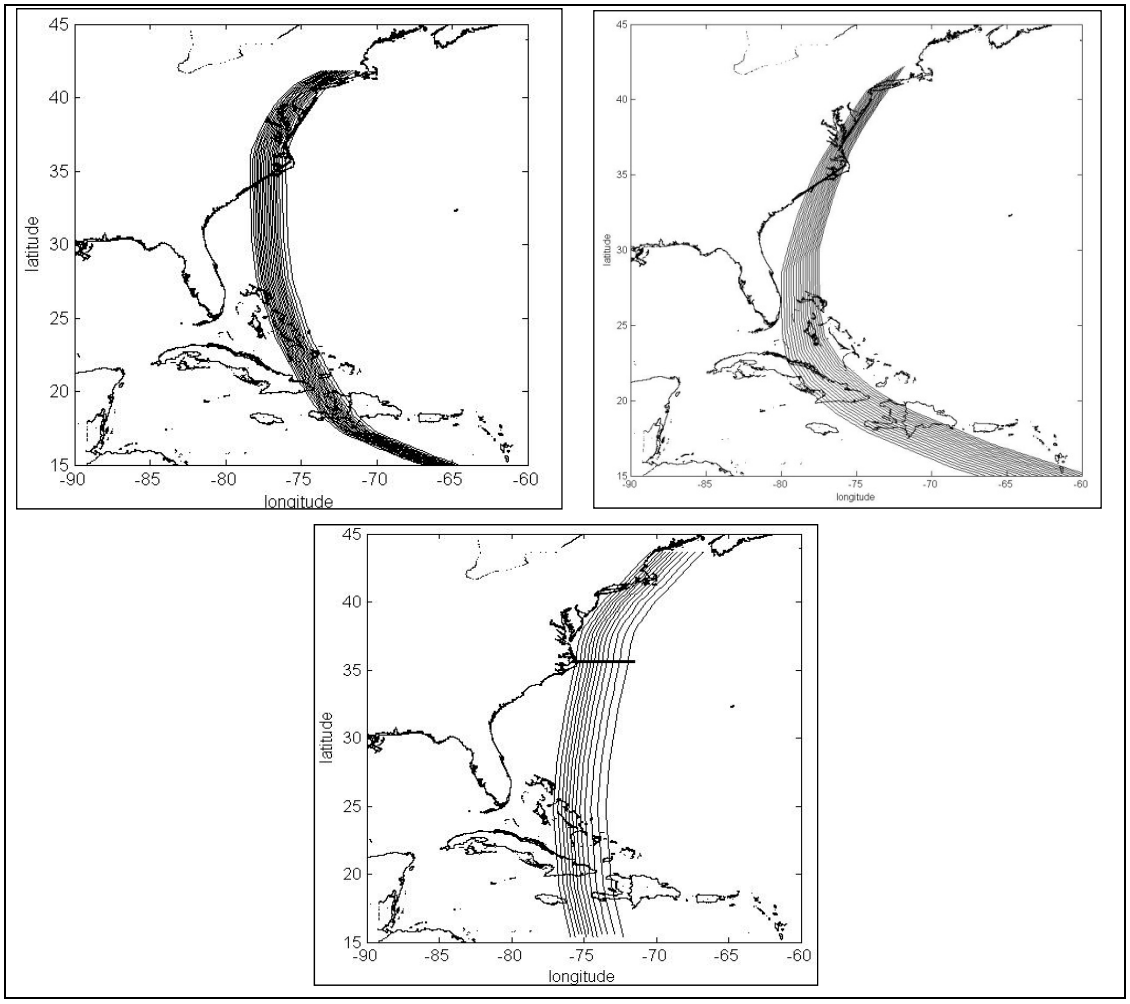

Figure 2-22. (concluded)

pressure-heading-translation speed combination (Vickery and Wadhera 2008). These rates are further multiplied by an additional term equal to $1/N_B$, where N_B is the number of B values used in the simulation (N_B is one out of the 156 storm cases and three out of the 468 storm cases).

The probability that a hurricane-induced water elevation is exceeded during time period t is:

$$P_t(\eta > \eta_0) = 1 - \sum_{x=0}^{\infty} P(\eta > \eta_0 \mid \chi) P_t(\chi) \tag{2-1}$$

where $P(\eta>\eta_0 \mid x)$ is the probability that the water elevation η is greater than η_0, given that x storms occur, and $p_t(x)$ is the probability of x storms occurring during time period t. From Equation 2-1, with $p_t(x)$ defined as Poisson and defining t as one year, the annual probability of exceeding a storm surge elevation is:

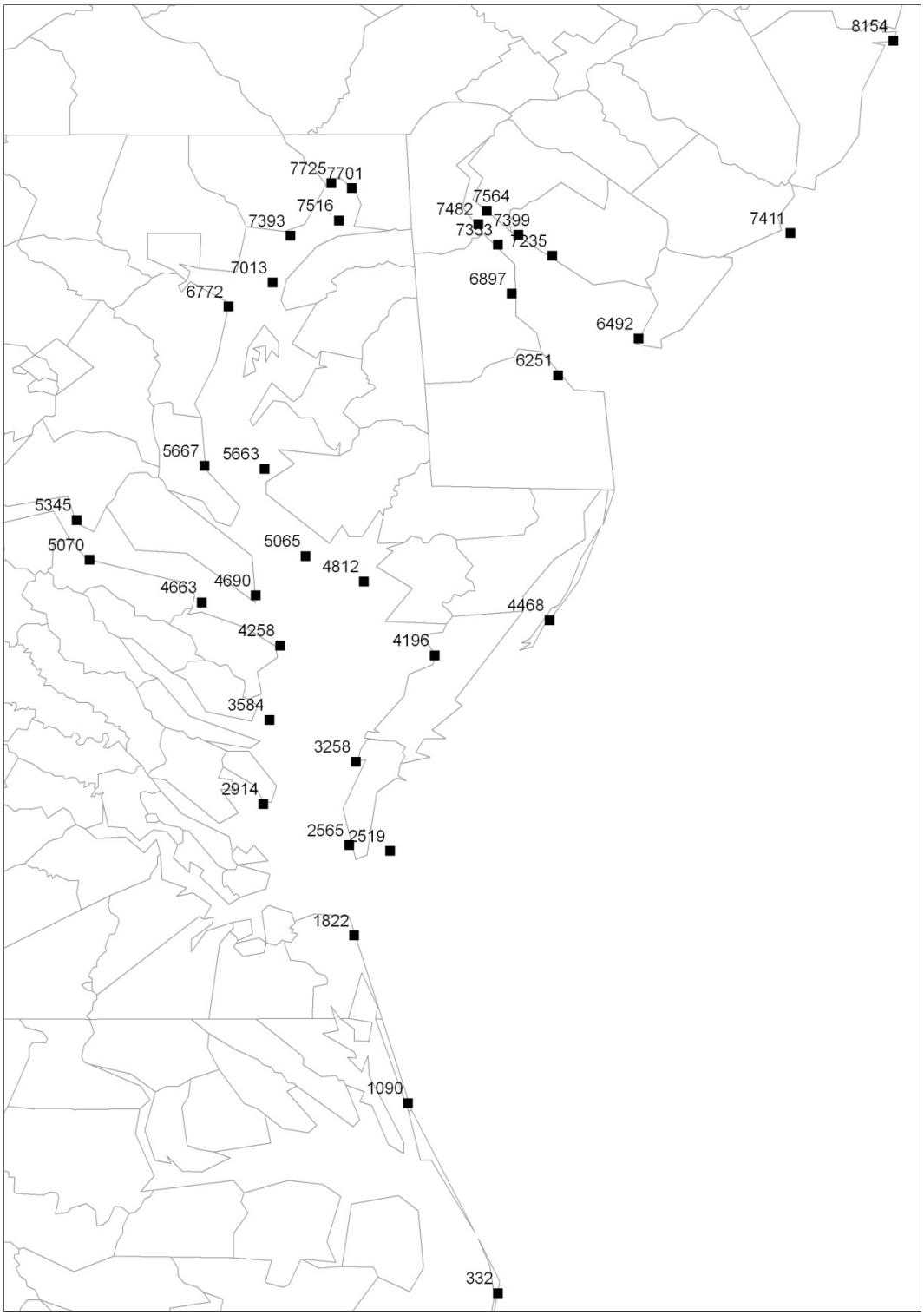

Figure 2-23. Map showing the locations of the 35 points used for comparisons of storm surge elevations that were computed using the full storm set and the reduced JPM storm set.

$$P_a(\eta > \eta_0) = 1 - \exp\left[-\lambda P(\eta > \eta_0)\right] \quad (2\text{-}2)$$

where λ represents the average annual number of storms that cross any of the modeled coastline segments and $P(\eta>\eta_0)$ is the probability that the water elevation η is greater than η_0, given the occurrence of any one storm. Again, in the development of the conditional cumulative distribution function for water elevation, $P(\eta>\eta_0 \mid x)$, each simulated hurricane used to develop the distribution has a probability of occurrence of w_i, where w_i is the product of the individual storm weights given in Tables 2-1 through 2-3 (multiplied by the appropriate coastal, RMW and B weighting factors). The annual occurrence rate, λ, is 0.1561.

Figure 2-24 shows the comparisons of the estimated storm surge obtained using the JPM set of storm tracks with the full stochastic set for a return period range of 10 through 1,000 years. The storm surge estimates obtained using the JPM approach are reasonable for most of the locations up to a return period of 1,000 years. The cases where the JPM results are notably higher than the stochastic results are typically at the end of bays and estuaries. Maps showing the differences between the two sets of model results on a node-by-node basis are presented later in this report. These maps show the variation in the differences along the coast of the Region III study area.

Figure 2-25 presents the locations (not numbered) for all near coast surge points used in the coarse grid analysis. The full distribution of both the relative and absolute differences between the stochastic storm set and the JPM storm set are presented in Figure 2-26 for return periods of 10, 100 and 500 years. Figures 2-27 through 2-29 show the absolute differences in a map format. Figures 2-30 through 2-32 present the same information as provided in Figures 2-27 through 2-29, but here the relative differences are presented rather than the absolute differences. Each figure presents the maximum, minimum, and mean difference.

Appendix C presents the results for 468 equally spaced tracks and Appendix D presents the results for 156 equally spaced tracks. Appendices C and D also provide all of the information presented in Figures 2-20 through 2-32.

Tables 2-4 and 2-5 summarize the maximum, minimum, mean, RMS, and the 5th and 95th percentile differences associated with the data presented in Figures 2-24 through 2-32. The tables also present the difference statistics derived from the simulations summarized in Appendices C and D for the

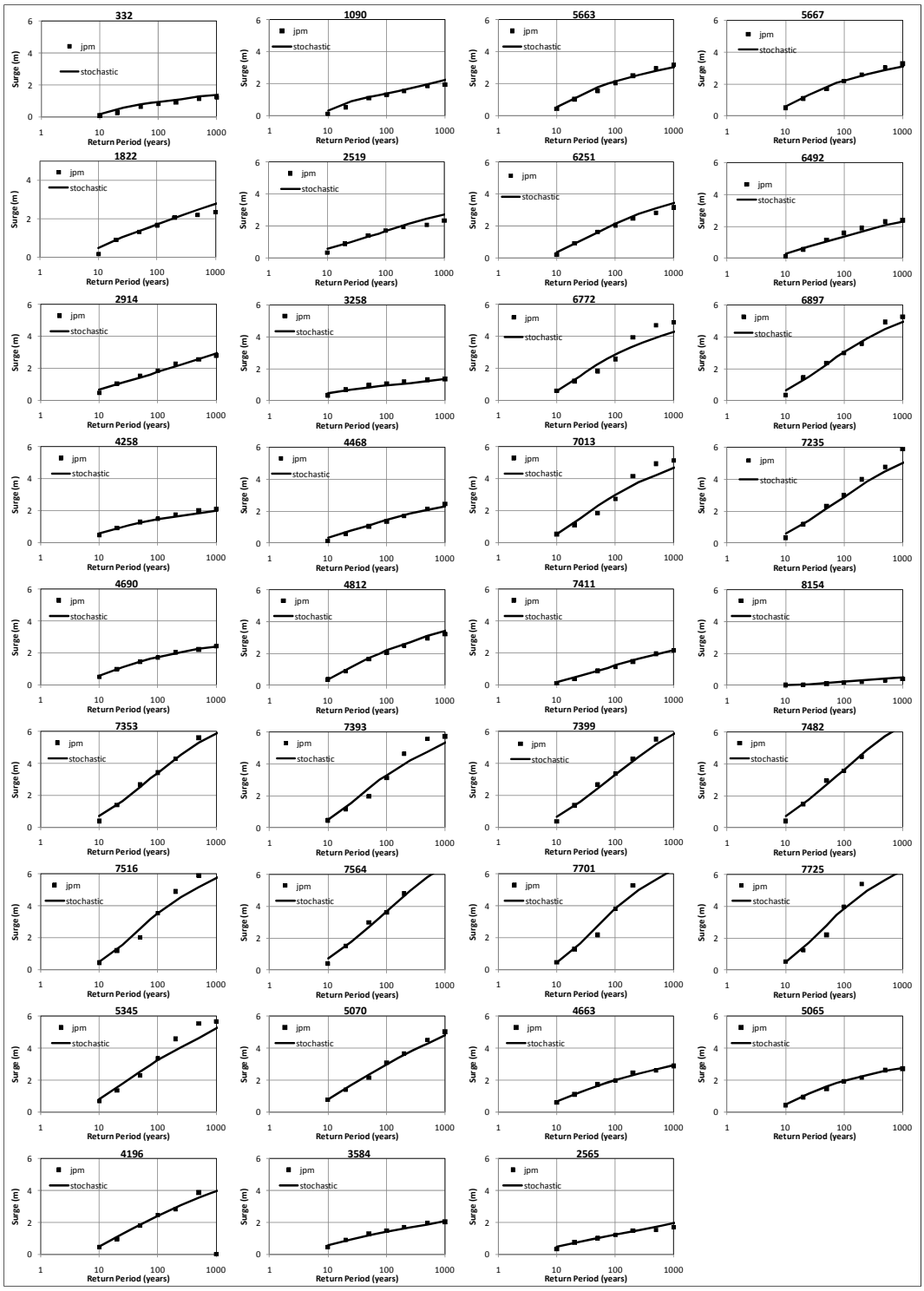

Figure 2-24 Comparisons of storm surge elevations computed using the full storm set and the JPM storm set.

Figure 2-25. Locations of all storm surge points used to derive distributions of the differences between the stochastic storm set elevations and the JPM storm set elevations. Storm tracks are shown in Figure 2-22.

other two storm sets (Appendix C contains the 468 storm track results and Appendix D contains the 156 equally spaced storms track results). Table 2-4 presents the statistics for the differences expressed in meters and Table 2-5 presents the statistics in terms of the percentage differences. In all cases, a negative difference indicates that the JPM results are lower than those obtained from the full stochastic simulation.

The results indicate that the 468 storm set yields the least amount of variability (as defined by the RMS difference), with the unequally spaced reduced storm set being next best. In the case of the 100-year return period surge elevations, the difference range as defined by the 5th to 95th percentiles for all three JPM sets is less 0.26 m (10.5 in.). In all three cases, there is a negative bias in the estimates of the 10-year return period surge elevations, with the negative bias being the least in the case of the 156 equally spaced storm tracks.

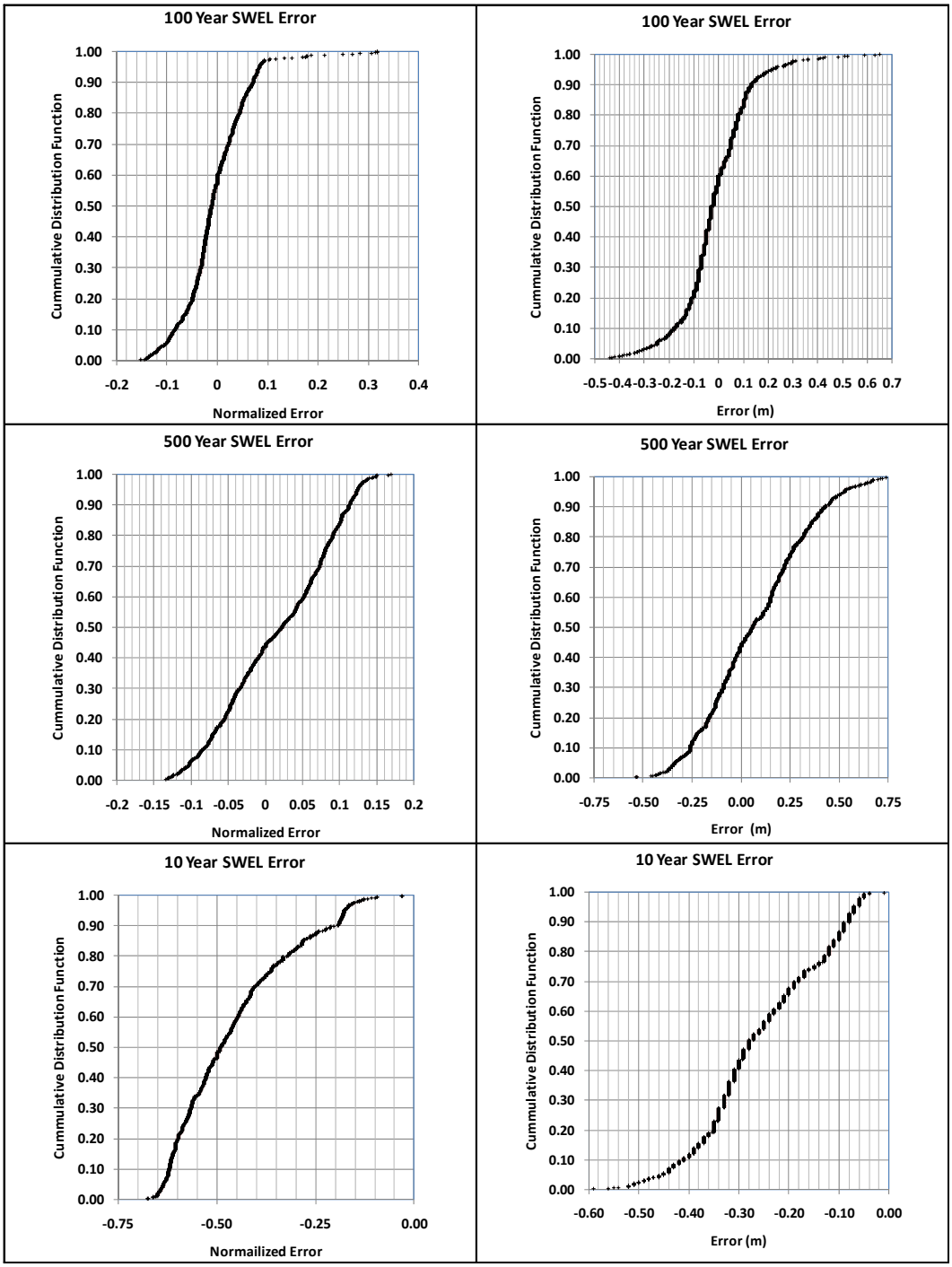

Figure 2-26. Cumulative distribution functions showing the differences in the modeled storm surge elevations at all nodal points shown in Figure 2-20. The differences are defined as the JPM results minus the stochastic results. Plots on the left present the relative (percentage) difference and plots on the right show the absolute difference, expressed as meters.

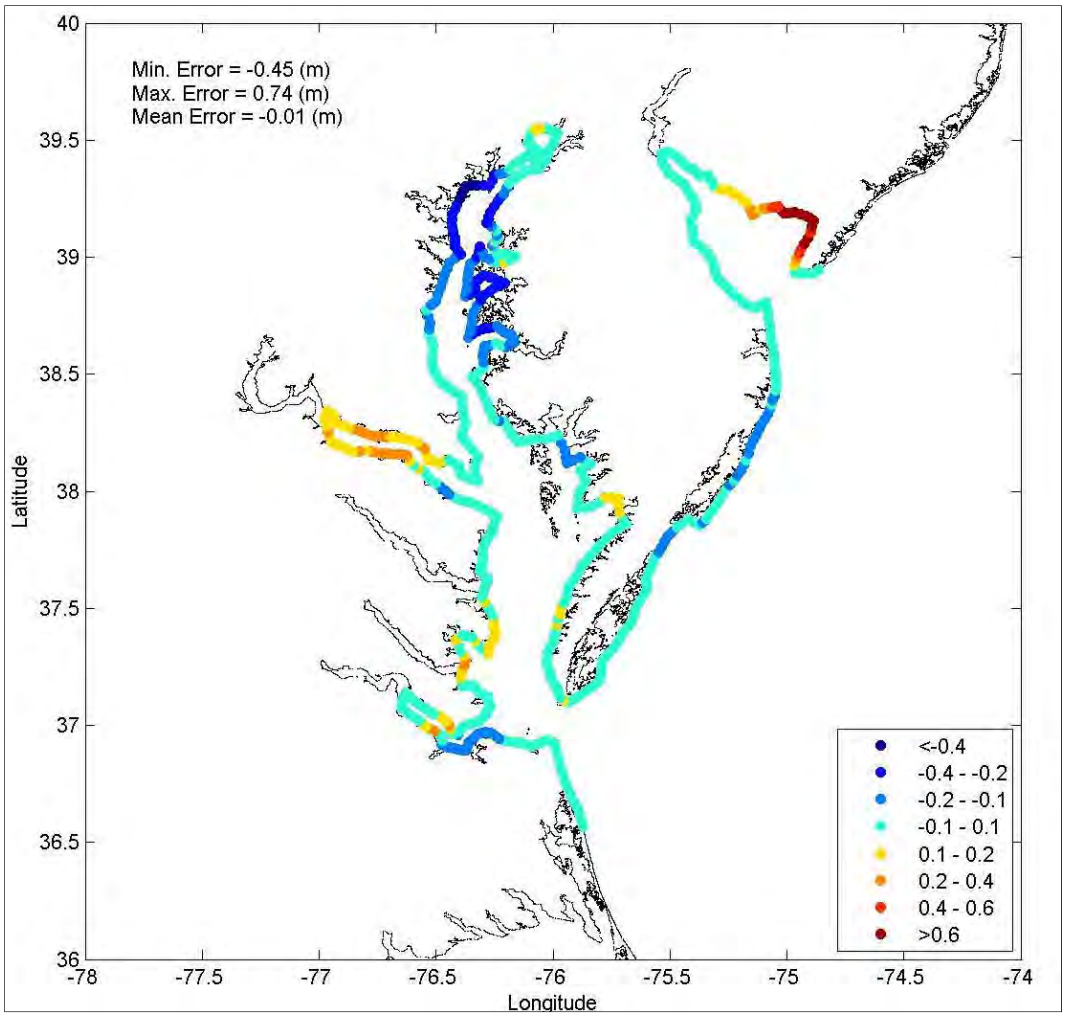

Figure 2-27. Difference between the stochastic and JPM-predicted, 100-year return period storm surge elevations. Positive values indicate that the JPM methodology produces higher storm surge values than the stochastic model. Note that the largest positive differences occur on the north side of Delaware Bay, along the New Jersey Coast.

The difference statistics for the 500-year return period JPM storms show a small high bias, with the largest bias evident in the 156 equally spaced storm set. The distribution of the differences has a long positive (overestimate) tail that is not evident in the 10 year and 100 year return period comparisons.

Given the uncertainty in the entire modeling process, it is suggested that the equally spaced 156 storms presented herein be used as the simulation methodology basis for developing the FIRMs.

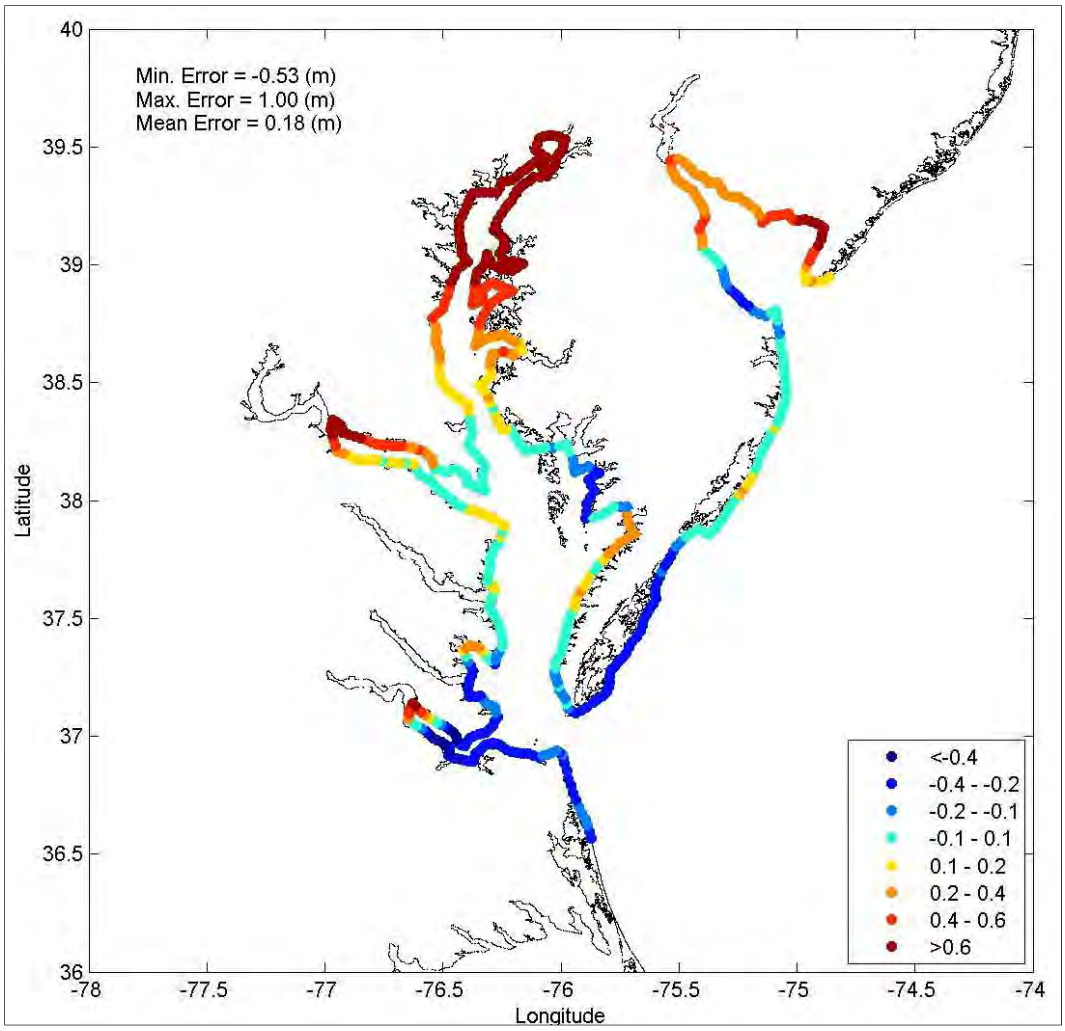

Figure 2-28. Difference between the stochastic and JPM-predicted, 500-year return period storm surge elevations. Positive values indicate that the JPM methodology produces higher storm surge values than the stochastic model. Note that the largest positive differences occur on the north side of Delaware Bay, and at the most extreme inland of Chesapeake Bay.

Table 2-4. Summary statistics of differences between the stochastic and JPM storms for the three different JPM storm sets. Differences are expressed in meters.

	156 Storms –Equally Spaced (Chapter 2)			468 Storms –Equally Spaced (Appendix C)			156 Storms –Unequally Spaced (Appendix D)		
	10 yr	100 yr	500 yr	10 yr	100 yr	500 yr	10 yr	100 yr	500 yr
Min	-0.49	-0.45	-0.53	-0.45	-0.28	-0.38	-0.59	-0.44	-0.54
Max	0.04	0.74	1.00	0.00	0.52	0.75	0.01	0.65	0.81
Mean	-0.14	-0.01	0.18	-0.19	0.01	0.20	-0.26	-0.01	0.07
RMS	0.12	0.16	0.37	0.08	0.10	0.26	0.12	0.14	0.26
5th	-0.37	-0.25	-0.31	-0.37	-0.13	-0.19	-0.45	-0.25	-0.34
95th	0.00	0.22	0.82	-0.07	0.20	0.65	-0.07	0.21	0.53

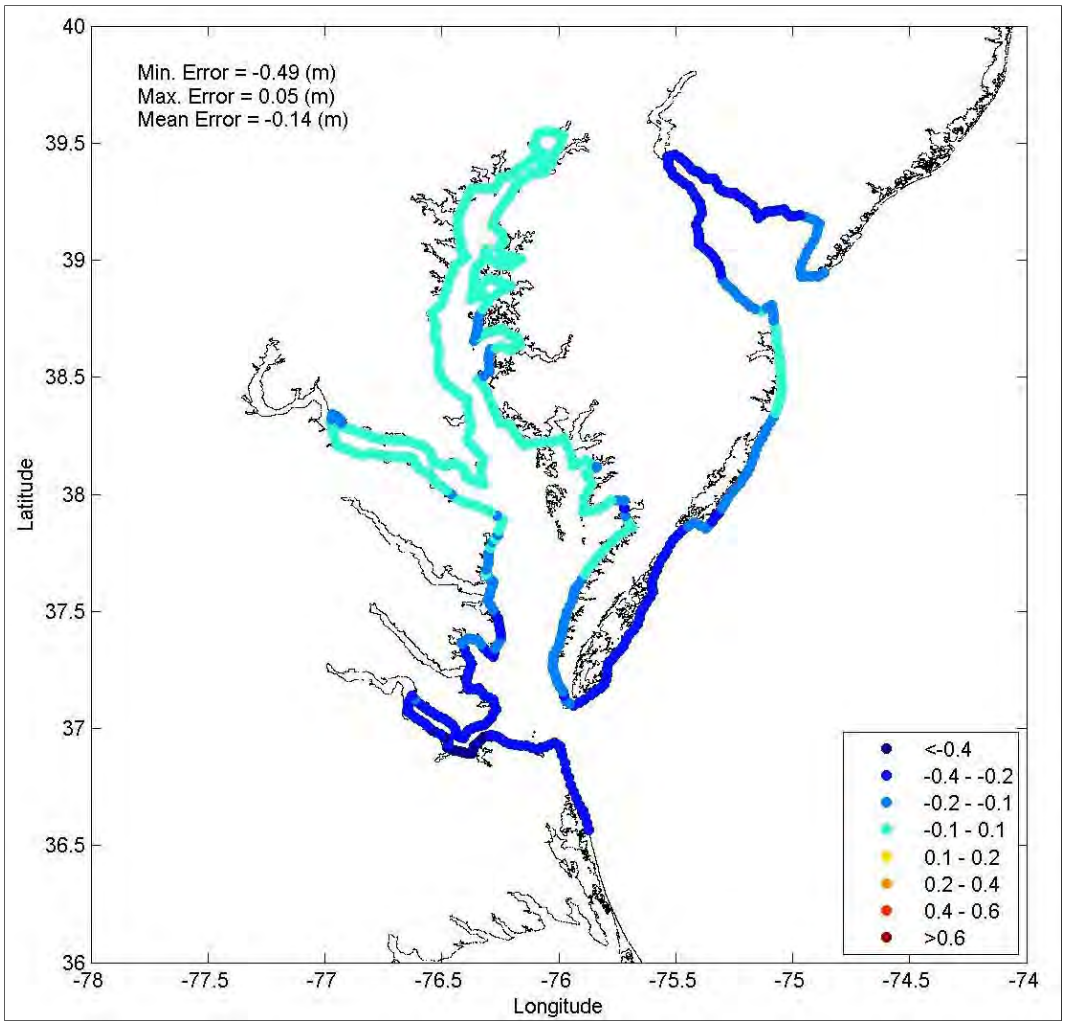

Figure 2-29. Difference between the stochastic and JPM-predicted, 10-year return period storm surge elevations. Positive values indicate that the JPM methodology produces higher storm surge values than the stochastic model. There is a clear bias, with the JPM results being lower than the stochastic results for all locations.

Table 2-5. Summary statistics of differences between the stochastic and JPM storms for the three different JPM storm sets. Differences are expressed as a percentage of the stochastic storm set results and have been computed on a point-by-point basis.

	156 Storms –Equally Spaced (Chapter 2)			468 Storms –Equally Spaced (Appendix C)			156 Storms –Unequally Spaced (Appendix D)		
	10 yr	100 yr	500 yr	10 yr	100 yr	500 yr	10 yr	100 yr	500 yr
Min	-73%	-14%	-16%	-58%	-12%	-10%	-68%	-15%	-14%
Max	11%	45%	22%	0%	26%	20%	3%	32%	17%
Mean	-27%	0%	4%	-34%	0%	6%	-46%	0%	2%
RMS	21%	5%	10%	8%	5%	7%	15%	6%	7%
5th	-60%	-9%	-11%	-50%	-9%	-7%	-63%	-11%	-10%
95th	0%	7%	19%	-24%	7%	16%	-18%	8%	12%

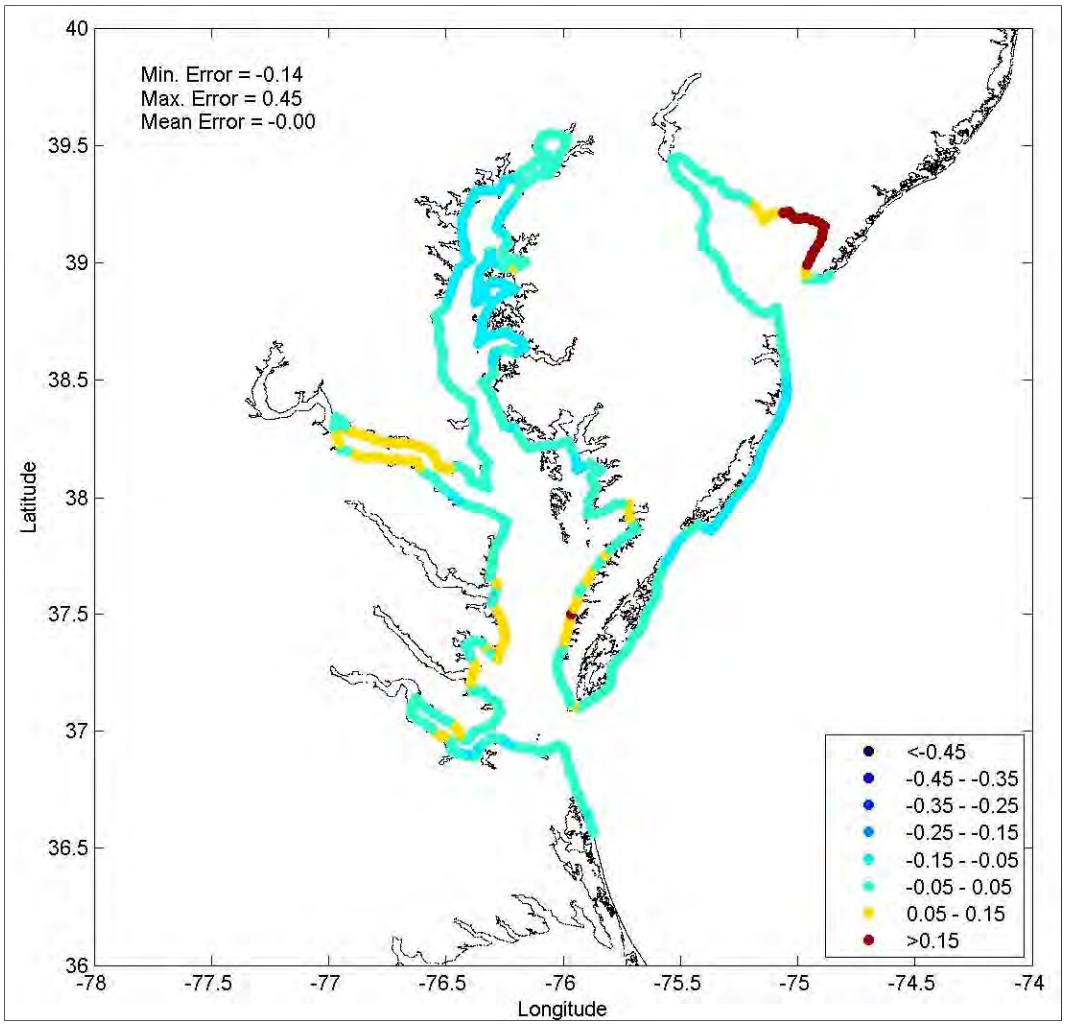

Figure 2-30. Relative (percentage) difference between the stochastic and JPM-predicted, 100-year return period storm surge elevations. Positive values indicate that the JPM methodology produces higher storm surge values than the stochastic model. Note that the largest positive differences occur on the north side of Delaware Bay, along the New Jersey Coast.

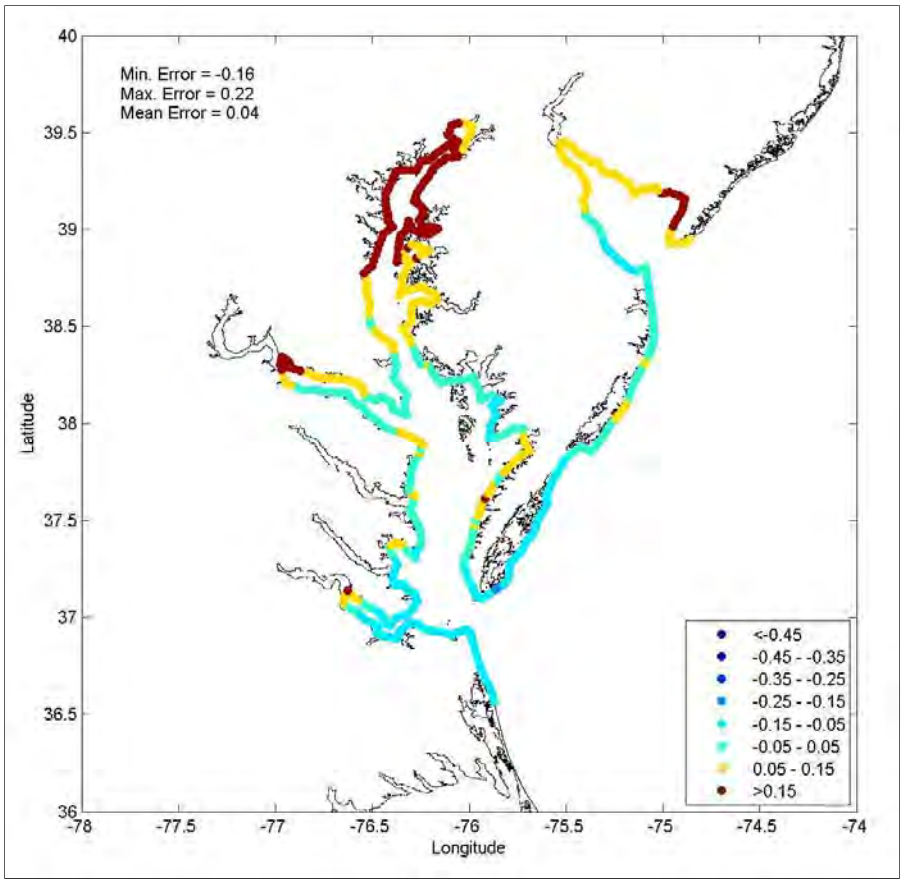

Figure 2-31. Relative (percentage) difference between the stochastic and JPM-predicted, 500-year return period storm surge elevations. Positive values indicate that the JPM methodology produces higher storm surge values than the stochastic model. Note that the largest positive differences occur on the north side of Delaware Bay, along the New Jersey Coast, and at the inland most extreme of Chesapeake Bay.

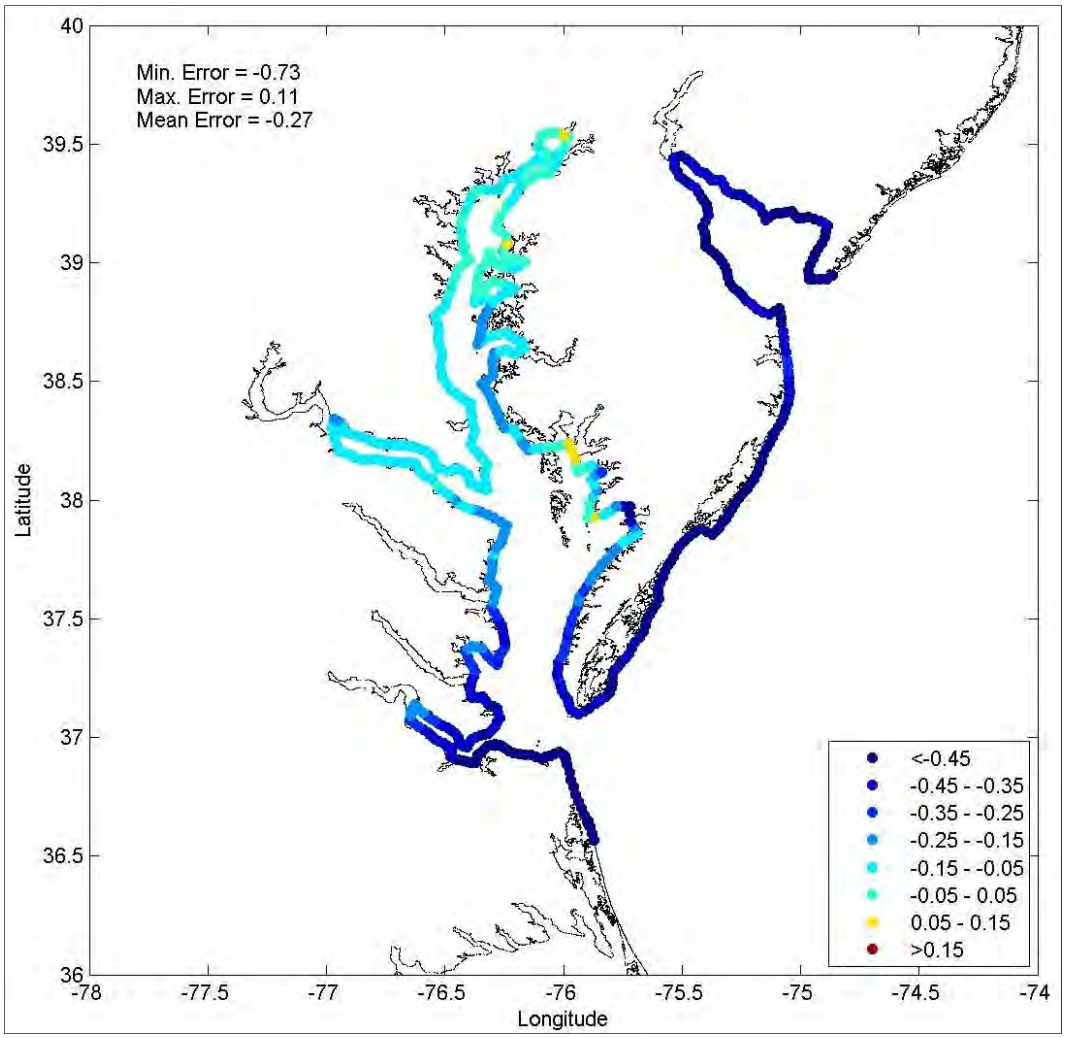

Figure 2-32. Relative (percentage) difference between the stochastic and JPM-predicted, 10-year return period storm surge elevations. Positive values indicate that the JPM methodology produces higher storm surge values than the stochastic model. There is a clear bias with the JPM results being lower than the stochastic results for all locations.

3 Extratropical Cyclones

The selection and development of extratropical cyclones (ETC) and associated wind and pressure fields for the FEMA Region III storm surge study was performed by Oceanweather, Inc. Initially, a set of 30 extratropical cyclones were identified for hindcast based on a ranking of historical measured water levels from seven stations in the NOS archive. After the completion of this work, in November 2009, ETC Ida made a significant impact on the study area. Ida originated as Hurricane Ida in the Gulf of Mexico and resulted in water levels 8.0-9.0 ft above MLLW at some locations in the study domain and 5.0-6.0 ft above MLLW in the Chesapeake Bay. Sample ETC Ida water levels from two NOS stations in the Chesapeake Bay appear in Figure 3-1. Predicted (tides only), observed, and residual water levels are depicted. The significant increase of observed water levels above the tidal prediction is a measure of the Ida storm surge and flooding at this location. As a result of this widespread impact, Ida was added to the list of extratropical cylones selected for the study. Furthermore, Ida has been added to the list of validation storms that will be used to quantify the performance of the modeling system prior to production.

The documentation for this work was provided by Oceanweather and appears in a series of two appendices. Appendix A, updated after ETC Ida was added, provides a summary of the work performed by Oceanweather to identify the extratropical cyclone dataset and reconstruct these events. Appendix B describes the extratropical cyclone selection process for the study. Included are the NOS station data used to rank the events, and samples of the reconstructed water levels and pressure fields.

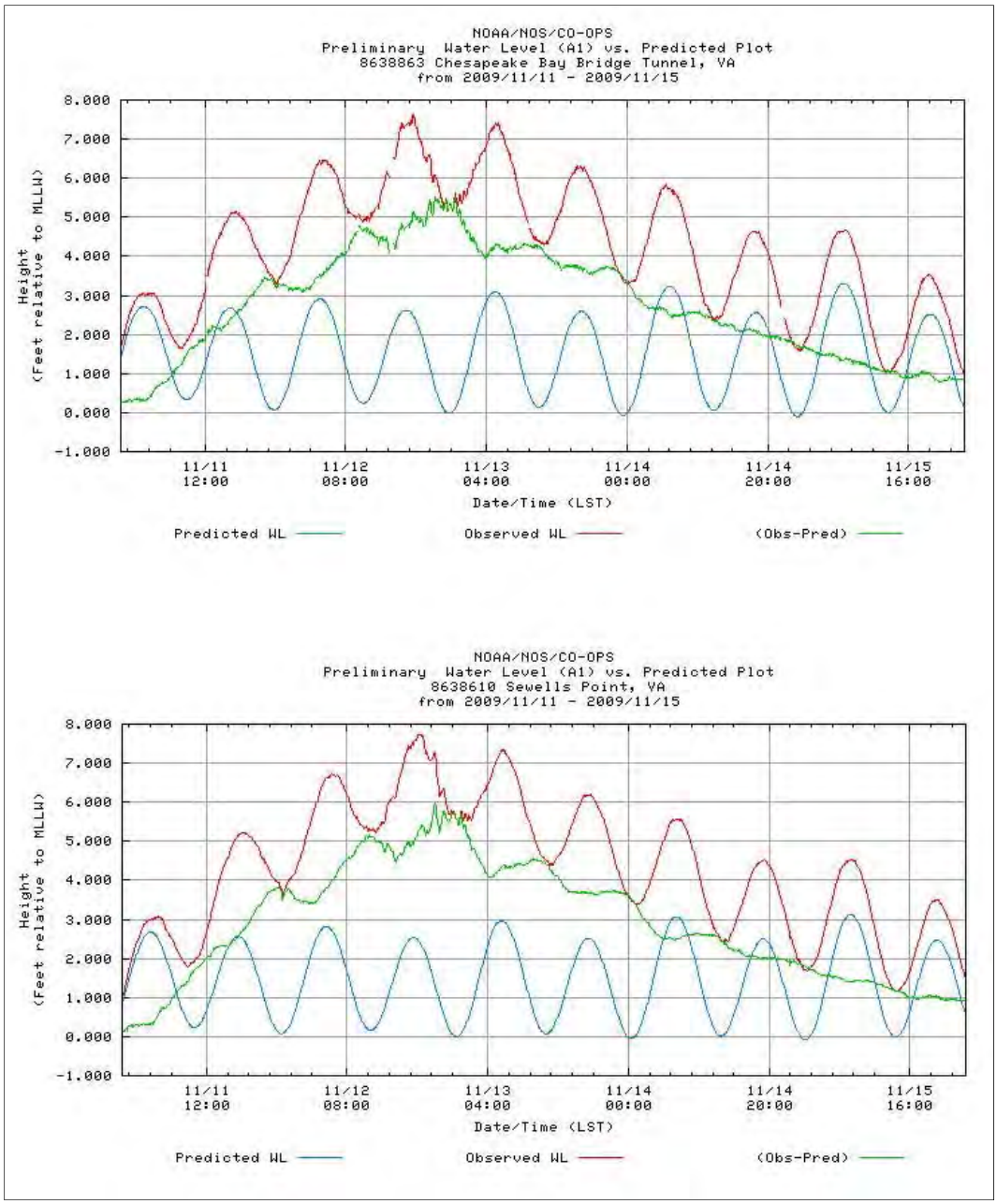

Figure 3-1. NOS water levels at Chesapeake Bay Bridge Tunnel (upper) and Sewells Point, VA (lower) during Extratropical Cyclone Ida in November 2009.

References

Blanton, B., S. Madry, K. Galluppi, K. Gamiel, H. Lander, M. Reed, L. Stillwell, M. Blanchard-Montgomery. Draft report for the State of North Carolina, Floodplain Mapping Project: Coastal Flood Analysis System. http://www.renci.org/wp-content/pub/techreports/TR-08-06.pdf

Blanton, B., L. Stillwell, H. Roberts, J. Atkinson, S. Zou, M. Forte, J. Hanson and R. Luettich. 2011. *Coastal storm surge analysis: Computational system*. Submittal 1.2 to FEMA. ERDC/CHL TR-11-1. Vicksburg, MS: US Army Engineer Research and Development Center.

Emanuel, K. A. 1988. The maximum intensity of hurricanes. *Journal of Atmospheric Sciences* 45(7):1143-1155.

Emanuel, K., C. DesAutels, C. Holloway, and R. Korty. 2004. Environmental Control of Tropical Cyclone Intensity. *Journal of Atmospheric Sciences* 61:843–858.

Federal Emergency Management Agency (FEMA). 2007. *Atlantic Ocean and Gulf of Mexico coastal guidelines update. Guidelines and specifications for flood hazard mapping partners Technical Report*. Washington, DC.

Forte, M. F., J. L. Hanson, L. Stillwell, M. Blanchard-Montgomery, B. Blanton, R. Leuttich, H. Roberts, J. Atkinson, and J. Miller. 2011. *Coastal storm surge analysis system: Digital elevation model*. Submittal 1.1 to FEMA. ERDC/CHL TR-11-1. Vicksburg, MS: US Army Engineer Research and Development Center.

Holland, G. J. 1980. An analytic model of the wind and pressure profiles in hurricanes. *Monthly Weather Review* 108:1212-1218.

Resio, D. T, S. J. Boc, L. Borgman ,V. J. Cardone, A. Cox, W. R. Dally, R. G. Dean, D. Divoky, E. Hirsh, J. L. Irish, D. Levinson, A. Niederoda, M. D. Powell, J. J. Ratcliff, V. Stutts, J. Suhada , G. R. Toro and P. J. Vickery. 2007. White Paper on Estimating Hurricane Inundation Probabilities.

Russell, L. R. 1968. Probability distribution for Texas Gulf Coast hurricane effects of engineering interest. Ph.D. Thesis, Stanford University.

Vickery, P. J. 2005. Simple empirical models for estimating the increase in the central pressure of tropical cyclones after landfall along the coastline of the United States. *Journal of Applied Meteorology* 44:1807-1826

Vickery, P. J., P. F. Skerlj, and L. A. Twisdale, Jr. 2000. Simulation of hurricane risk in the US using an empirical track model. *Journal of Structural Engineering*. 126:10.

Vickery, P. J., and D. Wadhera. 2008. Statistical Models of the Holland Pressure Profile Parameter and Radius to Maximum Winds of Hurricanes from Flight Level Pressure and H*Wind Data. *Journal of Applied Meteorology and Climatology* 47:2497-2517

Vickery, P. J., D. Wadhera, M. D. Powell, and Y. Chen. 2009a. A Hurricane boundary layer and wind field model for use in engineering applications. *Journal of Applied Meteorology and Climatology* 48:381-405

Vickery, P. J., D. Wadhera, L.A. Twisdale, Jr., and F. M. Lavelle. 2009b. United States hurricane wind speed risk and uncertainty. *Journal of Structural Engineering* 135:301-320.

Appendix A: Storm Reanalysis in Support of FEMA Region III Storm Surge Modeling

Submitted to:

Jeff Hanson (ERDC-CHL-MS) USACE Office
1261 Duck Road
Kitty Hawk, NC 27949
(252) 261-6840 x239

Updated February 9, 2010

Oceanweather, Inc.
5 River Road
Cos Cob, CT, USA
Tel: 203-661-3091
Fax: 203-661-6809
Email: oceanwx@oceanweather.com
Web: www.oceanweather.com

Introduction

This report describes work performed under contract W912BU-08-P-0291 for the US Army Engineer District, Philadelphia, for storm reanalysis in support of FEMA Region III storm surge modeling. The objective of the project is to update the coastal flood risk analysis for Chesapeake Bay (CB) and eventually all of Region III. The project will incorporate the latest approaches, modeling, and statistical methodologies applied in similar studies carried out post-Katrina to Regions VI (Gulf of Mexico) and IV (Southeast Coast of US). Region III is subject to both extreme extratropical cyclones (ETC) and tropical cyclones (TC), so both regimes need to be addressed.

This project consists of the following major tasks and deliverables:

1. ETC storm selection
2. Hindcast of 25 ETC storms for Chesapeake Bay support
3. Hindcast of 5.0 additional ETC and 2.0 TC for Region III support

4. Transfer of TC96 Tropical Planetary Boundary Layer model
5. Additional ETC case of the "Nor'Ida" storm of November 2009

Extratropical storm selection

A total of 30 ETCs were identified for hindcast using historical measured water levels from the National Ocean Service (NOS) archive. Seven stations in the Region III area with long term continuous records during the 1975-2008 period were identified for the storm selection process. A summary report titled *Extra-Tropical Storm Selection In Support of FEMA Region III Storm Surge Modeling* provides details about the selection process.

After the 30 ETC storm work was completed, an extratropical system (so-called "Nor'Ida") which originated as Hurricane Ida in the Gulf of Mexico impacted the study area during the period of November 11-15, 2009. This storm resulted in water levels 8.0-9.0 ft above MLLW at The Battery, New York (NOS 8518750), Sandy Hook, New Jersey (NOS 8531680), and Cape May, New Jersey (8536110), and impacted numerous other NOS gauges in the study area. This storm was hindcast using the same ETC methodology outlined below and added to the project.

Extratropical storm hindcast

The 30 ETC storms plus the Nor'Ida storm identified for hindcast are shown in Table A1 and include the approximately five-day spin-up and three-day spin-down period from the storm's peak surge. Storms were hindcast using the Interactive Objective Kinematic Analysis (IOKA) system as described in Cox et al. 1995. Wind and pressure data were obtained from the following sources:

1. National Centers for Environmental Prediction/National Center for Atmospheric Research (NCEP/NCAR) reanalysis wind and pressure fields
2. Buoy and Coastal Manned Station (C-MAN) data from National Data Buoy Center (NDBC)
3. National Weather Service (NWS) and National Ocean Service (NOS) land station data provided by the National Climatic Data Center (NCDC)
4. Ship reports from Comprehensive Ocean-Atmosphere Data Set (COADS)
5. Scatterometer wind estimates from the QUIKSCAT, ERS-1, ERS-2 instruments

Table A1. Extratropical storm hindcast list.

Storm Reference	Start (UTC)	End (UTC)
19750926	Sep-21-1975 00:00	Sep-29-1975 00:00
19780126	Jan-21-1978 00:00	Jan-29-1978 00:00
19780427	Apr-22-1978 00:00	Apr-30-1978 00:00
19790226	Feb-21-1979 00:00	Mar-01-1979 00:00
19821025	Oct-20-1982 00:00	Oct-28-1982 00:00
19830404	Mar-30-1983 00:00	Apr-07-1983 00:00
19840216	Feb-11-1984 00:00	Feb-19-1984 00:00
19840329	Mar-24-1984 00:00	Apr-01-1984 00:00
19850212	Feb-07-1985 00:00	Feb-15-1985 00:00
19851107	Nov-02-1985 00:00	Nov-10-1985 00:00
19870102	Dec-28-1986 00:00	Jan-05-1987 00:00
19911031	Oct-26-1991 00:00	Nov-03-1991 00:00
19920105	Dec-31-1991 00:00	Jan-08-1992 00:00
19921211	Dec-06-1992 00:00	Dec-14-1992 00:00
19930305	Feb-28-1993 00:00	Mar-08-1993 00:00
19931128	Nov-23-1993 00:00	Dec-01-1993 00:00
19940104	Dec-30-1993 00:00	Jan-07-1994 00:00
19960108	Jan-03-1996 00:00	Jan-11-1996 00:00
19960119	Jan-14-1996 00:00	Jan-22-1996 00:00
19961009	Oct-04-1996 00:00	Oct-12-1996 00:00
19980128	Jan-23-1998 00:00	Jan-31-1998 00:00
19980205	Jan-31-1998 00:00	Feb-08-1998 00:00
19980309	Mar-04-1998 00:00	Mar-12-1998 00:00
20000125	Jan-20-2000 00:00	Jan-28-2000 00:00
20021017	Oct-12-2002 00:00	Oct-20-2002 00:00
20051025	Oct-20-2005 00:00	Oct-28-2005 00:00
20061007	Oct-02-2006 00:00	Oct-10-2006 00:00
20061028	Oct-23-2006 00:00	Oct-31-2006 00:00
20061122	Nov-17-2006 00:00	Nov-25-2006 00:00
20080512	May-07-2008 00:00	May-15-2008 00:00
20091113	Nov-08-2009 00:00	Nov-16-2009 00:00

Wind fields from individual storms were reanalyzed using kinematic analysis, a man-intensive process for which wind speeds (isotachs) and wind directions (streamlines) are hand-drawn to best represent the available observations while preserving the primary meteorological principles of storm development and continuity. Figure A1 shows an example of a kinematic analysis valid during the October 2006 event.

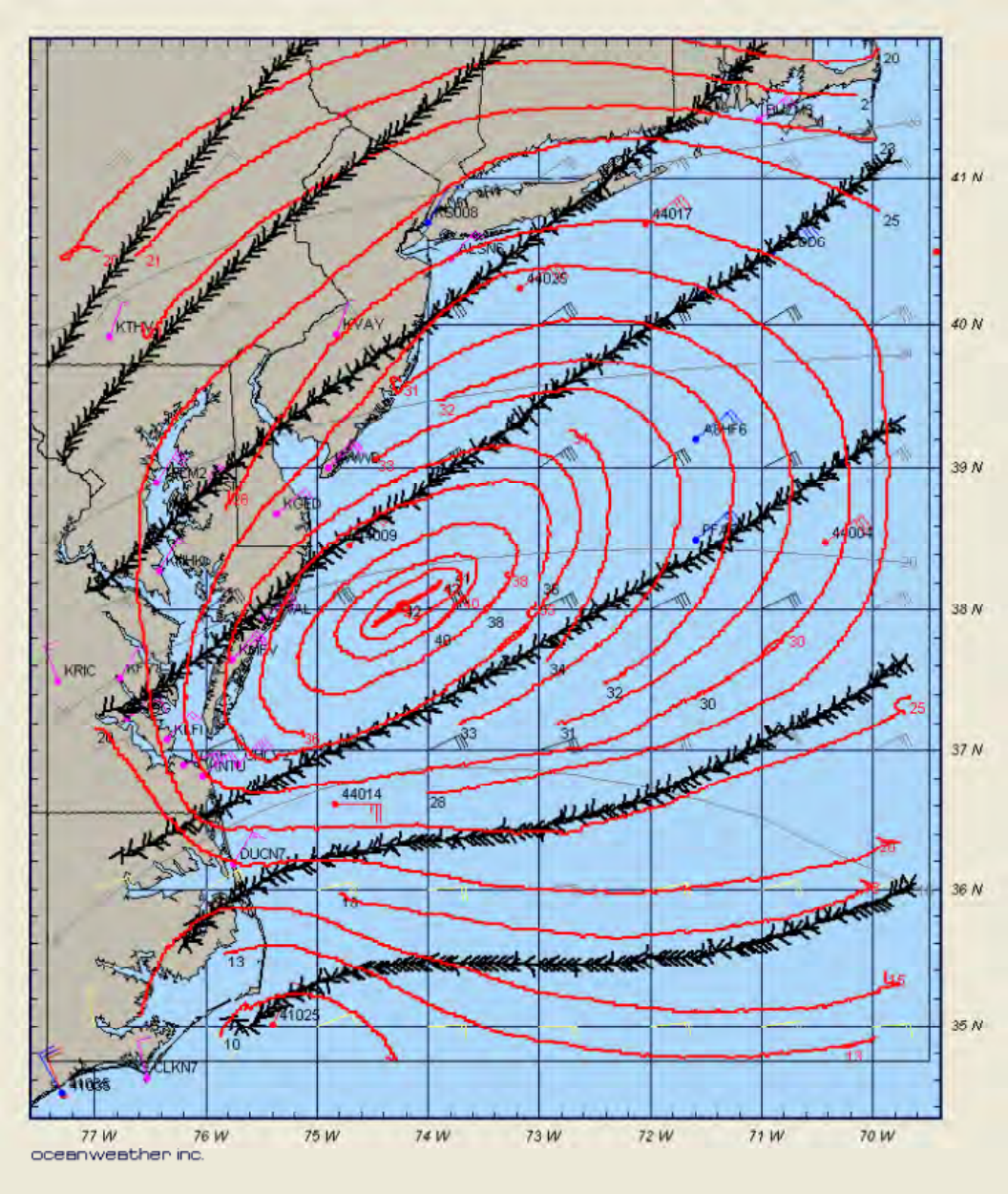

Figure A1. Kinematic analysis of wind speed (red knots) and wind direction (streamlines, black) valid October 7, 2006 00:00 UTC.

Wind fields were developed on two grid systems: a basin grid covered the domain 15-58N, 85- 55W at a 0.125-deg latitude-longitude grid with time step of 30 min. A fine grid covered the domain 36-40N, 78-74W at 0.025-deg with 15 min time step. All winds are 10-m neutral representing a 30-min average. Pressures from the NCEP/NCAR data were interpolated onto the same working grids as the wind fields.

Tropical cyclone hindcasts

The reference set of historical storms selected for calibration of the modeling consist of Isabel (2003) and Ernesto (2006). Copious meteorological data exist and have been processed to develop wind and pressure fields to drive ocean response models. The pertinent data sets for wind field analysis consist of

1. historical track and intensity data from NOAA's (National Oceanographic and Atmospheric Administration) HURDAT (Hurricane Data) archive;
2. aircraft reconnaissance obtained from NOAA and US Air Force hurricane hunter aircraft, including vortex messages and continuous flight level wind speed, direction, DValue;
3. gridded and image fields of marine surface wind composites from the HRD (Hurricane Research Division) HWnd analysis;
4. synoptic observations from NOAA buoy and C-MAN (Coastal Manned) stations;
5. synoptic observations from transient ships, coastal and land stations;
6. composite NWS (National Weather Service) radar imagery;
7. loops of NOAA visual, infrared and water vapor imagery;
8. NCEP (National Center for Environmental Prediction) model wind fields;
9. QUIKSCAT scatterometer winds;
10. TOPEX altimeter winds and waves;
11. ERS-2 altimeter winds and waves; and
12. data from offshore platforms equipped with met packages.

The meteorological parameters of greatest importance are the hurricane's track, forward speed, radius of maximum wind, barometric pressure distribution from the hurricane center to the periphery, and the ambient pressure system through which the hurricane is moving. In the hindcast method, these parameters are used to drive a numerical model (Thompson and Cardone 1996) (TC96) to determine a first guess of the surface wind field using OWI, Inc.'s (OWI's) tropical analyst workstation (Cox and Cardone 2000); next, the available direct wind measurements were

assimilated into the first guess fields to provide a refined specification using OWI's Interactive Objective Kinematic Analysis (IOKA) system (Cox et al. 1995). Since the 1950s, daily reconnaissance flights have been made into most storms by Air Force and NOAA personnel to collect pressure, temperature, and upper level wind data. Eye shape and diameter observations are also recorded. These data are used to fit the snapshot parameters required to drive the TC96 model.

Wind and pressure fields were developed on the same basin/fine grid systems applied in the ETC hindcast work. Pressure output from the TC96 model within the core of the system was blended into the larger domain of the NCEP/NCAR reanalysis pressures.

Validation of Ernesto (2006_06) and Extratropical cyclone 20051025

Table A2 and Figure A2 show the closest buoys and C-MAN station data locations for which data were verified against the hindcast. All data were obtained from the National Data Buoy Center and adjusted for both height and stability to a 10-m reference level. Where available, three consecutive 10-min wind observations were averaged 1-1-1 to produce a 30-min mean wind for direct comparison to the hindcast sets.

Time histories of each station and storm are shown in Figures A3 (20051025) and A4 (Ernesto). Mean wind speed bias during 20051025 was 0.22 m/sec with correlation coefficient of 92 %, wind direction bias was under 1.0 deg. Mean wind bias during Ernesto was 0.32 m/sec with correlation coefficient of 98 %; wind direction bias was also within 1.0 deg.

Table A-2 Buoys and C-MAN validation stations.

Station	Latitude	Longitude
44009	38.464	-74.702
44014	36.611	-74.836
CHLV2	39.910	-75.710
TPLM2	38.898	-76.437

Figure A2. Verification locations (image courtesy of NDBC).

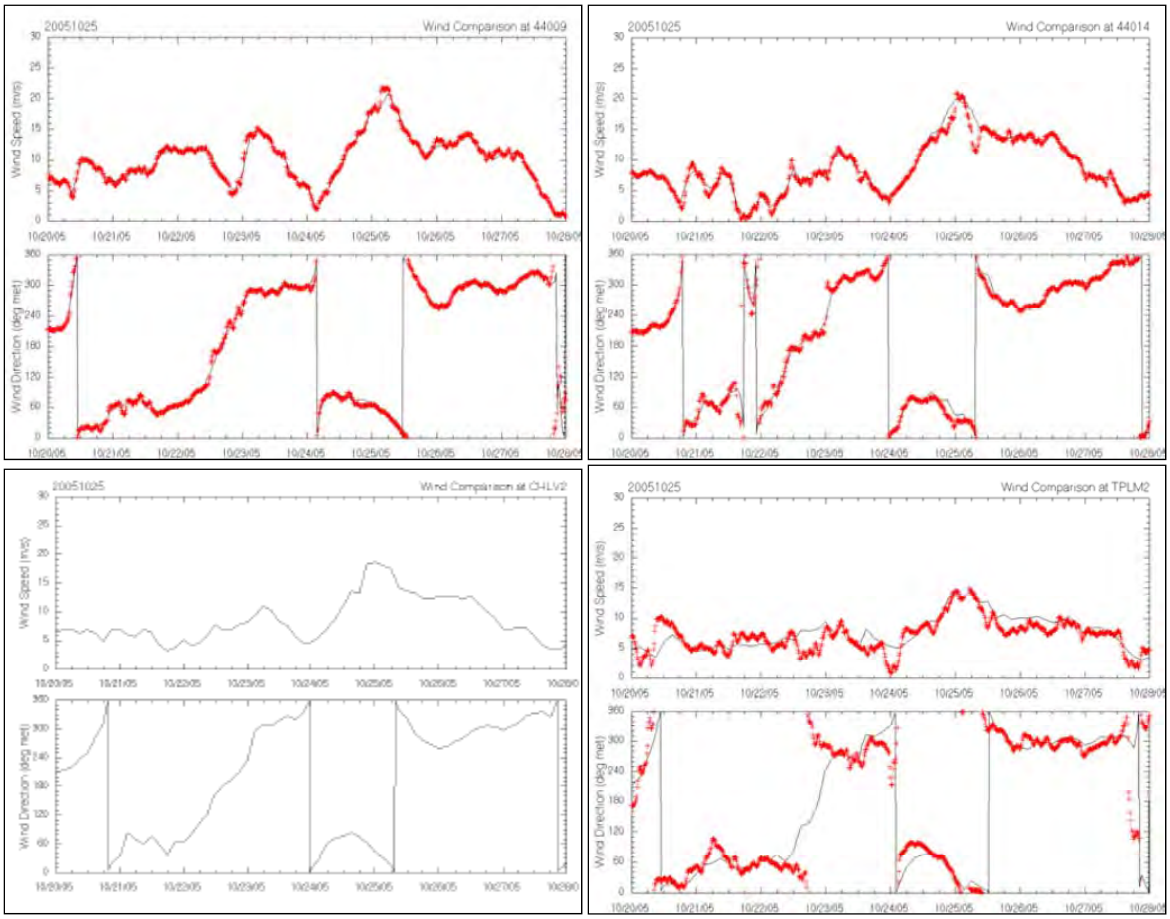

Figure A3. Comparison of wind speed (top) and direction (bottom) for four locations during extra-tropical cyclone 20051025. Red are NDBC observations, black is the hindcast.

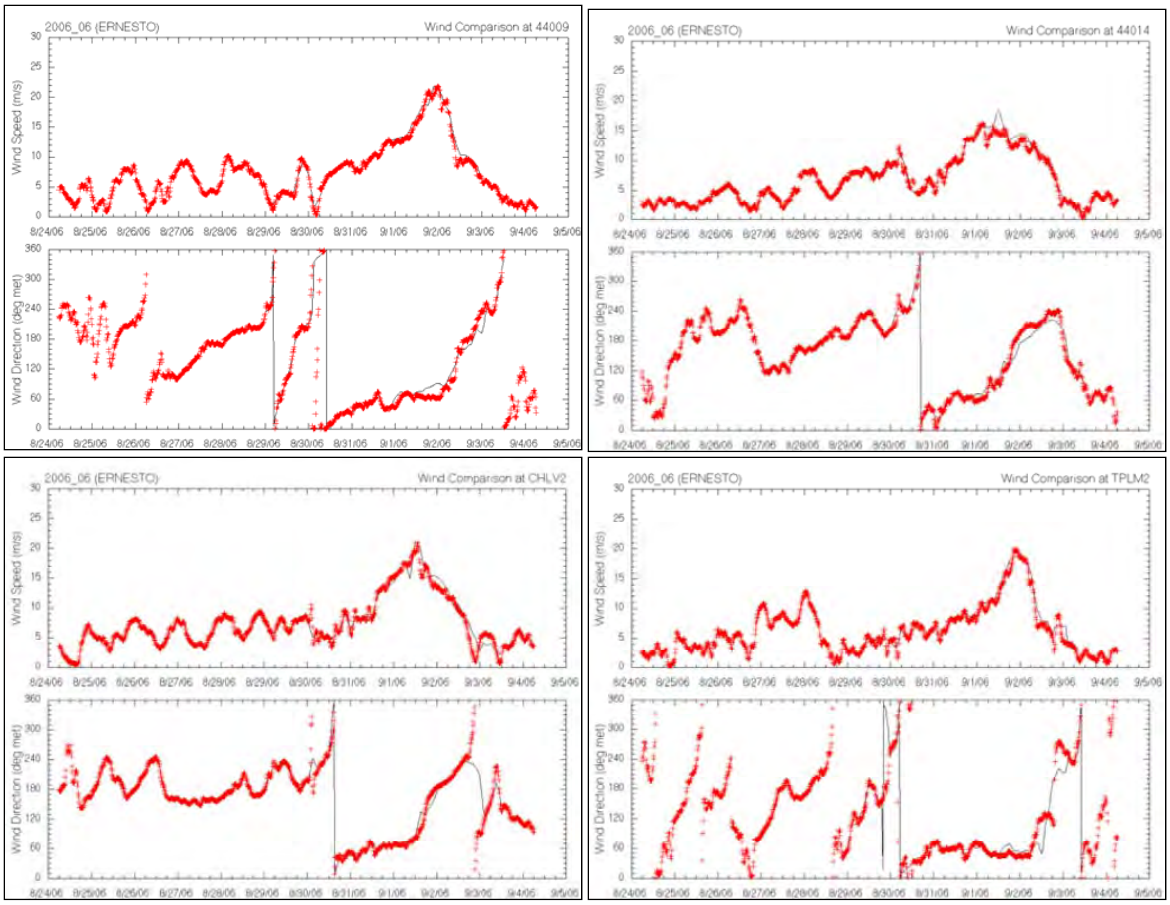

Figure A4. Comparison of wind speed (top) and direction (bottom) for four locations during Ernesto (2006_06). Red are NDBC observations, black is the hindcast.

TC96 tropical planetary boundary layer model transfer

The source code and documentation for the TC96 tropical boundary layer model use application were provided to RENCI for application in the Region III modeling work. The model is contained within a set of FORTRAN modules, which was delivered along with documentation pertaining to the model implementation.

References

Cox, A. T., J. A. Greenwood, V. J. Cardone, and V. R. Swail, 1995. An interactive objective kinematic analysis system. In *Proceedings 4th International Workshop on Wave Hindcasting and Forecasting*. 109-118. Banff, Alberta.

Cox, A. T., and V. J. Cardone. 2000. Operational System for the Prediction of Tropical Cyclone Generated Winds and Waves. *6th International Workshop of Wave Hindcasting and Forecasting*. Monterey, California.

Thompson, E. F., and V. J. Cardone. 1996. Practical modeling of hurricane surface wind fields. *Journal of Waterway, Port, Coastal, and Ocean Engineering* 195-205.

Appendix B: Extratropical Cyclone Selection in Support of FEMA Region III Storm Surge Modeling

Submitted to:

Jeff Hanson
ERDC-CHL-MS USACE Office
1261 Duck Road
Kitty Hawk, NC 27949
Tel: (252) 261-6840 x238
Jeffrey.L.Hanson@usace.army.mil

Work Performed under Contract W912BU-08-P-0291

October 20, 2008

Oceanweather, Inc.
5 River Road
Cos Cob, CT, USA
Tel: 203-661-3091
Fax: 203-661-6809
Email: oceanwx@oceanweather.com
Web: www.oceanweather.com

Approach

This report describes the extratropical cyclone selection process for the FEMA Region III coastal storm surge study. The primary area addressed includes both Chesapeake Bay and Delaware Bay and applies storm-ranking of surge events based on NOS measurements. Applying the measured NOS water level data — assuming a long continuous record is available at multiple stations — is consistent with other recent FEMA studies, such as that which was performed in North Carolina. A total of 30 storm events were identified for hindcast.

NOS station data

Historical NOS water level data are available for download from the NOS website and include both a measured and predicted (tide) component. The residual (measured-tide) water level was computed for all stations to remove the tidal response so that the storm selections are based on forcing, rather than tidal considerations. Measured data in the Chesapeake and Delaware Bays are shown in Figure B1 and include 20 measurement locations with indicated periods of record of at least 15-years length. In order to keep the storm selection process as unbiased as possible, multiple long-term records of water level data are required. Stations with large gaps, or short time records were not considered. Figure B2 shows the measured

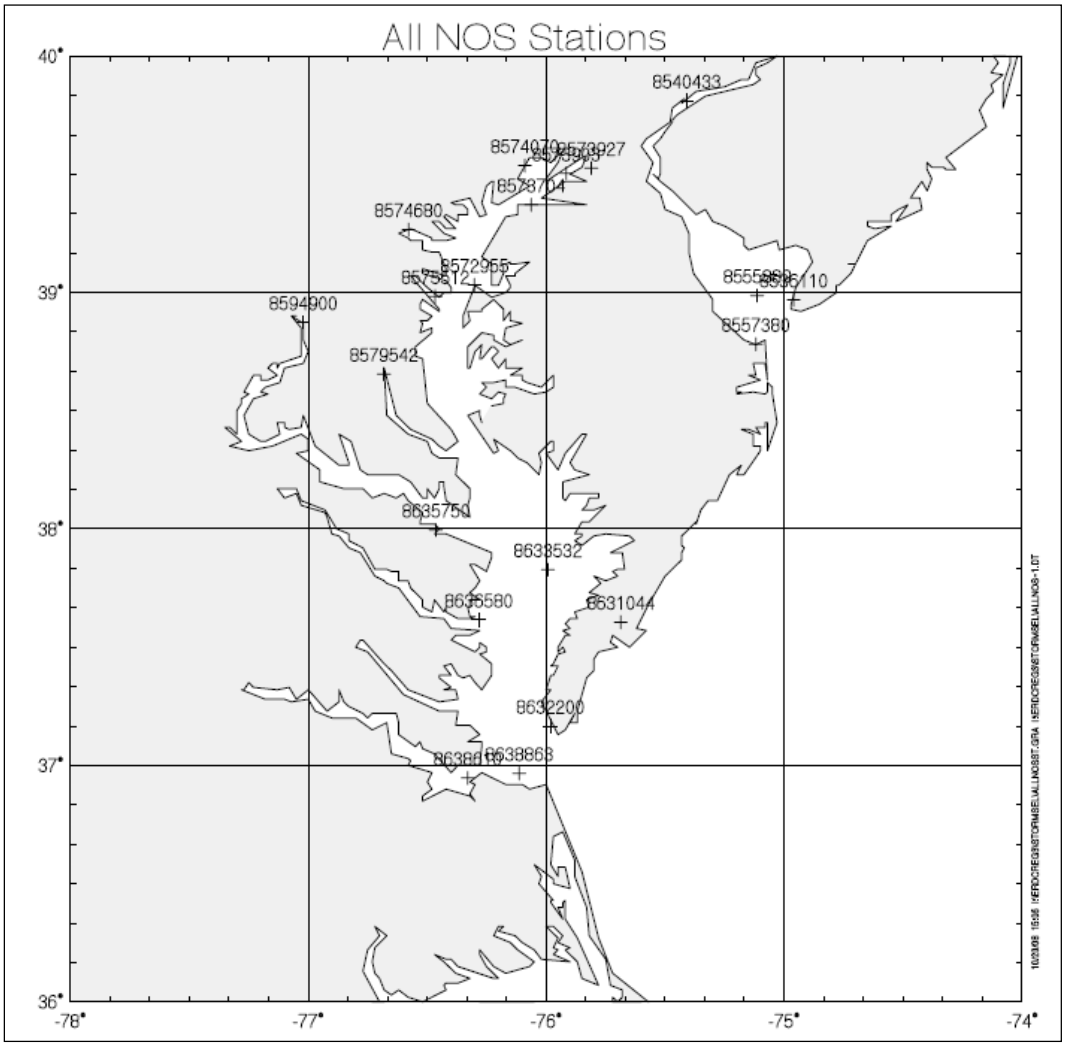

Figure B1. Available NOS station data in Chesapeake and Delaware Bay with records greater than 15 years length.

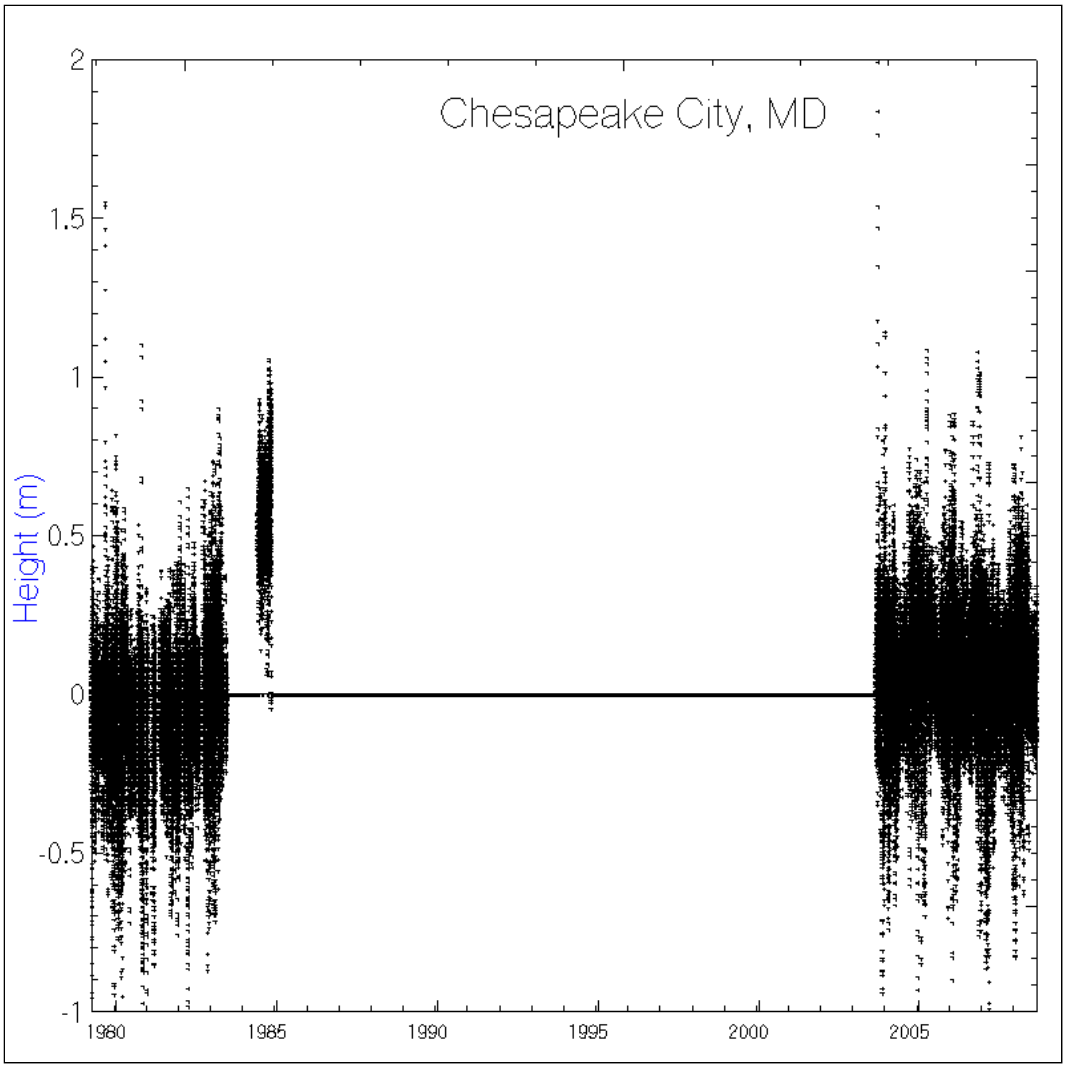

Figure B2. Historical residual water level measurements at Chesapeake City, MD (NOS 8573927) shown as an example of a record with large gaps.

residual water level at Chesapeake City, Maryland (NOS station 8573927), for which there are no reports from 1985-2004. When each of the NOS records are examined, only seven stations (Figure B3 and Table B1) are found to have good coverage during the period January 26, 1975 (based on NOS 8638863) to August 31, 2008 (present time when the selection was performed).

Storm ranking

At each selected NOS station, the water level peaks greater than the 99th percentile residual water level were identified individually as candidate storm events. Figure B4 shows the residual water level record at Chesapeake Bay Bridge Tunnel, VA (NOS 8638863) where peaks are identified

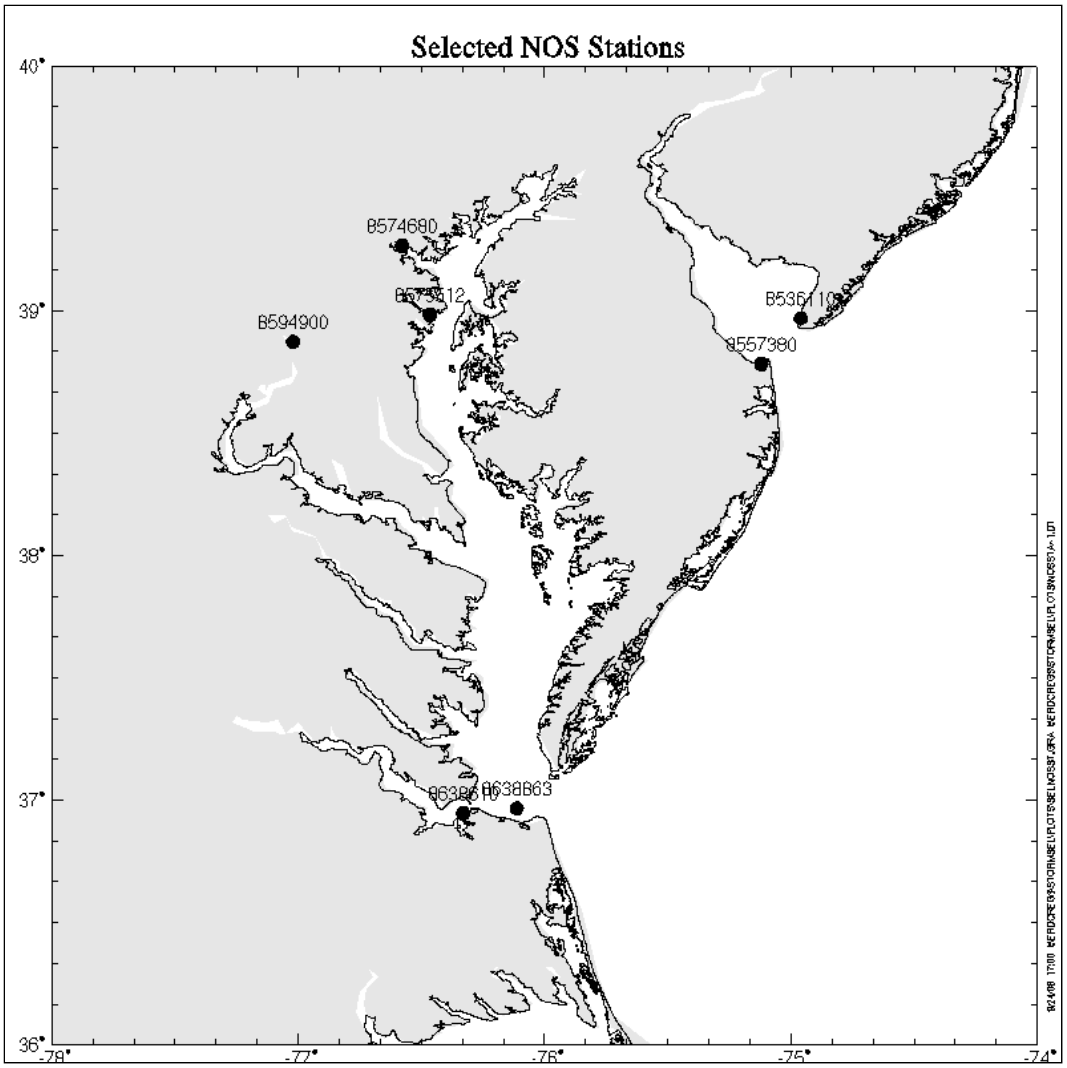

Figure B3. Selected NOS stations applied in the storm selection process.

Table B1. Select NOS stations applied in the storm selection process.

Station ID	Lat	Long	Record Began (YMD)	Record Ended (YMD)	Station Location
8638863	36.966	-76.113	19750126	20080831	Chesapeake Bay Bridge, VA
8638610	36.946	-76.33	19270701	20080831	Sewells Point, VA
8575512	38.983	-76.466	19280801	20080731	Annapolis, MD
8574680	39.266	-76.578	19020701	20080831	Baltimore, MD
8557380	38.781	-75.12	19570101	20080831	Lewes, DE
8536110	38.968	-74.96	19651101	20080831	Cape May, NJ
8594900	38.873	-77.021	19310401	20080831	Washington, DC

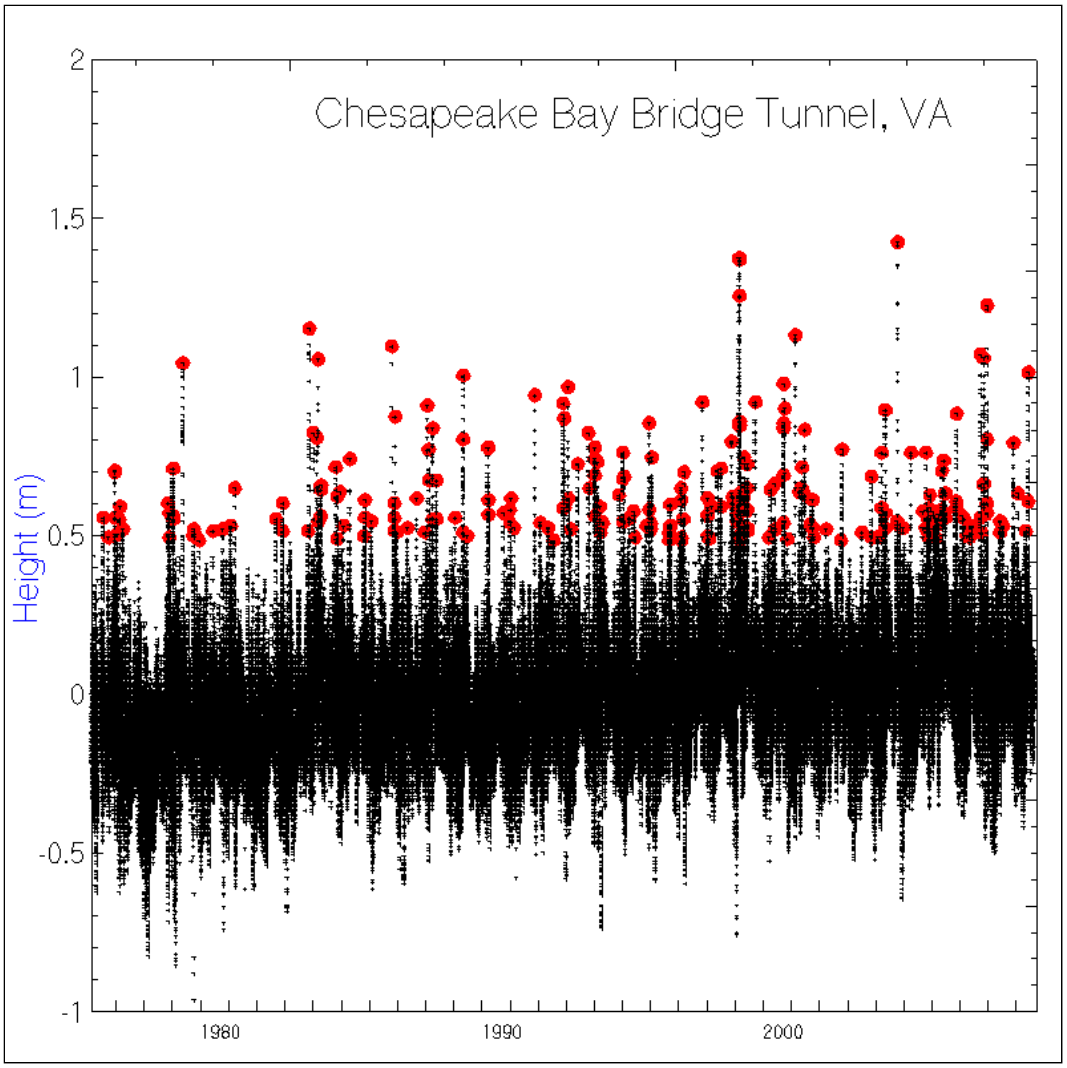

Figure B4. Peaks (red) greater that the 99th percentile residual water level identified at Chesapeake Bay Bridge Tunnel, VA NOS station.

(filled red circles in Figure B4) in the January 1975 to August 2008 period. Storm peaks were then ranked by station and the top ranked events matched with those from the other NOS stations within a 3.0-day window. A population of 30 events was obtained by taking the top-ranked storms from each of the NOS stations sequentially and removing dates found to be tropical in nature, as determined by historical tropical storm/hurricane tracks. During this period, the tropical cyclones of David (1979), Gloria (1985), Josephine (1996), Isabel (2003), and Ernesto (2006) were identified and removed from the storm list. Multiple storm peaks at a single NOS site within a 3.0-day period were merged into a single storm event. The storm-surge-ranked table represents at least the top six measured events at each individual station (Table B2). Storms with missing surge values typically

indicate that the measured water level was under the 99th percentile threshold, rather than missing from the archive entirely.

NOS stations in the mid-Chesapeake region and between the Chesapeake and Delaware Bays were removed in the selection process due to poor temporal coverage. However, their removal leaves a large portion of the mid-Chesapeake not represented by a NOS measurement station for the storm ranking. To test for missing storms, a separate storm ranking was performed for the period 1998-2005 using the Lewisetta, Virginia (NOS 8635750), Wachapreauge, Virginia (NOS 8631044); and Brandywine Shoal Light, Delaware (NOS 8555889) stations. Table B3 shows the top five extra-tropical events at each station. This ranking indicates that four of the five top storms at Lewistetta, three of five at Wachapreauge, and three of five at Brandywine Shoal Light were identified for hindcast, and the top events in the 1998-2003 period at each station are also represented in the hindcast. Figure B5 shows plots of residual water level and sea level pressures for each storm.

Table B2. Extratropical cyclones selected from the period Jan-1975 to Aug-2008 based on seven NOS stations.

Storm Date	Chesapeake Bay Bridge Tunnel, VA 8638863 Date (YMD)	Residual (m)	Rank	Sewells Point, VA 8638610 Date	Residual	Rank	Annapolis, MD 8575512 Date (YMD)	Residual (m)	Rank	Baltimore, MD 8574680 Date (YMD)	Residual (m)	Rank	Lewes, DE 8557380 Date (YMD)	Residual (m)	Rank	Cape May, NJ 8536110 Date (YMD)	Residual (m)	Rank	Washington, DC 8594900 Date (YMD)	Residual (m)	Rank
19750926										19750926	0.4687	25+							19750926	1.435	5
19780126							19780126	0.993	3	19780126	1.152	1				19780126	0.803	25+	19780126	1.23	12
19780427	19780427	1.044	8	19780426	1.219	5							19780427	0.648	25+	19780427	0.592	25+	19780427	0.643	25+
19790226										19790226	0.6696	25+	19790226	0.7357	25+				19790226	1.816	3
19821025	19821025	1.152	4	19821025	1.312	3							19821025	0.88	25+	19821025	0.731	25+			
19830404							19830403	0.751	14	19830403	0.916	7				19830404	0.6276	25+	19830403	0.8488	25+
19840216										19840215	0.499	25+							19840216	1.523	4
19840329	19840329	0.741	25+	19840329	0.725	25+							19840329	1.219	5	19840329	1.05	9	19840329	0.885	59
19850212							19850213	0.818	9	19850213	0.993	5	19850212	0.6328	25+	19850212	0.7511	25+	19850212	0.8694	72
19851107	19851104	0.875	21	19851104	0.967	17	19851105	1.024	1	19851105	1.127	2	19851105	0.9	25+	19851105	0.849	25+	19851108	2.078	2
19870102	19870102	0.911	17	19870102	0.921	21	19870103	0.4836	25+	19870102	0.4687	25+	19870102	1.158	8	19870102	0.962	19			
19911031	19911031	0.916	16	19911101	0.89	25+	19911101	0.772	13	19911101	0.737	25	19911031	1.147	9	19911031	1.08	6	19911101	0.7788	25+
19920105	19920104	0.937	12	19920104	0.865	25+	19920105	0.628	25+	19920105	0.6328	25+	19920104	1.219	6	19920104	1.07	7	19920105	0.6533	25+
19921211	19921212	0.777	25+	19921211	0.751	25+	19921211	0.689	25+	19921211	0.756	25+	19921211	1.142	10	19921211	1.343	2	19921211	1.07	18
19930305							19930305	0.7099	25+	19930305	0.89	14	19930304	0.8848	25+	19930304	0.6996	25+	19930306	1.302	7
19931128							19931128	0.983	4	19931128	1.06	4	19931125	0.5144	25+	19931128	0.5762	25+	19931128	1.086	14
19940104	19940104	0.6642	25+	19940104	0.6842	25+	19940104	0.839	8	19940104	0.911	8	19940104	1.1678	7	19940104	1.111	5	19940104	0.6636	25+
19960108	19960107	0.6482	25+	19960107	0.6636	25+				19960109	0.5042	25+	19960108	1.523	2	19960108	1.549	1			
19980119							19980119	0.689	25+	19980119	0.8385	13							19980121	2.572	1
19981009	19981003	0.921	14	19981008	1.178	8	19981010	0.53	25+	19981010	0.54	25+	19981008	0.916	25+	19981008	0.756	25+	19981010	0.561	25+
19980128	19980123	1.374	1	19980128	1.41	2	19980130	0.725	19	19980130	0.737	24	19980128	1.42	3	19980128	1.168	4	19980130	1.065	19
19980205	19980205	1.338	2	19980205	1.528	1	19980205	0.854	6	19980206	0.808	19	19980205	1.559	1	19980205	1.322	3	19980207	1.368	6
19980309							19980309	0.844	7	19980309	0.933	6							19980309	0.9383	25+
20000125	20000125	1.132	5	20000125	1.235	4				20000120	0.499	25+	20000125	1.014	21	20000125	0.9	25			
20021017	20021013	0.634	25+	20021016	0.6996	25+				20021019	0.4687	25+	20021016	1.044	19	20021016	1.034	10	20021016	0.5556	25+
20051025	20051025	0.835	20	20051025	0.9	25+	20051025	0.592	25+	20051025	0.5402	25+	20051025	1.096	12	20051025	1.07	8	20051025	0.7459	25+
20061007	20061007	1.06	6	20061007	1.194	7	20061008	0.53	25+	20061007	0.478	4	20061007	0.941	25+	20061007	0.777	25+	20061006	0.659	25+
20061028							20061028	0.869	5	20061028	1.038	8				20061028	0.5865	25+	20061028	0.8385	25+
20061122	20061122	1.224	3	20061122	1.199	6	20061117	1.014	2	20061117	1.111	3	20061123	0.993	24	20061123	0.89	25+	20061117	0.936	25+
20080512	20080513	1.014	9	20080513	0.972	16	20080512	0.725	20	20080512	0.737	32	20080512	1.26	4	20080512	1.029	11	20080514	1.055	20

Table B3. 1998-2005 storms found at mid-Chesapeake NOS stations.

Lewisetta, VA 8635750				Wachapreauge, VA 8631044				Brandywine Shoal Light, DE 8555889			
Date (YMD)	Residual (m)	Rank	In Storm List?	Date (YMD)	Residual (m)	Rank	In Storm List?	Date (YMD)	Residual (m)	Rank	In Storm List?
19980205	0.9517	1	Yes	19980205	1.6874	1	Yes	20051025	1.1009	1	Yes
19990916	0.9003	2	No	19980128	1.6822	2	Yes	20080512	1.1009	2	Yes
20080512	0.7871	3	Yes	19990830	1.0803	3	No	20021016	1.0906	3	Yes
19961008	0.7665	4	Yes	19961008	1.0752	4	Yes	20031214	1.0083	4	No
20051025	0.7357	5	Yes	19970424	0.9363	5	No	20031206	1.0032	5	No

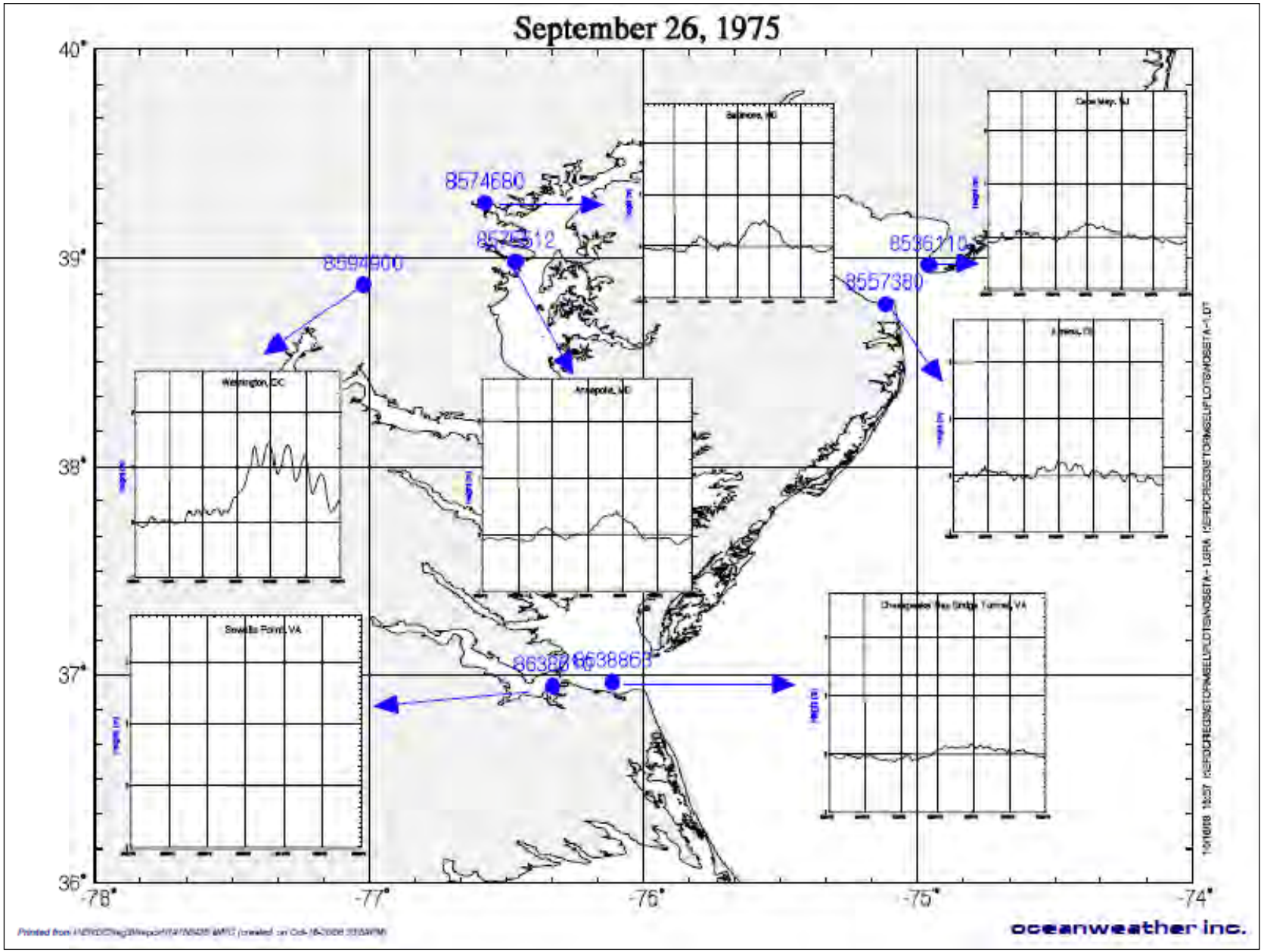

Figure B5. Plots of residual water level and sea level pressures for each storm. (Sheet 1 of 60)

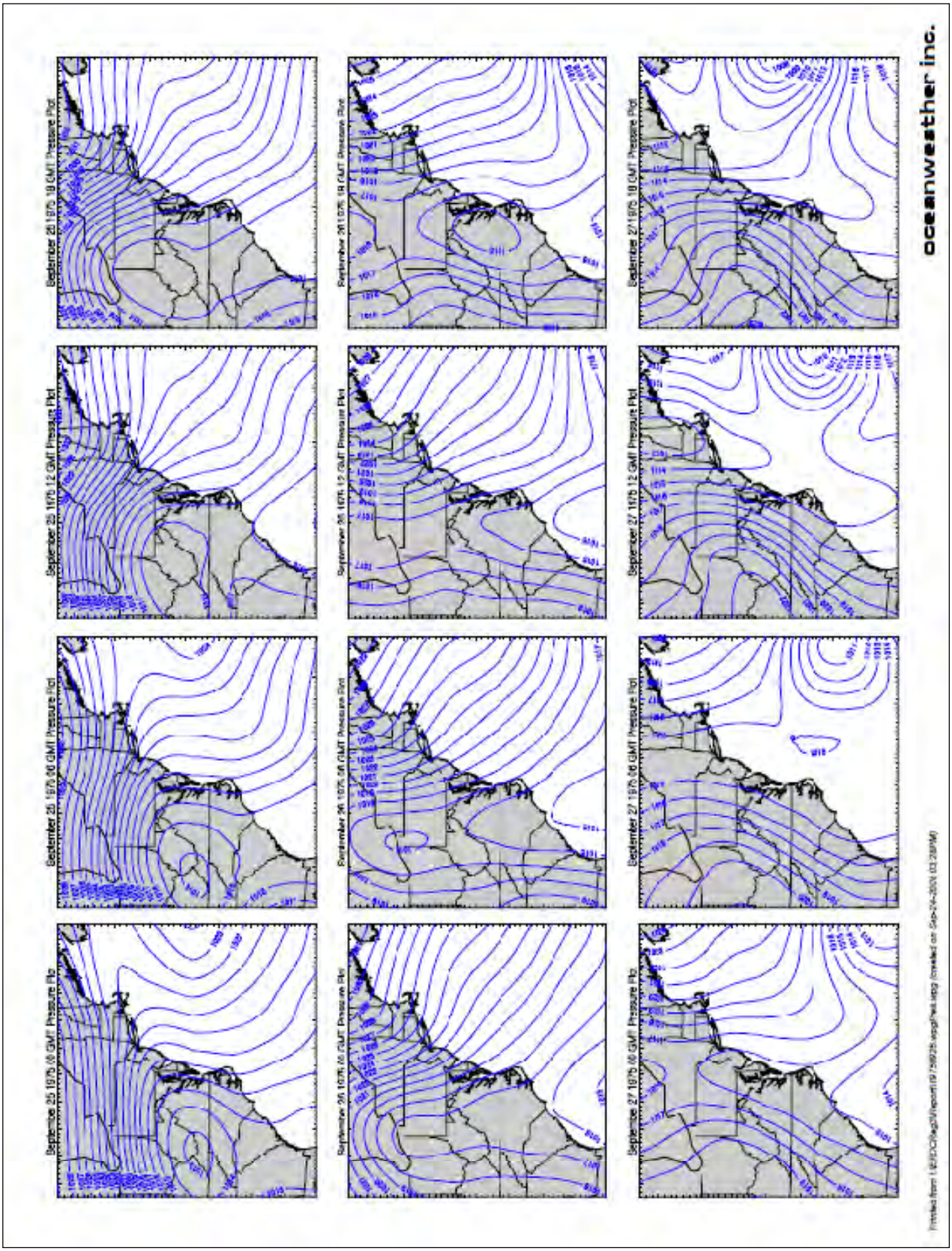

Figure B5. (Sheet 2 of 60)

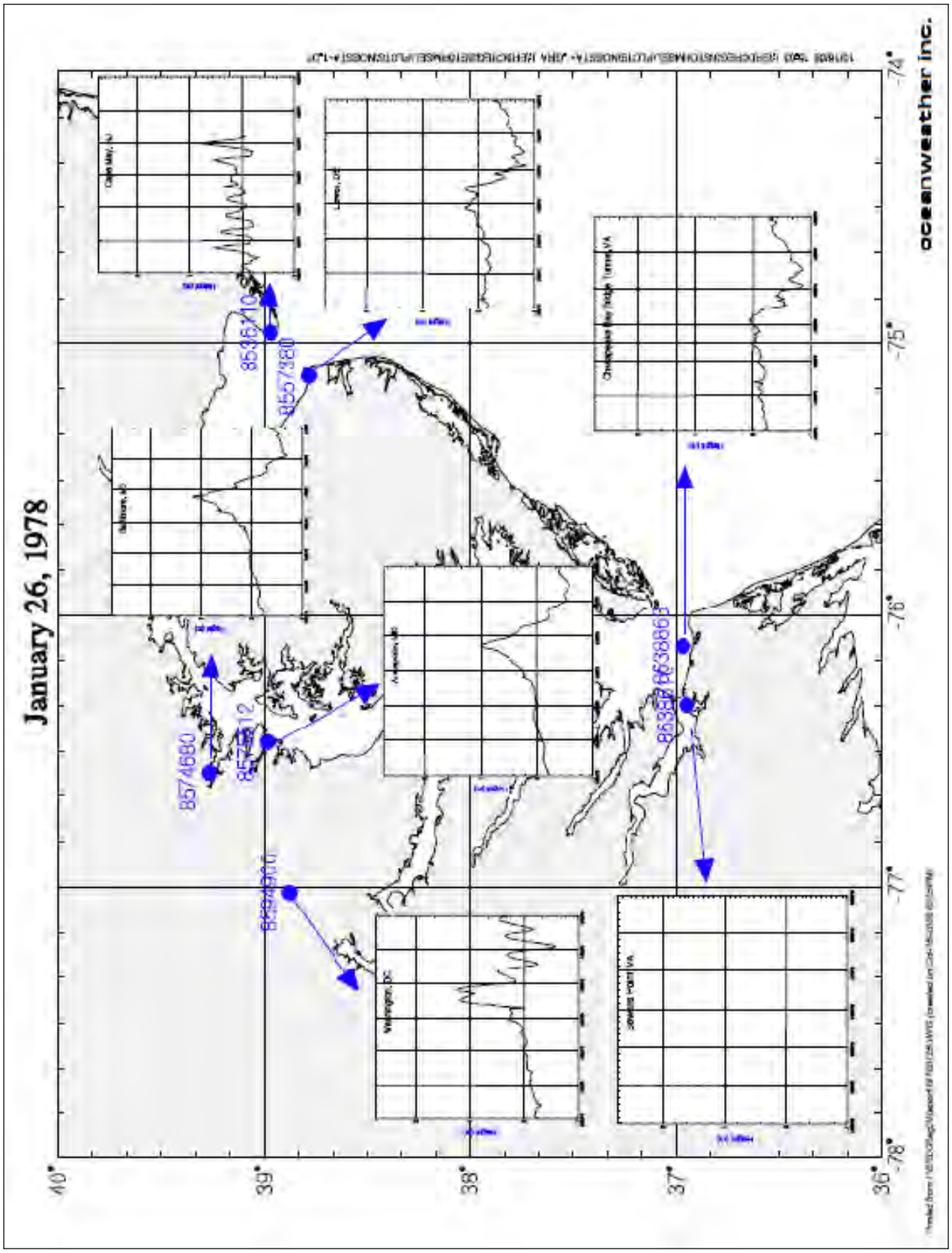

Figure B5. (Sheet 3 of 60)

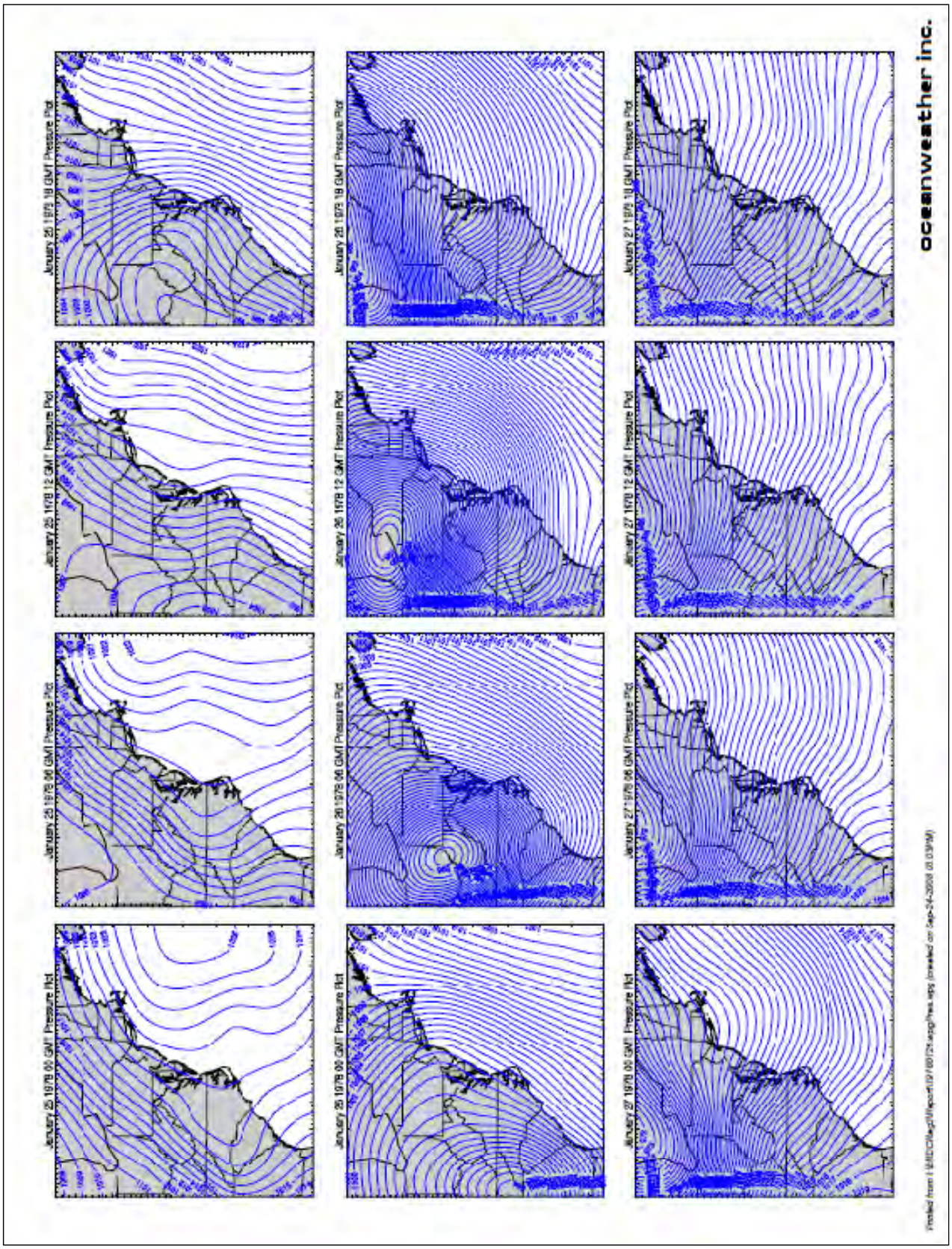

Figure B5. (Sheet 4 of 60)

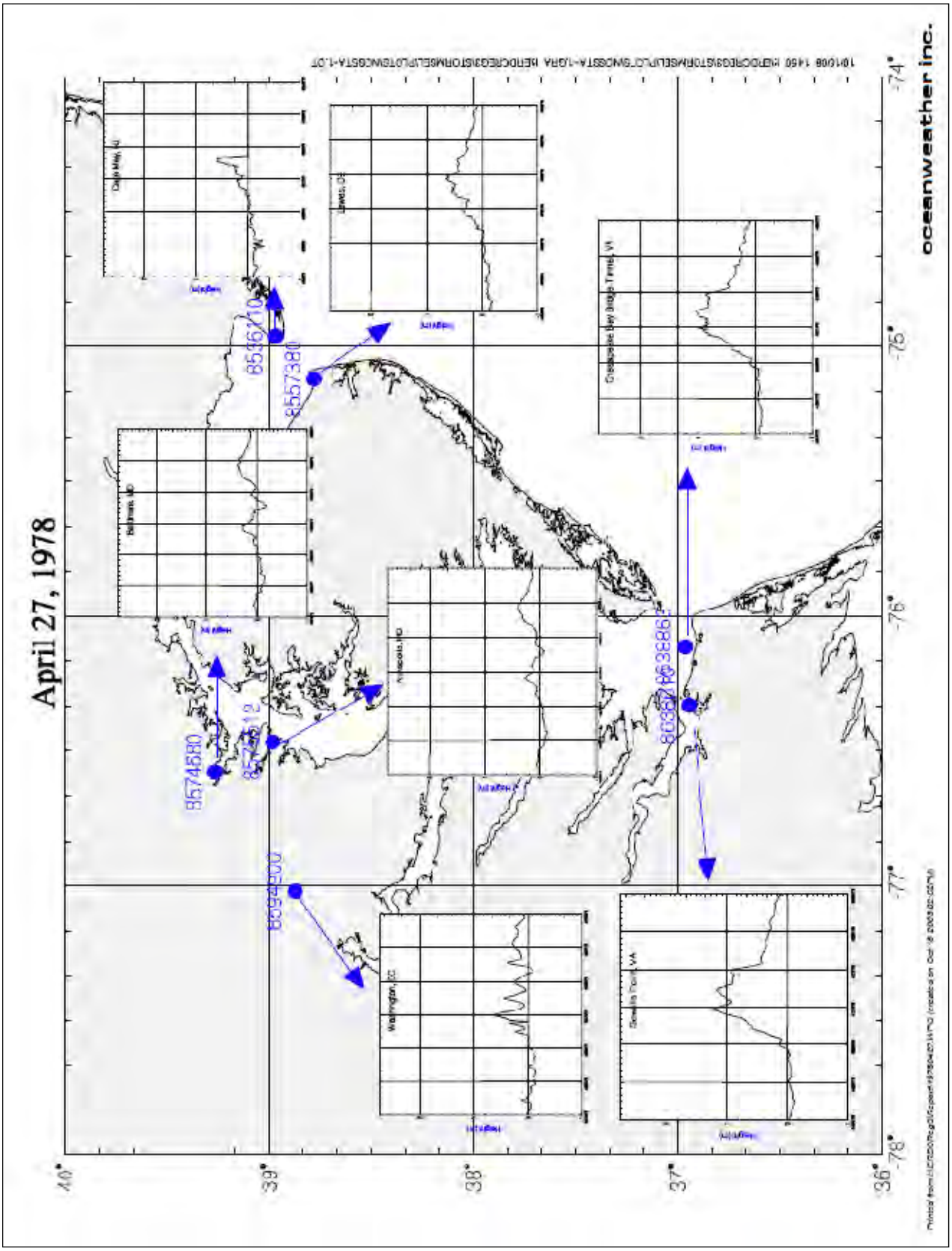

Figure B5. (Sheet 5 of 60)

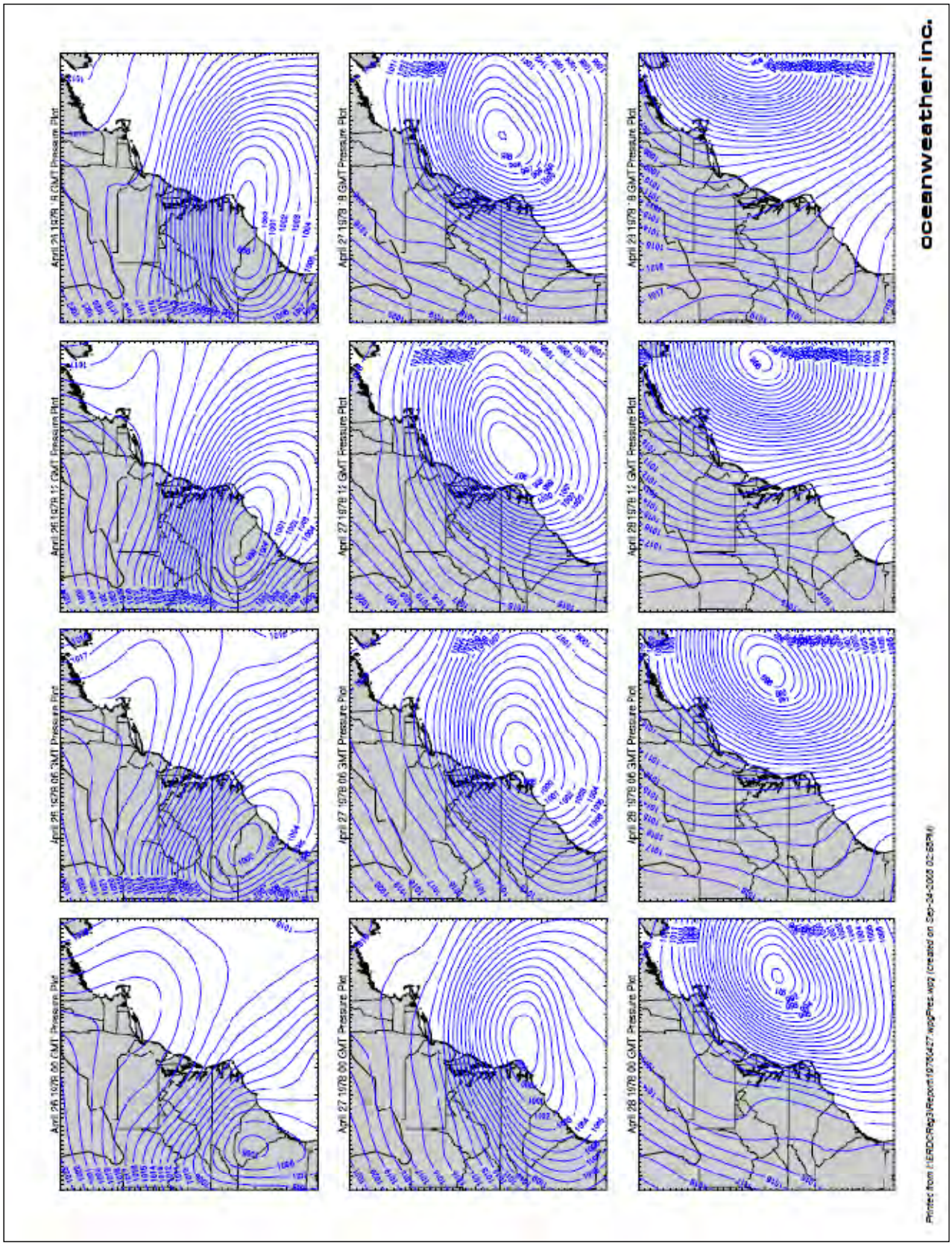

Figure B5. (Sheet 6 of 60)

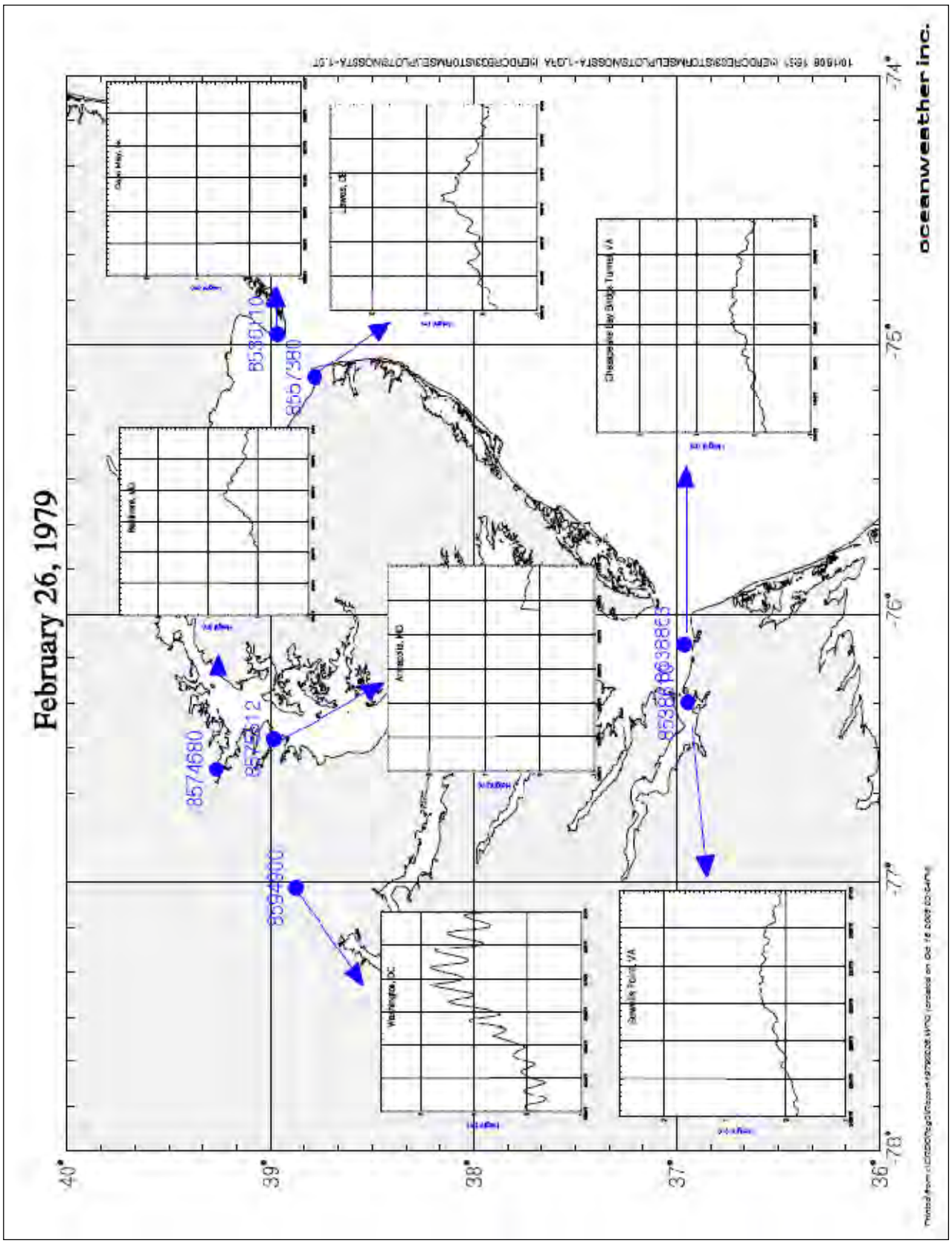

Figure B5. (Sheet 7 of 60)

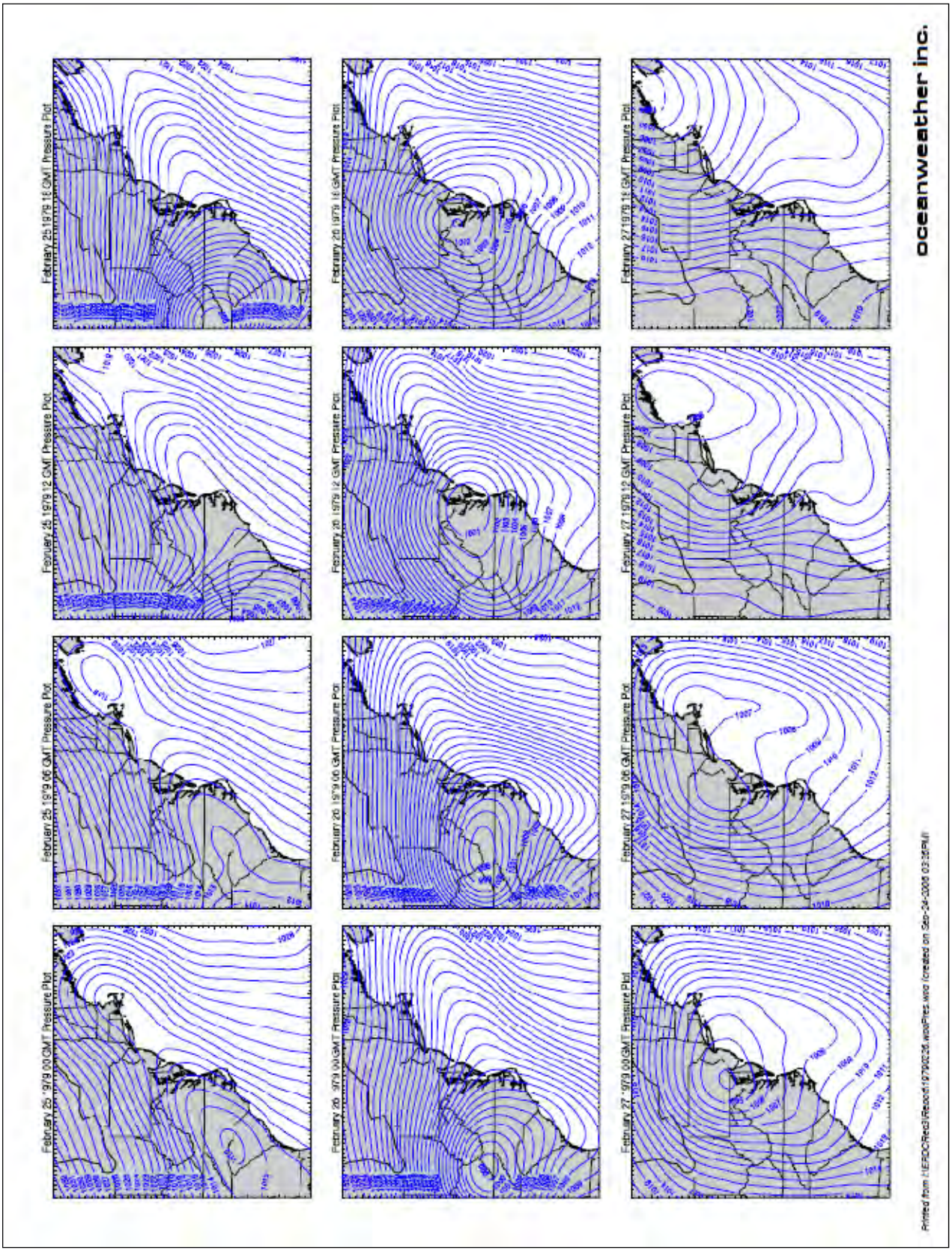

Figure B5. (Sheet 8 of 60)

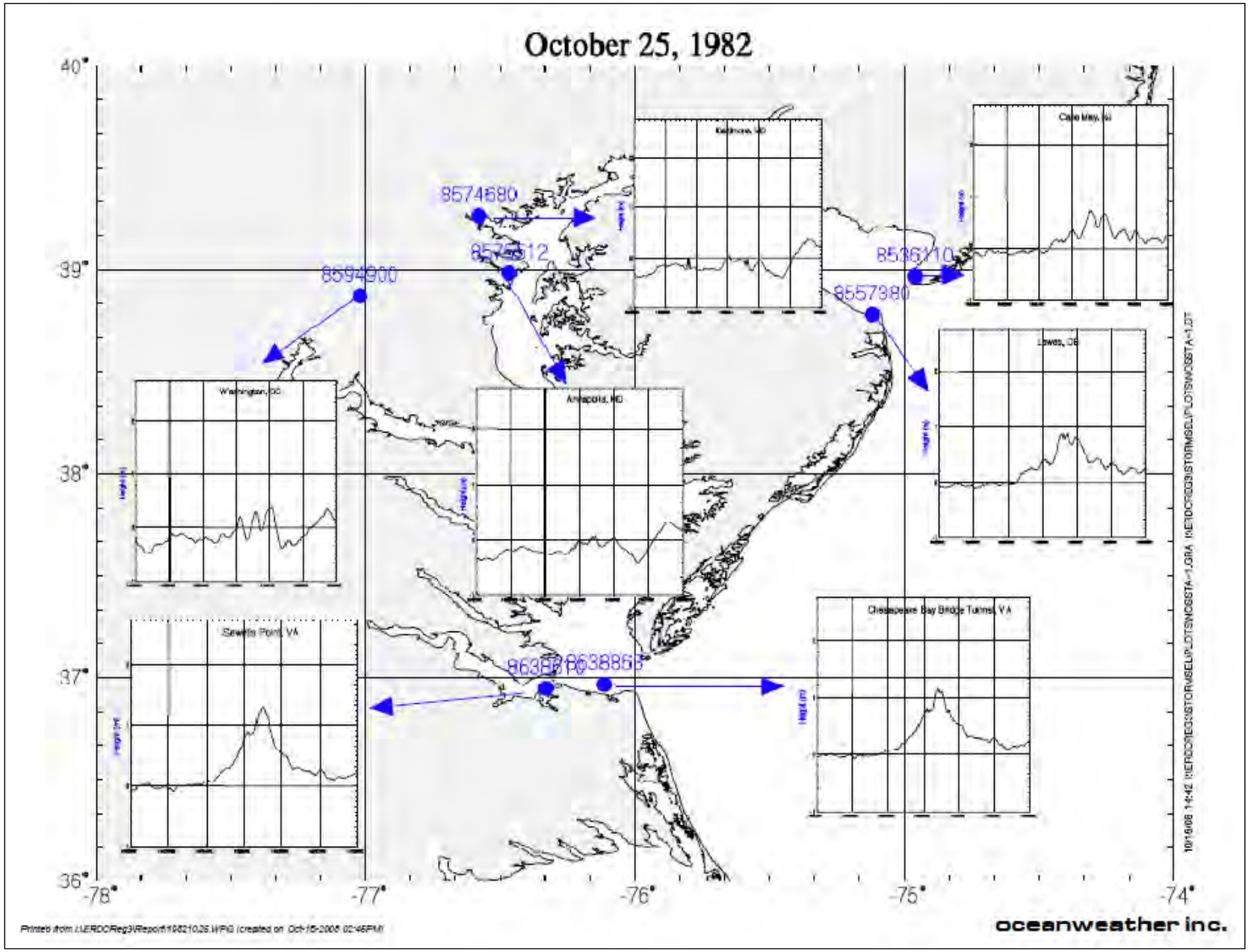

Figure B5. (Sheet 9 of 60)

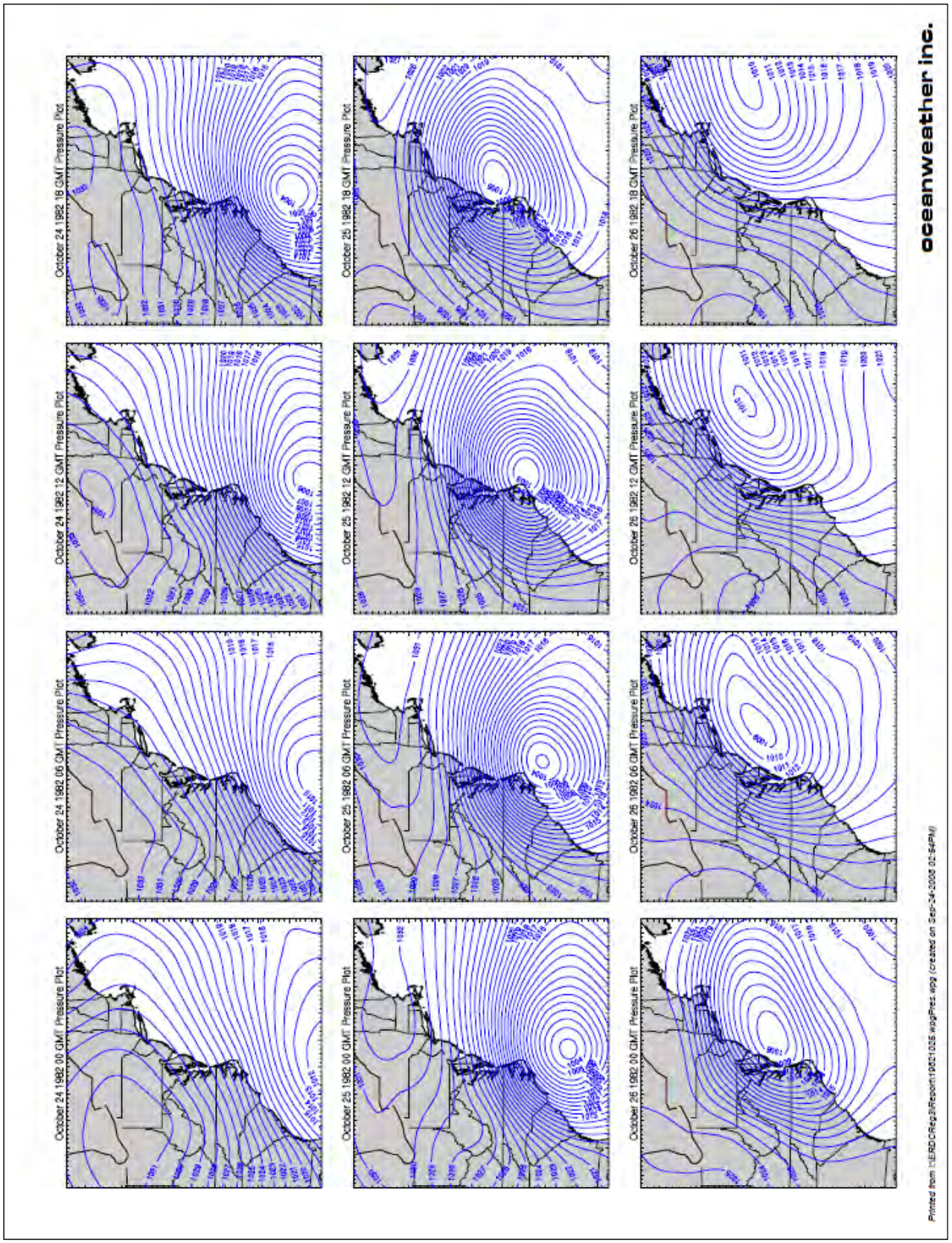

Figure B5. (Sheet 10 of 60)

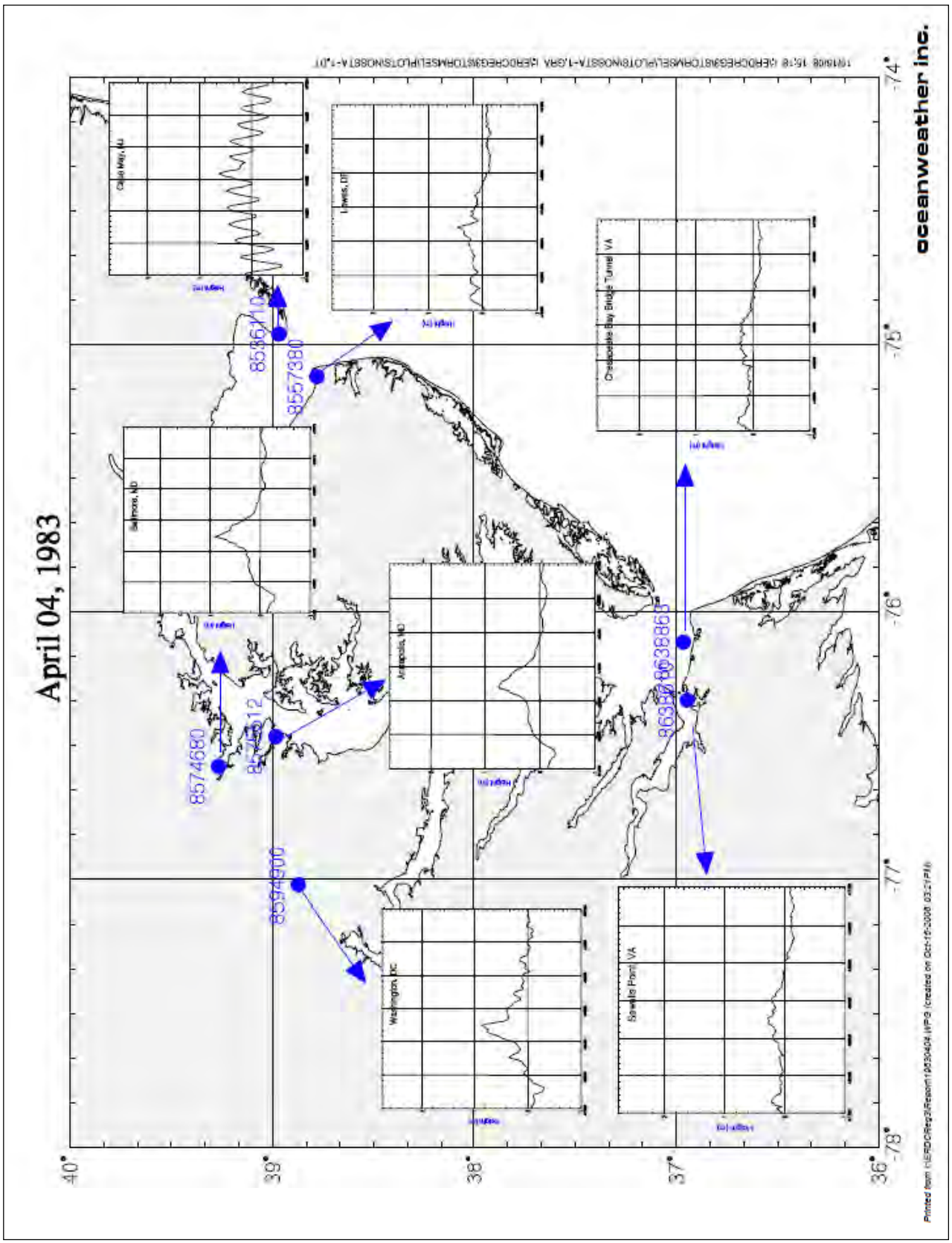

Figure B5. (Sheet 11 of 60)

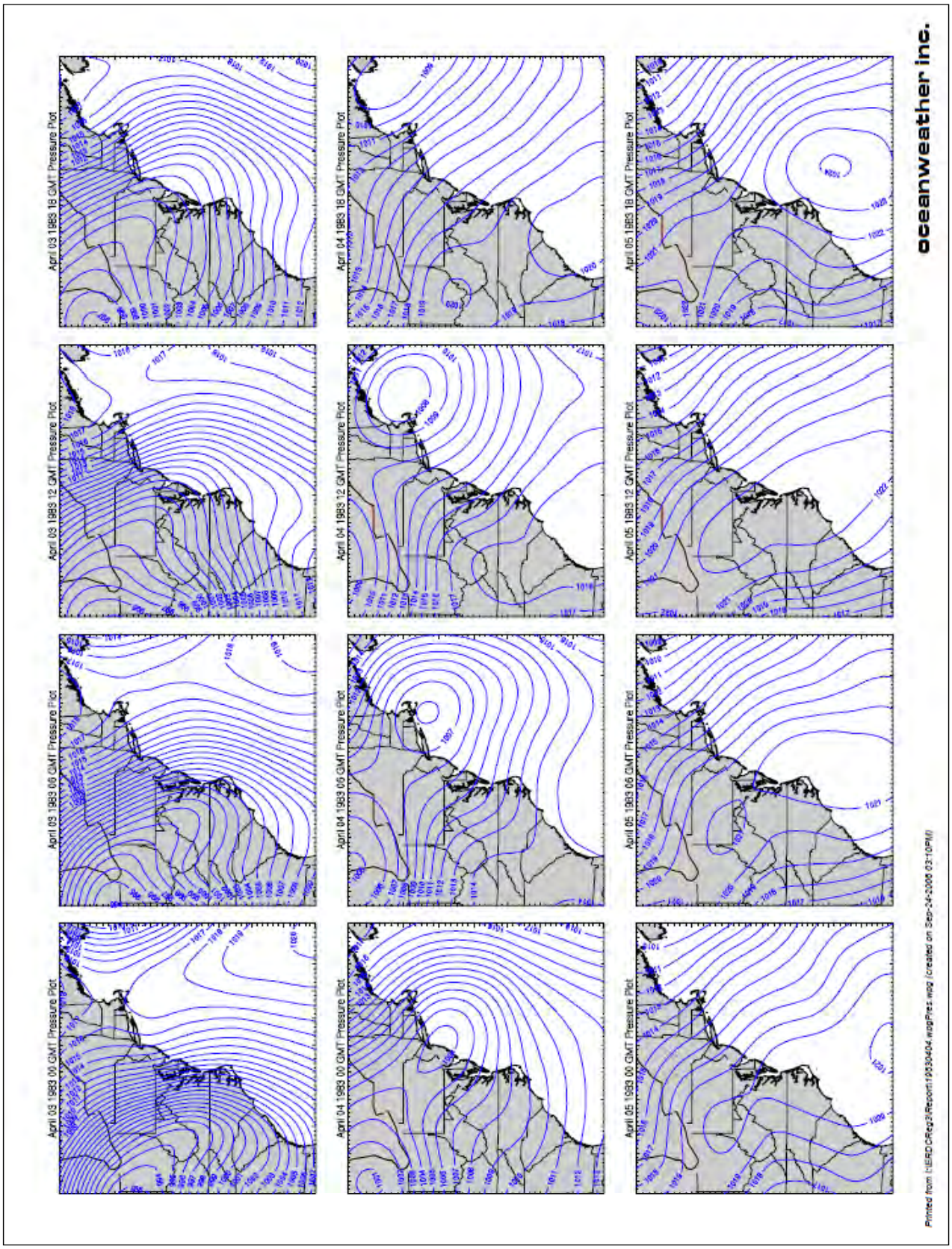

Figure B5. (Sheet 12 of 60)

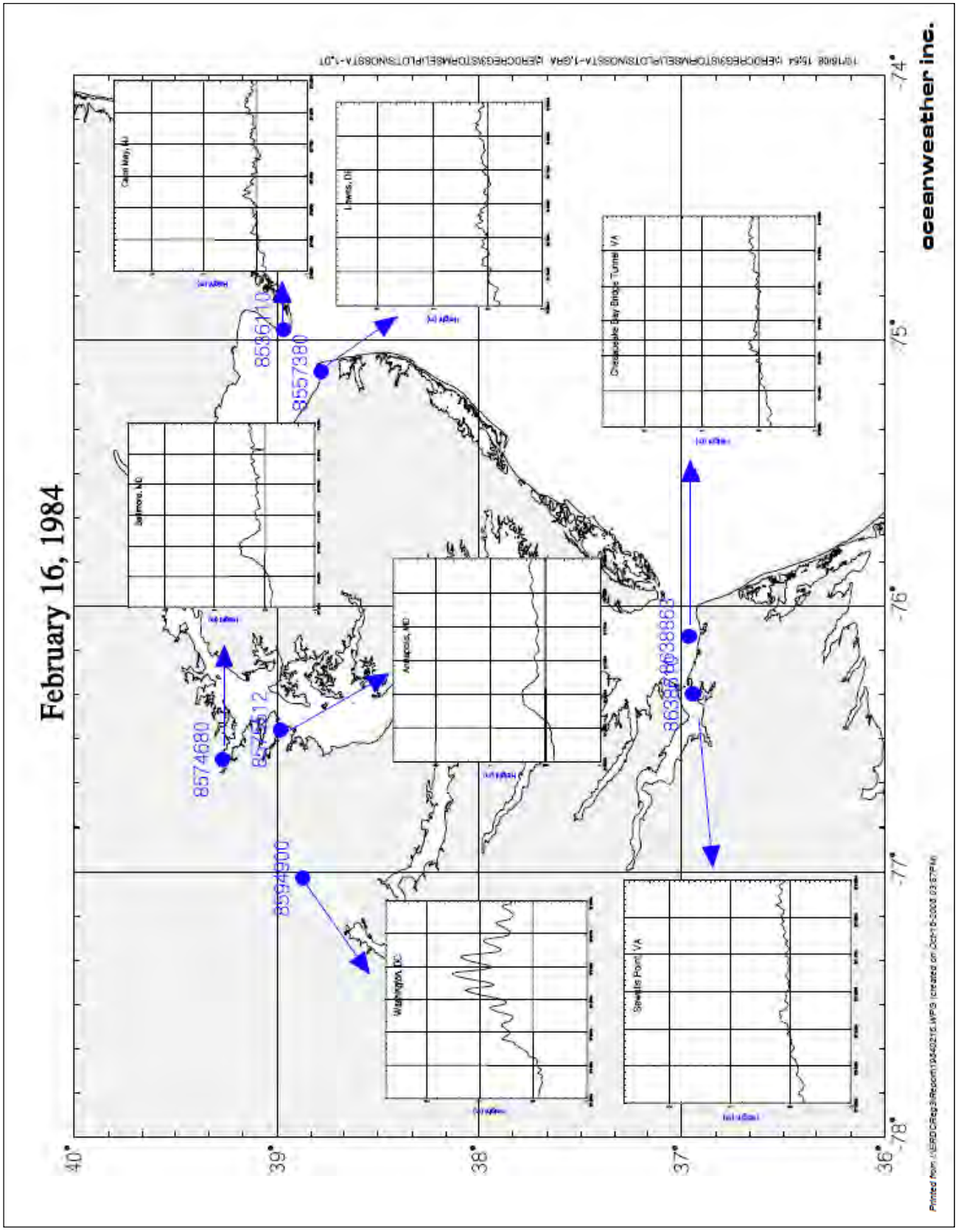

Figure B5. (Sheet 13 of 60)

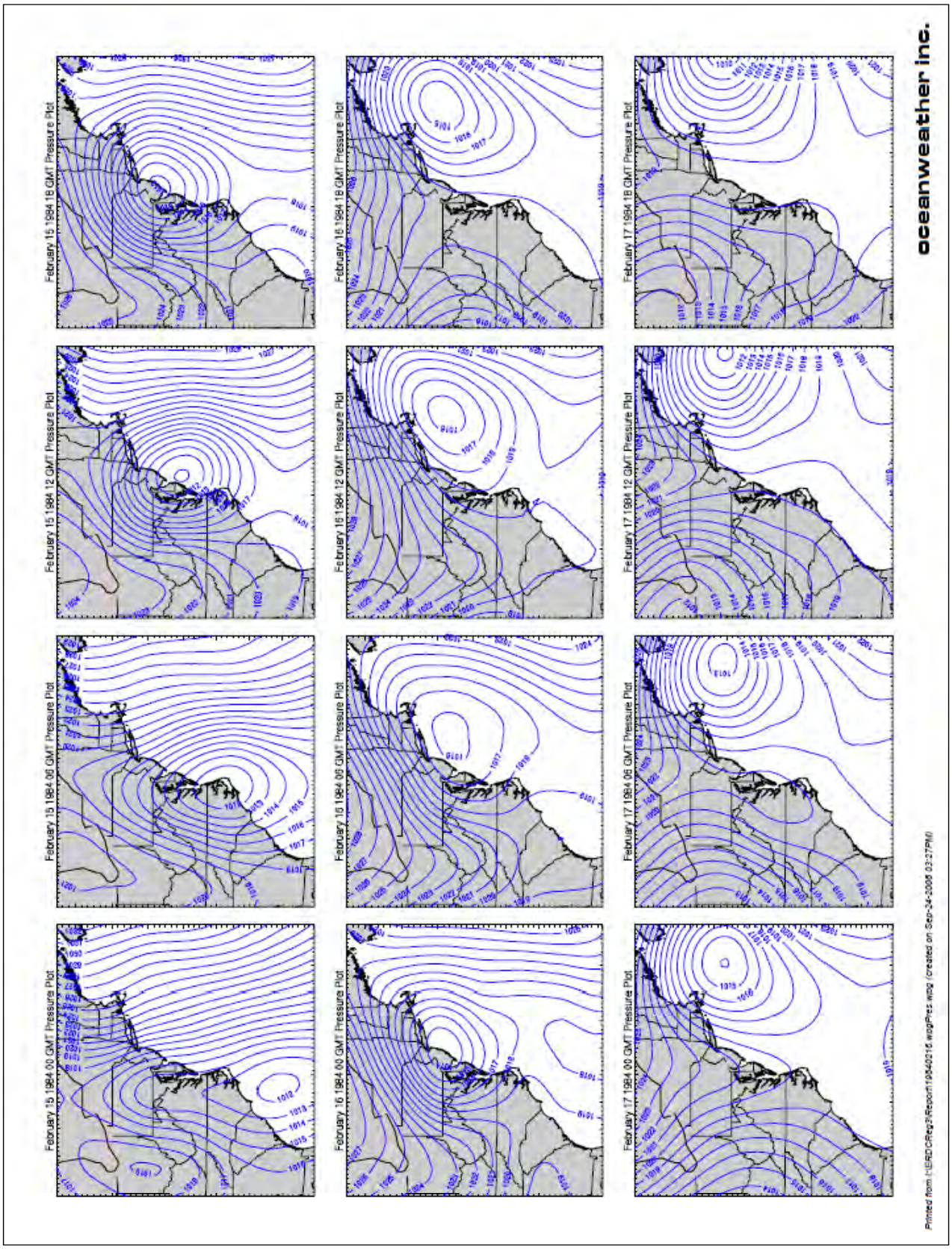

Figure B5. (Sheet 14 of 60)

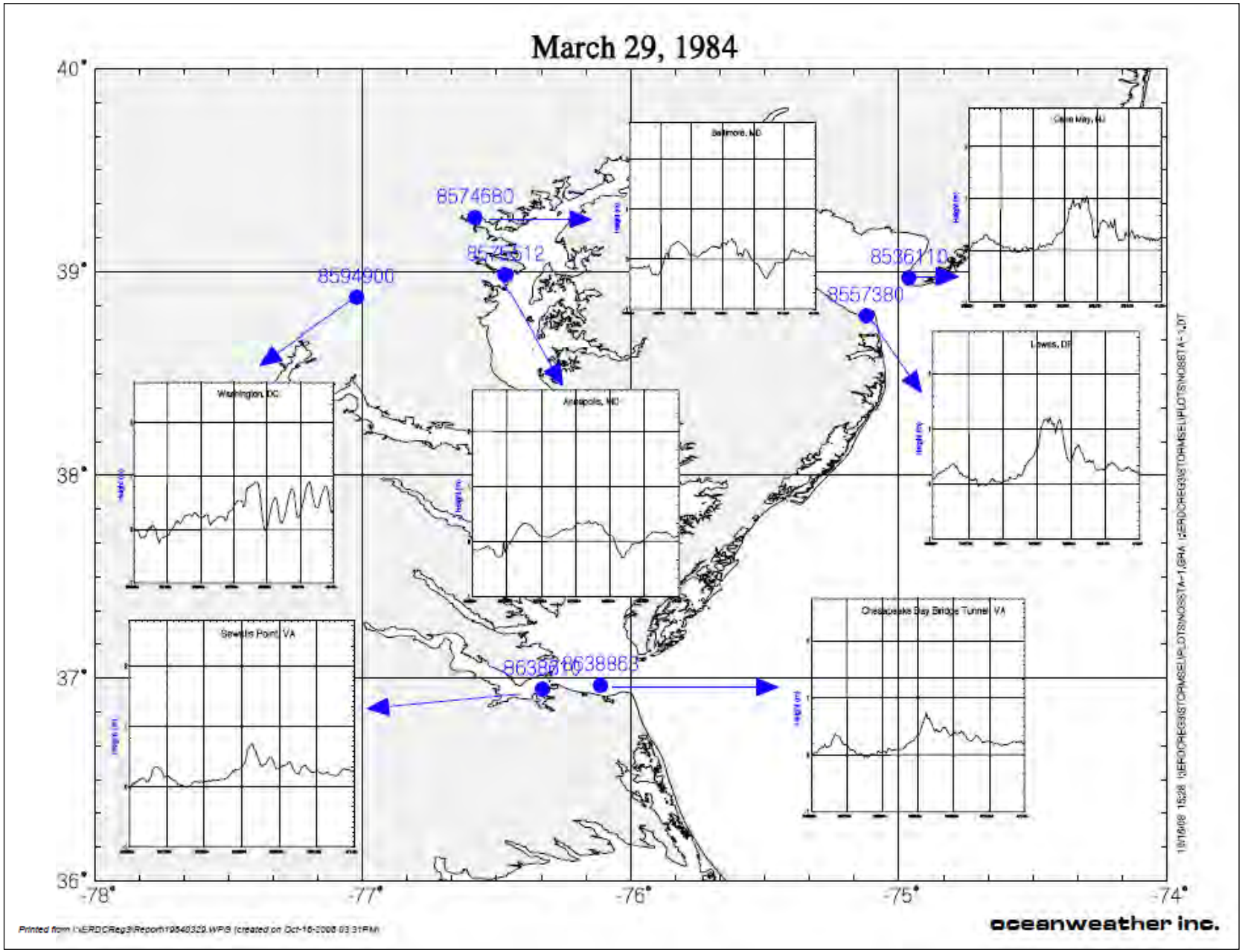

Figure B5. (Sheet 15 of 60)

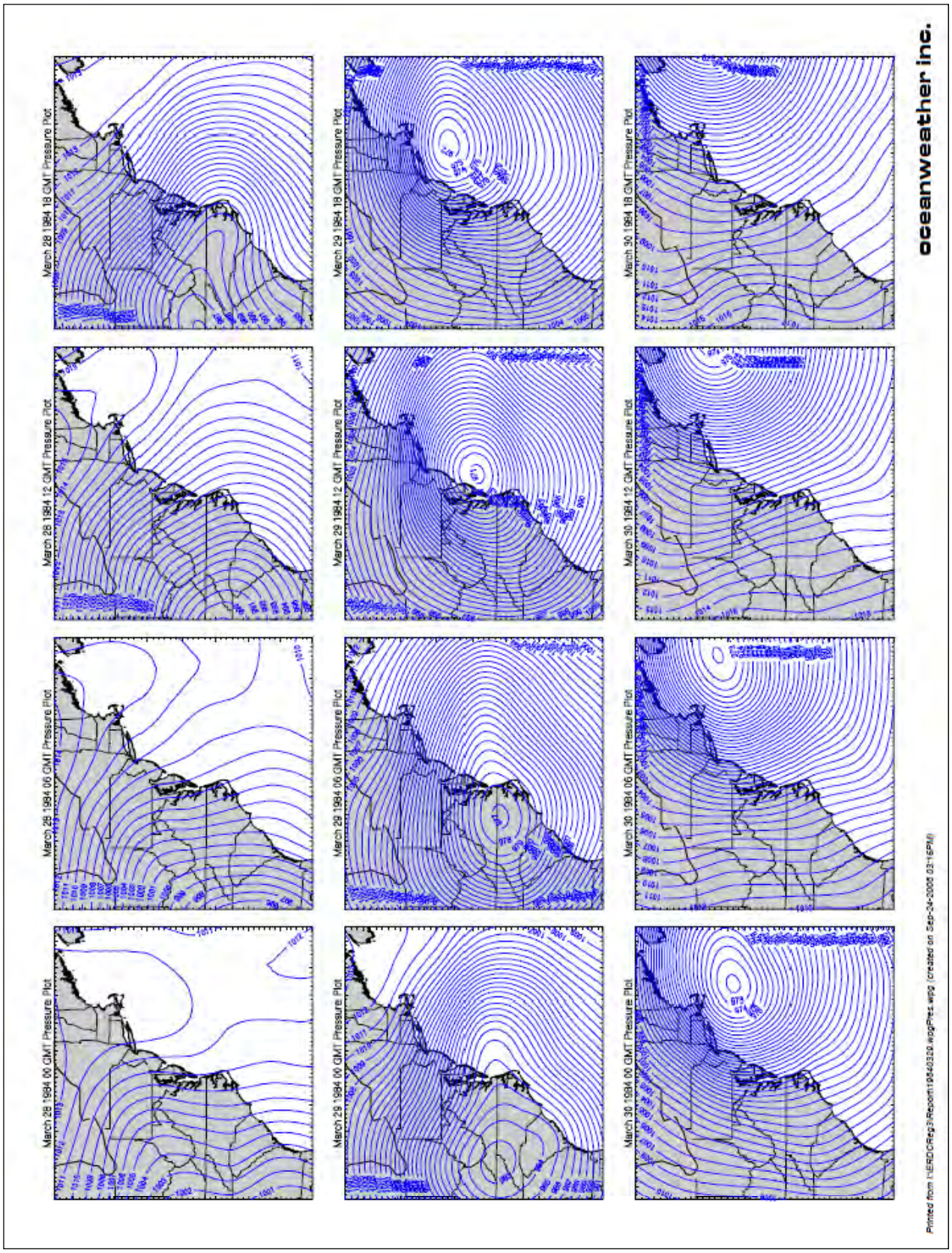

Figure B5. (Sheet 16 of 60)

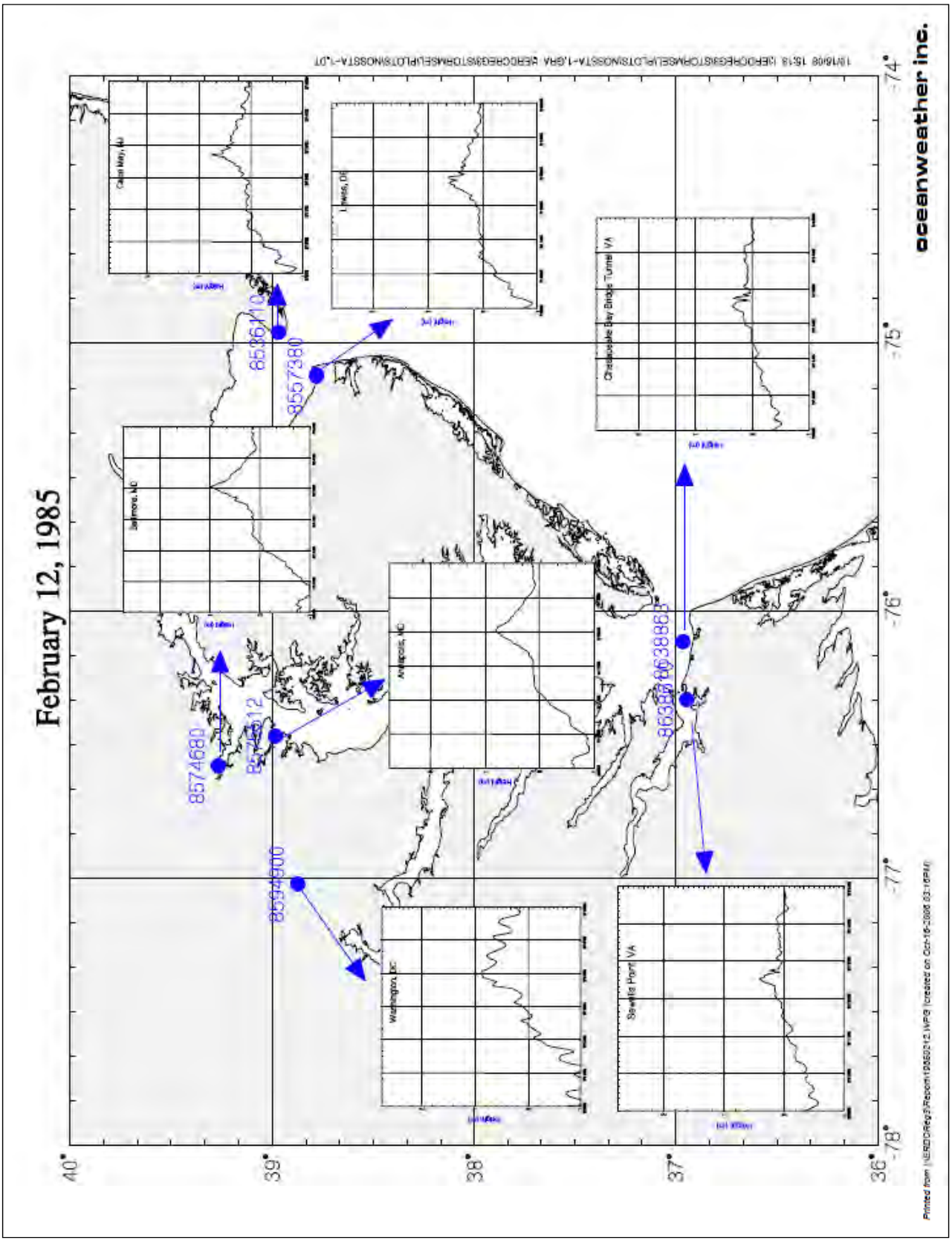

Figure B5. (Sheet 17 of 60)

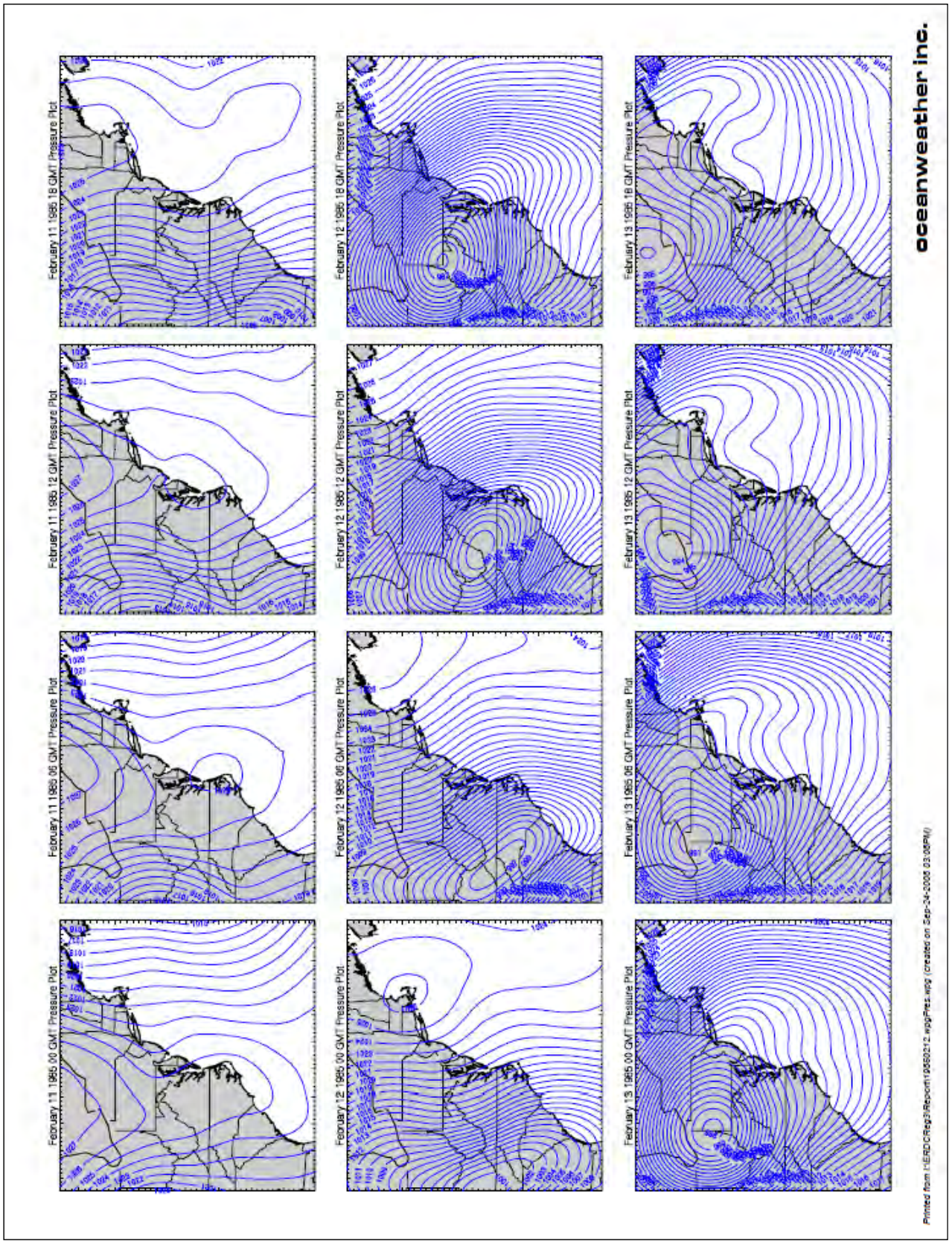

Figure B5. (Sheet 18 of 60)

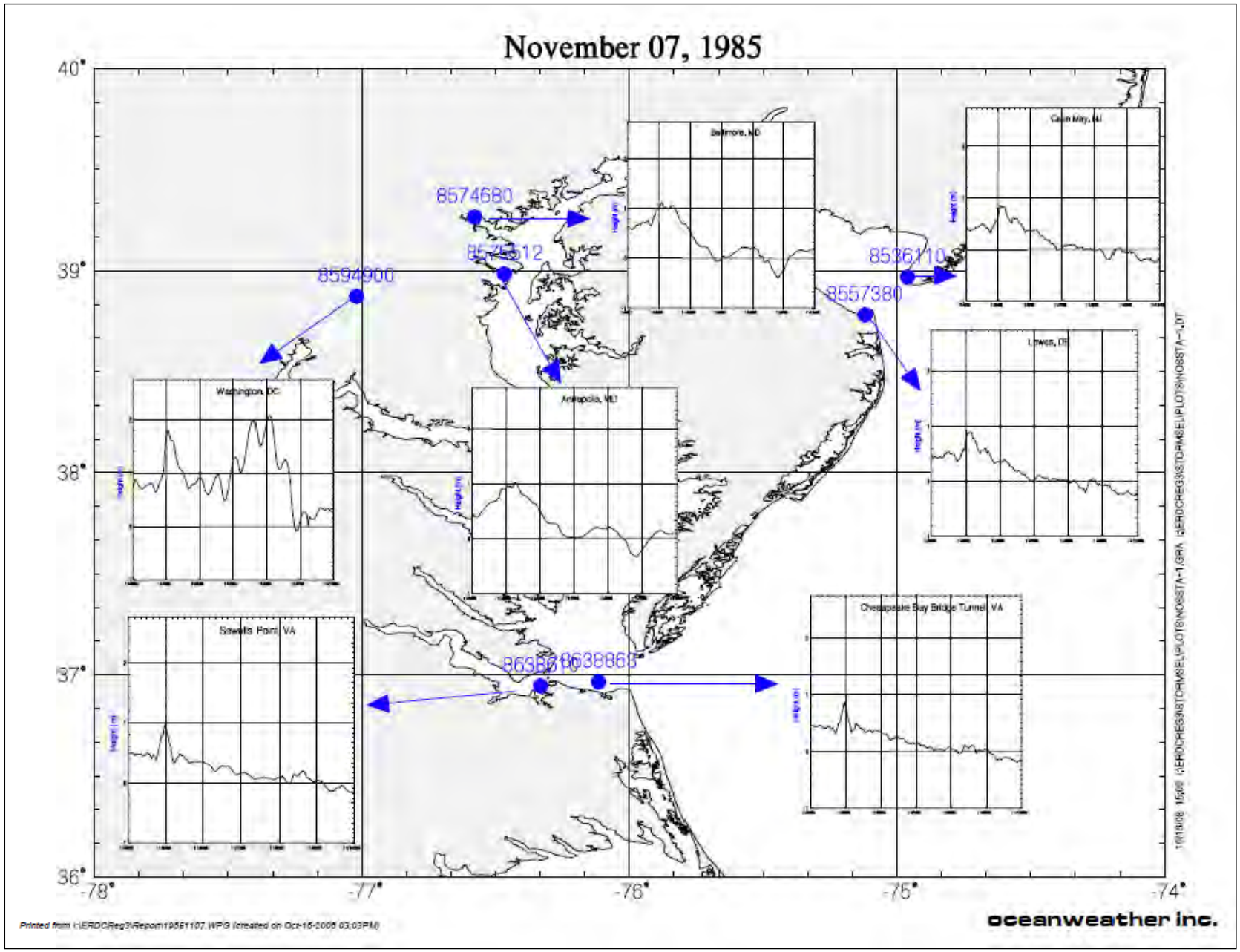

Figure B5. (Sheet 19 of 60)

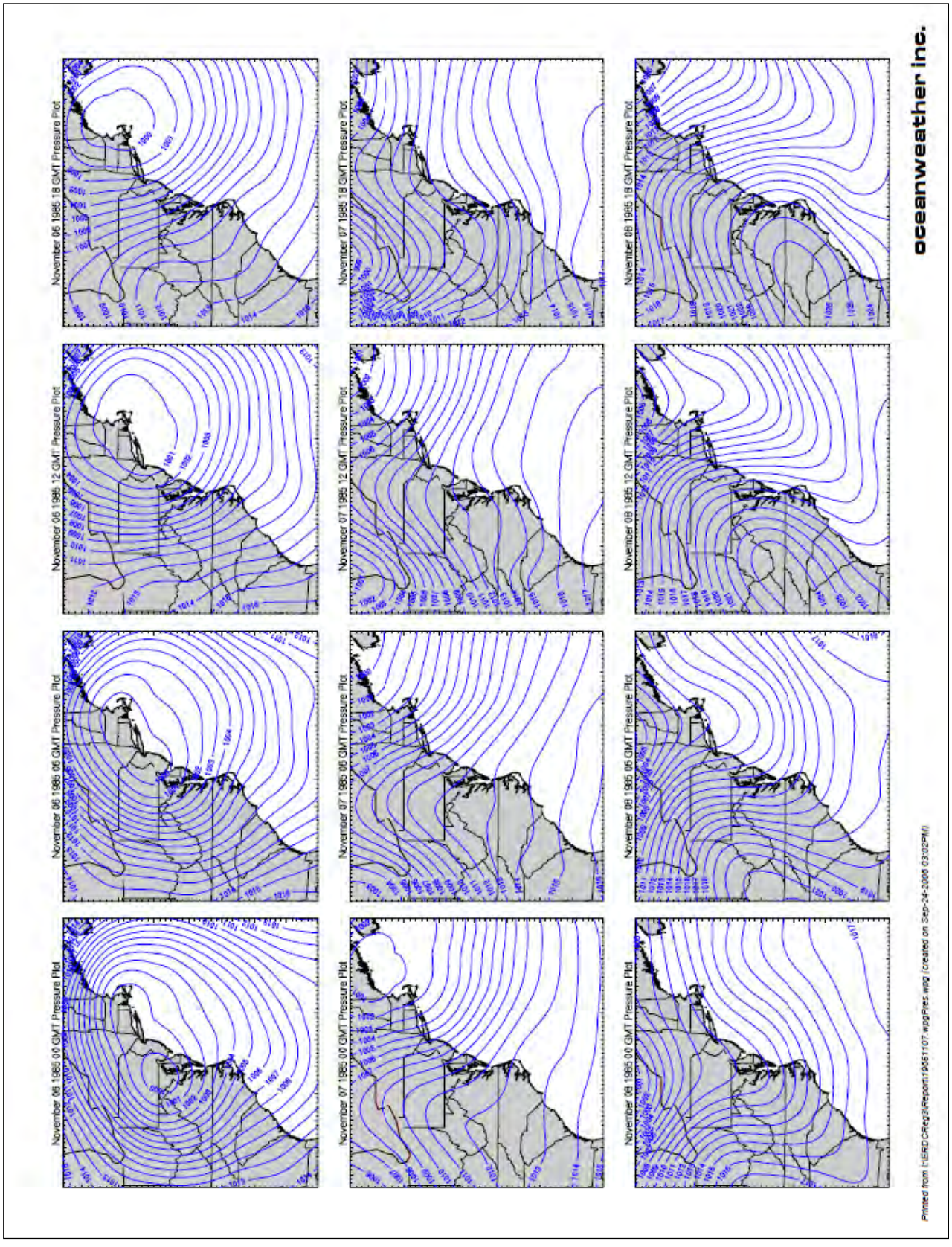

Figure B5. (Sheet 20 of 60)

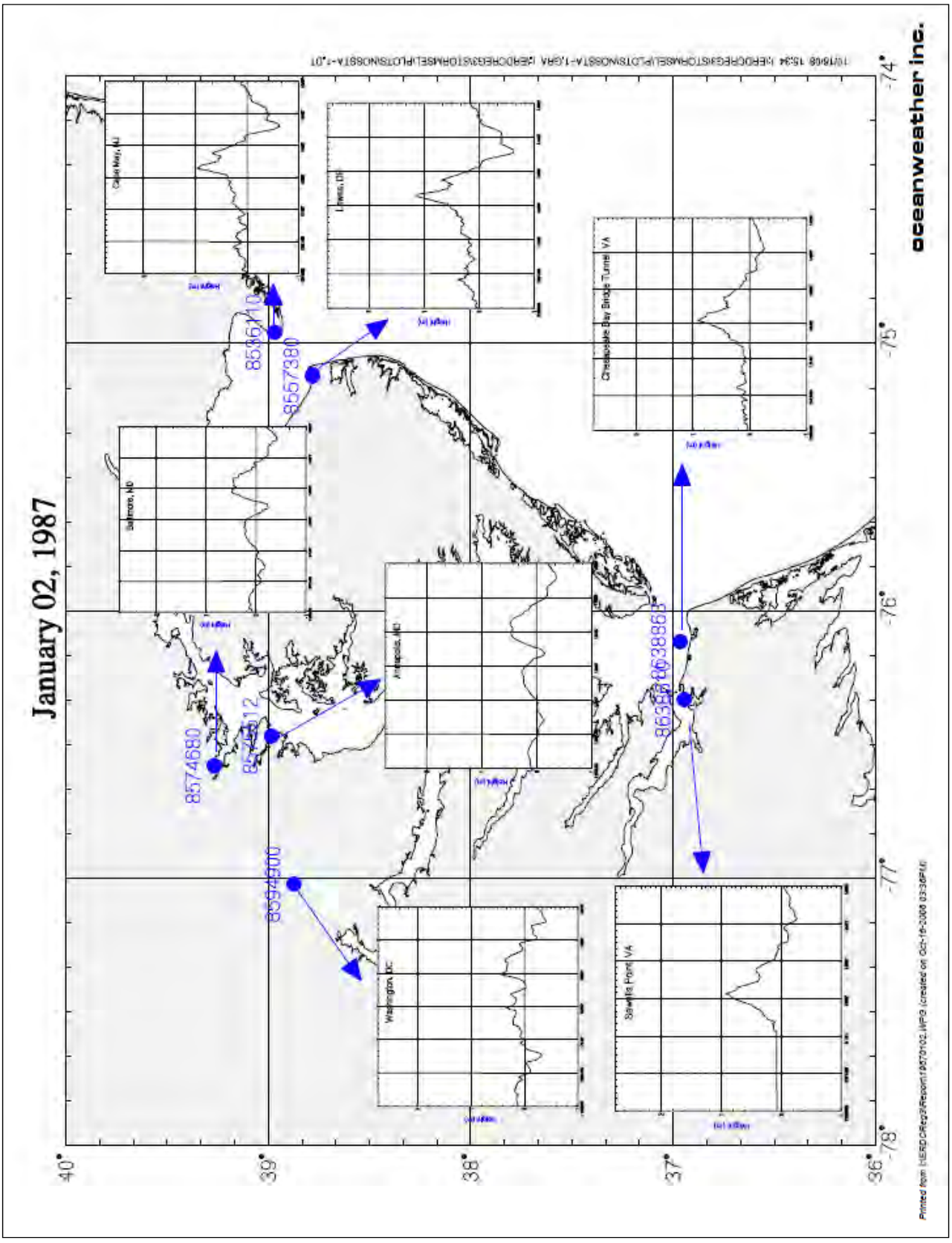

Figure B5. (Sheet 21 of 60)

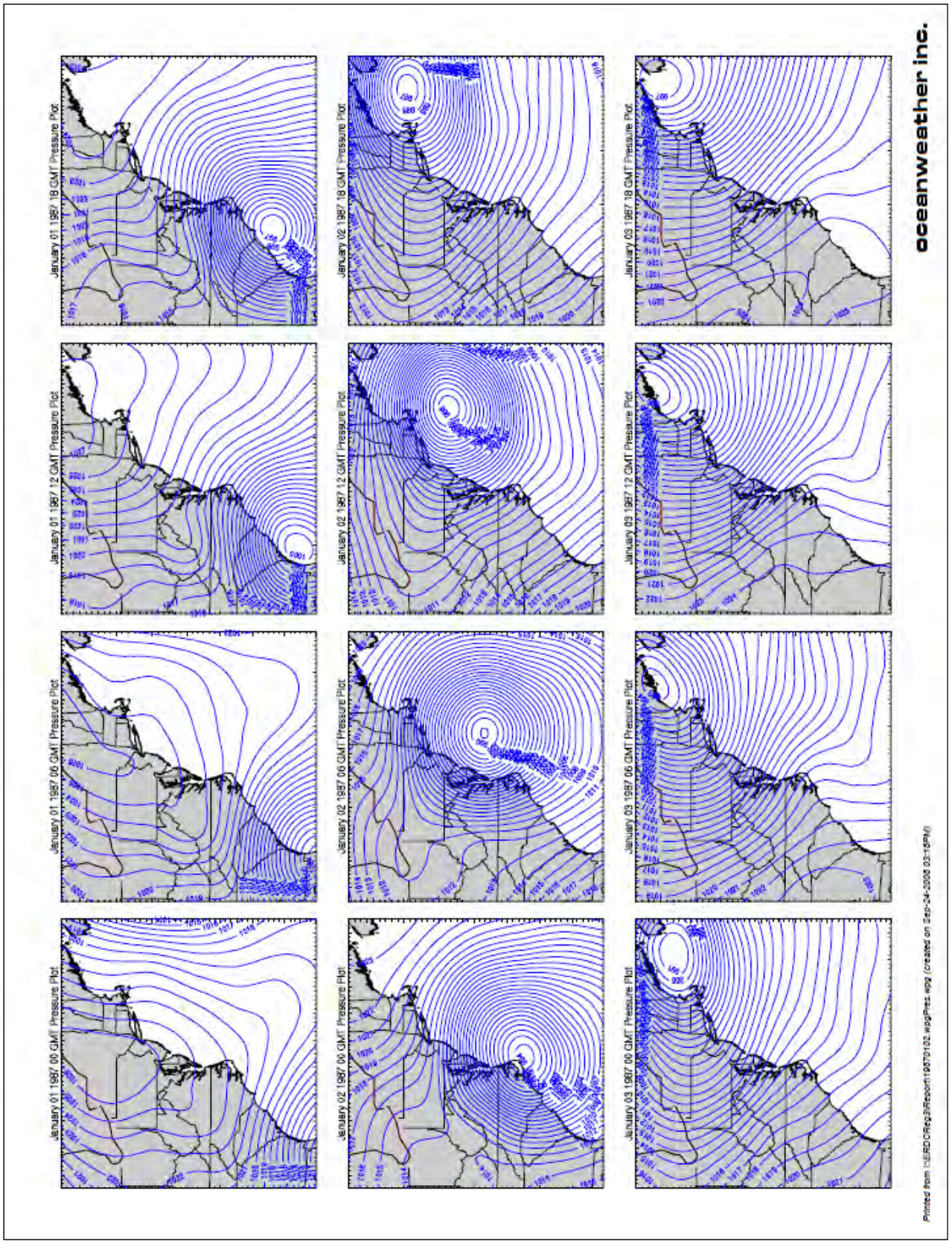

Figure B5. (Sheet 22 of 60)

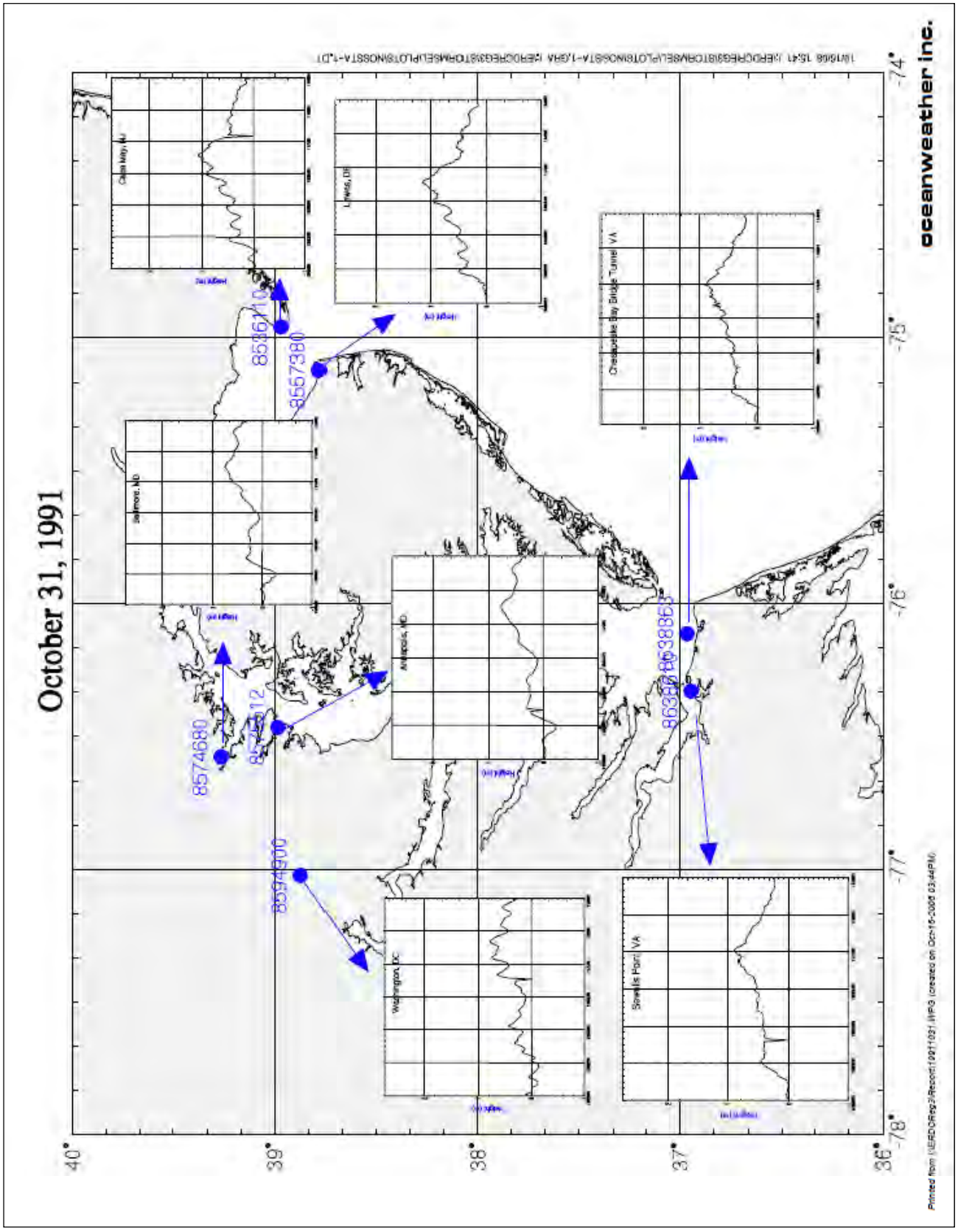

Figure B5. (Sheet 23 of 60)

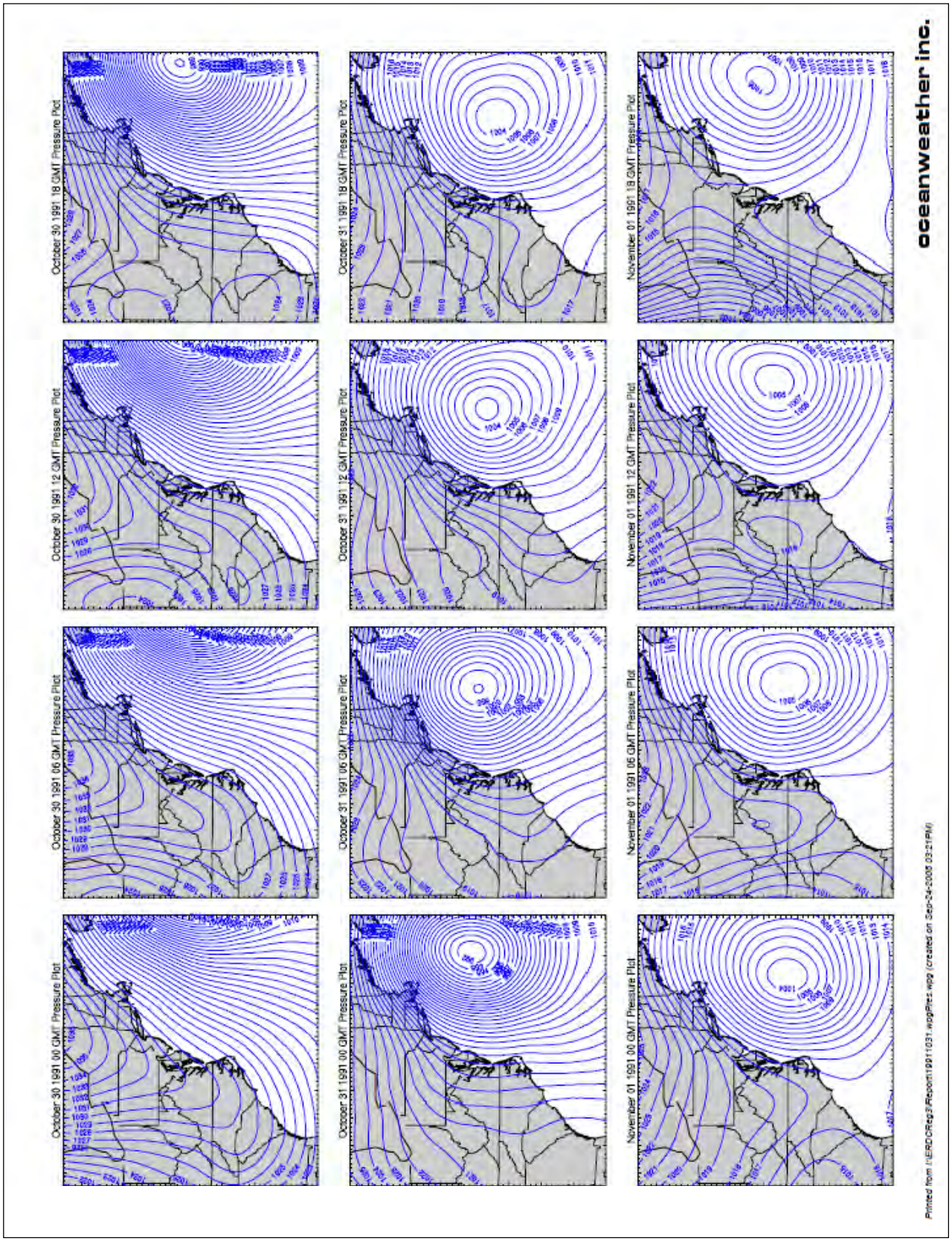

Figure B5. (Sheet 24 of 60)

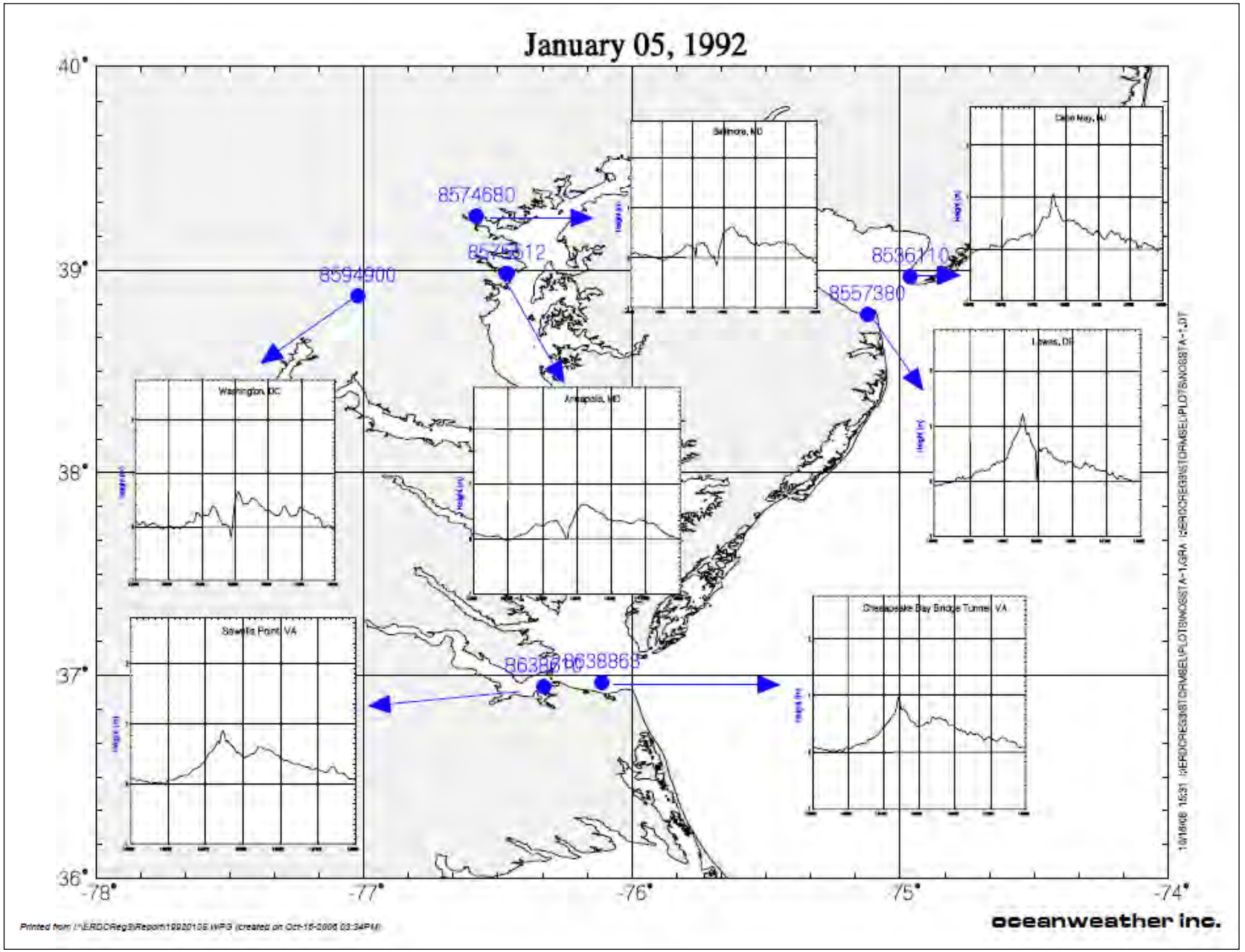

Figure B5. (Sheet 25 of 60)

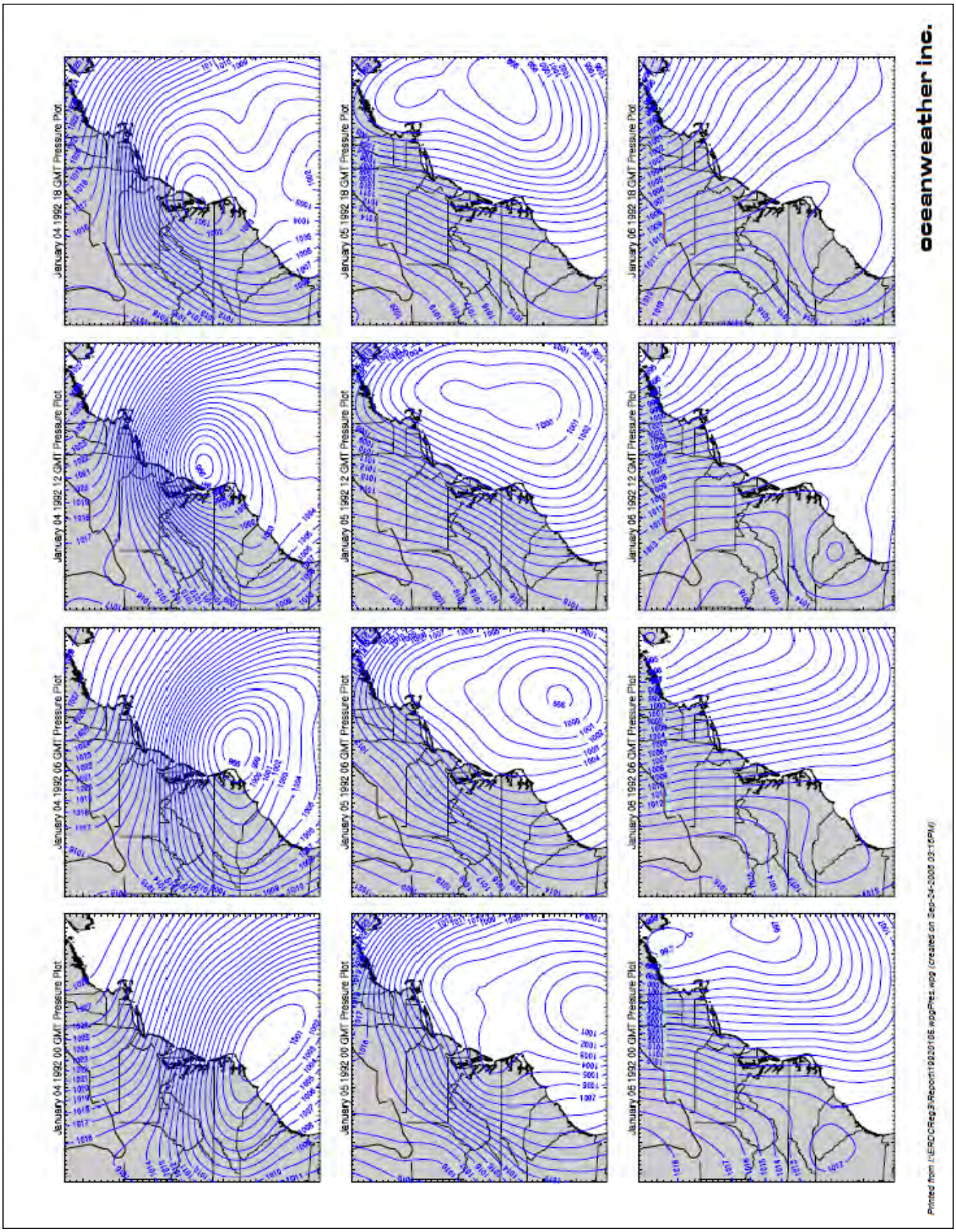

Figure B5. (Sheet 26 of 60)

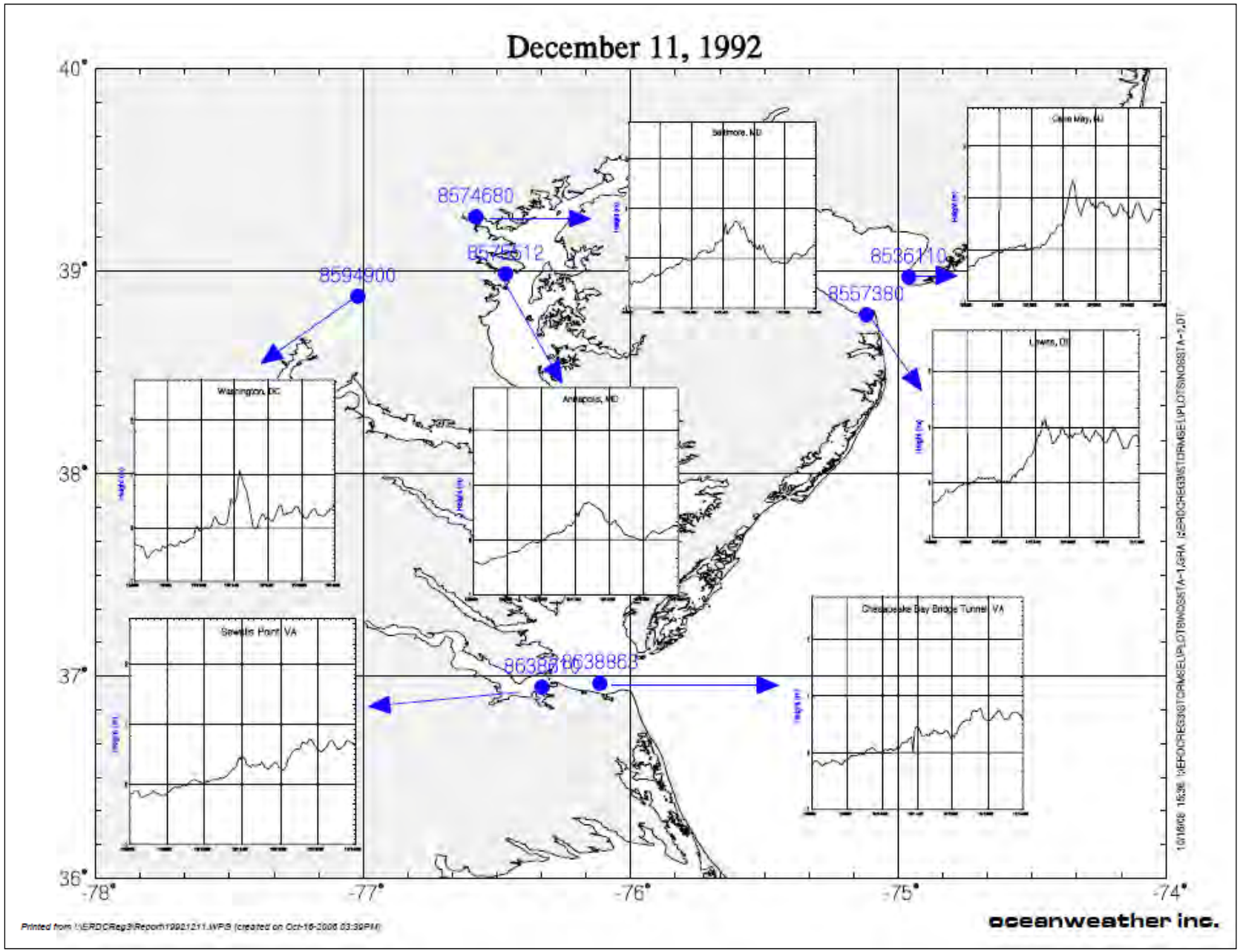

Figure B5. (Sheet 27 of 60)

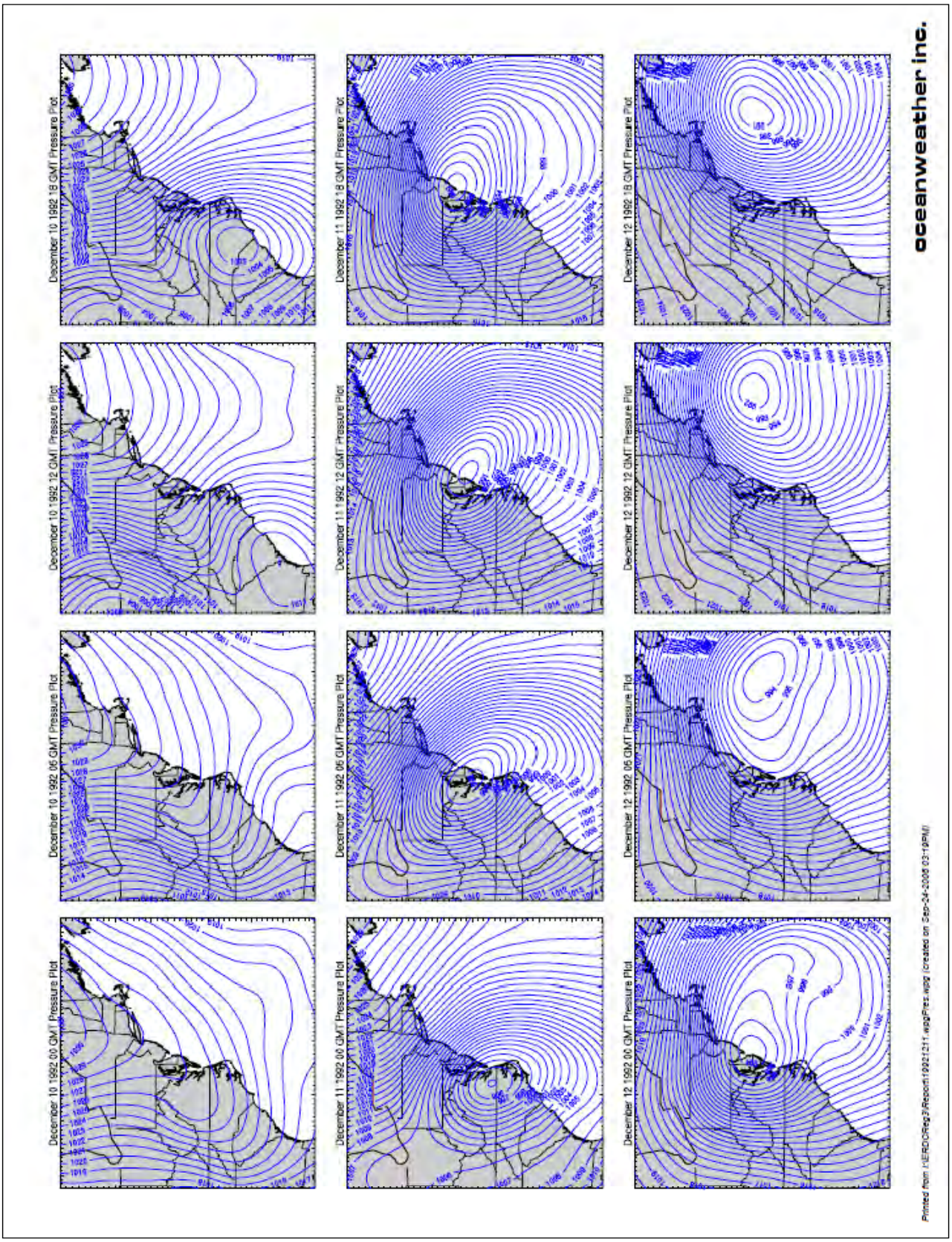

Figure B5. (Sheet 28 of 60)

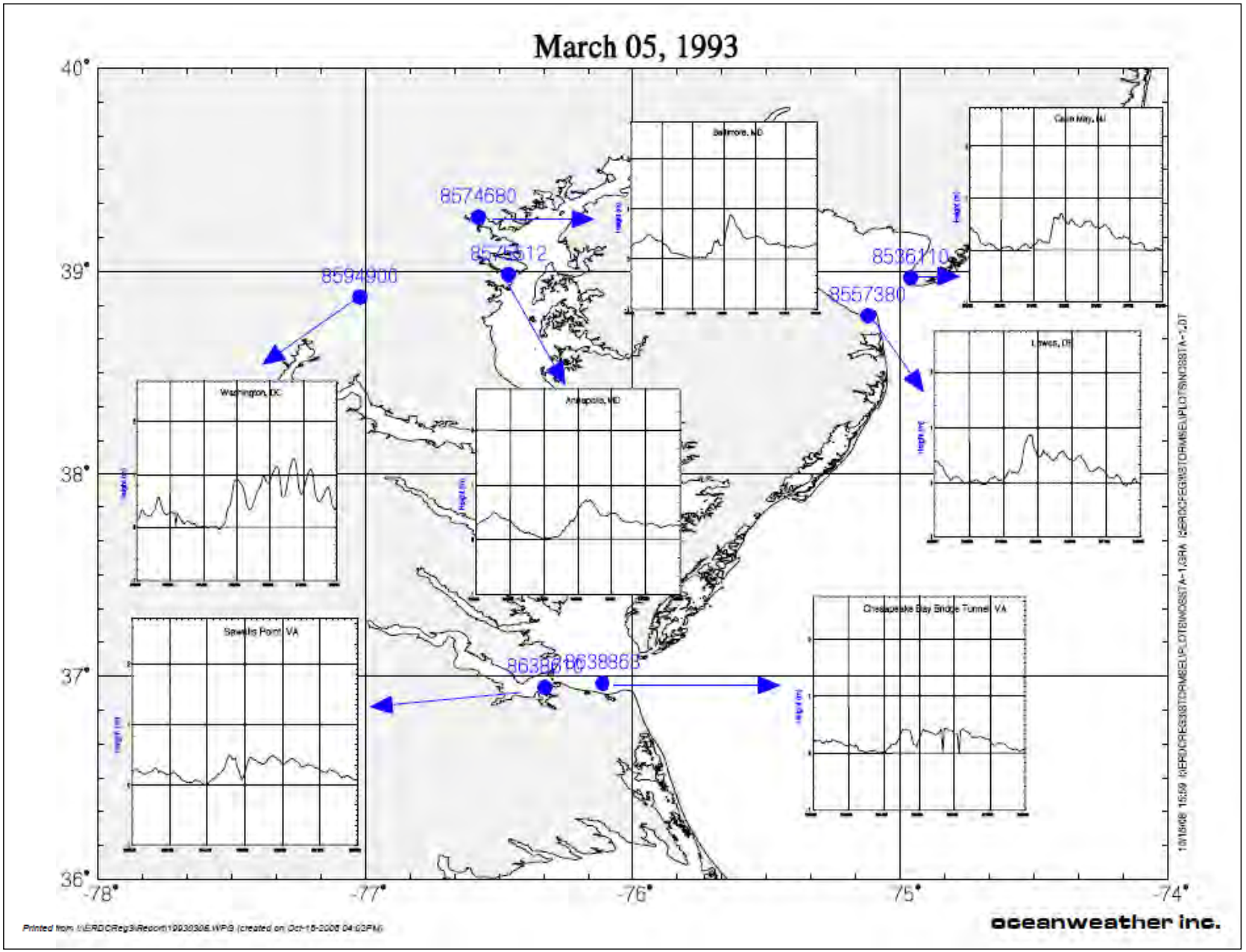

Figure B5. (Sheet 29 of 60)

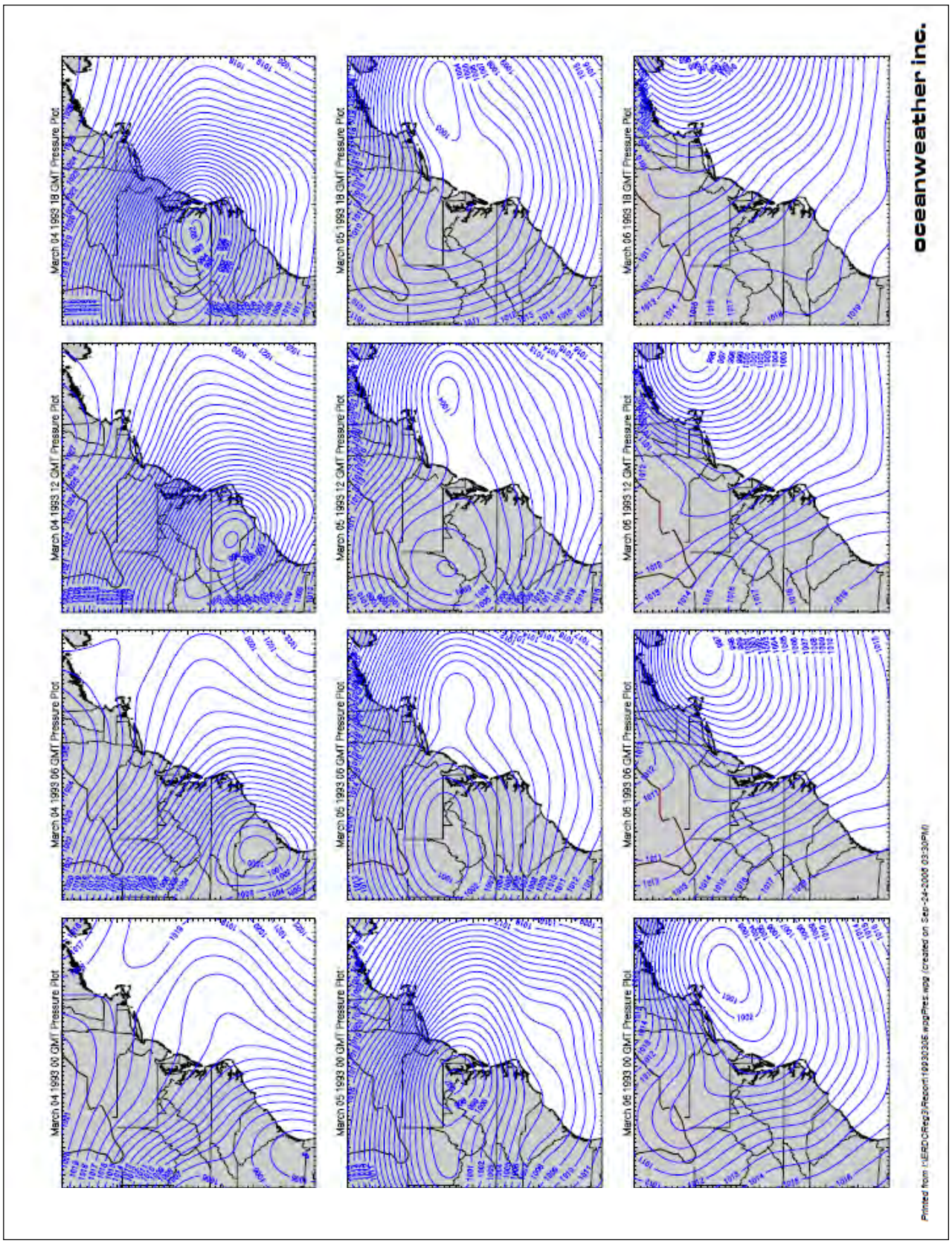

Figure B5. (Sheet 30 of 60)

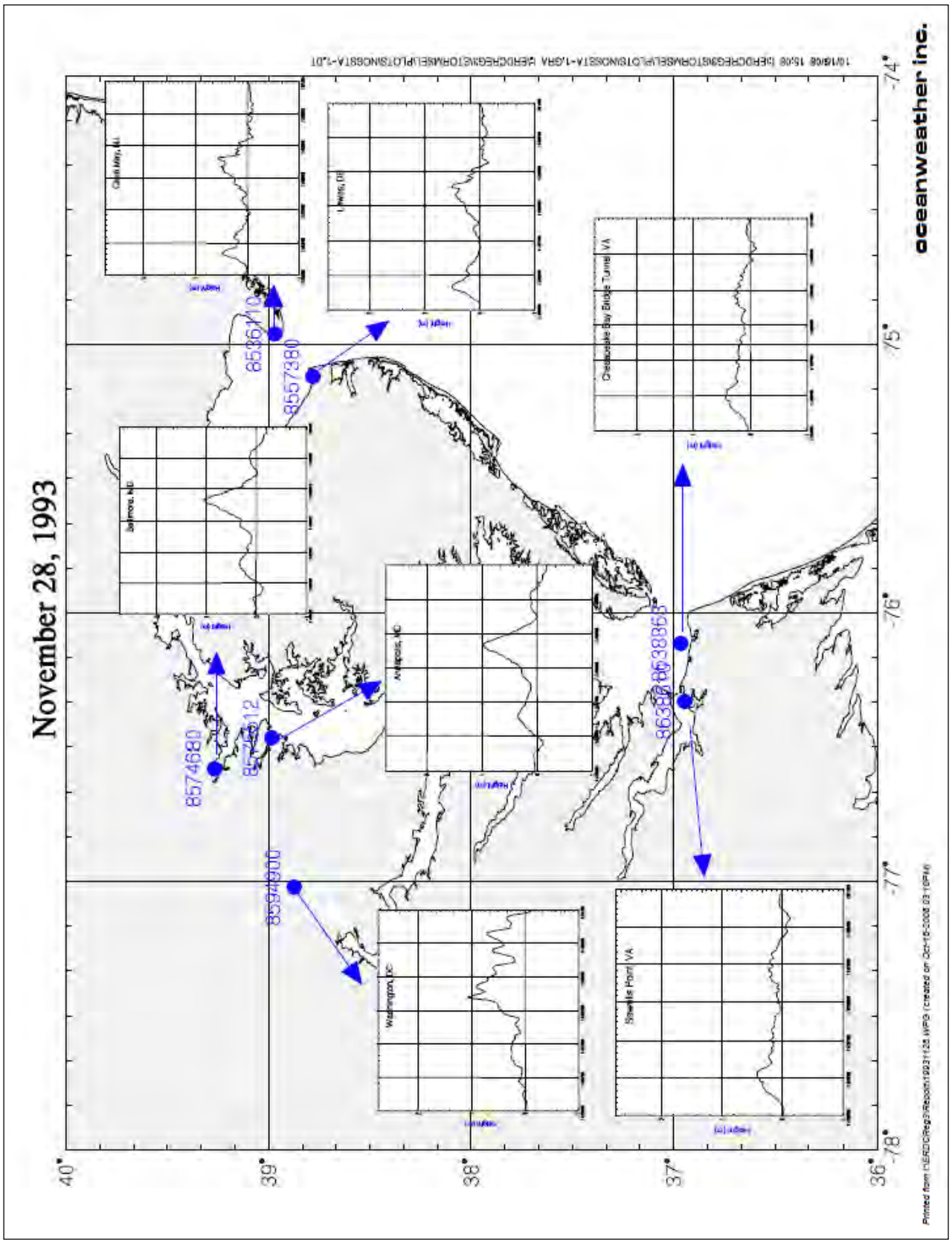

Figure B5. (Sheet 31 of 60)

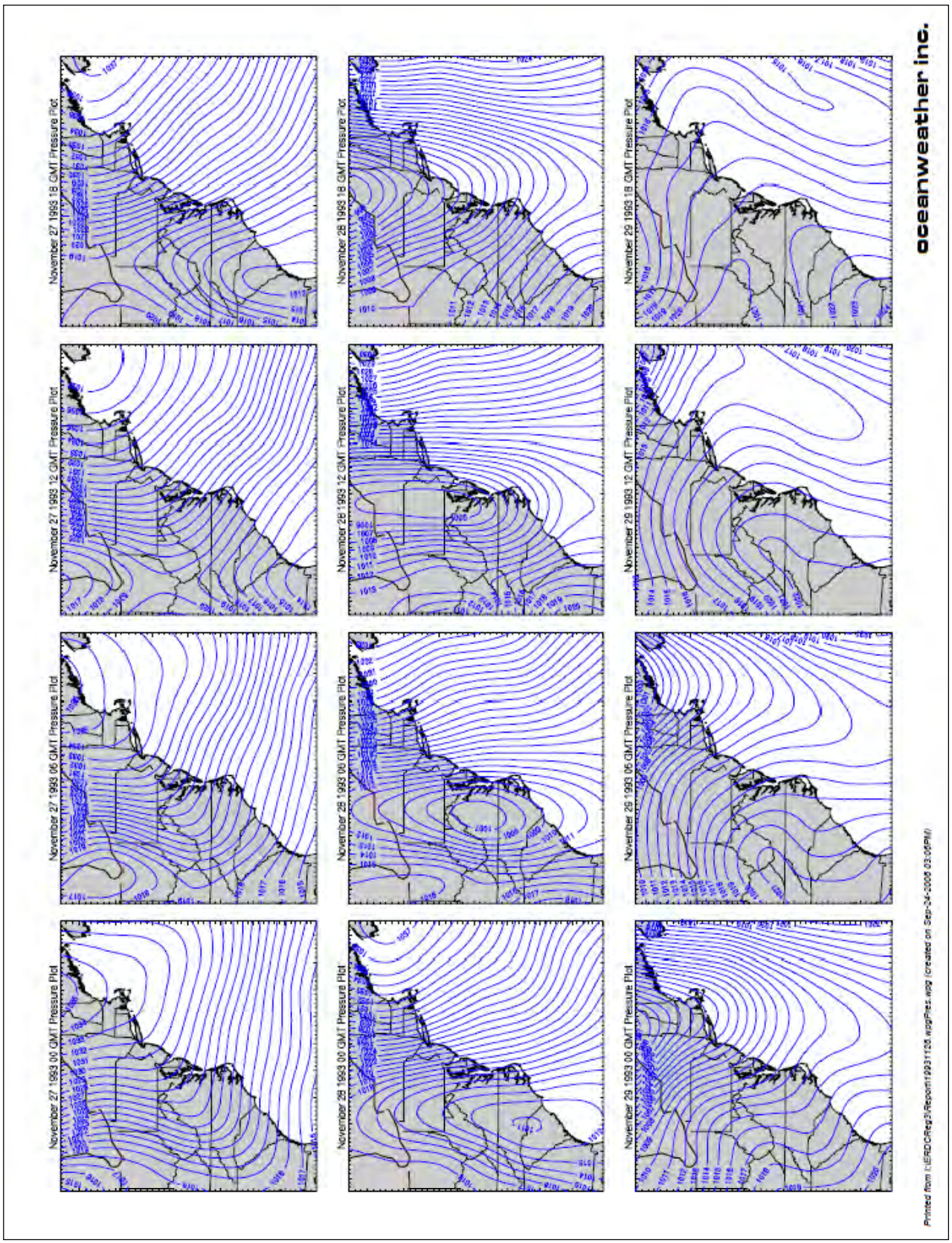

Figure B5. (Sheet 32 of 60)

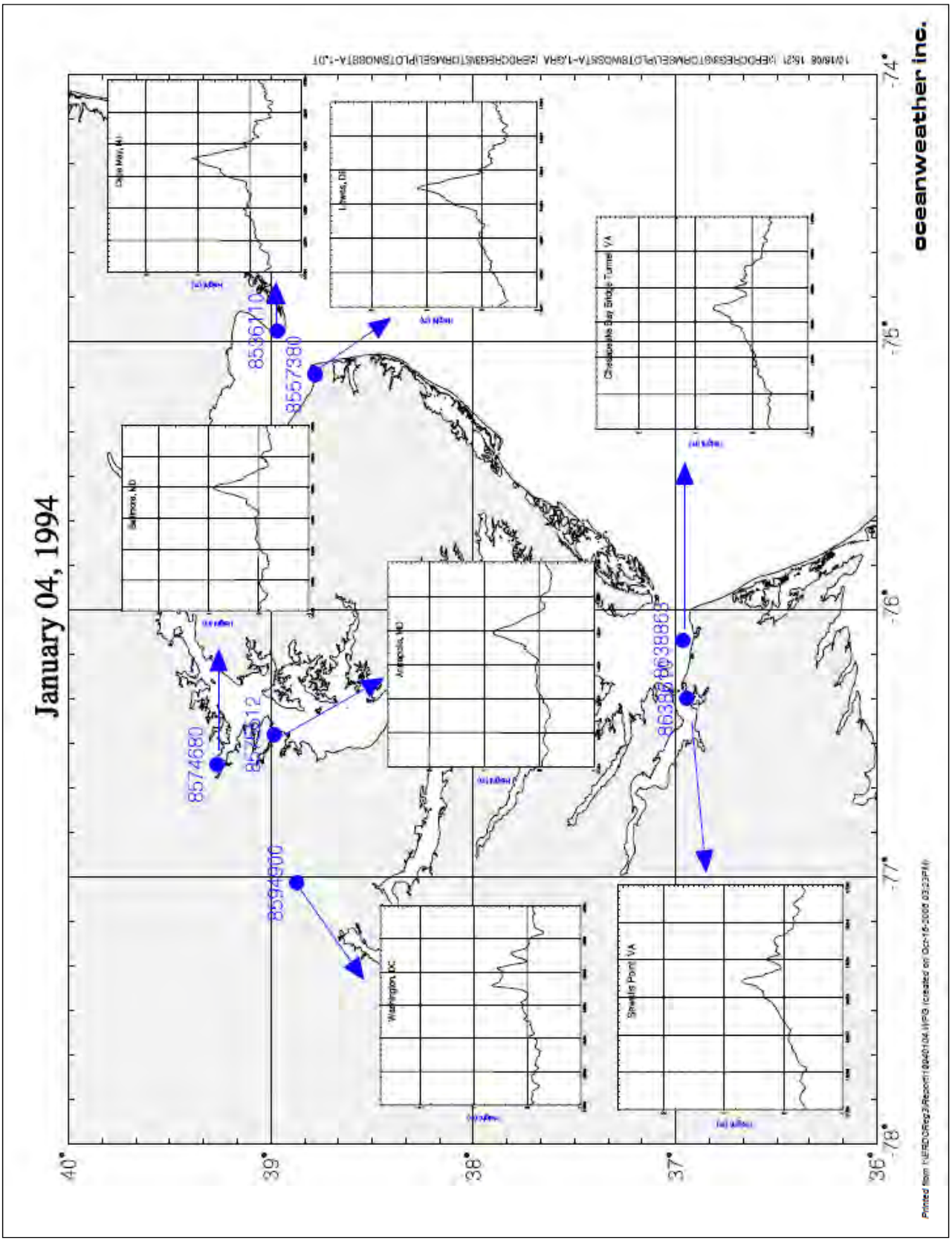

Figure B5. (Sheet 33 of 60)

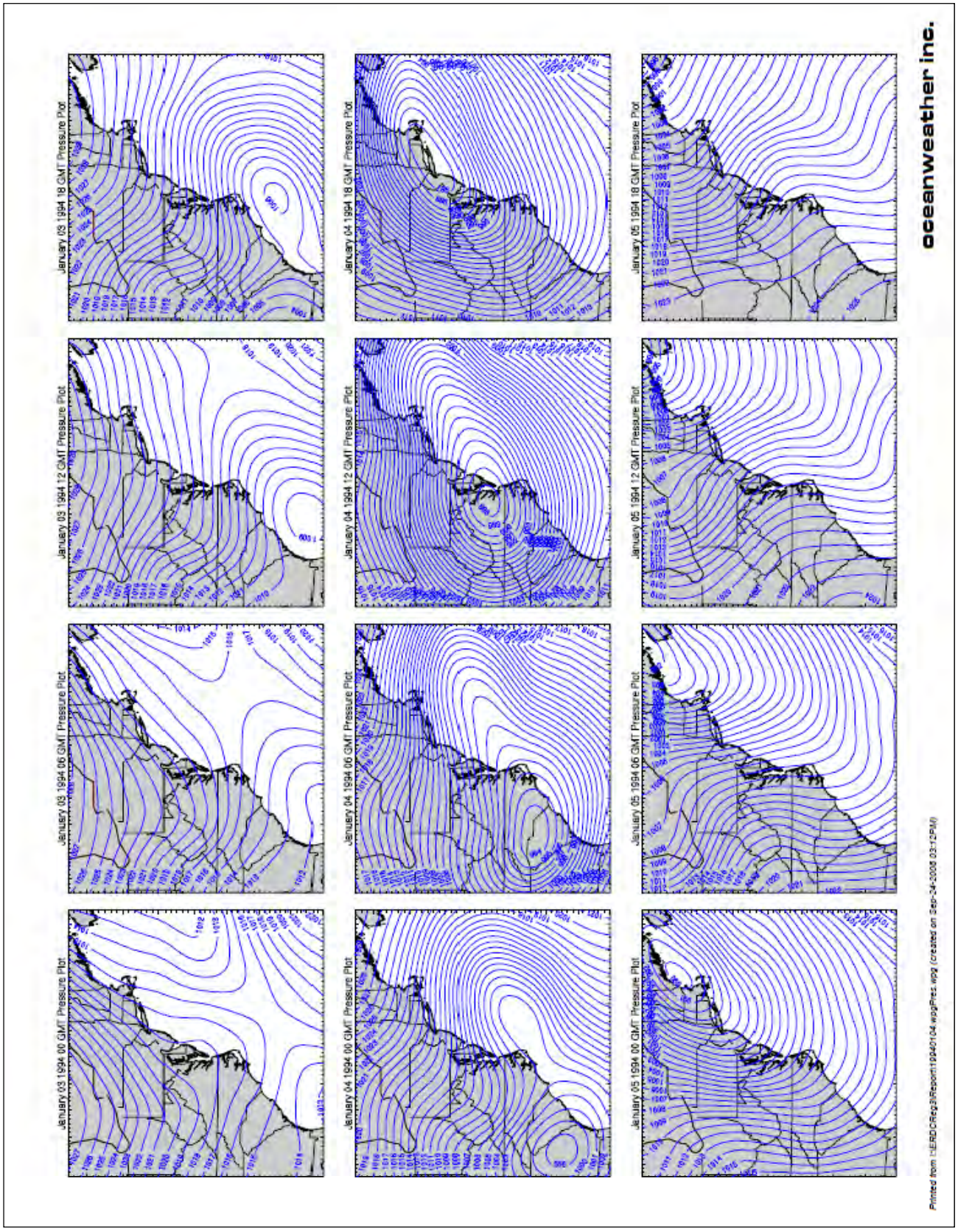

Figure B5. (Sheet 34 of 60)

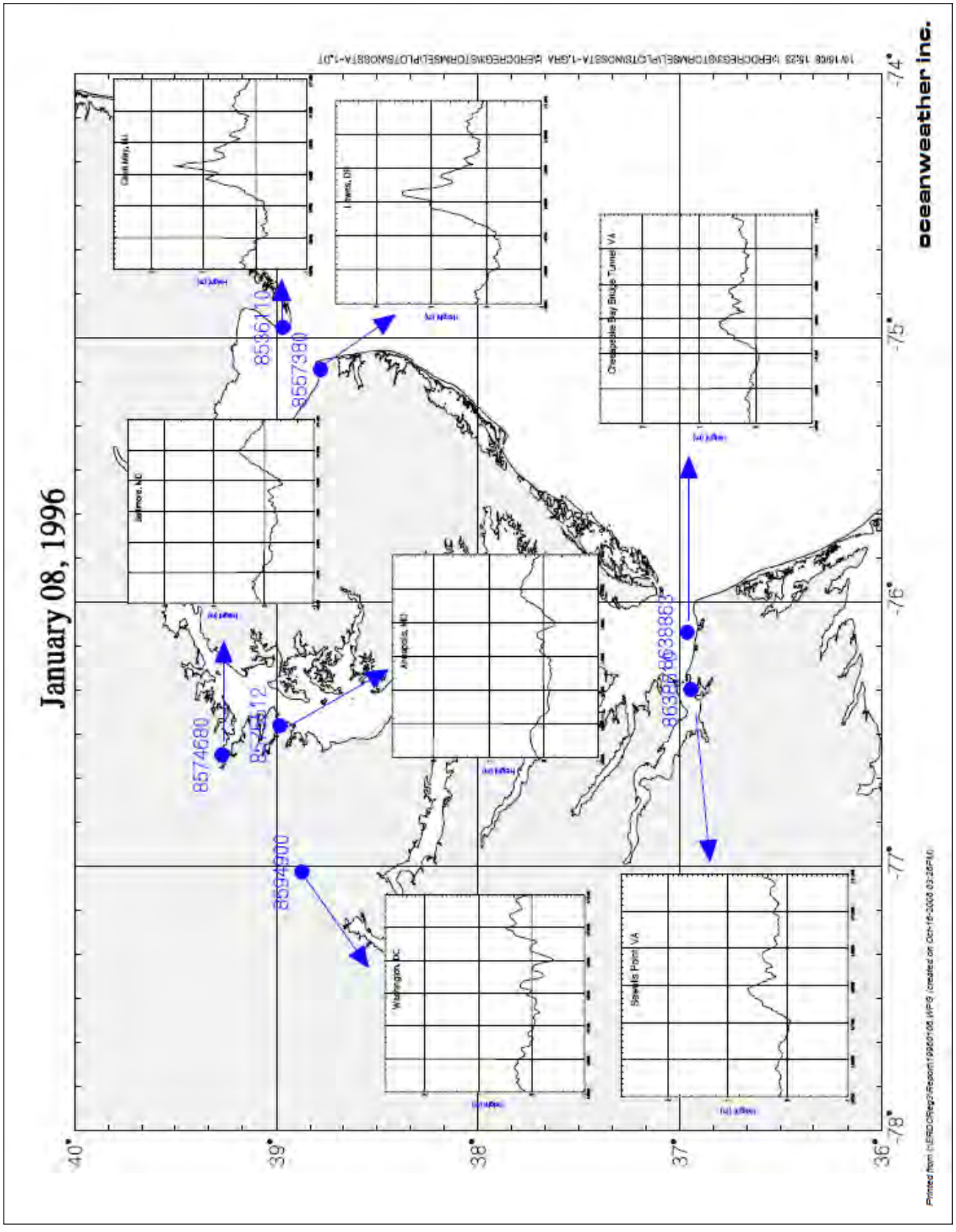

Figure B5. (Sheet 35 of 60)

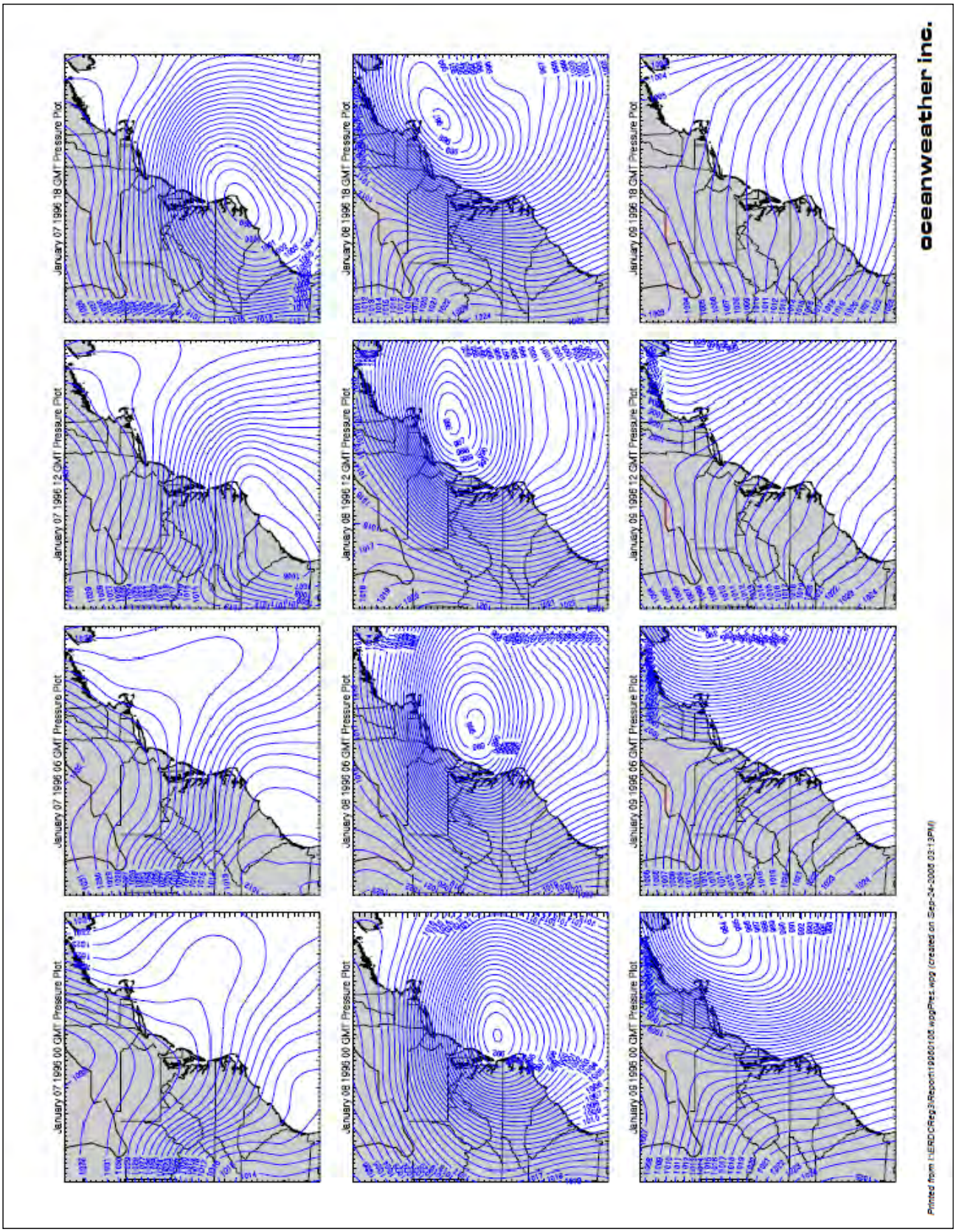

Figure B5. (Sheet 36 of 60)

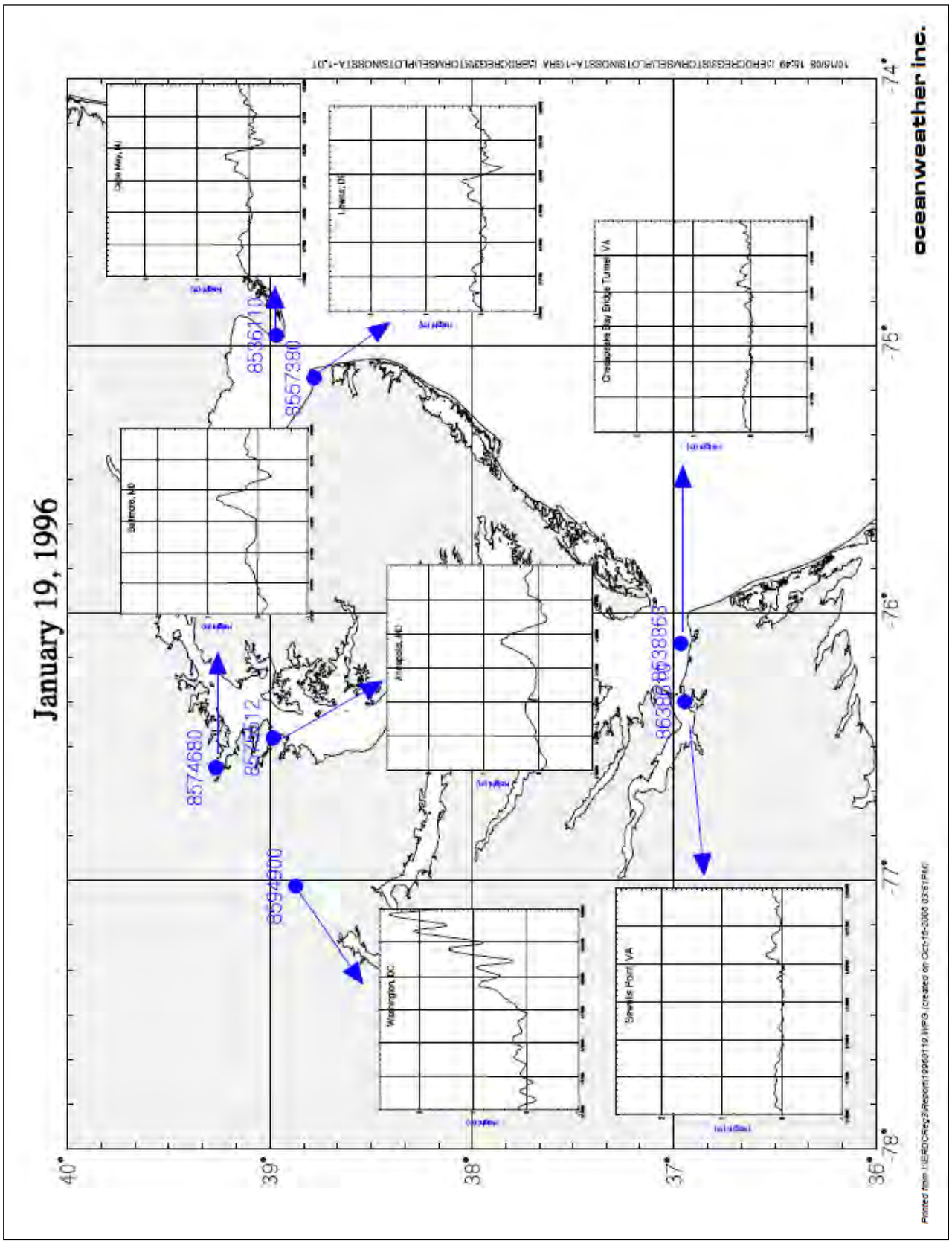

Figure B5. (Sheet 37 of 60)

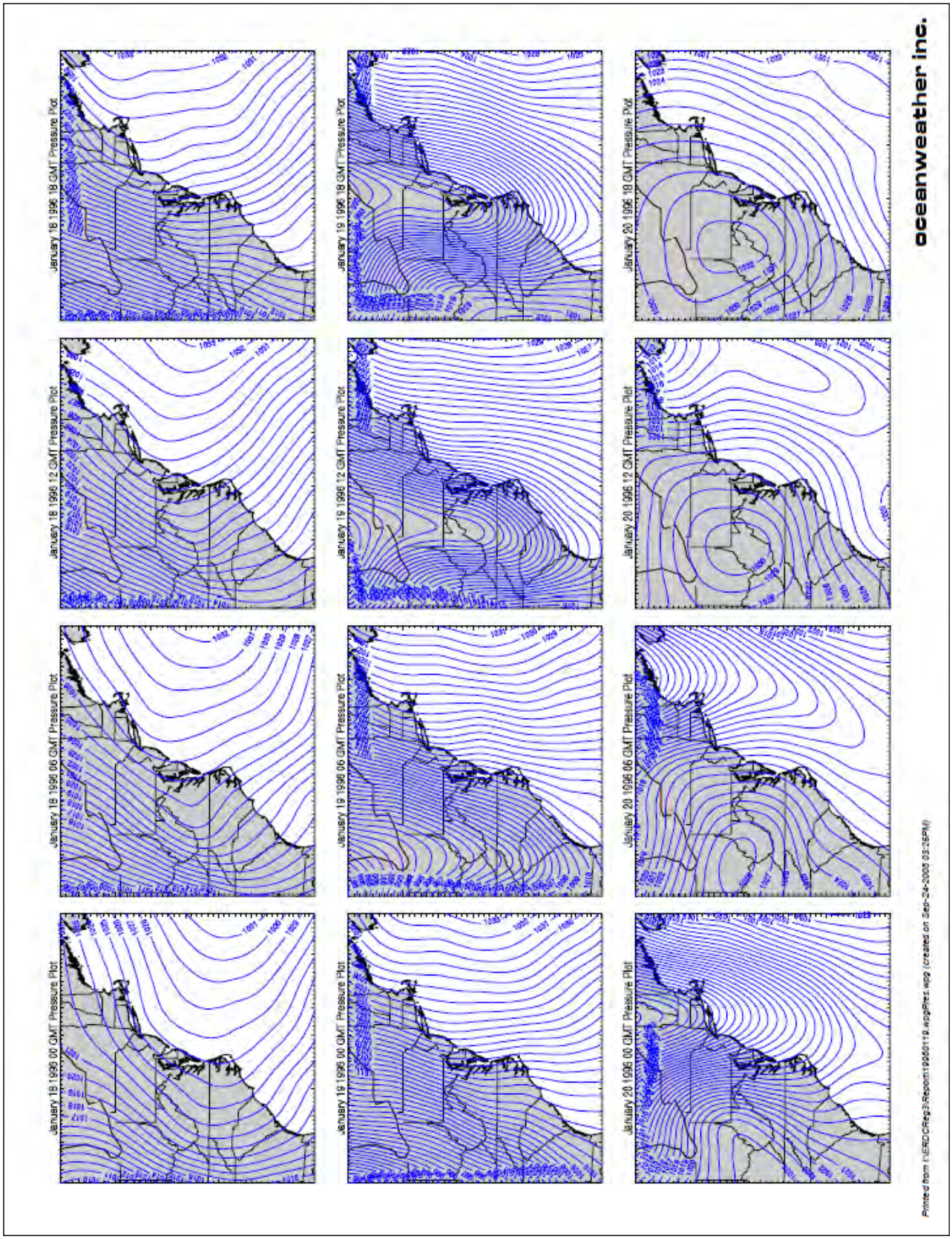

Figure B5. (Sheet 38 of 60)

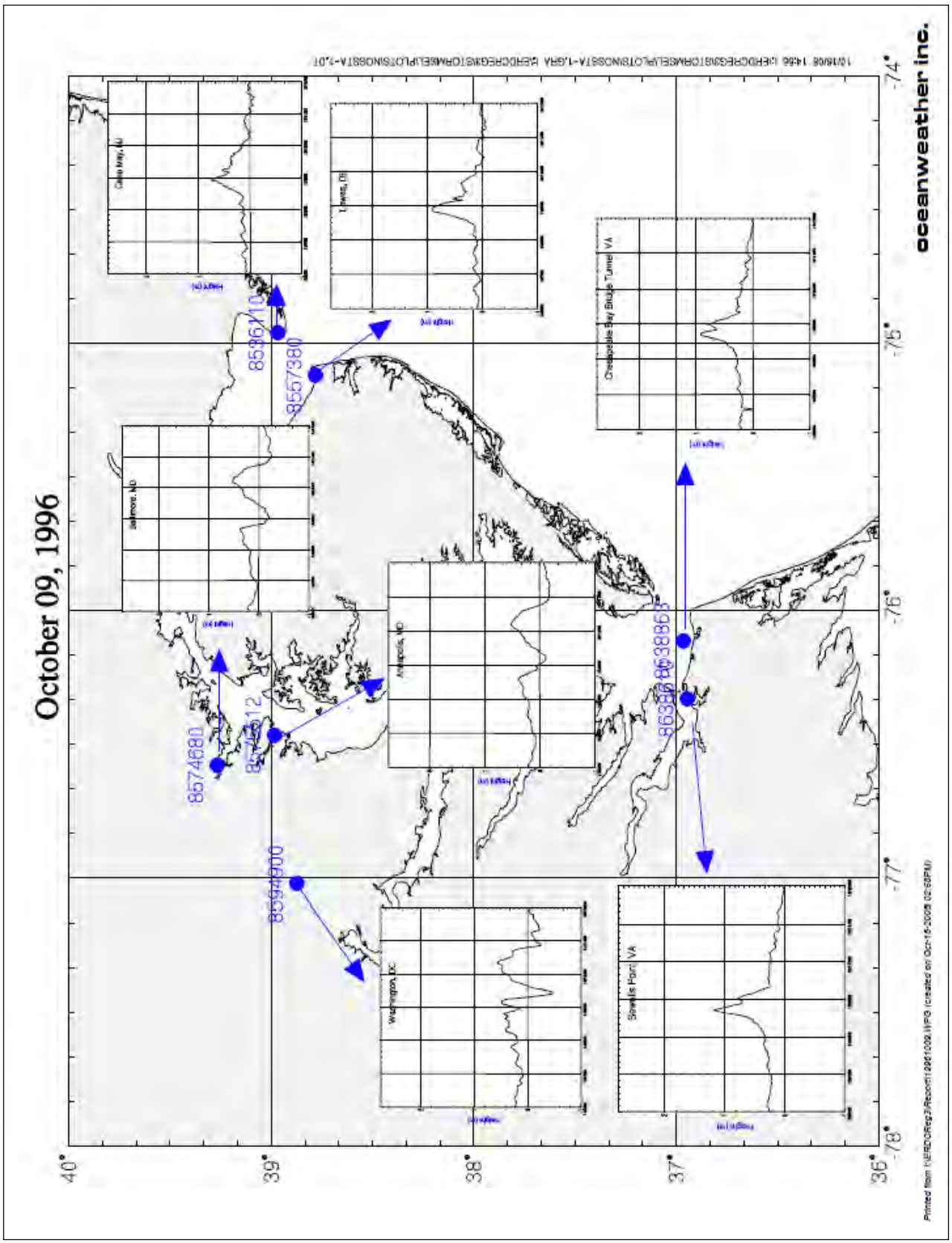

Figure B5. (Sheet 39 of 60)

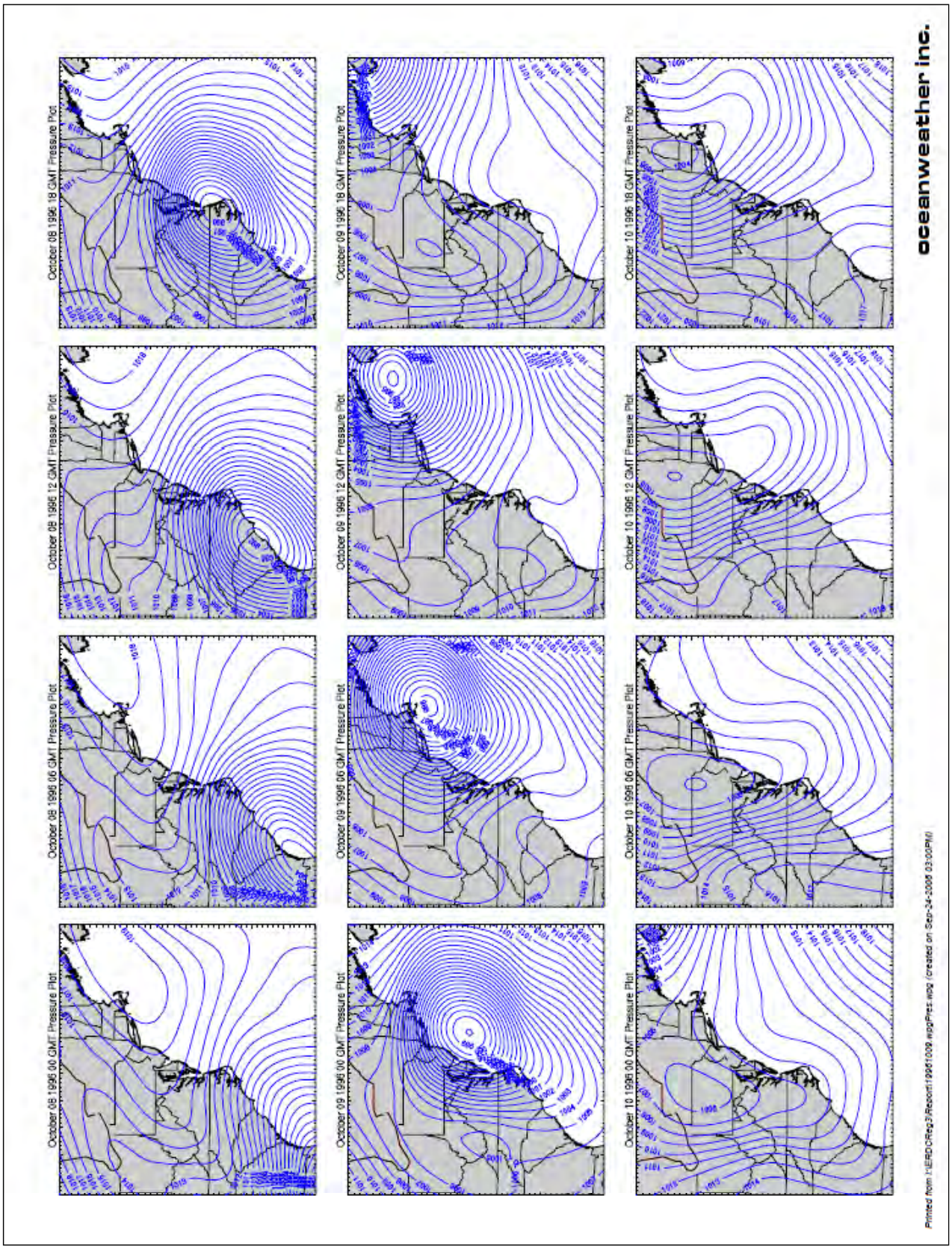

Figure B5. (Sheet 40 of 60)

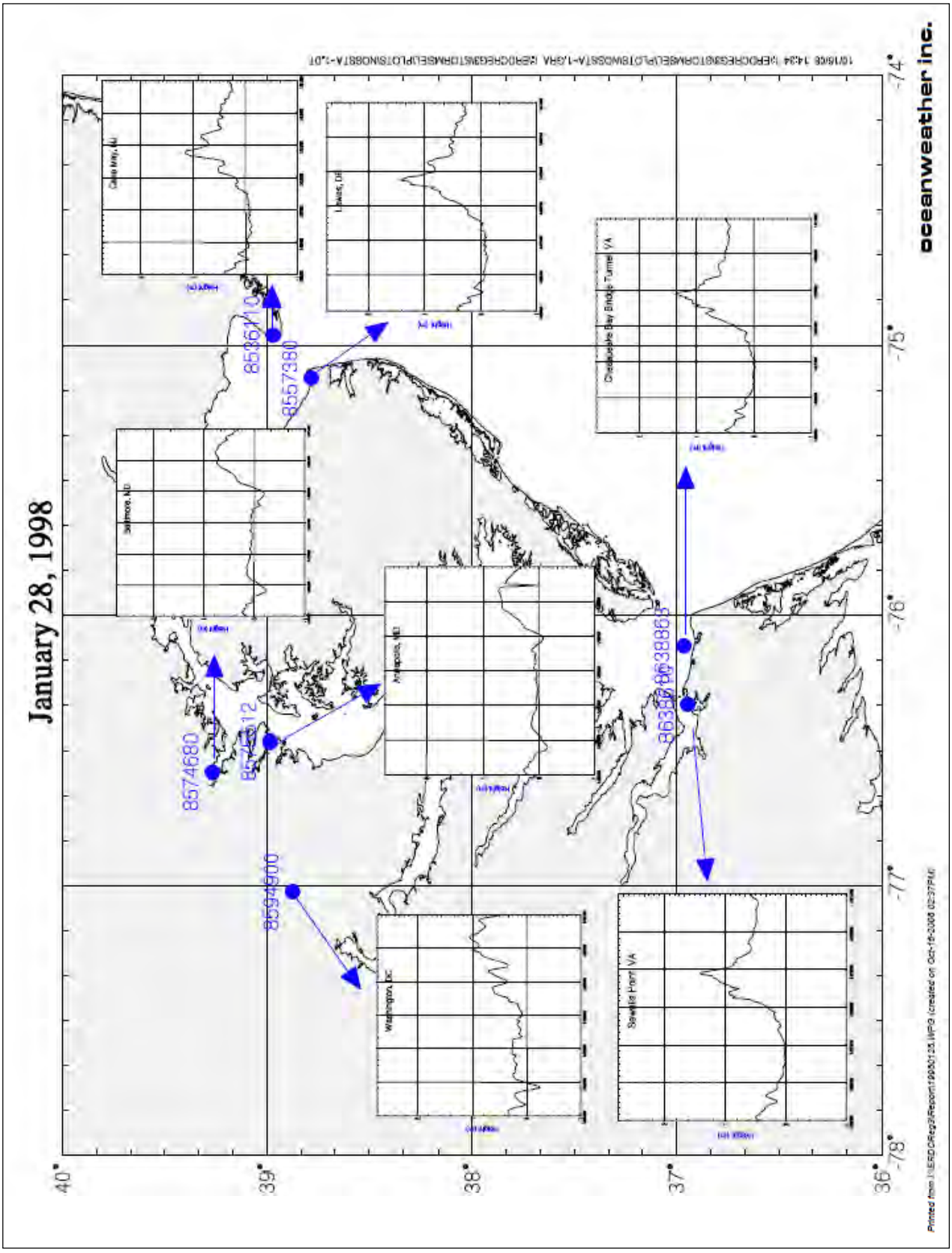

Figure B5. (Sheet 41 of 60)

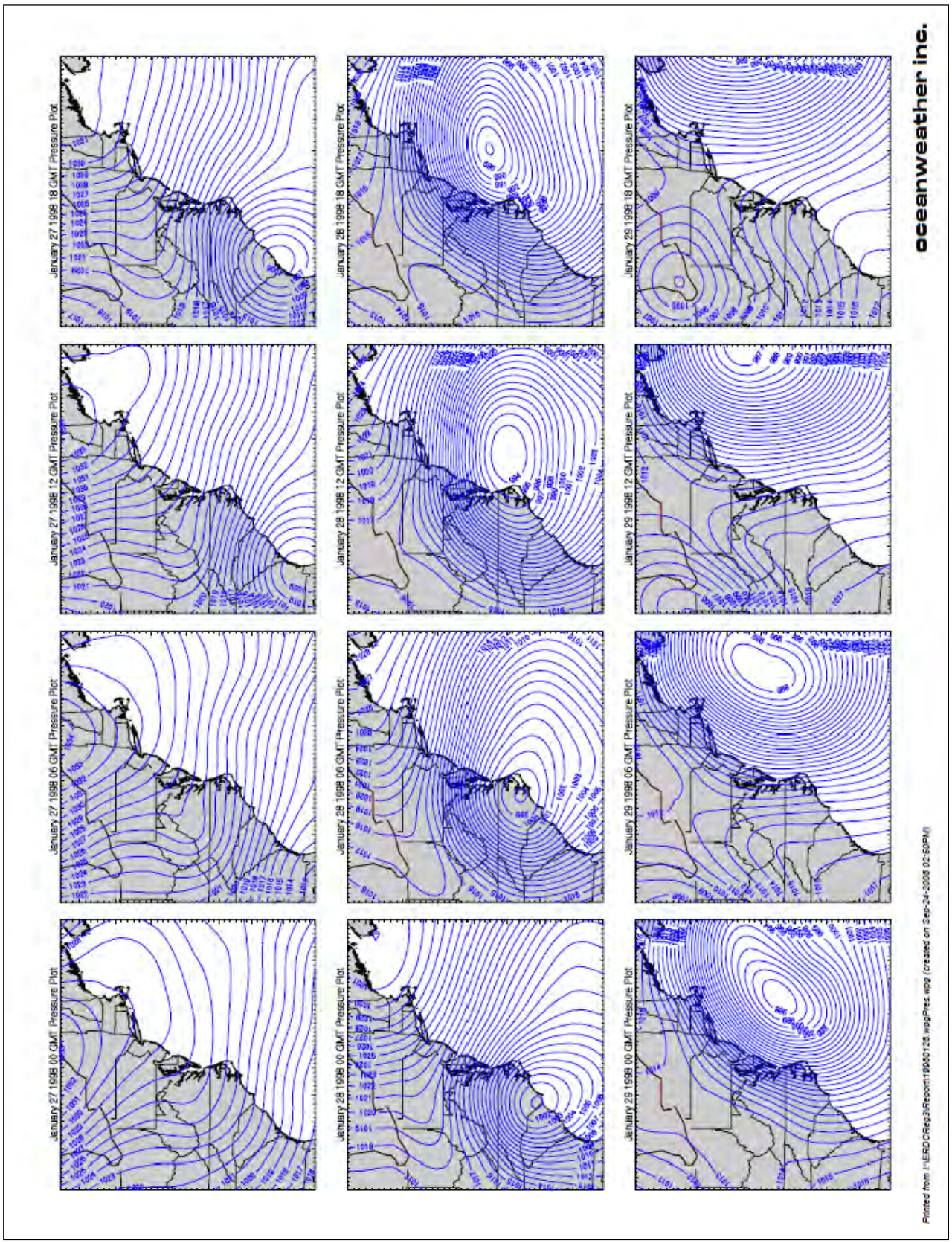

Figure B5. (Sheet 42 of 60)

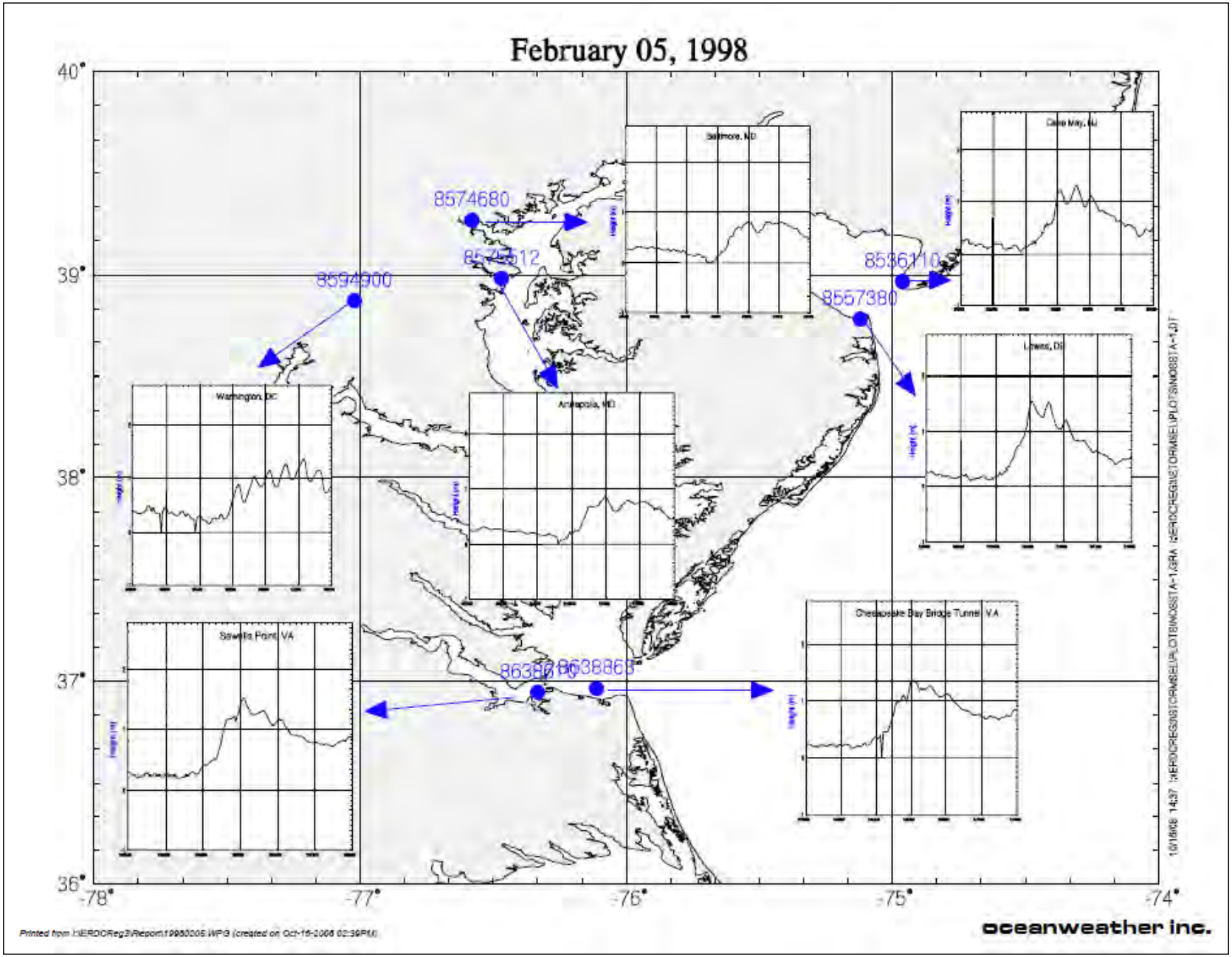

Figure B5. (Sheet 43 of 60)

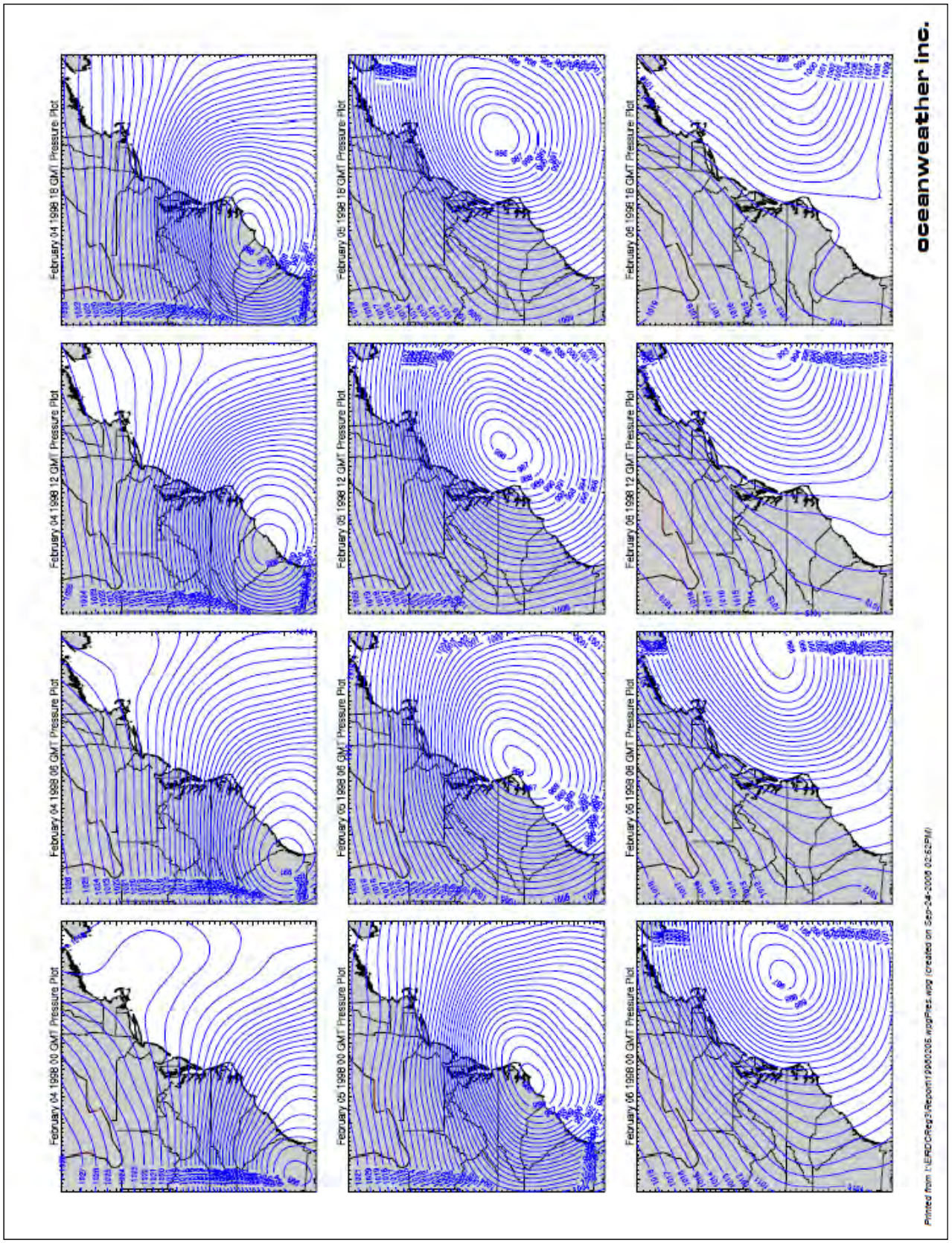

Figure B5. (Sheet 44 of 60)

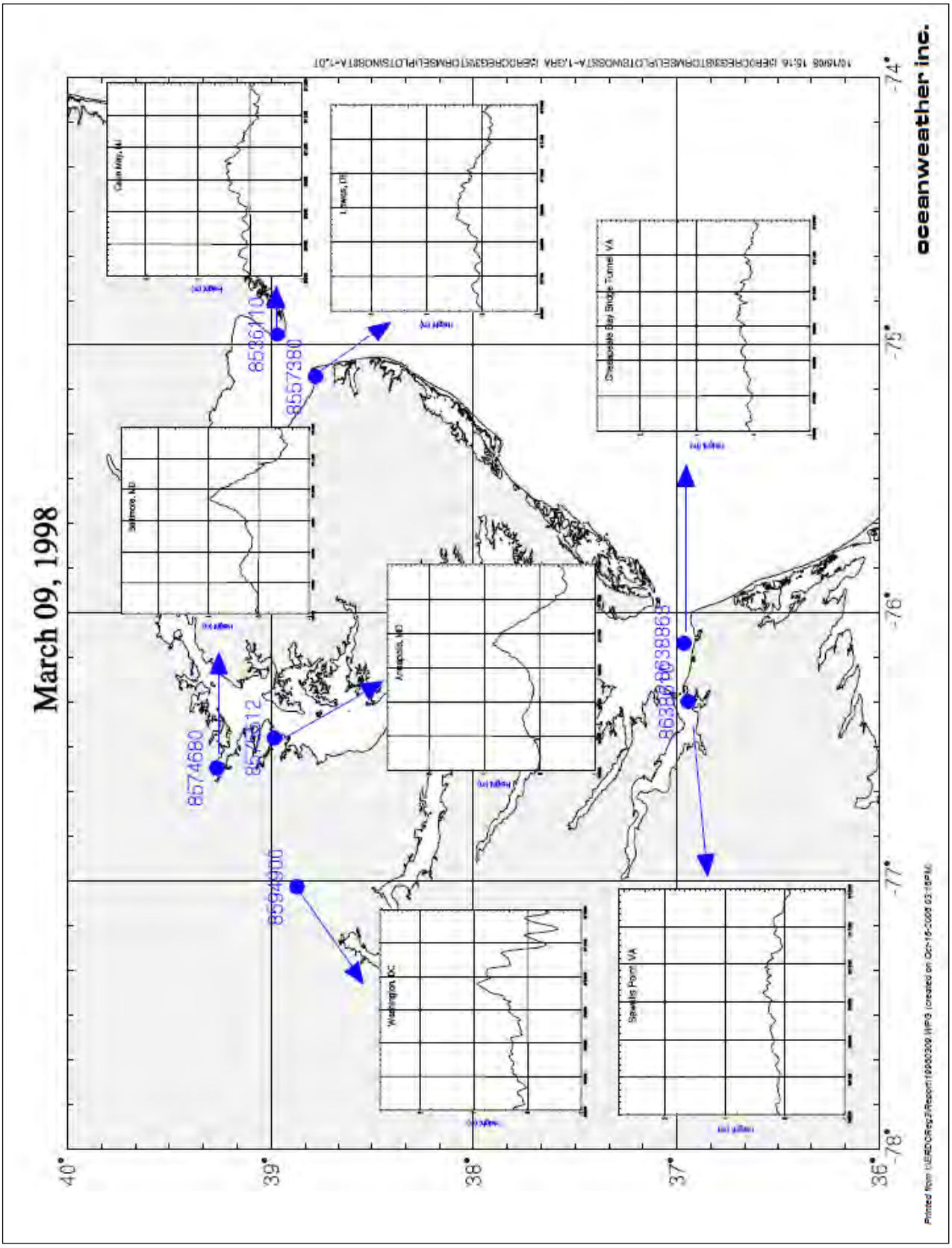

Figure B5. (Sheet 45 of 60)

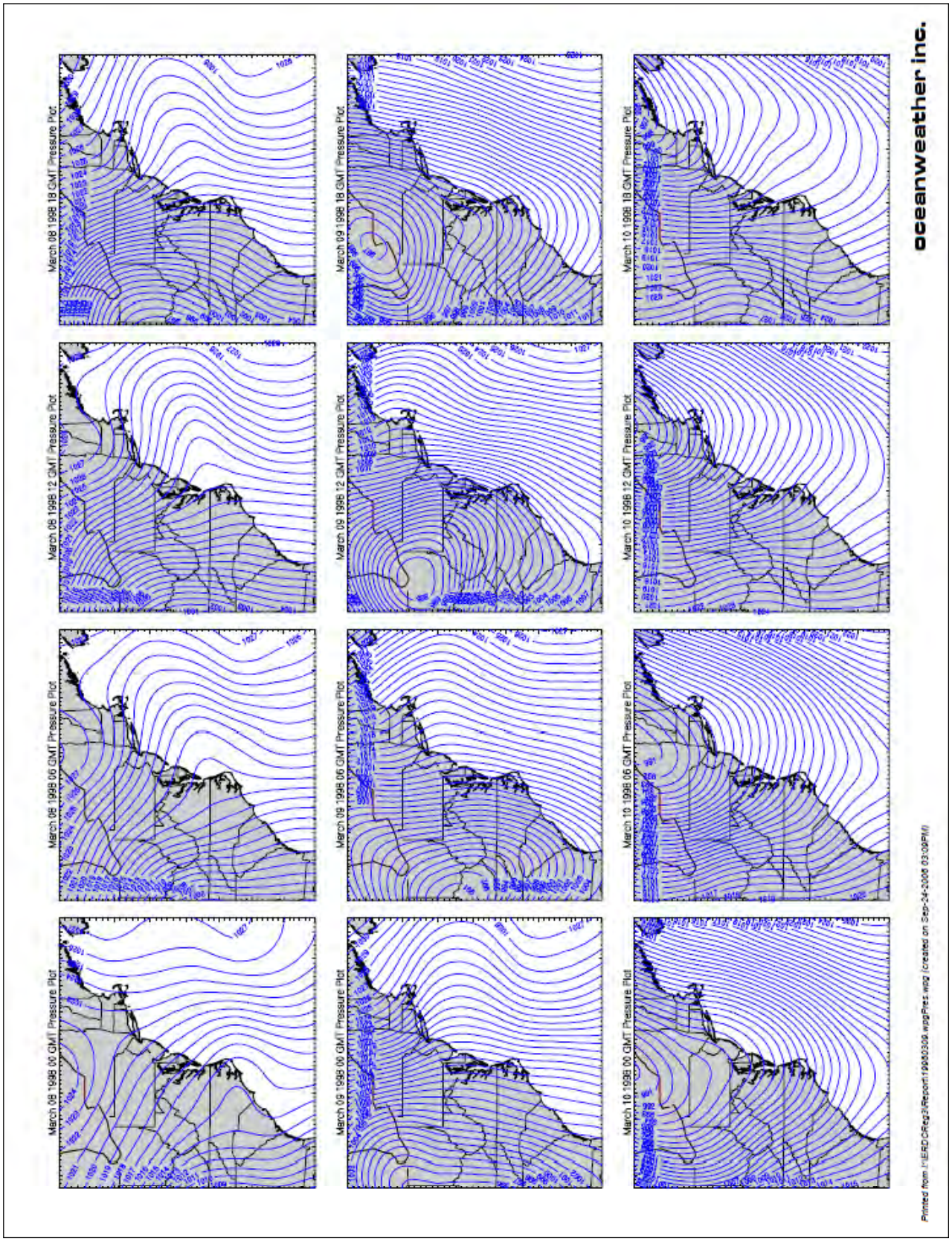

Figure B5. (Sheet 46 of 60)

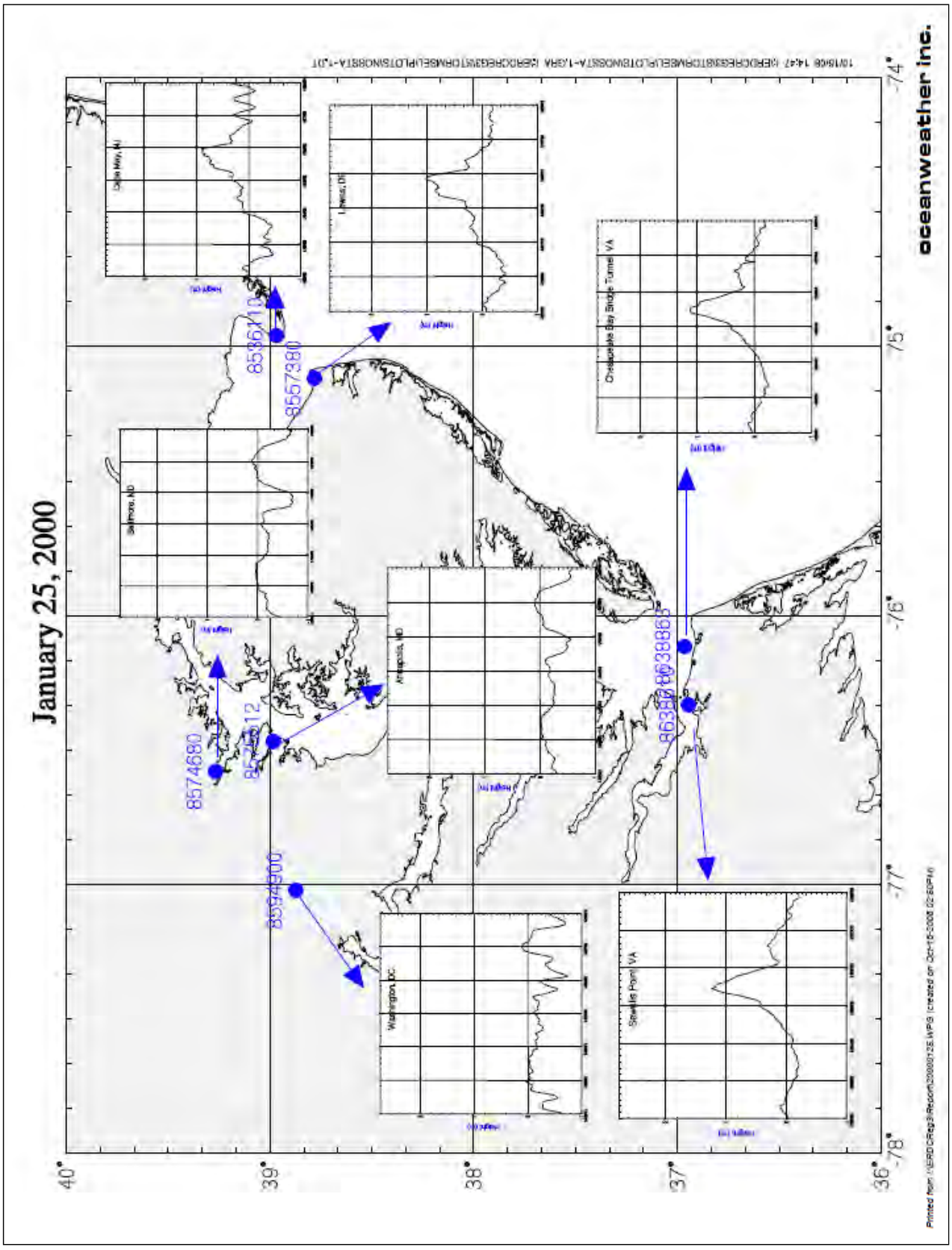

Figure B5. (Sheet 47 of 60)

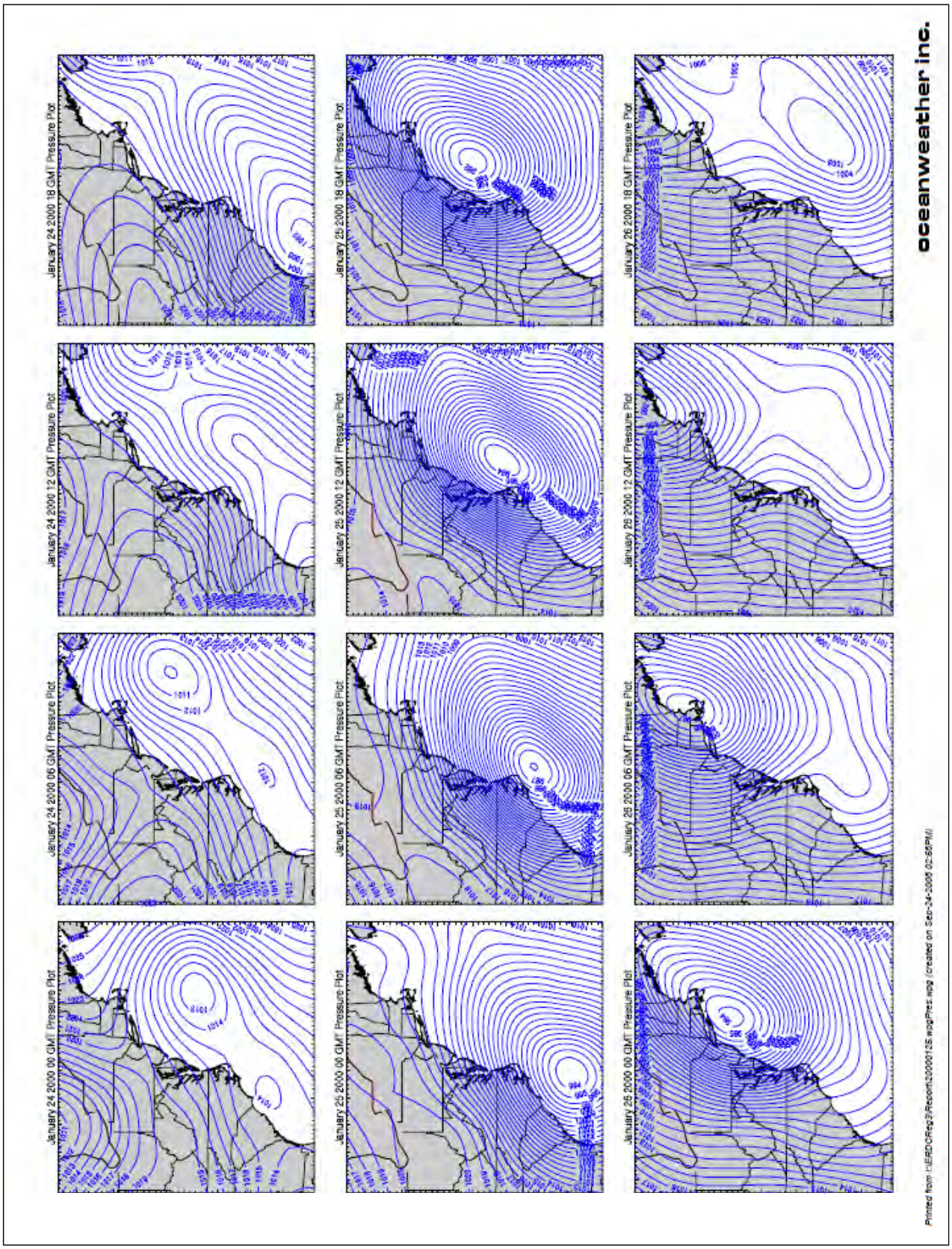

Figure B5. (Sheet 48 of 60)

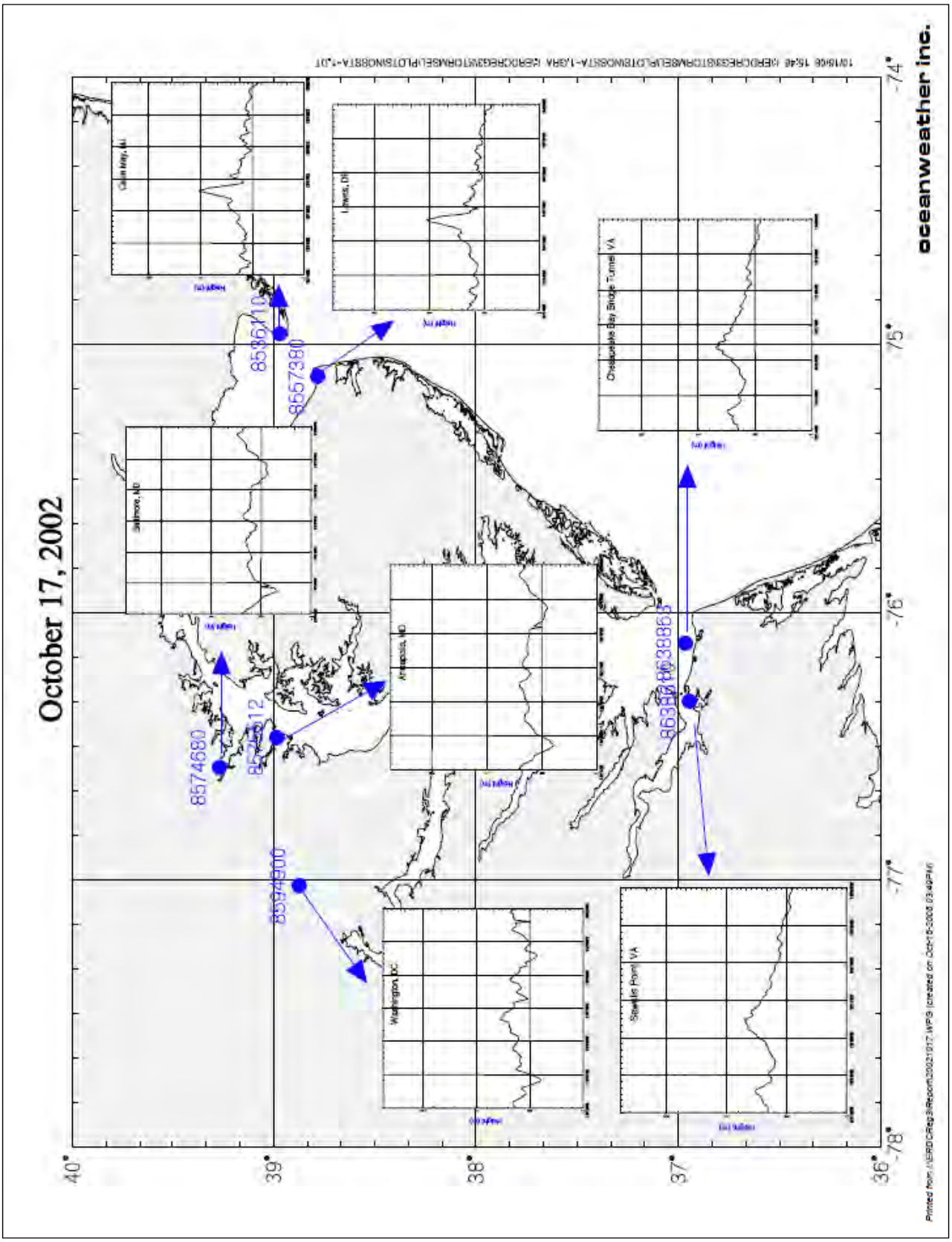

Figure B5. (Sheet 49 of 60)

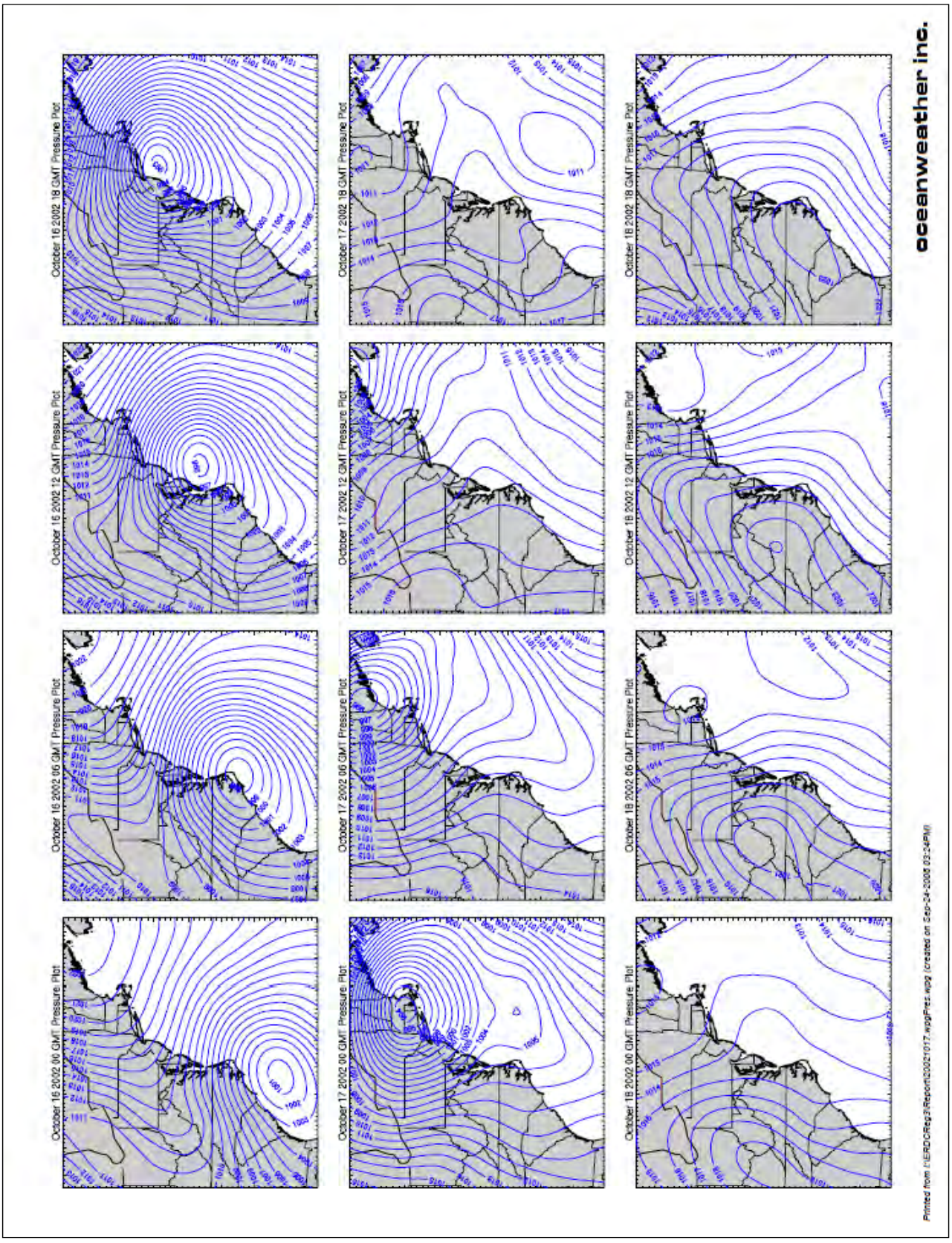

Figure B5. (Sheet 50 of 60)

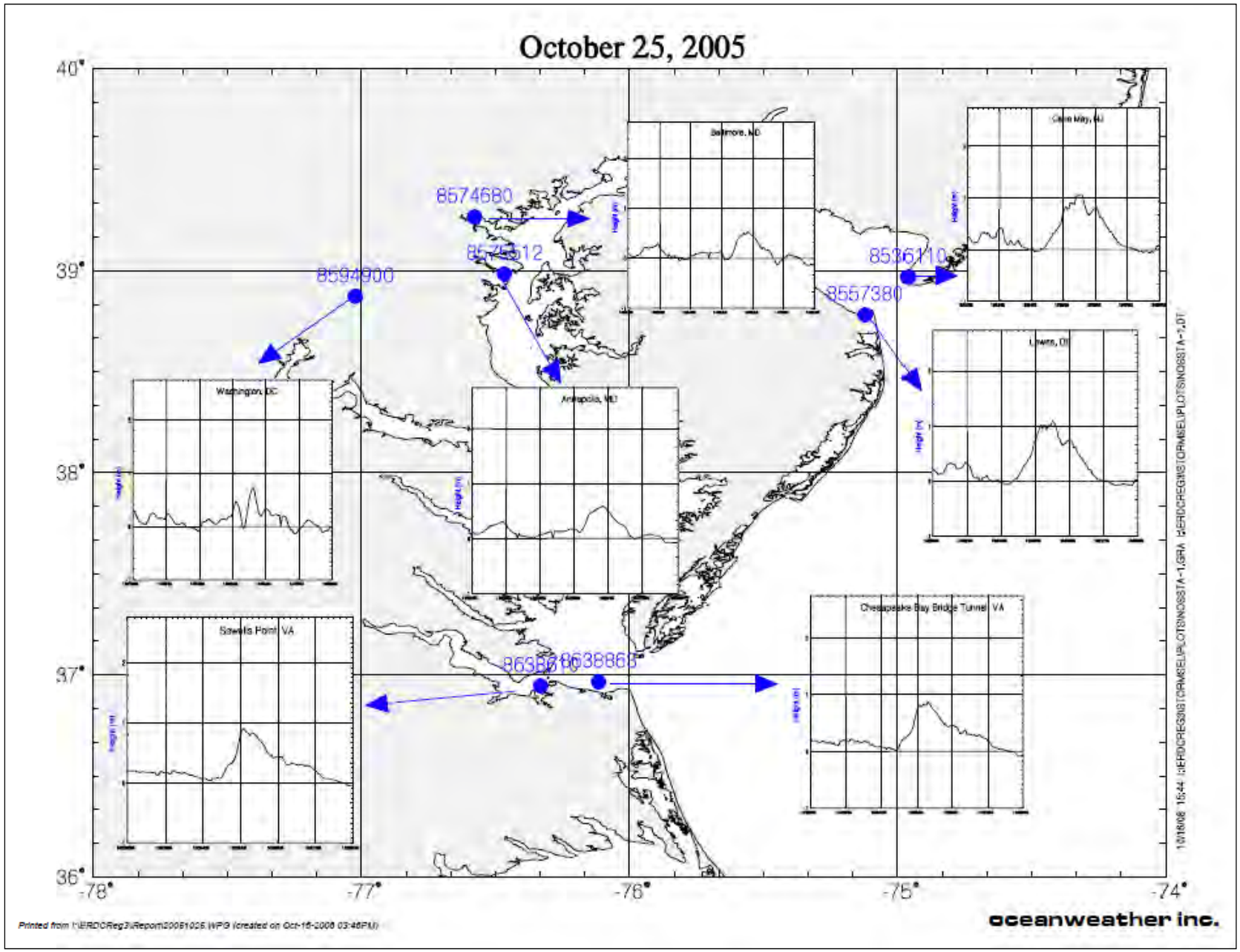

Figure B5. (Sheet 51 of 60)

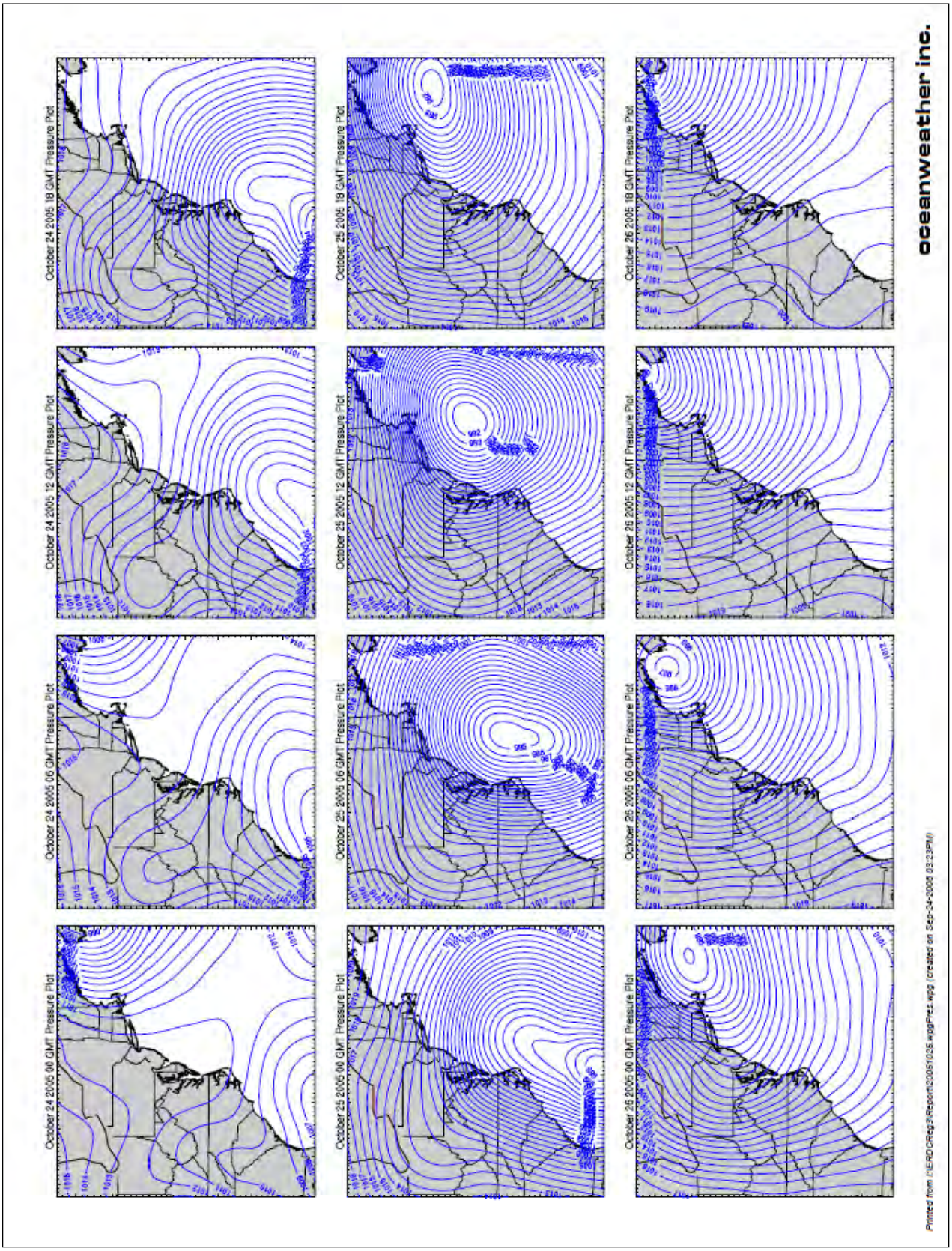

Figure B5. (Sheet 52 of 60)

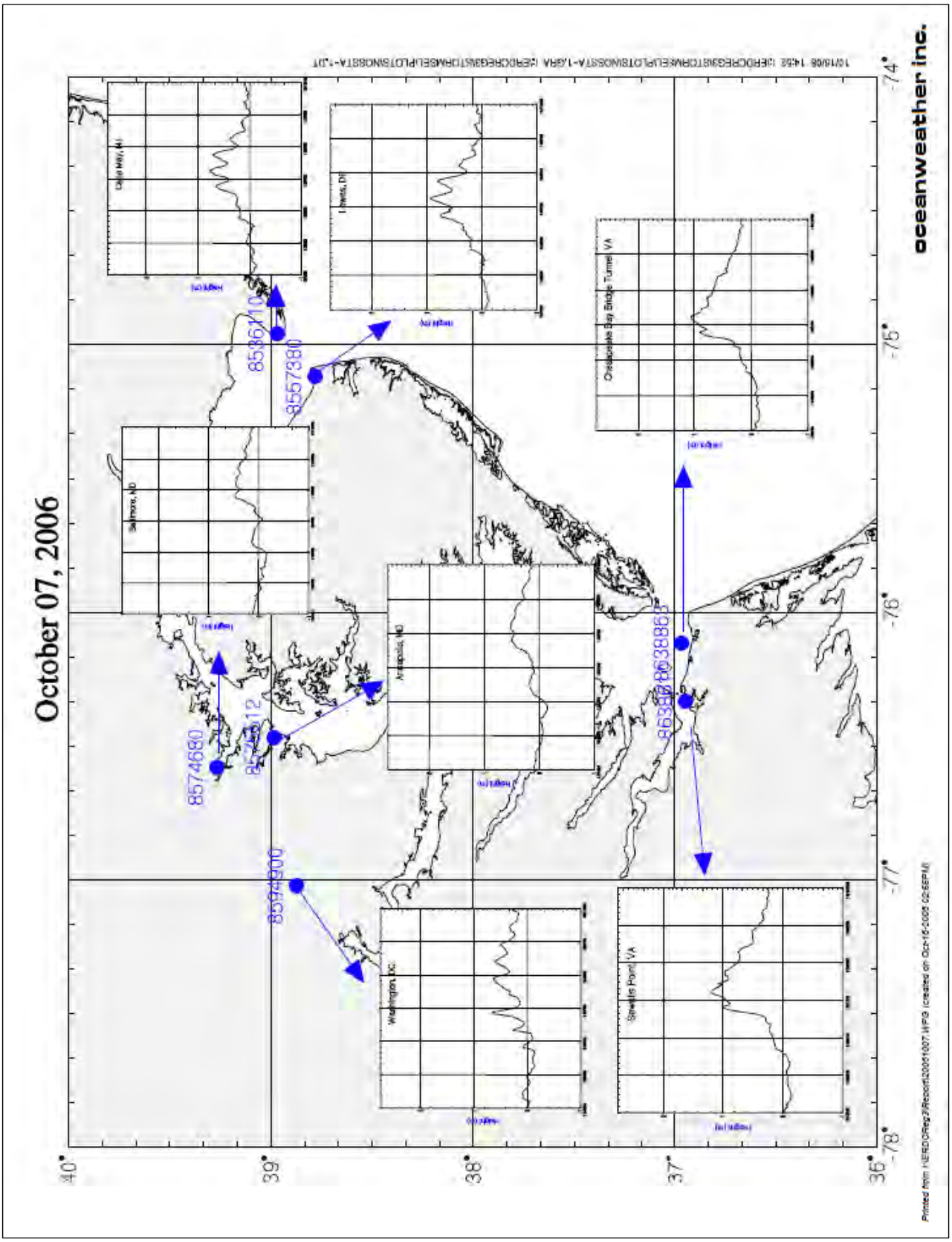

Figure B5. (Sheet 53 of 60)

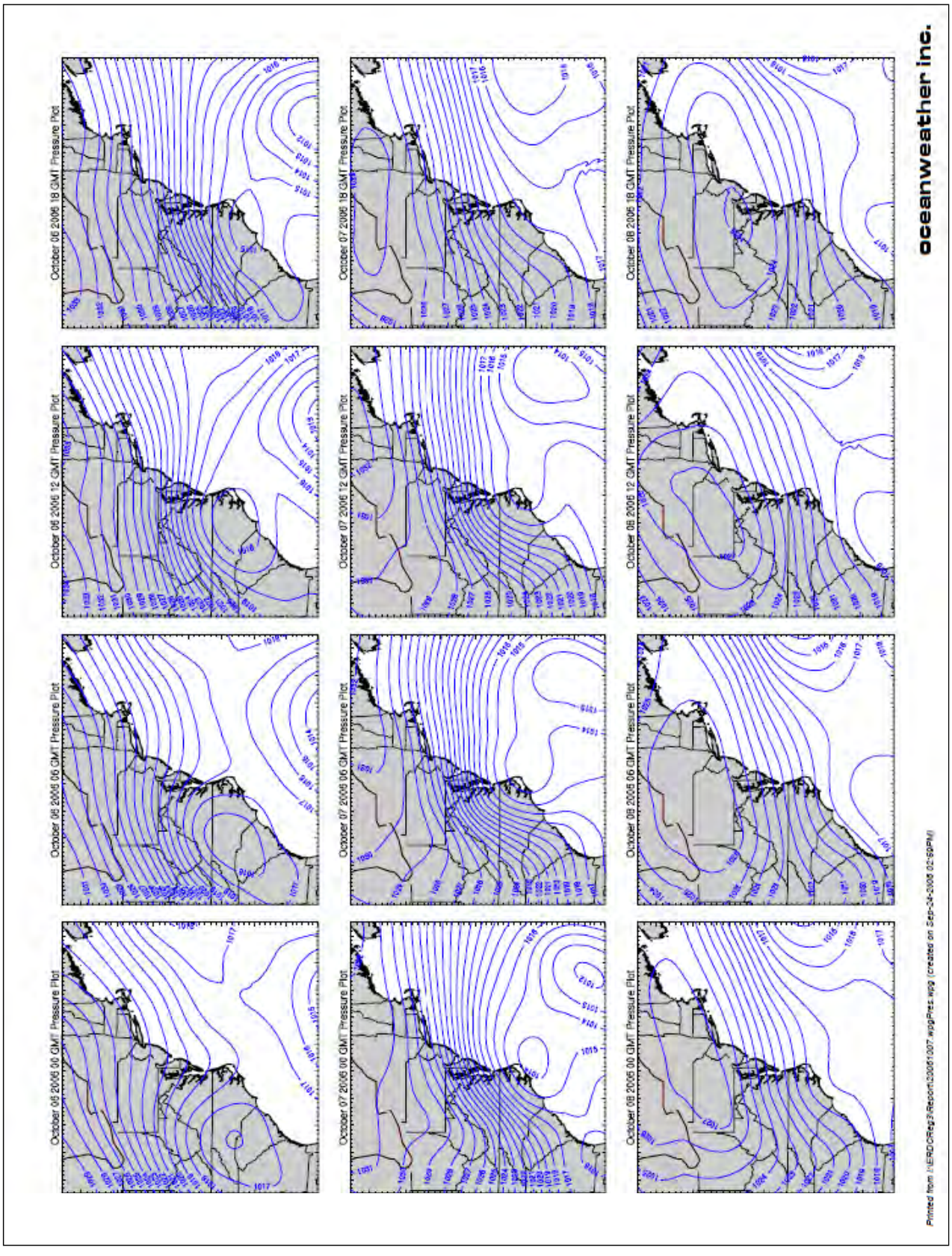

Figure B5. (Sheet 54 of 60)

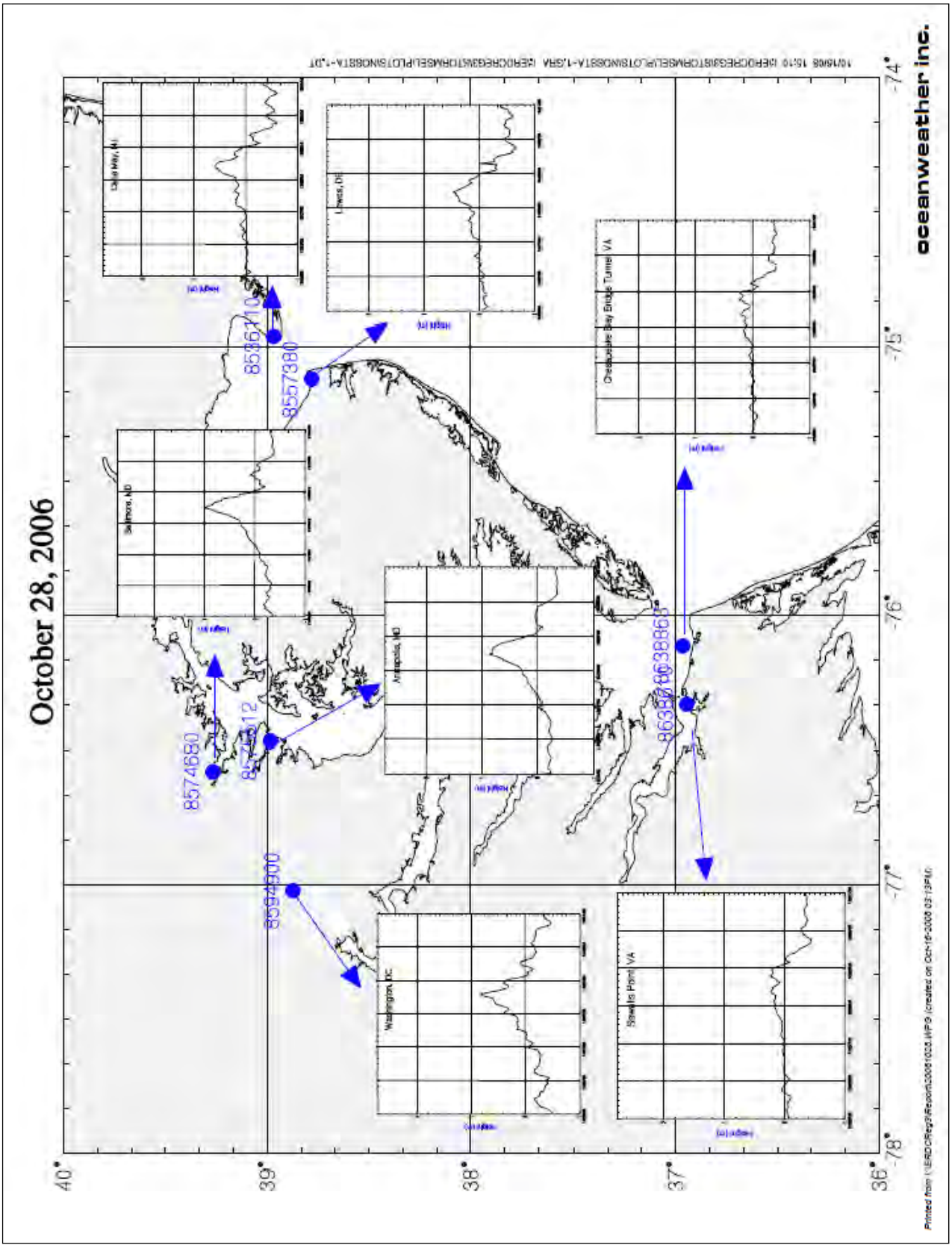

Figure B5. (Sheet 55 of 60)

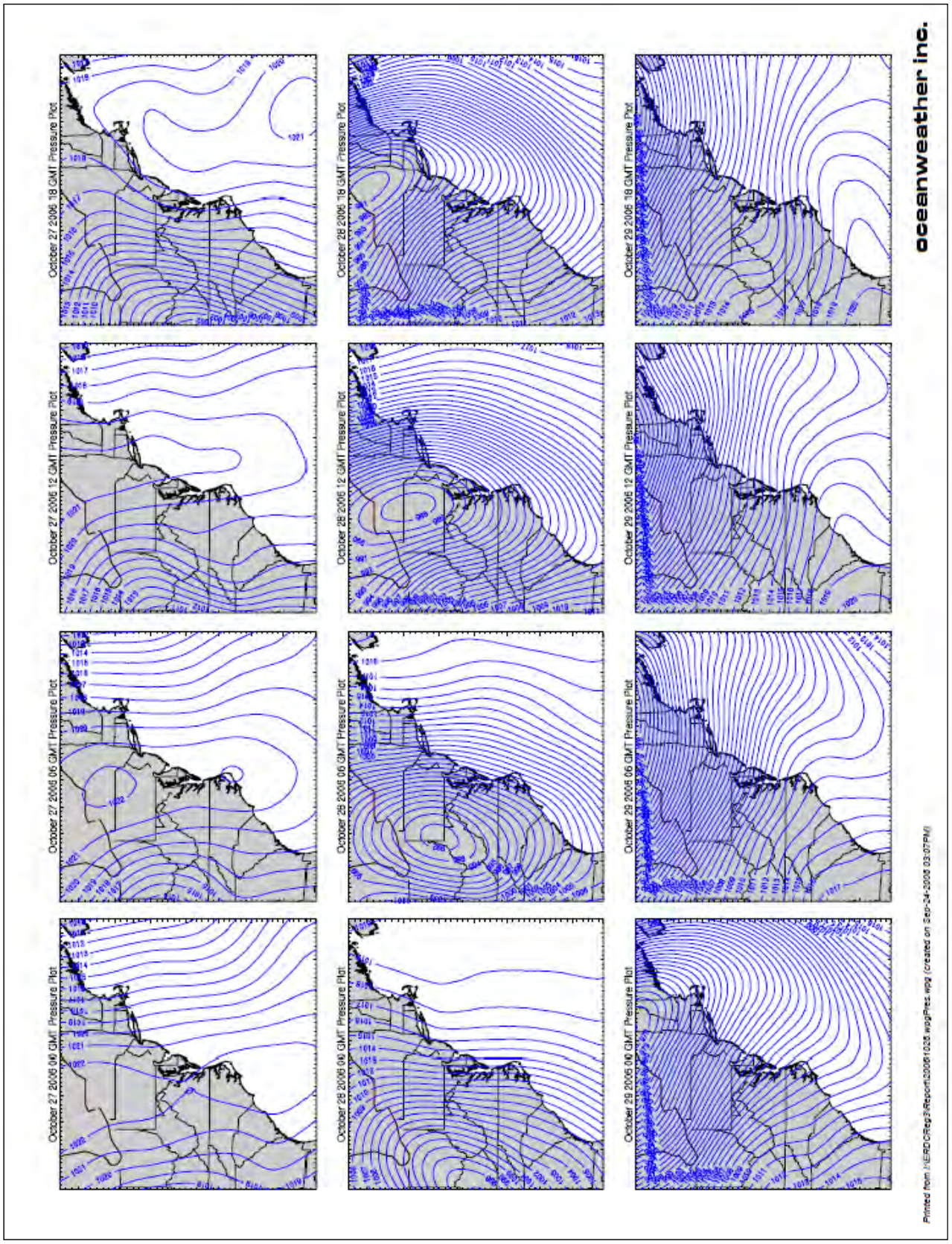

Figure B5. (Sheet 56 of 60)

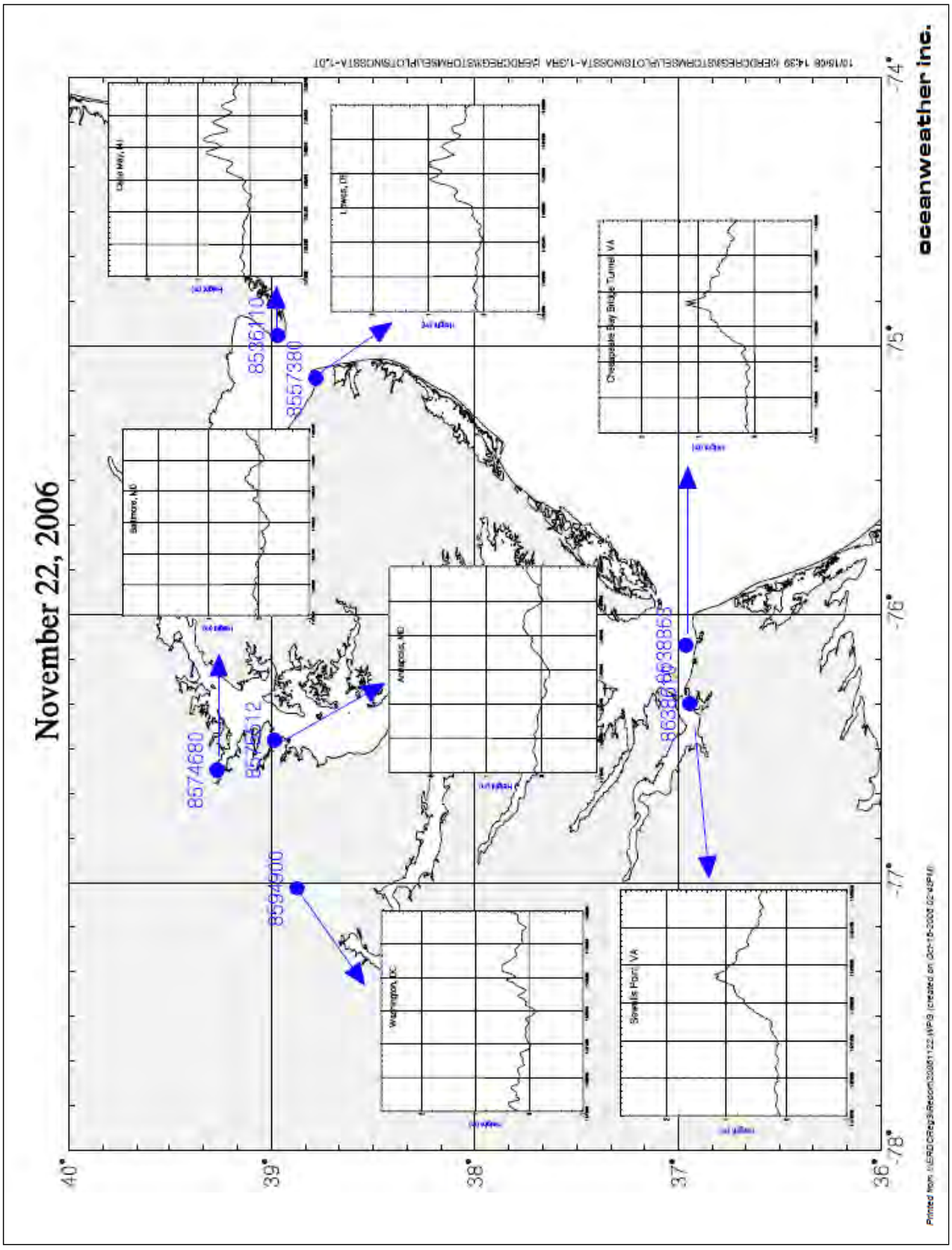

Figure B5. (Sheet 57 of 60)

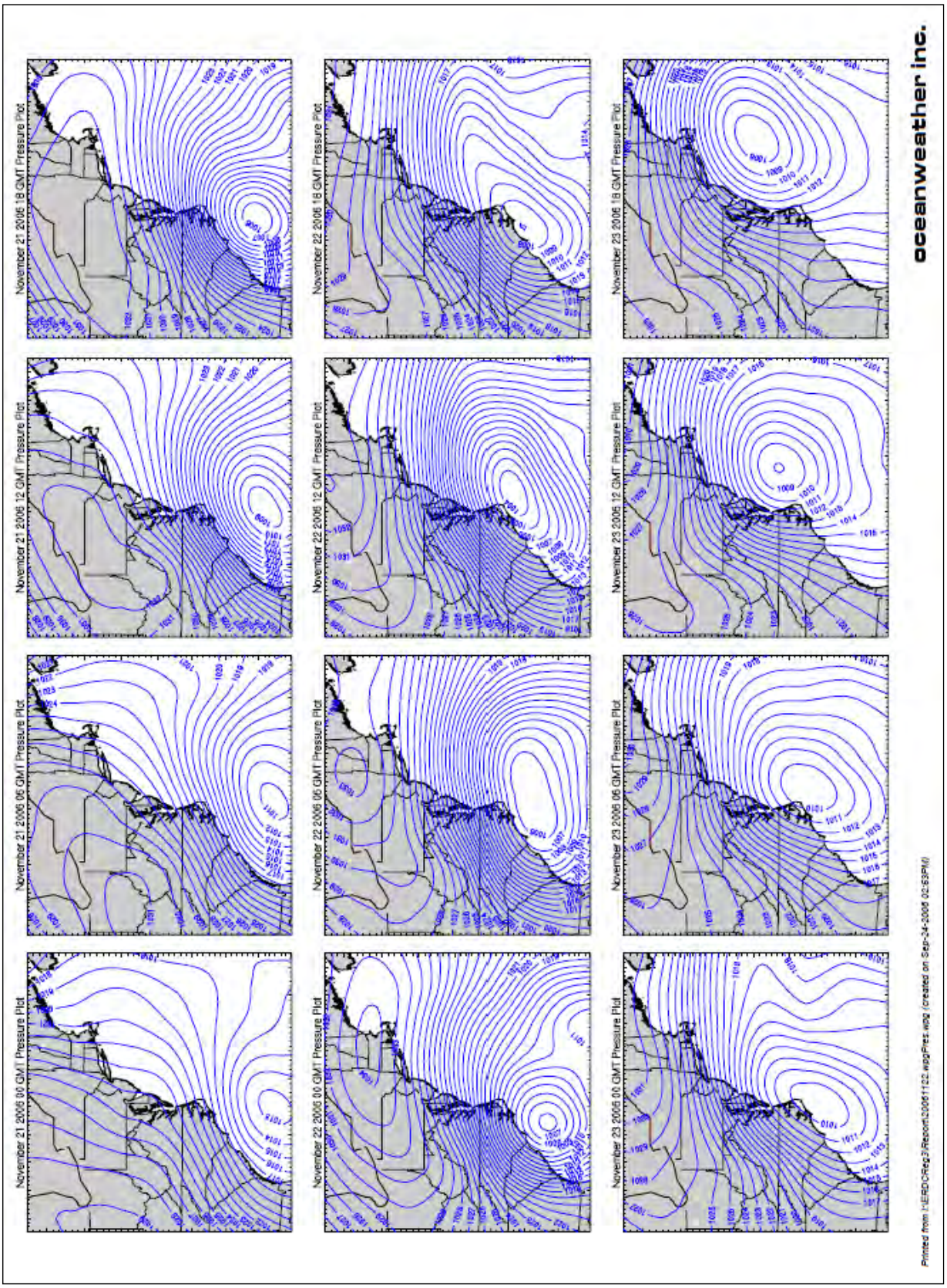

Figure B5. (Sheet 58 of 60)

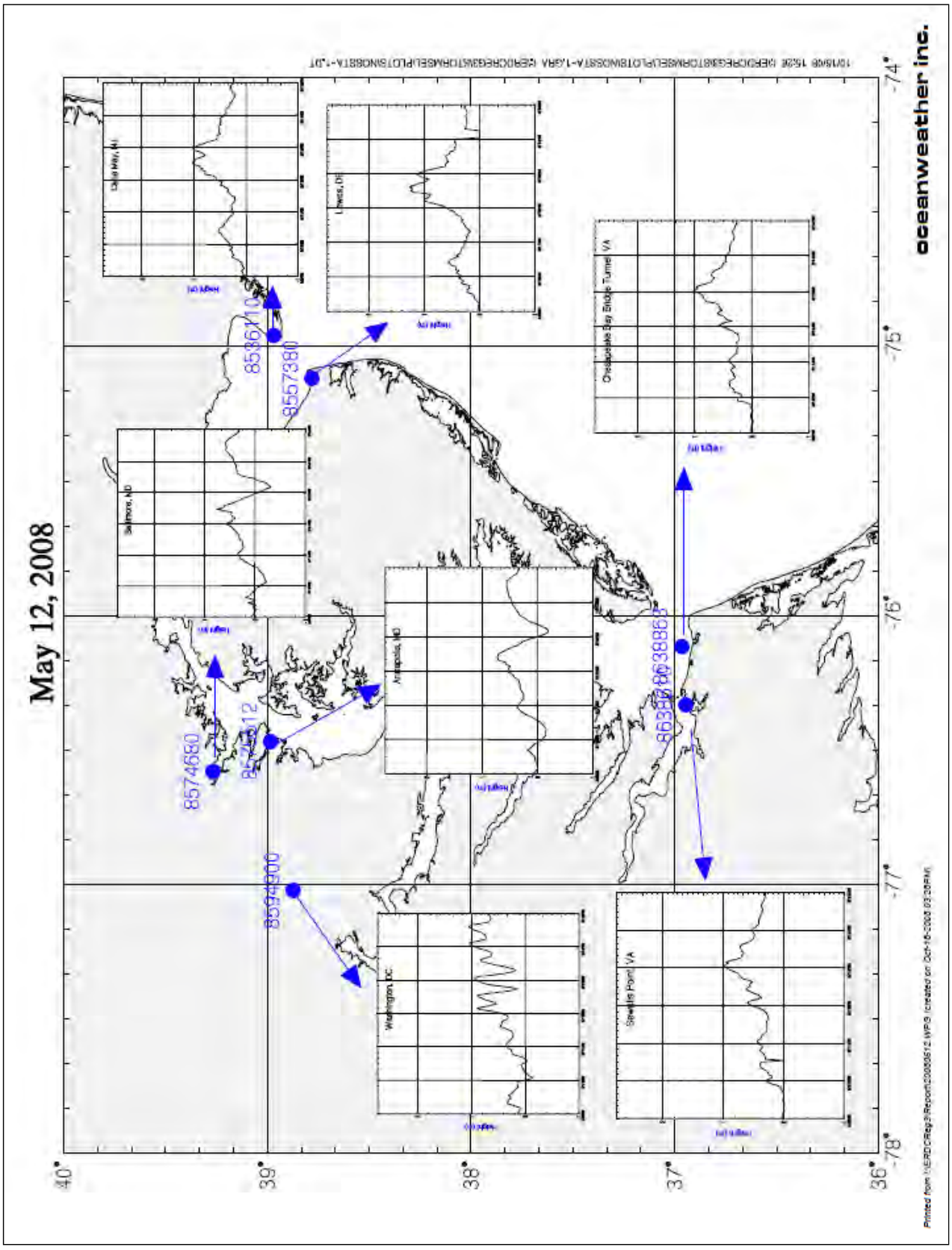

Figure B5. (Sheet 59 of 60)

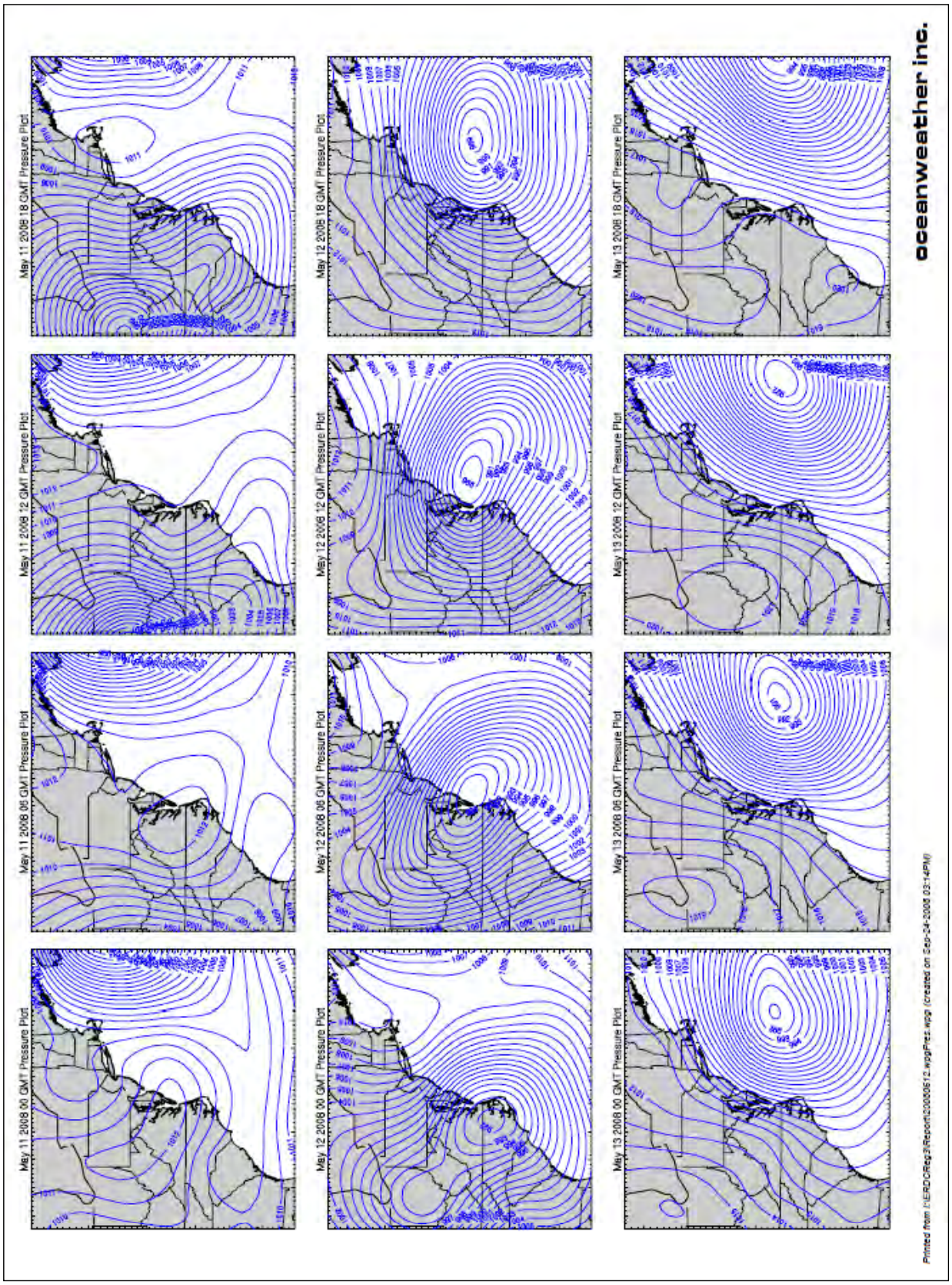

Figure B5. (Sheet 60 of 60)

Appendix C: 468 JPM Track Results

This Appendix discusses the results of and comparisons to the stochastic model values resulting from the 468 storm JPM set.

The probability distributions of the key landfall parameters and associated weights used in the JPM approach using the 468 storms are the same as those used for the 156-storm case and are reflected in Figures 2-14 through 2-17 and Tables 2-1 through 2-3, as given in Chapter 2.

Figures C1 and C2 represent comparisons of the distributions of the landfall values of central pressure, etc. from the 468 storm JPM set to the stochastic simulation results. The comparisons are essentially the same as those discussed in Chapter 2 for the 156-storm case, with the exception that the complete distribution of *B* is retained in this larger set that contains both the mean model for *B*, as well as the upper and lower bound models.

Figure C3 presents the nine sets of tracks used in the 468-JPM storm set. Figure C4 shows the comparisons of the estimated storm surge obtained using the JPM set of storm tracks and full stochastic set for a return period range of 10 through 1,000 years. As seen in Chapter 2, the storm surge estimates obtained using the JPM approach are reasonable for most of the locations up to a return period of 1,000 years. The cases where the JPM results are notably higher than the stochastic results are typically at the end of bays and estuaries.

The full distribution of both the relative and absolute differences between the stochastic and the JPM storm sets are presented in Figure C5 for return periods of 10, 100 and 500 years. Figures C6 through C8 represent the absolute differences in a map format. Figures C9 through C11 present the same information as given in Figures C6 through C8, but here the differences are presented in a relative sense rather than the absolute errors. Each figure presents the maximum, minimum, and mean error.

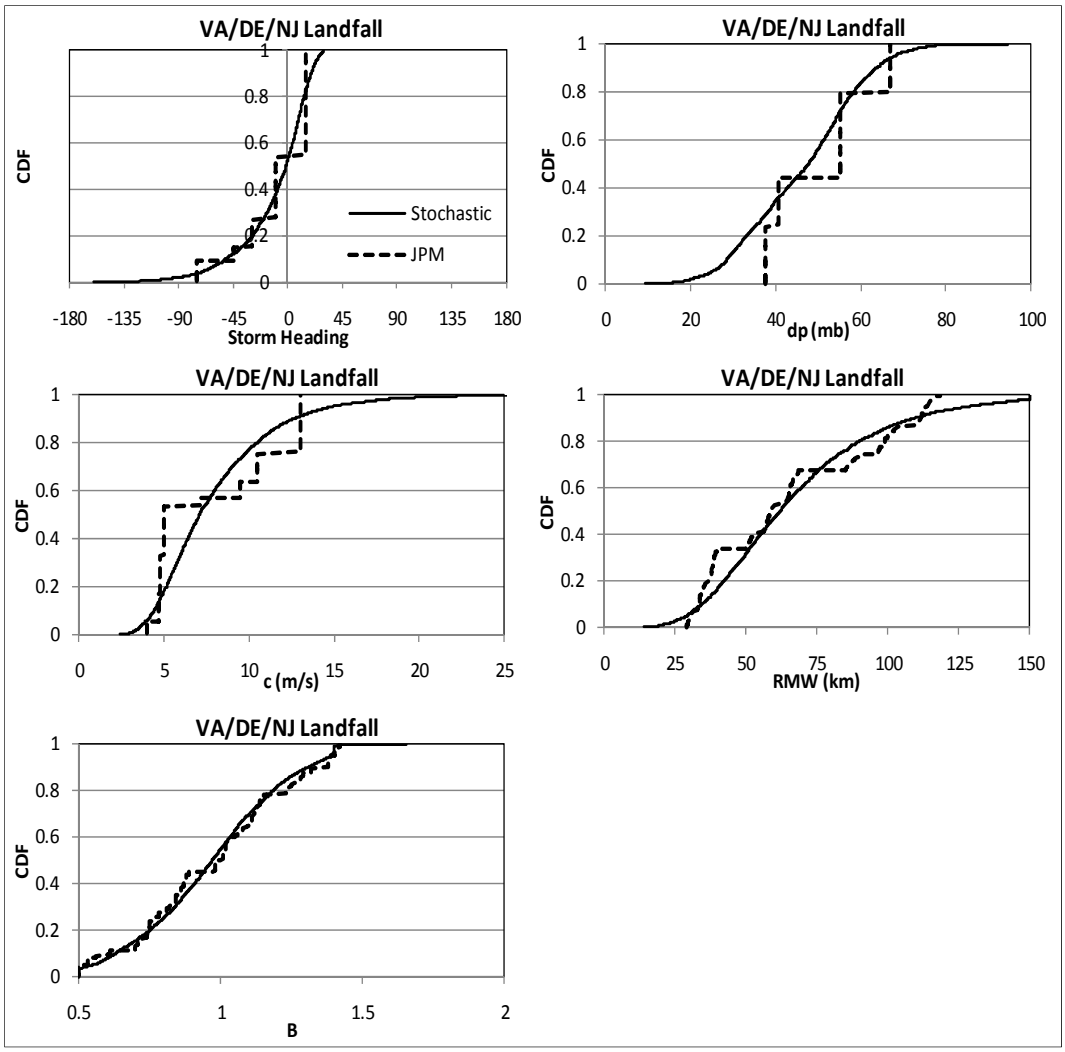

Figure C1. Comparison of JPM and stochastic representations of hurricane parameters at landfall along the VA/DE/NJ coastal segment. Heading is defined as the direction of motion of the storm measured clockwise from north. Storms with a positive heading have an eastward component. The translation speed is denoted *c*, the central pressure difference is denoted *dP* and *RMW* is the radius to maximum winds.

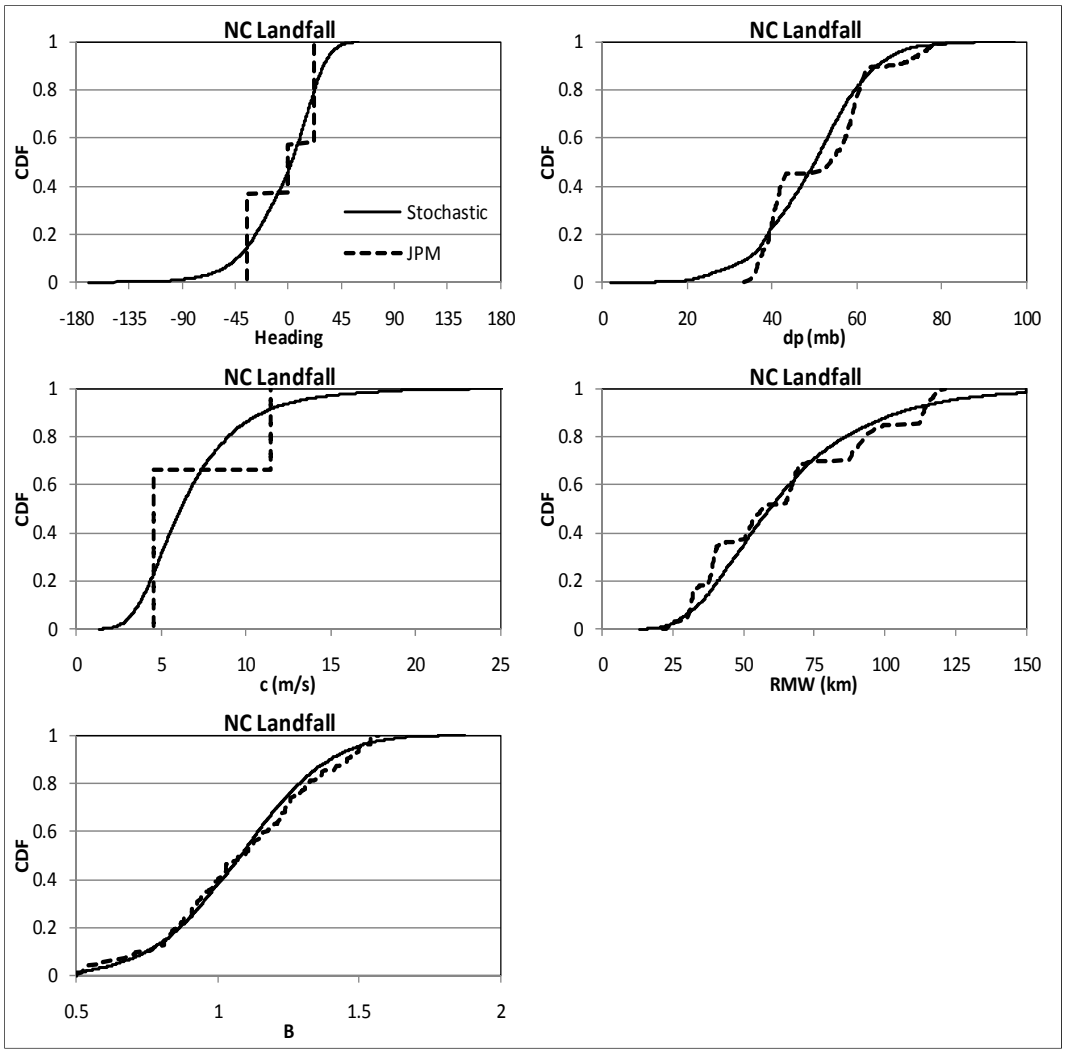

Figure C2. Comparison of JPM and stochastic representations of hurricane parameters at landfall along the NC coastal segment. Heading is defined as the direction of motion of the storm measured clockwise from north. Storms with a positive heading have an eastward component. The translation speed is denoted *c*, the central pressure difference is denoted *dP* and *RMW* is the radius to maximum winds.

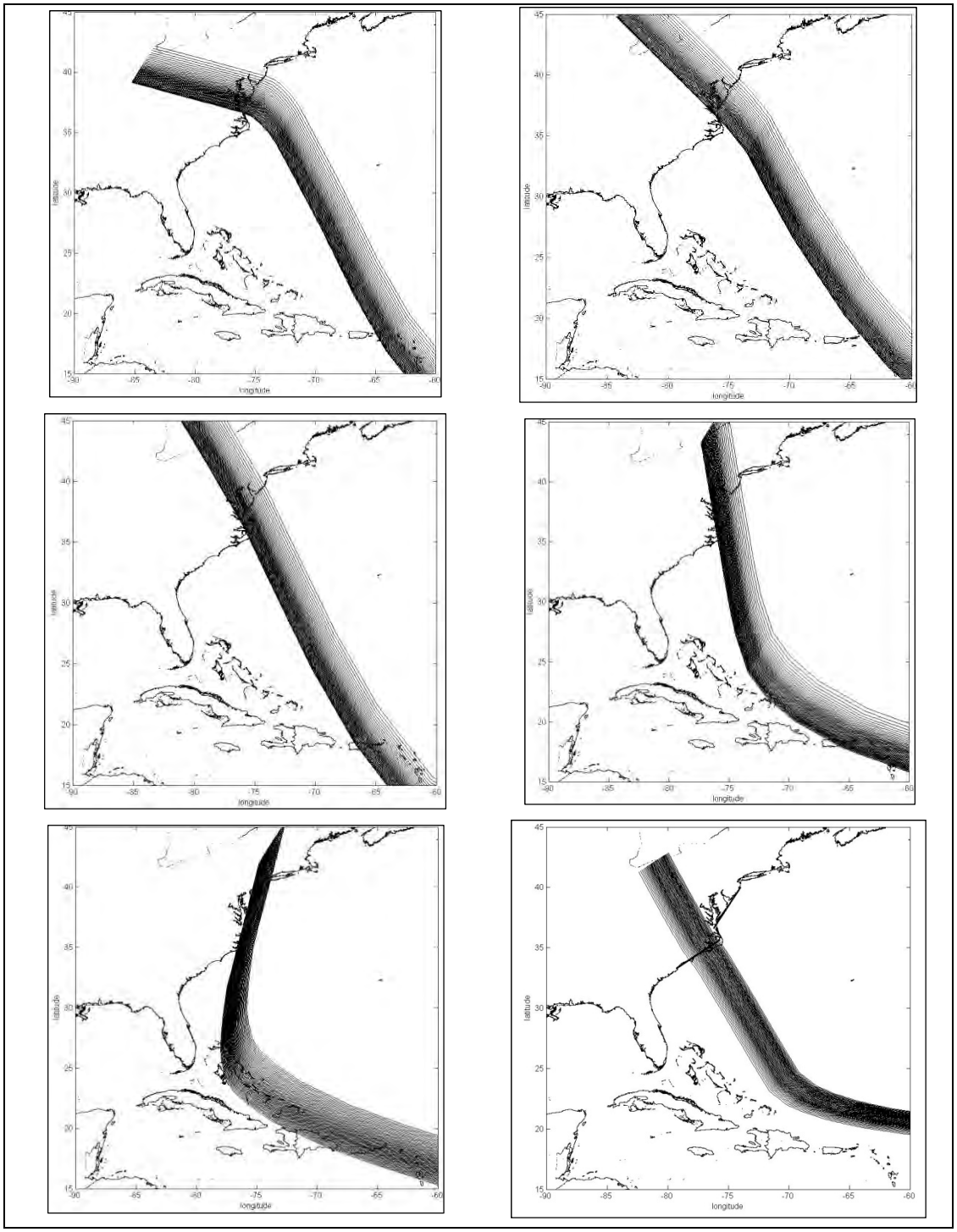

Figure C3. Tracks used to define the reduced (JPM) storm set. (continued)

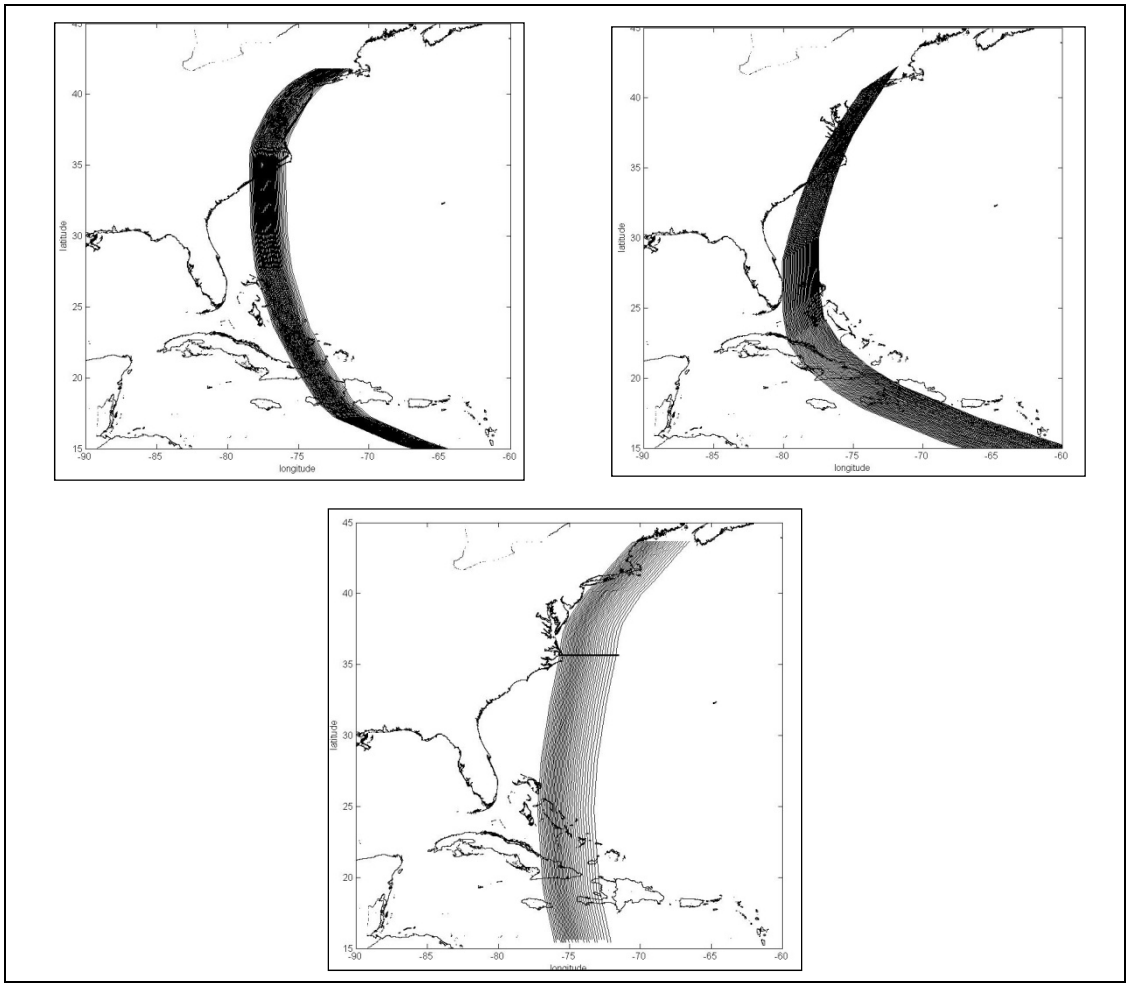

Figure C3. (concluded)

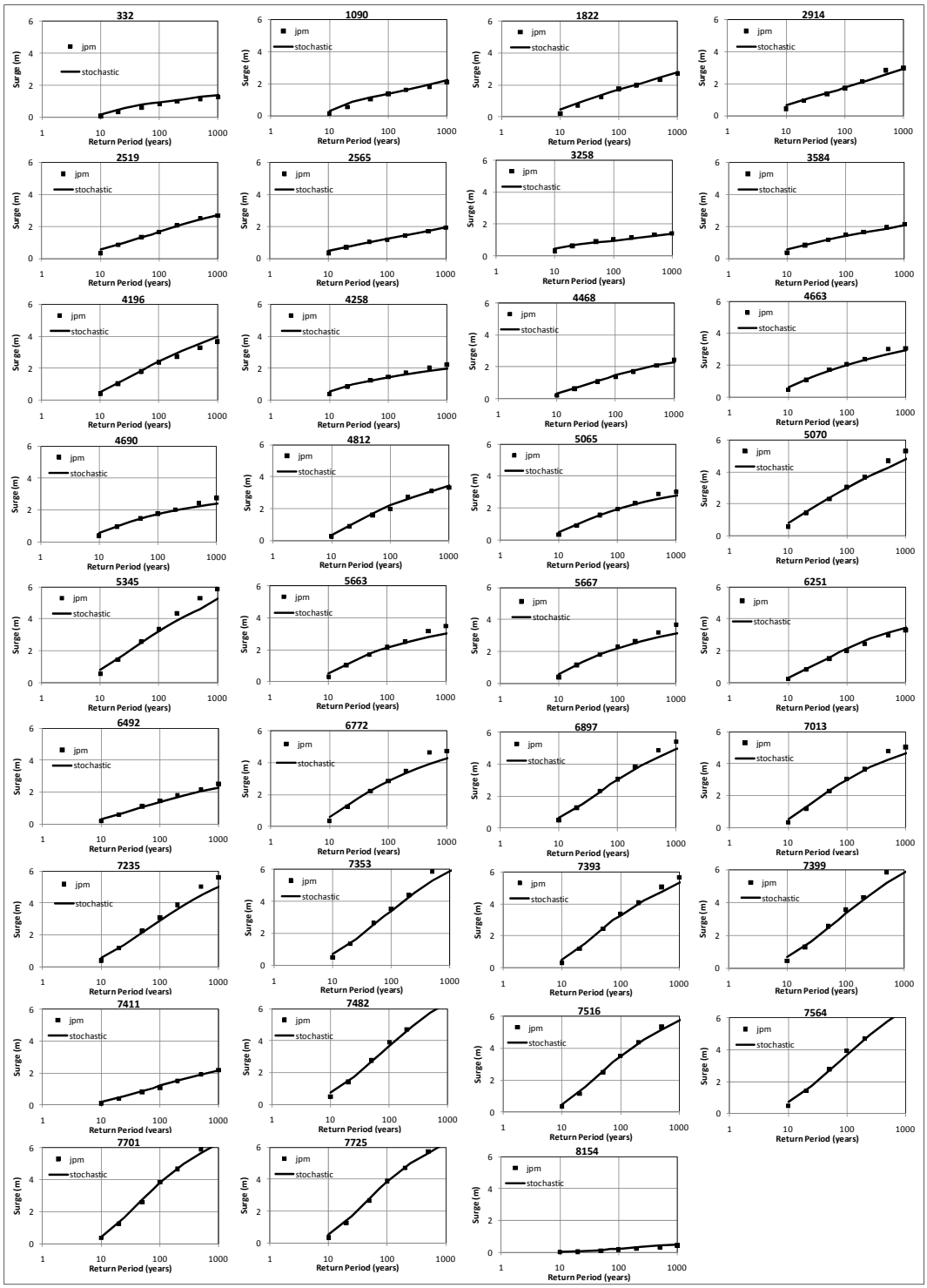

Figure C4. Comparisons of storm surge elevations computed using the stochastic and the JPM storm sets represented with 468 simulated tracks.

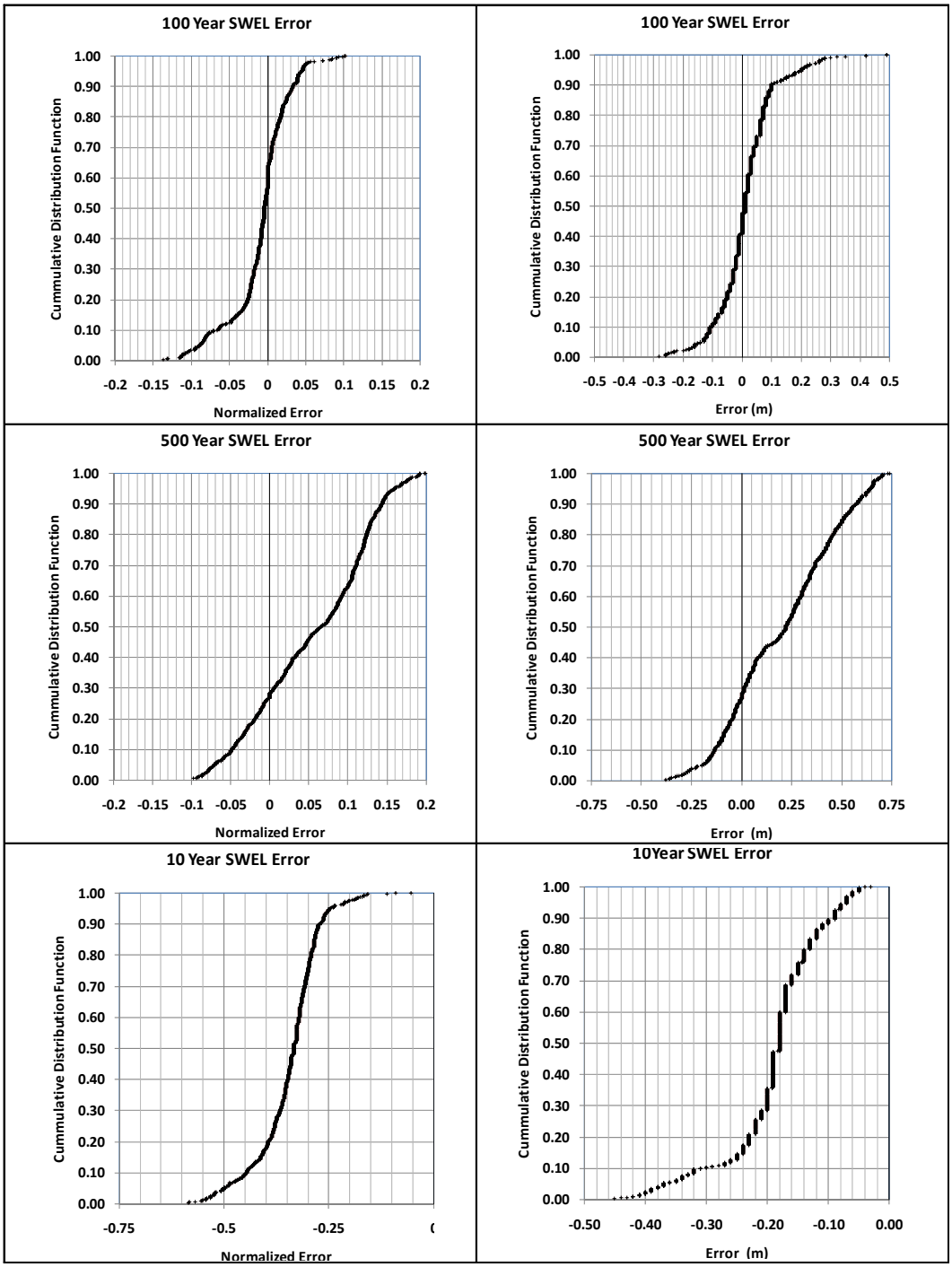

Figure C5. Cumulative distribution functions showing the differences in the modeled storm surge elevations at all nodal points shown in Figure 2-20. The differences are defined as the JPM results minus the stochastic results. Plots on the left present the relative difference and plots on the right show the absolute difference, expressed as meters.

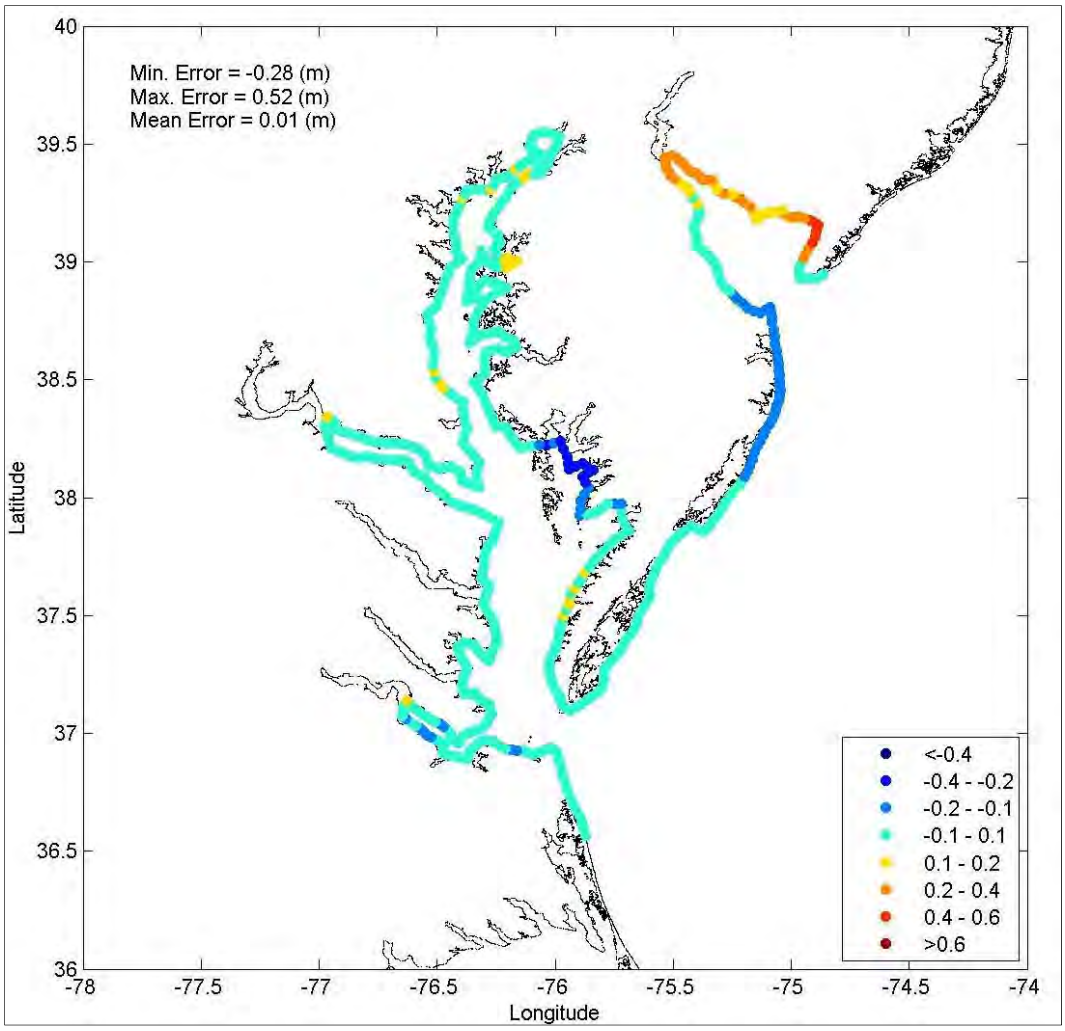

Figure C6. Difference between the stochastic and JPM-predicted 100-year return period storm surge elevations. Positive values indicate that the JPM methodology produces higher storm surge values than the stochastic model. The largest positive differences occur on the north side of Delaware Bay, along the New Jersey coast.

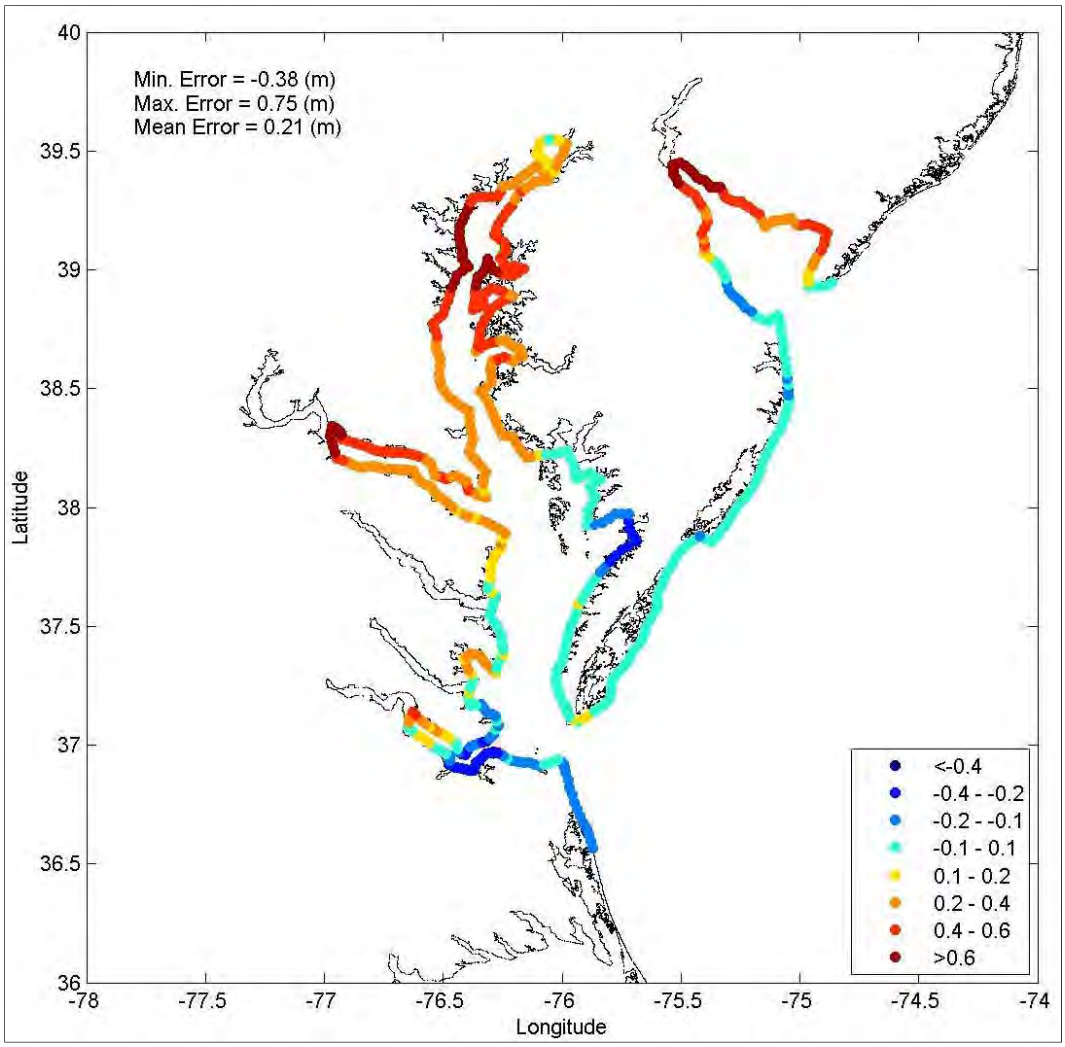

Figure C7. Difference between the stochastic and JPM-predicted 500-year return period storm surge elevations. Positive values indicate that the JPM methodology produces higher storm surge values than the stochastic model. Note the largest positive differences occur on the north side of Delaware Bay, along the New Jersey coast and at the inland most extreme of the Delaware Bay.

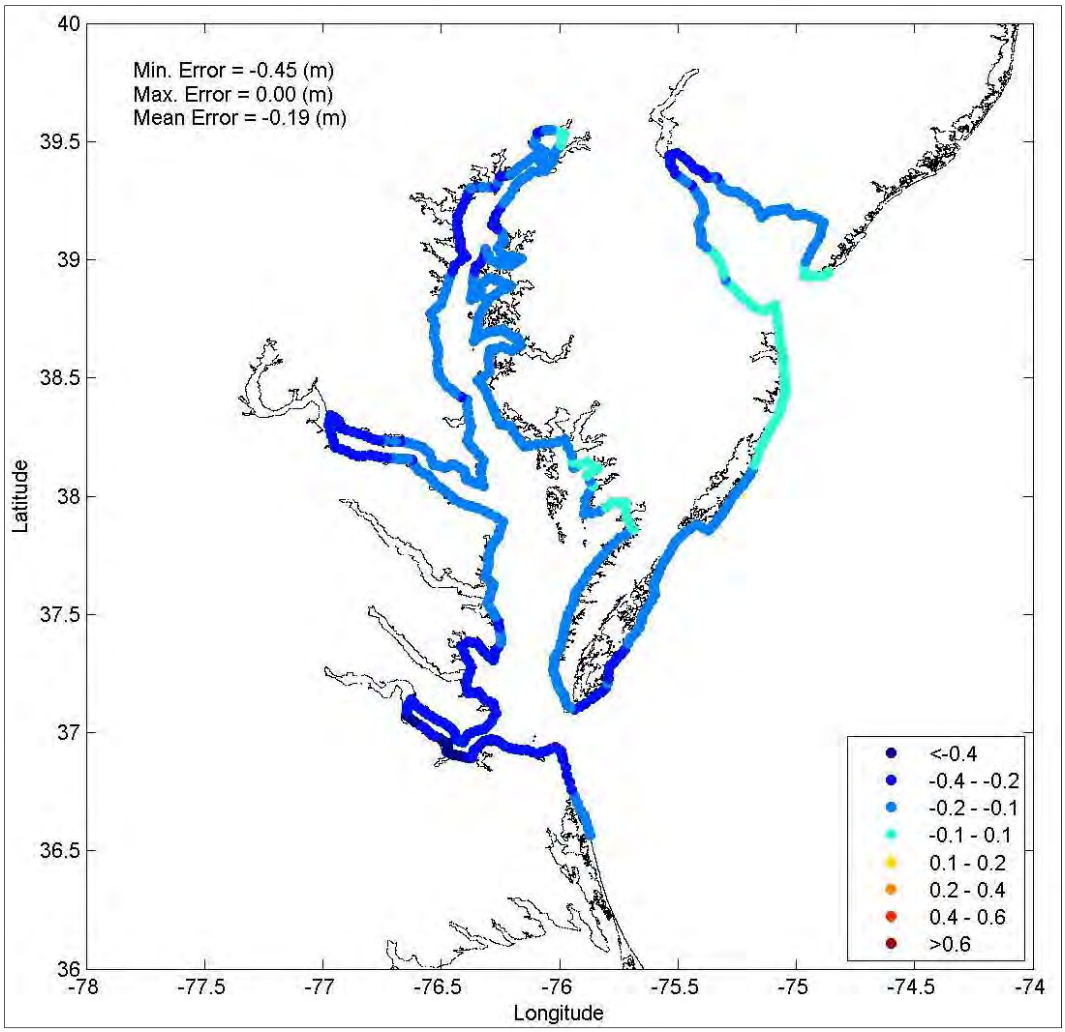

Figure C8. Difference between the stochastic and JPM-predicted 10-year return period storm surge elevations. Positive values indicate that the JPM methodology produces higher storm surge values than the stochastic model. There is a clear bias, with the JPM results being lower than the stochastic results for all locations.

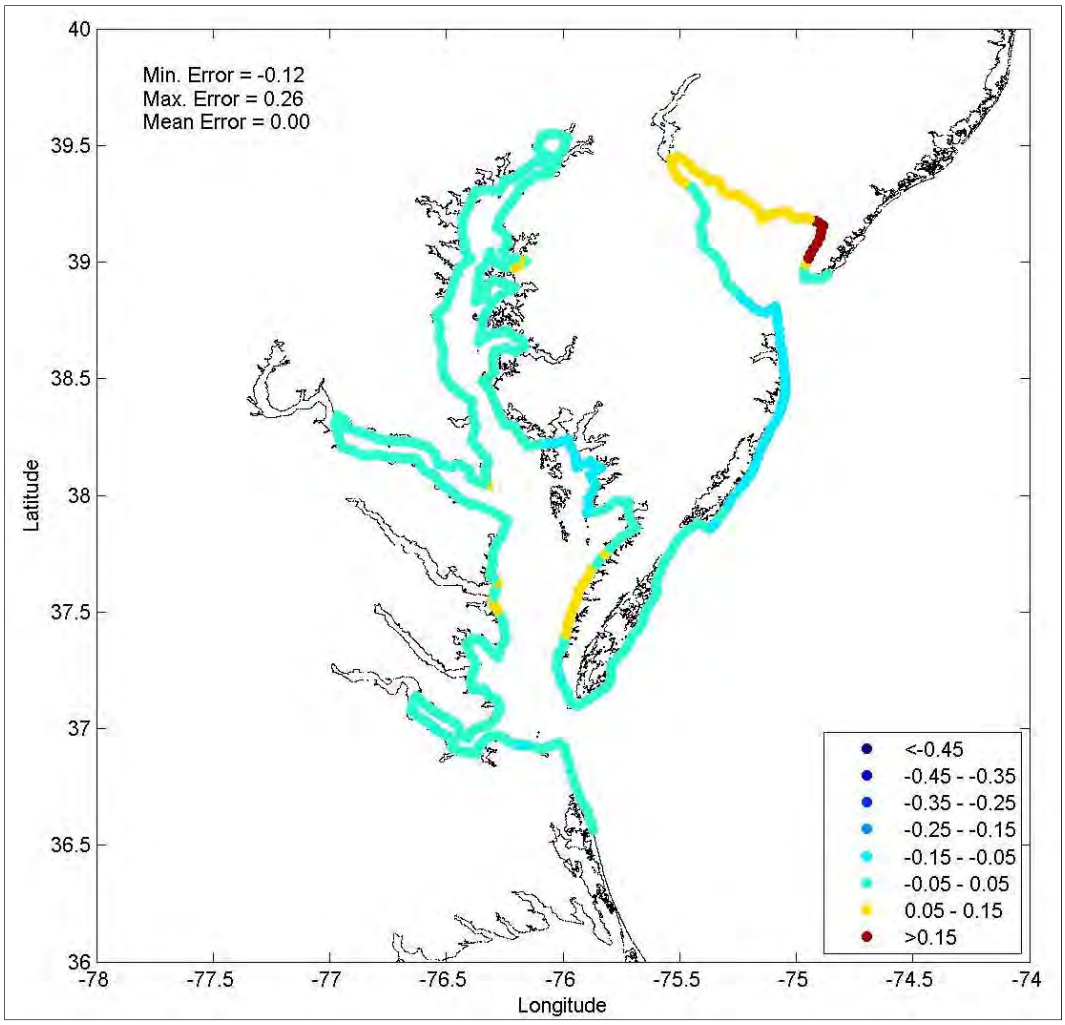

Figure C9. Relative (percentage) difference between the stochastic and JPM-predicted 100-year return period storm surge elevations. Positive values indicate that the JPM methodology produces higher storm surge values than the stochastic model. The largest positive differences occur on the north side of Delaware Bay, along the New Jersey coast.

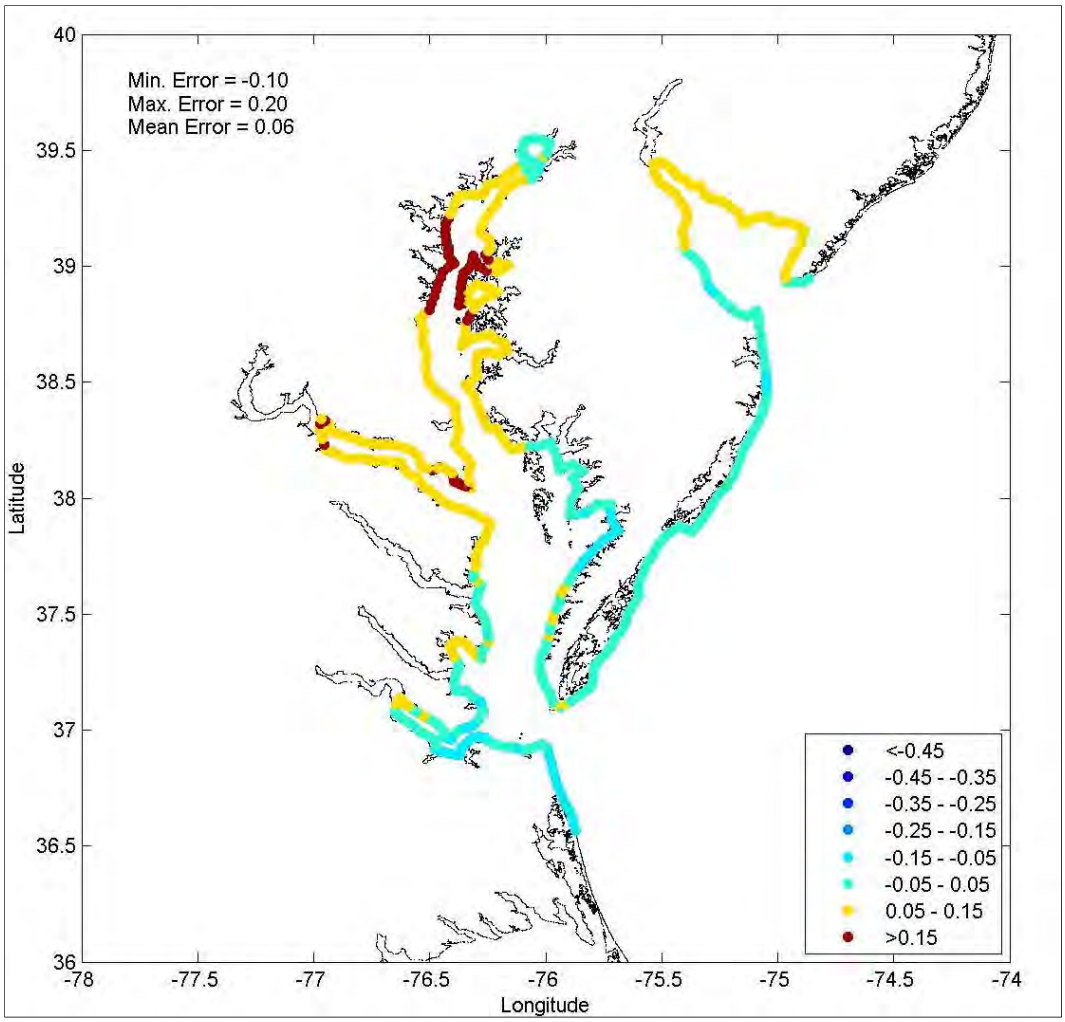

Figure C10. Relative (percentage) difference between the stochastic and JPM-predicted 500-year return period storm surge elevations. Positive values indicate that the JPM methodology produces higher storm surge values than the stochastic model. The largest positive differences occur on the north side of Delaware Bay, along the New Jersey coast and at the inland most extreme of the Delaware Bay.

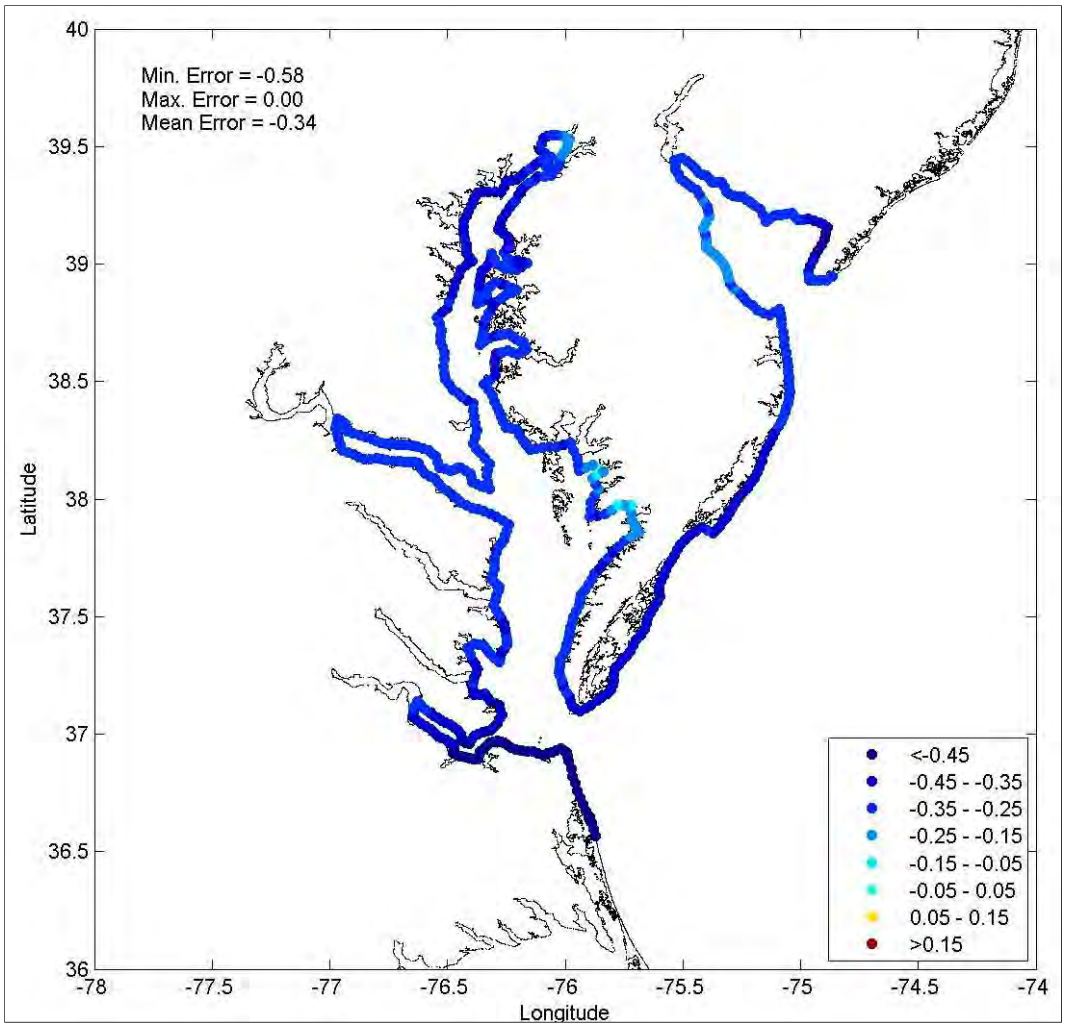

Figure C11. Relative (percentage) difference between the stochastic and JPM-predicted 10-year return period storm surge elevations. Positive values indicate that the JPM methodology produces higher storm surge values than the stochastic model. There is a clear bias, with the JPM results being lower than the stochastic results for all locations.

Appendix D: 156 Unequally Spaced JPM Track Results

This Appendix discusses the results and comparisons to the stochastic model values resulting from the 156 unequally spaced JPM storm set. This set of tracks was developed by removing 2/3 of the tracks from the full set of 468, which included the modeling of the variance associated with the Holland *B* parameter. The removal of 2/3 of the storms resulted in unequally spaced tracks, but it enabled the rapid assessment of the impact of removing the results associated with the upper and lower bound representations of the Holland *B* parameter without the need to rerun the ADCIRC simulations.

The probability distributions of the key landfall parameters and associated weights used in the JPM are the same as those used for the 156-storm case and are reflected in Figures 2-14 through 2-17 and Tables 2-1 through 2-3, (Chapter 2);therefore they will not be presented here again.

Comparisons of the distributions of the landfall values of central pressure, etc. between the JPM set to the stochastic simulation results are the same as those seen in the 156 set of equally spaced tracks presented in Section 2.5 and are not reproduced here.

Figure D1 presents the nine sets of tracks used in this storm set of 156 equally spaced tracks. Figure D2 shows the comparisons of the storm surge estimated using the JPM set of storm tracks and full stochastic set for a return period range of 10 through 1,000 years. As seen in Chapter 2, Appendix C, and again here, the storm surge estimates calculated using the JPM approach are reasonable for most of the locations, up to a return period of 1,000 years. The cases where the JPM results are notably higher than the stochastic results are typically at the end of bays and estuaries.

The full distribution of both the relative and absolute differences between the stochastic and the JPM storm sets are presented in Figure D3 for return periods of 10, 100, and 500 years. Figures D4 through D6 show the absolute differences in a map format. Figures D7 through D9 present the same information as given in Figures D4 through D6, but here the differences are presented in a relative sense rather than as absolute errors. Each figure presents the maximum, minimum, and mean error.

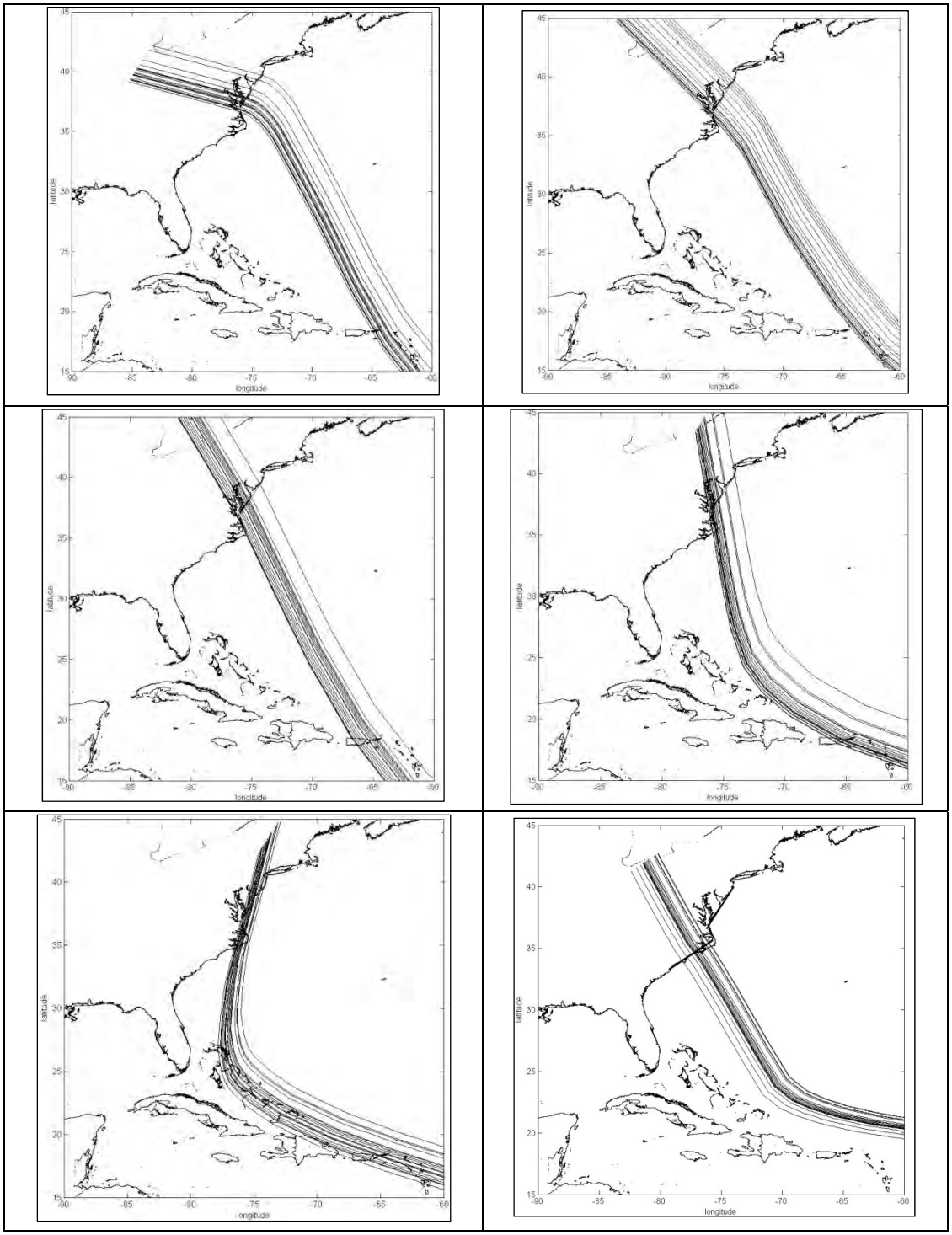

Figure D1. Tracks used to define the reduced (JPM) storm set. (continued)

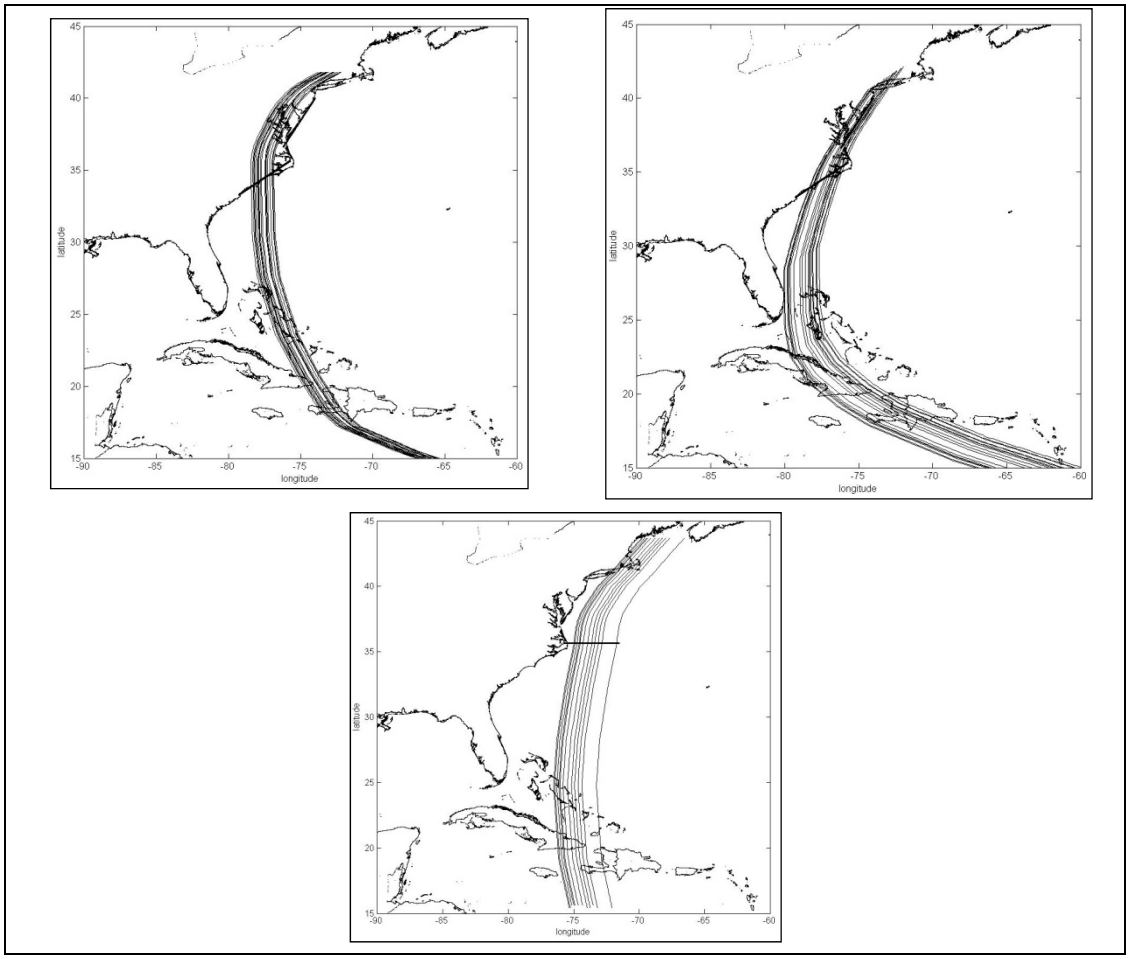

Figure D1. (concluded)

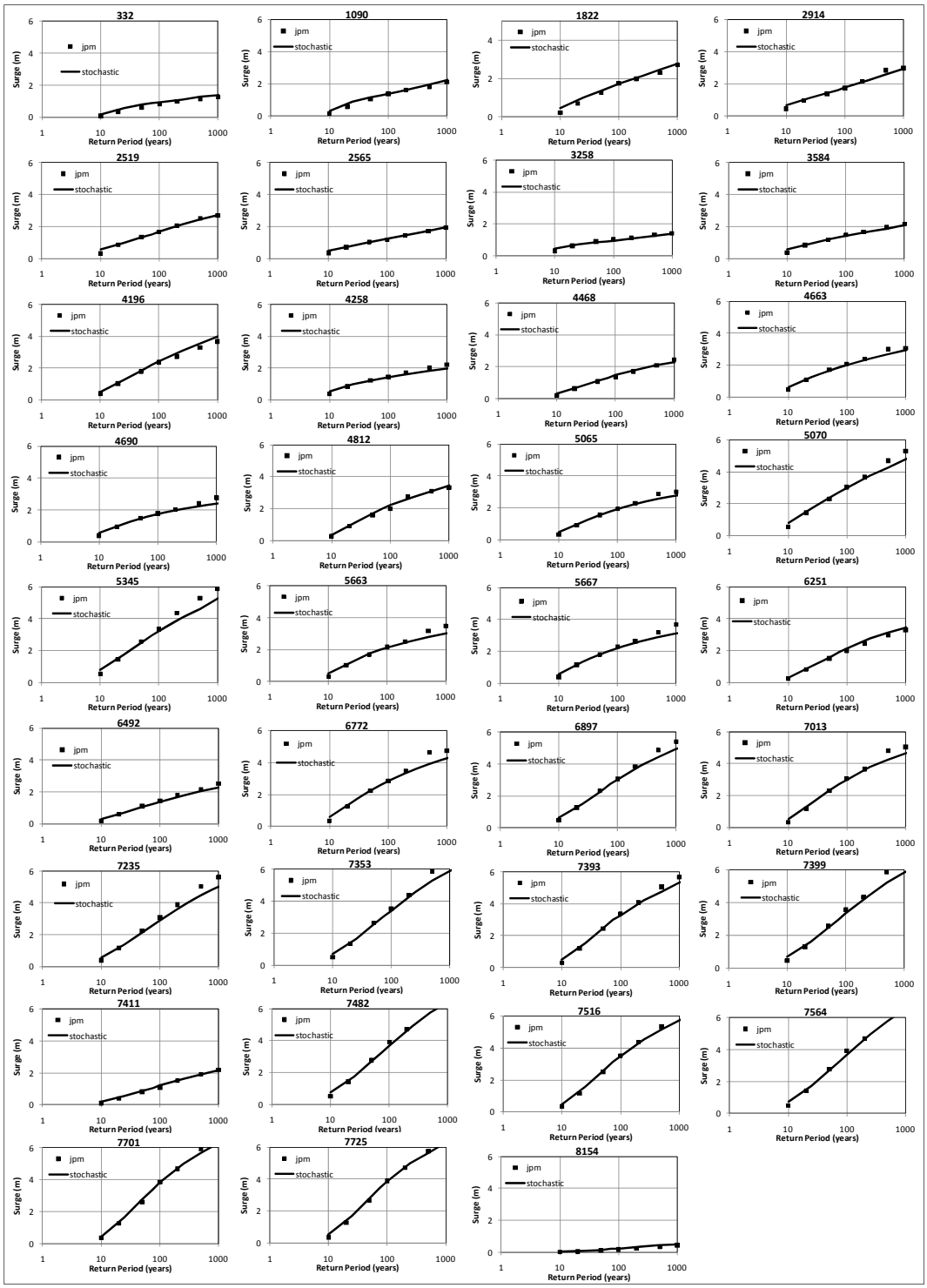

Figure D2 Comparisons of storm surge elevations computed using the stochastic and the JPM storm sets, represented with 156 unequally spaced simulated tracks.

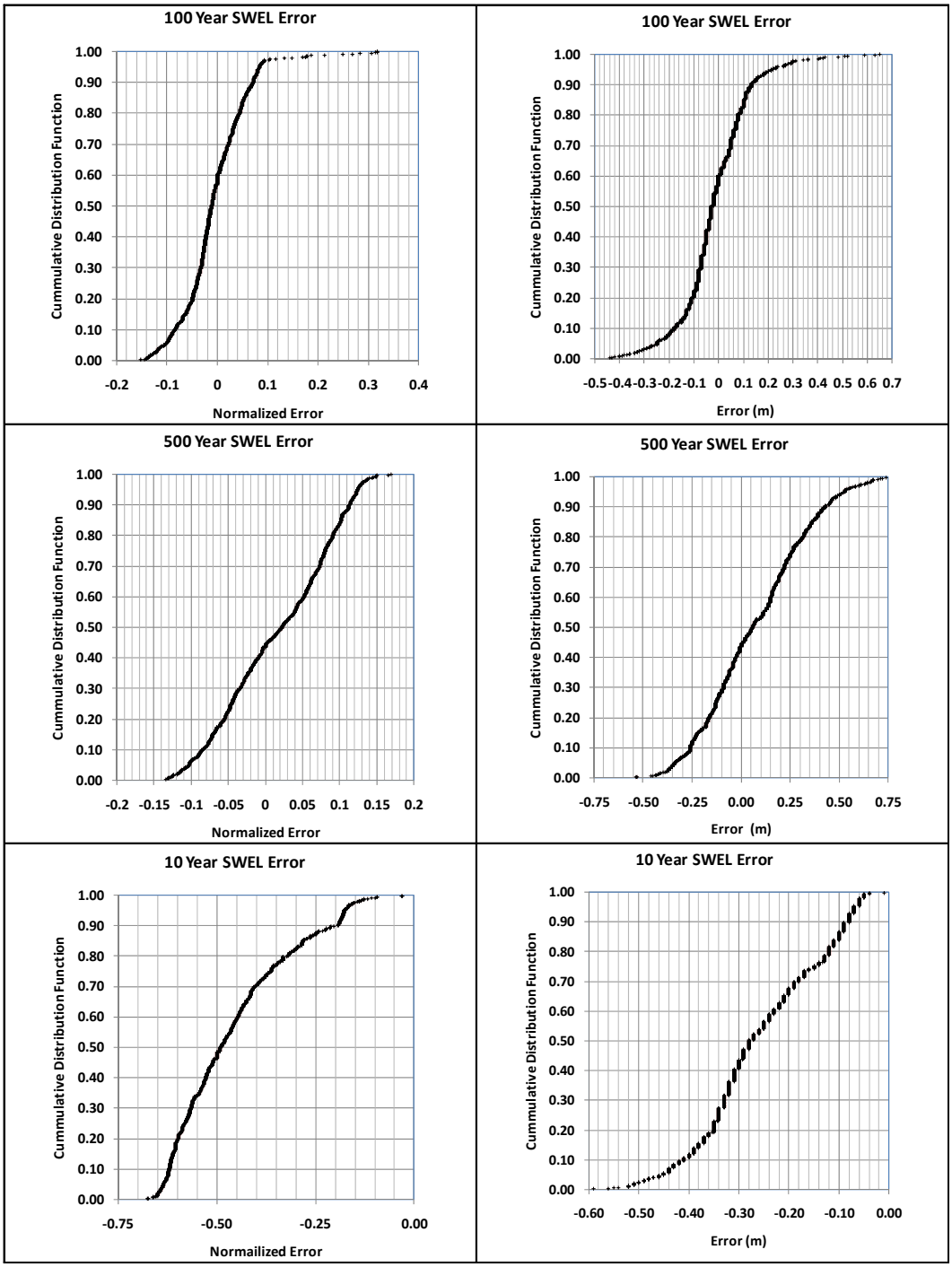

Figure D3. Cumulative distribution functions showing the differences in the modeled storm surge elevations at all nodal points shown in Figure 2-20. The differences are defined as the JPM results minus the stochastic results. Plots on the left represent the relative difference and plots on the right show the absolute difference, expressed as meters.

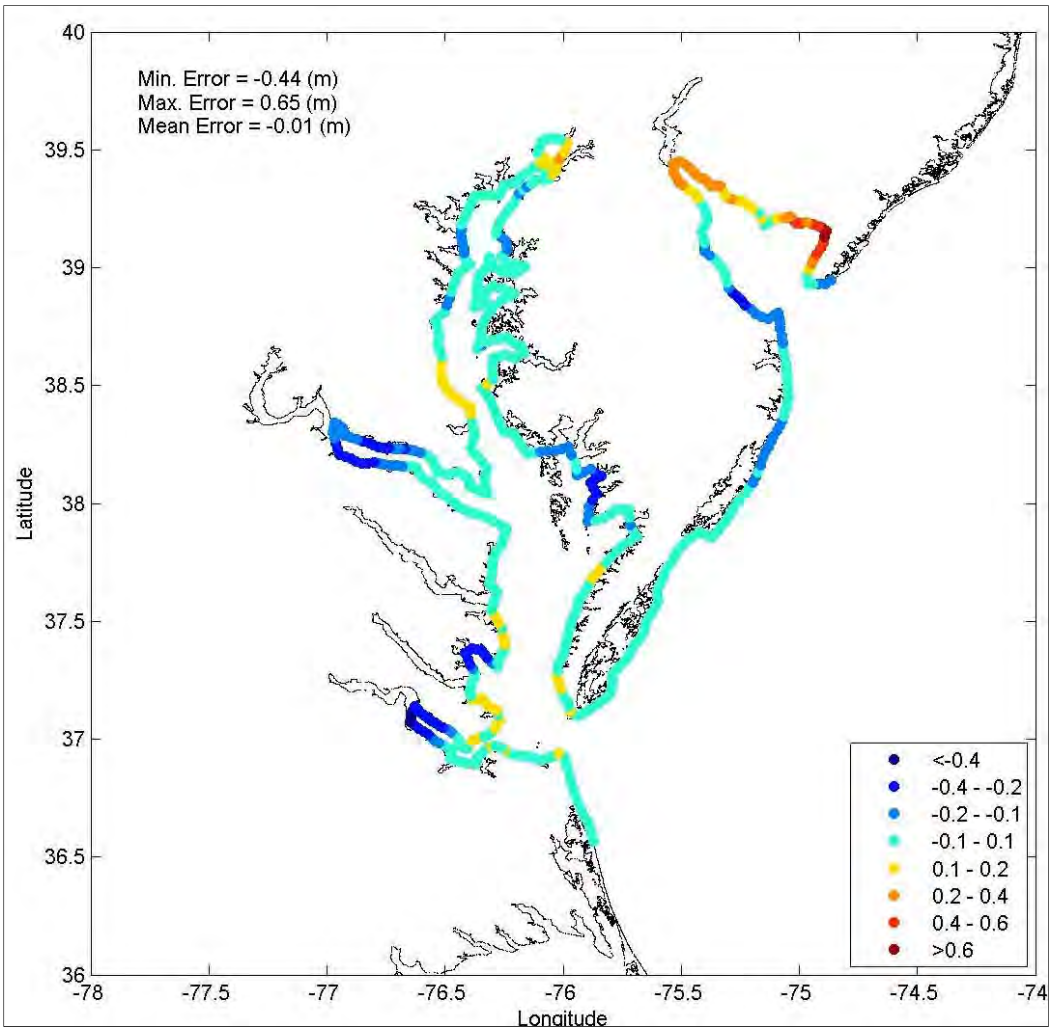

Figure D4. Difference between the stochastic- and JPM-predicted 100-year return period storm surge elevations. Positive values indicate that the JPM methodology produces higher storm surge values than the stochastic model. The largest positive differences occur on the north side of Delaware Bay, along the New Jersey coast.

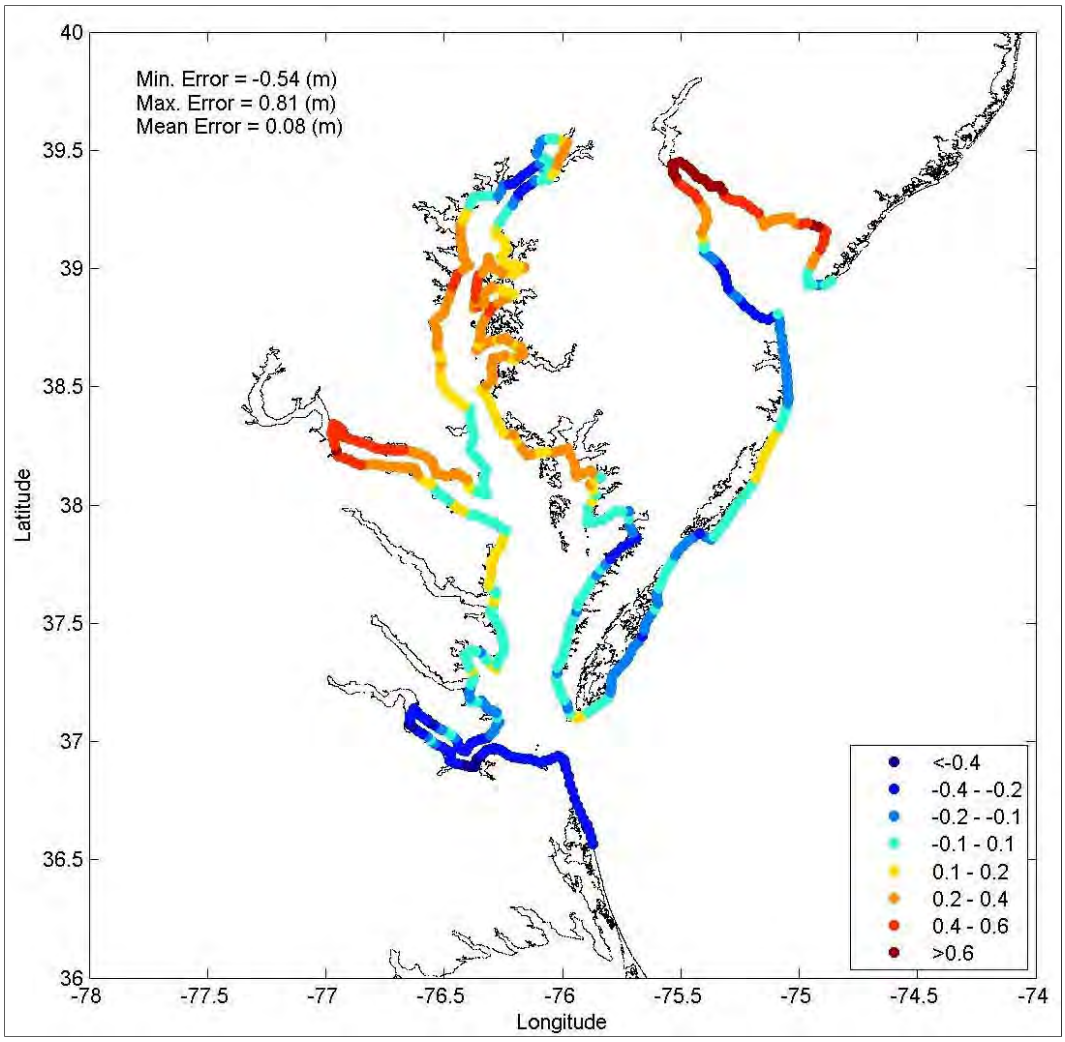

Figure D5. Difference between the stochastic- and JPM-predicted 500-year return period storm surge elevations. Positive values indicate that the JPM methodology produces higher storm surge values than the stochastic model. The largest positive differences occur on the north side of Delaware Bay, along the New Jersey coast and at the inland most extreme of the Delaware Bay.

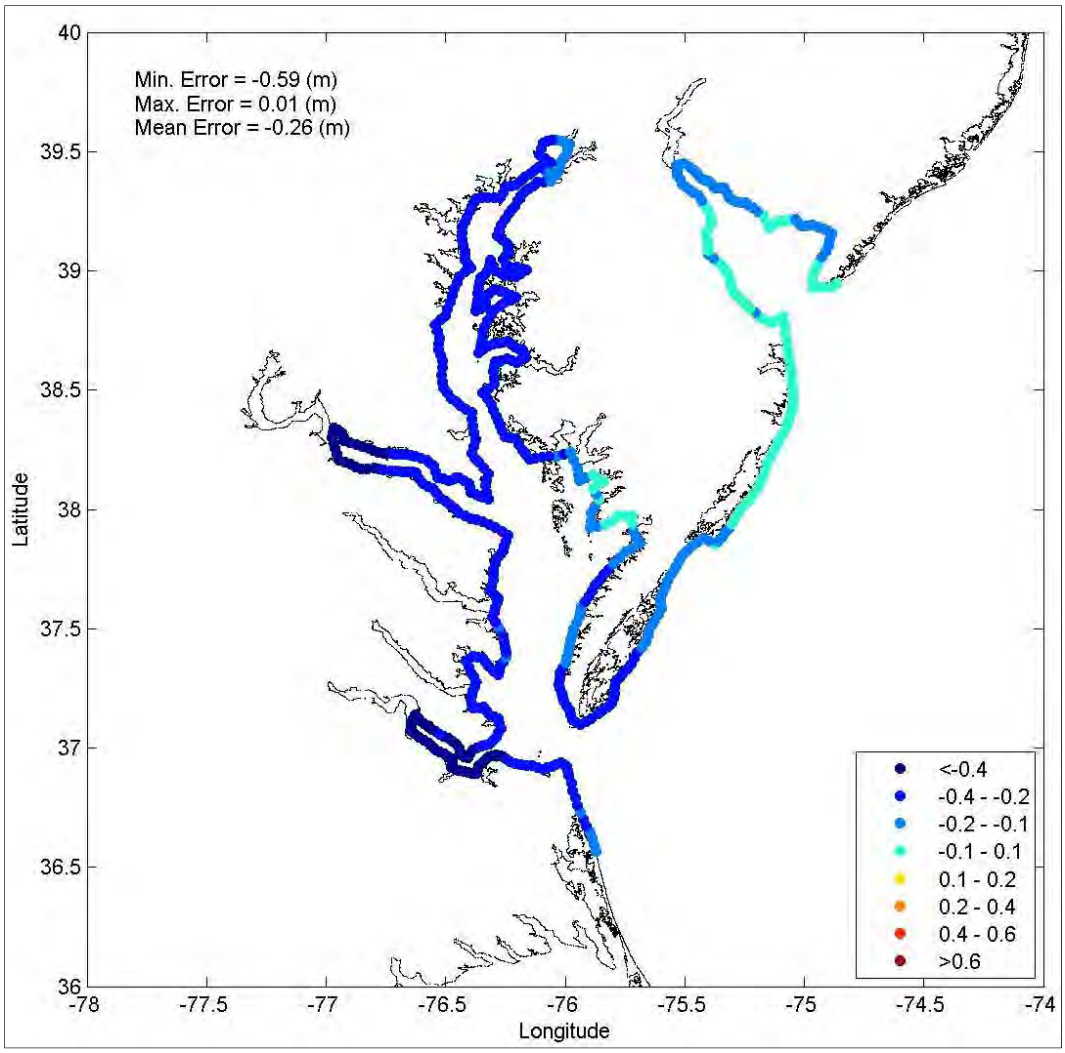

Figure D6. Difference between the stochastic- and JPM-predicted 10-year return period storm surge elevations. Positive values indicate that the JPM methodology produces higher storm surge values than the stochastic model. There is a clear bias, with the JPM results being lower than the stochastic results for all locations.

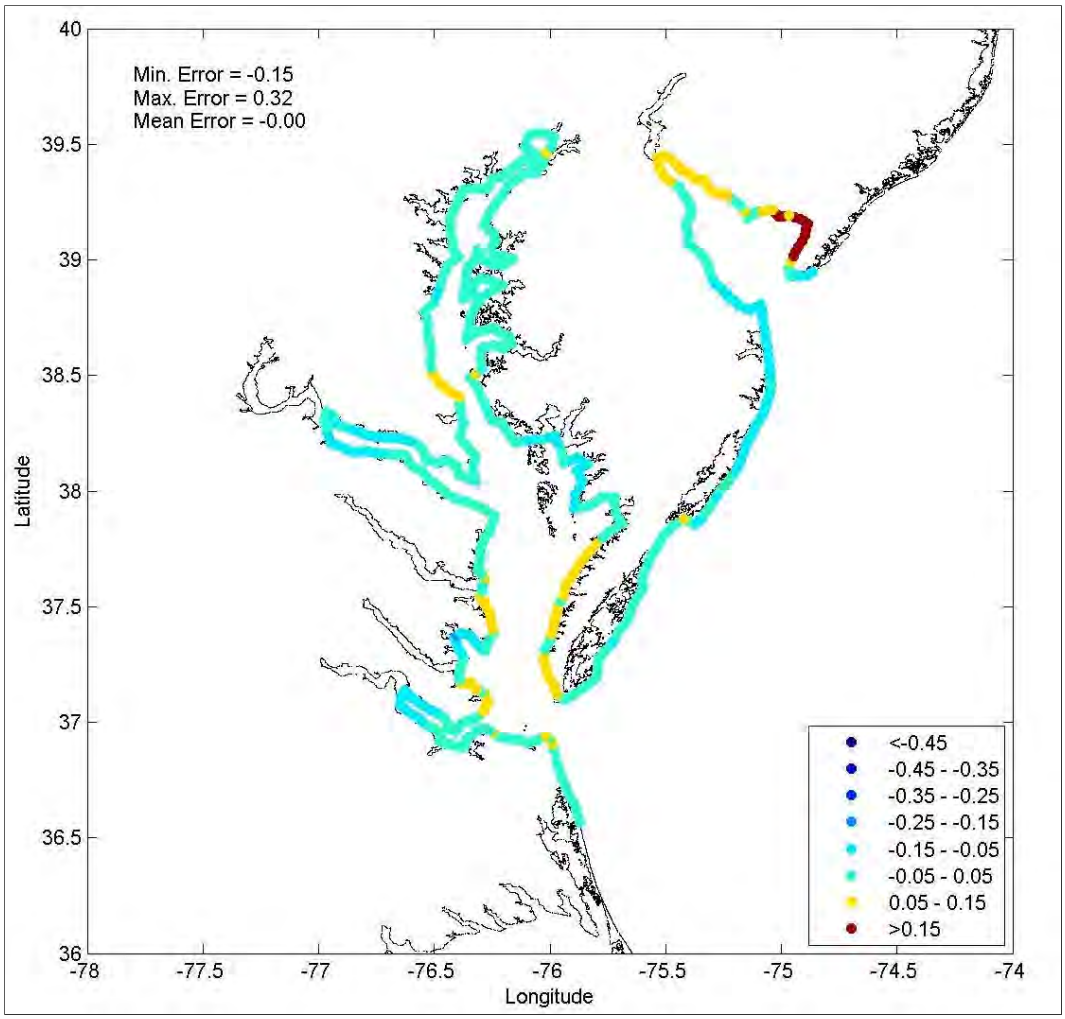

Figure D7. Relative (percentage) difference between the stochastic- and JPM-predicted 100-year return period storm surge elevations. Positive values indicate that the JPM methodology produces higher storm surge values than the stochastic model. The largest positive differences occur on the north side of Delaware Bay, along the New Jersey coast.

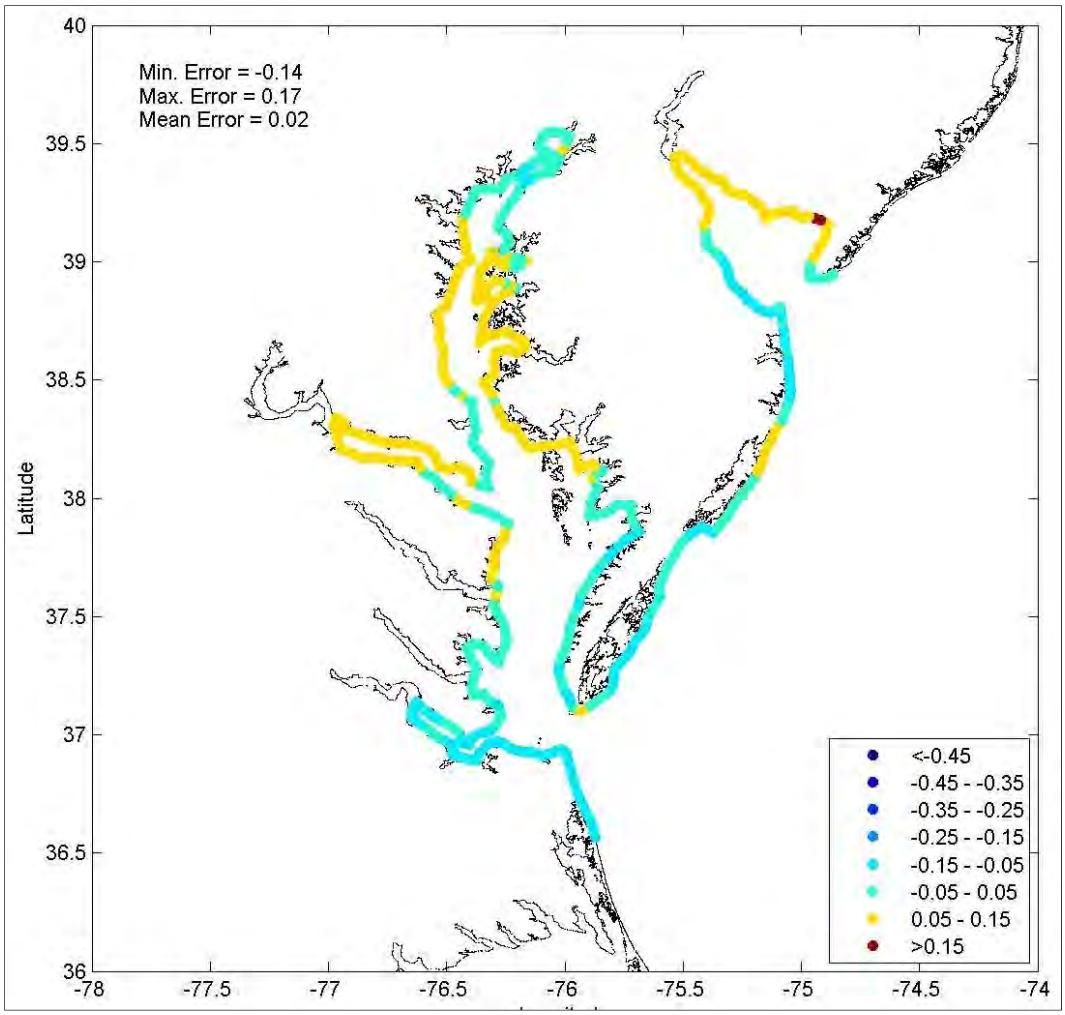

Figure D8. Relative (percentage) difference between the stochastic- and JPM-predicted 500-year return period storm surge elevations. Positive values indicate that the JPM methodology produces higher storm surge values than the stochastic model. The largest positive differences occur on the north side of Delaware Bay, along the New Jersey coast and at the inland most extreme of the Delaware Bay.

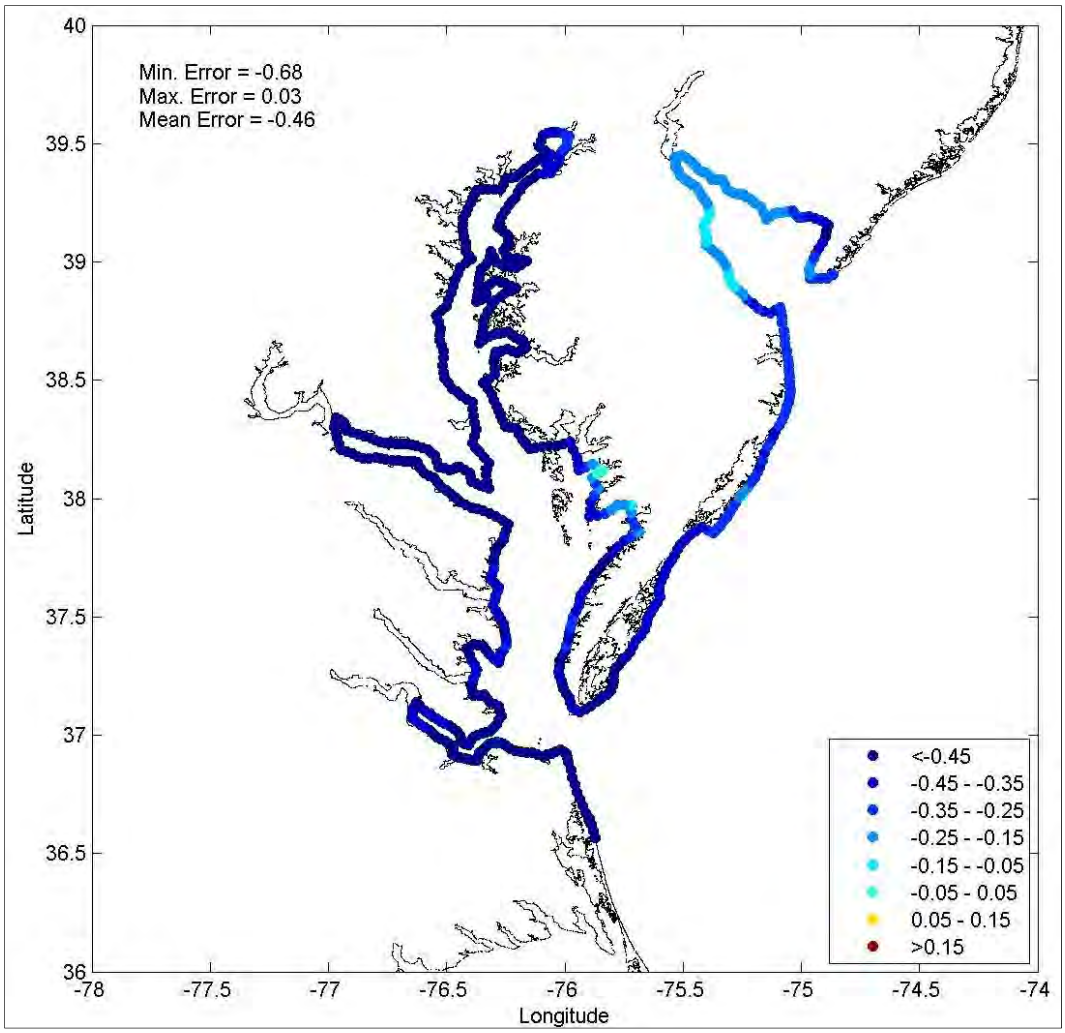

Figure D9. Relative (percentage) difference between the stochastic- and JPM-predicted 10-year return period storm surge elevations. Positive values indicate that the JPM methodology produces higher storm surge values than the stochastic model. There is a clear bias with the JPM results being lower than the stochastic results for all locations.

REPORT DOCUMENTATION PAGE

Form Approved
OMB No. 0704-0188

1. REPORT DATE ***(DD-MM-YYYY)***		**3. DATES COVERED** ***(From - To)***
July 2013	Final-TR	

4. TITLE AND SUBTITLE

Coastal Storm Surge Analysis: Storm Forcing
Report 3: Intermediate Submission No. 1.3

5a. CONTRACT NUMBER

5b. GRANT NUMBER

5c. PROGRAM ELEMENT NUMBER

6. AUTHOR(S)

Peter Vickery, Dhiraj Wadhera, Andrew Cox, Vince Cardone, Jeffrey Hanson, and Brian Blanton

5d. PROJECT NUMBER

5e. TASK NUMBER

5f. WORK UNIT NUMBER
81DFG1

7. PERFORMING ORGANIZATION NAME(S) AND ADDRESS(ES)

Field Research Facility
US Army Engineer Research and Development Center
1261 Duck Rd
Kitty Hawk, NC 27949

8. PERFORMING ORGANIZATION REPORT NUMBER

ERDC/CHL TR-11-1

9. SPONSORING / MONITORING AGENCY NAME(S) AND ADDRESS(ES)

Federal Emergency Management Agency Region III
615 Chestnut St
Philadelphia, PA 19106
Attn: Ms. Robin Danforth

10. SPONSOR/MONITOR'S ACRONYM(S)

11. SPONSOR/MONITOR'S REPORT NUMBER(S)

12. DISTRIBUTION / AVAILABILITY STATEMENT
Approved for public release; distribution is unlimited.

13. SUPPLEMENTARY NOTES

14. ABSTRACT

The Federal Emergency Management Agency (FEMA), Region III office, has initiated a study to update the coastal storm surge elevations within the states of Virginia, Maryland, and Delaware, and the District of Columbia. The area includes the Atlantic Ocean, the Chesapeake Bay, including its tributaries, and the Delaware Bay. This effort is one of the most extensive coastal storm surge analyses to date, encompassing coastal floodplains in three states and including the largest estuary in the world. The study will replace outdated coastal storm surge stillwater elevations for all Flood Insurance Studies in the study area, and serve as the basis for new coastal hazard analysis and — ultimately — updated Flood Insurance Rate Maps (FIRMs). Study efforts were initiated in August of 2008, and are expected to conclude in 2012.

The storm surge study considers both tropical storms and extratropical cyclones for determination of return period storm surge elevations. The historical record of events in the region has been used to reconstruct wind and pressure fields for significant extratropical cyclone events and to develop a synthetic suite of tropical storm tracks and associated parameters to drive the models. This will support the statistical analysis of storm surge return period elevations. This report, the third of three reports comprising the required Submittal 1 documentation, describes development of the wind and pressure fields required for FEMA Region III storm surge modeling.

15. SUBJECT TERMS		
Chesapeake Bay	Delaware Bay	Historical storms
Coastal flooding	FEMA flood study	Hurricane risk
	FEMA Region III	Storm surge modeling

16. SECURITY CLASSIFICATION OF:			**17. LIMITATION OF ABSTRACT**	**18. NUMBER OF PAGES**	**19a. NAME OF RESPONSIBLE PERSON: Jeffrey L. Hanson**
a. REPORT	**b. ABSTRACT**	**c. THIS PAGE**			**19b. TELEPHONE NUMBER** ***(include area code)***
Unclassified	Unclassified	Unclassified	Unclassified	154	(252) 261-6840 x238